THE ANALYSIS OF MIXING IN CONTINUOUS FLOW SYSTEMS

by

Abul Faiz Syed Abdul Aowal

B.E.,D.I.C.,M.Sc.(Eng.)(London)

A thesis submitted to the

University of London

for the Degree of

Doctor of Philosophy

in the

Faculty of Engineering

Department of Civil Engineering
Imperial College of Science and Technology
London S.W.7.

April, 1969.

ABSTRACT

The complex phenomena of mixing in a flow system are studied by assuming the "system" to be composed of a number of independent components or zones of flow connected in series or parallel with each other. Flow zones such as plug flow, perfect mixing, short circuit and recirculation are assumed and a method for determining them in proportion to the total volume is presented. Control theory is used in developing six different mathematical models described in this work.

The mathematical models are verified by direct simulation, using turbulent flow in a tube to simulate plug flow and a diffused aeration tank to simulate perfect mixing. The mathematical models are found to agree with experiment fairly well. In a second series of experiments, flow curves obtained from a small rectangular tank are analysed by the proposed models. It is shown that these models can deal with multipeaked flow curves, when these peaks are due to a combination of main flow, short circuit and/or recirculation.

Two methods of determining the optimum values of the parameters which give the best fit of the models to the experimental curves are presented. The first is a direct application of linear programming technique to the experimental data. The second method is indirect, involving the "Pulse Technique". Both these methods have been found to be satisfactory and useful for this type of problem.

ACKNOWLEDGEMENTS

The author wishes to express his gratitude to Mr F.E. Bruce, Reader in Public Health Engineering, for supervising the work presented herein.

He is ever indebted to Mr A.L. Dowley, Lecturer in the Department of Civil Engineering, Imperial College, for his continuous assistance and guidance throughout the project. His anglicising of the text is gratefully acknowledged.

He also wishes to thank his friend and colleague George (G.M. Ayoub) for the assistance lent to him by his good humour and practical knowledge of everything and Mr Gupta for helping him on numerous occasions.

It would be most appropriate to thank Mrs U.O. Fowler for her painstaking typing of the thesis with such speed and accuracy.

Financial support, in the form of an Overseas Scholarship, from the Government of Assam is gratefully acknowledged.

CONTENTS

NOTATIONS

C = Concentration of tracer

C_a = Average concentration of tracer

= Total weight of the tracer added divided by system volume

= Area of the input pulse/nominal detention time.

C_i = Concentration of the input pulse = height of the input pulse

f, f_1 = Fraction of short circuiting flow

f_2 = Fraction of recirculating flow

FT = Fourier Transform of

m = Perfect mixing fraction

p = Plug flow fraction

Q = Flow rate

r = Recirculation fraction, also perfect mixing fraction in the short circuit path of the 5 parameter model

s = Short circuiting fraction of the total volume

S = Laplace complex variable

t = Time

T = Nominal detention time = volume of the system/flow rate

θ = Dimensionless time = $t/_T$

T_1 = Input pulse width in time units = duration of input

θ_1 = Dimensionless input pulse width = $T_1/_T$

TF = Transfer Function

ϕ = Least square error

$*$ is used as a multiplication sign from Chapter 2 onward and does not stand for convolution.

All other symbols used are described in the text whenever they appear.

CHAPTER I

REVIEW OF LITERATURE

1.1 The analysis of flow systems

An analysis of the flow behaviour in a flow through system is of the utmost importance in giving a physical insight into the operation of the system. Many attempts at such analysis have been made by research scientists in Chemical Engineering. Much work has been done (1)(2)(3) on chemical reactors and different theories have been put forward which attempt to relate the flow system to changes in temperature, or concentration of the reacting components, with time.

One of the commonest procedures adopted is the stimulus-response technique. The stimulus may be a pulse, an impulse, a ramp or a step change in some property of the flow into the system at the input. Generally, a tracer or a dye is used. The response to such a stimulus is measured and plotted against time. Such a response curve, known as a "Flow curve" (4), or "Detention time distribution curve" (4), or "Dispersion curve" (5) is assumed to reflect the various components of the system, since each component contributes towards its formation. Hence an analysis of this flow curve can reveal valuable information on the behaviour of the components of the system.

A flow through system (which will be referred to henceforth as a reactor) may be subdivided into a number of idealised zones of flow in which plug flow (piston flow), perfect mixing, dead space (stagnant zone), short circuiting or recirculation are combined. Different combinations of these zones give rise to different flow patterns in the reactor which are reflected in the shape of the flow curve.

Mixing, the most important unit operation in chemical engineering and perhaps the most intractable problem, has been the subject of intense study in recent years. Since no real system can produce ideal mixing or ideal plug flow research has been largely concentrated on the deviations from these ideal conditions (1)(2)(3)(4)(5).

These deviations have been represented more in qualitative than in quantitative terms. Recently attempts have been made to supplement the qualitative approach with quantitative information and thereby give meaning to the previous analysis in more specific terms.

Work done on this topic may be divided into two broad categories, that based on a statistical approach or that based on a quantitative or deterministic approach.

The forerunners in analysing the flow curve were MacMullin and Weber (1). However Danckwerts (2) was the first to represent it in terms of a number of distribution functions. Since these functions form the basis of a large number of works using the statistical approach, they will be described in some detail in the following section.

1.2 Definitions of Age-Distribution Functions

The "Residence Time" of a fluid element is the time that elapses from the instant the element enters the vessel to the instant it leaves it. The "Age" of an element at a particular instant is the time that elapses after the entry of the element into the system up to that instant. In what follows, the existence of a system of volume V through which fluid flows at a steady rate Q is assumed.

From the above definition of "Age", it is clear that the vessel contains fluid of varying ages. The internal age distribution frequency is denoted by the functional notation I(t); I(t) has the units of fraction of ages per unit time. In accordance with probability theory in statistics, the fraction of the fluid elements between ages "t" and "t + Δt" is given by $I(t).\Delta t$. Since the internal age distribution function I(t) is a continuous function it is normalised by making the sum of all the fractions equal to unity:-

$$\int_0^\infty I(t)dt = 1 \qquad \ldots\ldots \qquad 1.2.1$$

The time t = 0 is an arbitrary initial point and not the starting time of the fluid flow. Physically equation (1.2.1) means that all the fluid in the vessel has an age between 0 and ∞.

The fraction of the vessel contents younger than a certain age "t" is :-

$$\int_0^t I(t')dt' \qquad \ldots\ldots \qquad 1.2.2$$

while the fraction older than "t" is

$$\int_t^\infty I(t')dt' = 1 - \int_0^t I(t')dt' \quad .. \qquad 1.2.3$$

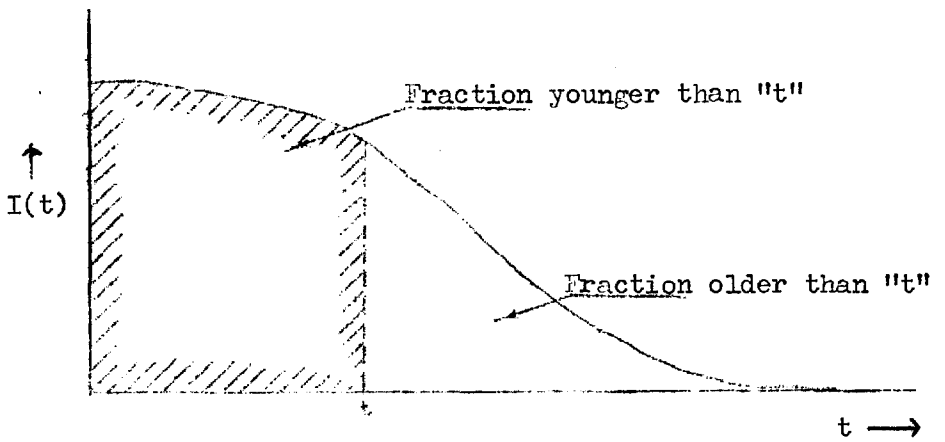

Fig.1.2.1.

The "Residence time distribution" or "Age Distribution Function" is defined as the exit age frequency distribution function E(t), which has the units of fraction of ages per unit time. As in the previous case E(t).Δt denotes the fraction of material leaving the system between ages t and t+Δt. On normalisation

$$\int_0^\infty E(t).dt = 1 \qquad \ldots\ldots \qquad 1.2.4$$

The fraction of the fluid in the exit stream younger than "t" is equal to :-

$$\int_0^t E(t')dt' \qquad \ldots\ldots \qquad 1.2.5$$

and the fraction older than t is equal to :-

$$\int_t^\infty E(t')dt' = 1 - \int_0^t E(t')dt' \quad .. \qquad 1.2.6$$

These are illustrated in figure 1.2.2

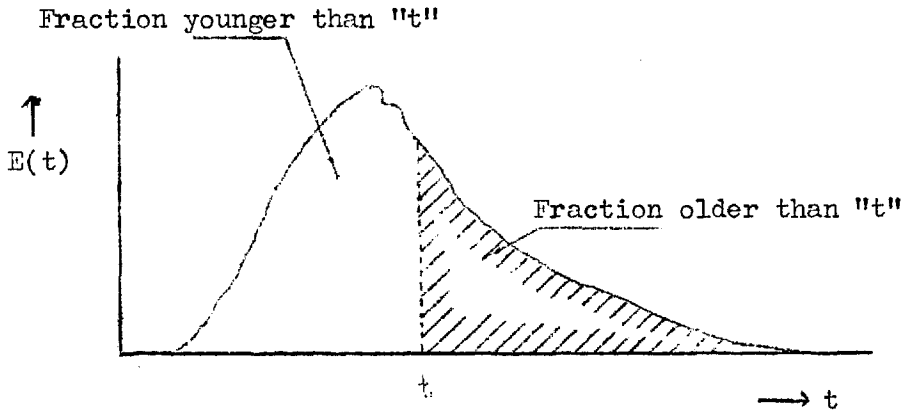

Fig. 1.2.2

Naor and Shinnar (7) introduced the "Intensity Function" $\Lambda(t)$ and defined it as the fraction of the fluid in the vessel of age "t" that will leave at a time between "t" and "t+Δt". This function gives the escape probability during the time interval Δt and will be discussed more fully at a later stage.

Himmelblau and Bischoff (8) related the above defined distribution functions to one another in the following way.

A vessel of constant volume "V" with a constant flow rate "Q" is considered. Let all the fluid entering the vessel at time $t > 0$ be called the "new" fluid. The existing content at time $t = 0$ is then the old fluid. At a time t equation 1.2.2 gives the fraction of new fluid in the vessel.

Therefore (Amount of "new" fluid in vessel at time t $= V \int_0^t I(t')dt'$

Equation 1.2.6 gives the fraction of the outgoing fluid at any instant of time, that has an age greater than t.

$$\text{Therefore } \left(\begin{matrix}\text{Amount of "old" fluid}\\ \text{gone from vessel at time t}\end{matrix}\right) = \int_o^t Q\,dt' \int_{t'}^{\infty} E(t'')\,dt''$$

Since the old fluid must be replaced by the new fluid it follows that :-

$$V \int_o^t I(t')\,dt' = \int_o^t Q\,dt' \int_{t'}^{\infty} E(t'')\,dt'' \qquad \ldots \quad 1.2.7$$

Differentiating both sides with respect to t'

$$V.I(t) = Q.1. \int_t^{\infty} E(t')\,dt'$$

or

$$\bar{t}.I(t) = \int_t^{\infty} E(t')\,dt' = 1 - \int_o^t E(t')\,dt' \qquad \ldots \quad 1.2.8$$

where $\bar{t} = \frac{V}{Q}$ = average detention time.

Differentiating again

$$E(t) = -\bar{t}\,\frac{d}{dt} I(t) \qquad \ldots \quad 1.2.9$$

The Intensity Function $\Lambda(t)$ may be related to the E(t) and I(t) functions in the following manner :-

$$\left(\begin{matrix}\text{Amount of fluid}\\ \text{leaving between}\\ \text{times t and t+}\Delta t\end{matrix}\right) = \left(\begin{matrix}\text{Amount of fluid}\\ \text{present at}\\ \text{time t}\end{matrix}\right) X \left(\begin{matrix}\text{Fraction of Age t}\\ \text{that will leave}\\ \text{between times t,}\\ \text{and t+}\Delta t\end{matrix}\right)$$

or

$$Q.E(t)dt = \left\{V.I(t)\right\} \quad x \quad \left\{\Lambda(t).dt\right\} \qquad \ldots\ 1.2.10$$

or

$$\Lambda(t) = \frac{1}{\bar{t}} \cdot \frac{E(t)}{I(t)} = -\frac{d}{dt}\left(\text{Ln } \bar{t}.I(t)\right) \qquad \ldots \quad 1.2.11$$

$$\because E(t) = -\bar{t}.\frac{d}{dt} I(t)$$

All of the above functions convey the same basic information i.e. the "age" of the fluid elements, and they are useful in studying deviations from ideal flow.

Again these distribution functions are generally written in dimensionless form, time being represented by θ in most literature (2), where

$$\theta = \frac{t}{\bar{t}} \qquad \ldots\ldots \qquad 1.2.12$$

thus $E(\theta).d\theta = E(t).dt$, $I(\theta).d\theta = I(t).dt$ and so on, so that :-

$$E(\theta) = \bar{t}E(t) \qquad \ldots\ldots \qquad 1.2.13$$

$$I(\theta) = \bar{t}I(t) \qquad \ldots\ldots \qquad 1.2.14$$

$$\Lambda(\theta) = \bar{t}\Lambda(t) \qquad \ldots\ldots \qquad 1.2.15$$

$$E(\theta) = -\frac{d}{d\theta} I(\theta) \qquad \ldots\ldots \qquad 1.2.16$$

$$\Lambda(\theta) = \frac{E(\theta)}{I(\theta)} = -\frac{d}{d\theta} \mathrm{Ln}\ I(\theta) \qquad \ldots\ldots \qquad 1.2.17$$

1.3 The Experimental Measurement of Age Distribution Functions

The stimulus response technique referred to in section 1.1 is used to measure the age distribution functions defined above. An injection of tracer is used as the stimulus to the flow system, and the response is the tracer concentration measured in the outlet stream. The tracer may be a coloured dye, a photosensitive material, an electrolyte or a radioactive compound, depending on the type of situation. The tracer should preferably have the same density, and viscosity and be hydrodynamically indistinguishable from the process stream in order to represent accurately the flow conditions.

The tracer may be injected in the form of a step change or in the form of an impulse and Danckwerts (2) defined "F" and "C" diagrams in relation to these two methods as follows.

Suppose some property of the inflowing fluid undergoes a sudden change from one steady value to another (i.e. step change). For example, let the colour change from white to red. Then let the fraction of the red material in the outflow at time "t" later be F(t). Then the dimensionless plot of $F(\theta)$ versus θ is called the "F" diagram. In $F(\theta)$, the concentration C of the outflowing tracer is made dimensionless by dividing by C_o, the concentration of the entering stream. The "F" curve rises from 0 to 1.

Danckwerts (2) defined the "C" curve as the concentration-time function of the tracer in the exit stream of a vessel in response to an idealised instantaneous or impulse tracer injection. Concentration and time are made dimensionless as above with the result that the area under the "C" curve is always equal to unity.

$$\int_o^\infty \frac{C}{C_o}\, d\theta = 1 \qquad \ldots\ldots \qquad 1.3.1.$$

The "F" and "C" diagrams are illustrated in Fig. 1.3.1. and 1.3.2 respectively.

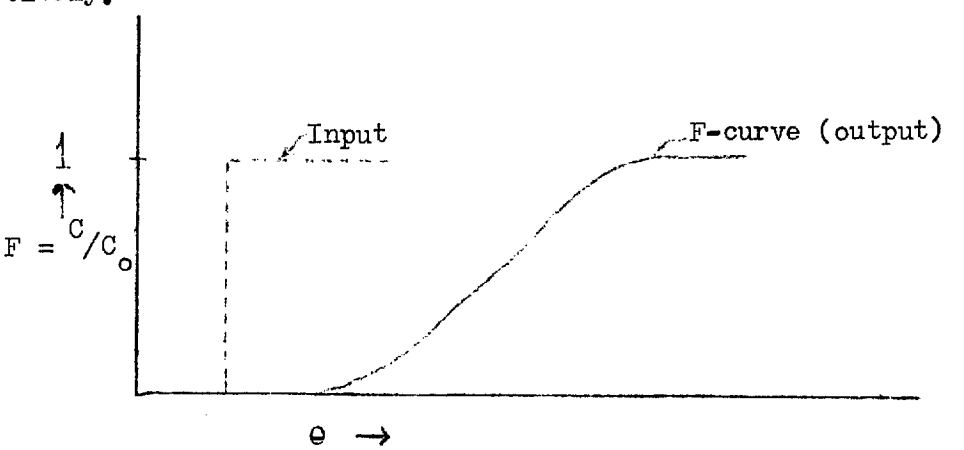

Fig. 1.3.1

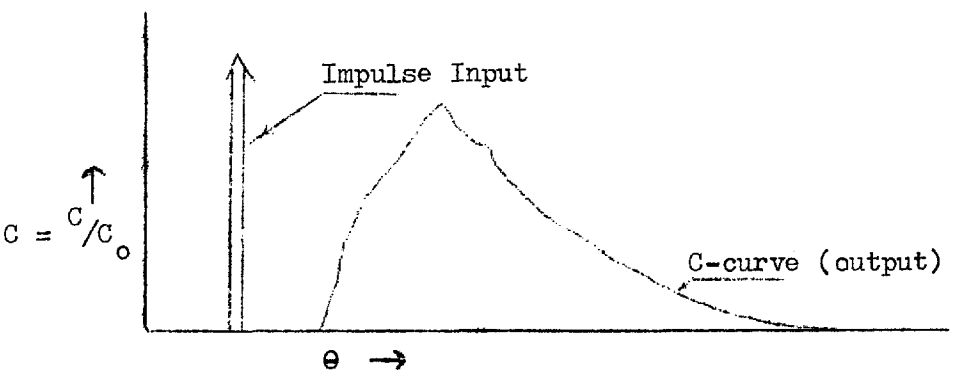

Fi . 1.3.2

Relationships between F, C, E and I functions are deduced by Danckwerts (2), Levenspiel (9), Himmelblau et al. (8), considering the reactor as a closed vessel. A closed vessel is defined as one in which the material flows in and out of the vessel by bulk flow only. Thus diffusion and dispersion are absent at entrance and exit so that, for example, we do not have materials moving upstream and out of the vessel entrance by swirling or eddying.

Considering the steady state flow of fluid through such a vessel and assuming that the tracer is introduced as a second fluid into the flow at time t = 0, in place of the original flowing fluid thus giving a step change in the input to the vessel. Then at time t and dimensionless time θ ($\theta > 0$), a material balance for the vessel gives :-

[Rate of tracer input] = [Rate of tracer output]

+ [Rate of tracer accumulation within the vessel]

$$Q = Q \times F + \frac{d}{dt}\left\{V \times \text{Fraction of second fluid within vessel}\right\}$$

$$\text{or} \quad Q = Q \times F + \frac{d}{dt}\left\{V \times \int_o^{\theta} I\,d\theta\right\}$$

$$\text{or} \quad 1 = F + \frac{d}{dt}\,\bar{t}\int_o^{\theta} I\,d\theta$$

$$\text{or} \quad 1 = F + \frac{d}{d\frac{t}{\bar{t}}}\int_o^{\theta} I\,d\theta$$

But $\frac{t}{\bar{t}} = \theta$.

$$\therefore\ 1 = F + \frac{d}{d\theta}\int_o^{\theta} I\,d\theta$$

$$\text{or} \quad F + I = 1 \qquad \ldots\ldots \qquad 1.3.2$$

$$\text{or} \quad F = 1 - I \qquad \ldots\ldots \qquad 1.3.3$$

Again at any time θ :-

[The fraction of the second fluid in the exit stream] = [Fraction of fluid in the exit stream younger than θ]

$$\text{By definition } F = \int_o^{\theta} E\,d\theta \qquad \ldots\ldots \qquad 1.3.4$$

This may ~~also~~ be obtained by comparing equations 1.28 and 1.33.

Now consider an input to the vessel in the form of an impulse of tracer. At the instant of tracer injection (t = 0) all elements of the tracer fluid have the same starting time for the measurement of their ages. Thus the outlet concentration curve or the "C" curve is a record of the fraction of the tracer elements that entered the vessel at time t = 0 and left at time t = t. This is obviously the same as the exit age distribution function "E".

Therefore $C = E = \bar{t} \times E(t)$ 1.3.5

From equations 1.3.4 and 1.3.5 :-

$$F = \int_0^\theta C d\theta \quad \text{.....} \quad 1.3.6$$

Also

$$C = \frac{dF}{d\theta} = -\frac{dI}{d\theta} \quad \text{.....} \quad 1.3.7$$

In all the above equations F, I, E and C are considered as functions of θ.

Equations 1.3.6 and 1.3.7 are special cases of the general theorem for linear systems. They show that an impulse is the derivative of a step function.

Denbigh (10) defined a function f(t) called the "Residence Time Frequency Function" in the same way as the function E(t) is defined above. The importance of this function will be discussed later on.

1.4 Idealised Flow Regimes

As mentioned in section 1.1 different flow patterns in the body of fluid in a reactor contribute to the formation of its characteristic flow curve. The frequency distribution functions defined above are used to analyse the flow curve and indicate the dominating regimes present in the reactor in a qualitative fashion. The different idealised regimes or zones and the ways in which they are defined and

determined by different authors are briefly outlined below.

The perfect mixing regime

Perfect mixing assumes that the vessel contents are perfectly homogeneous and have the same composition as the exit stream.

MacMullin and Weber (1) determined the F(t) and I(t) functions for a perfectly mixed vessel using a statistical probability approach. Consider a vessel of constant volume V with constant overflow rate Q. Assume that an increment or lump of fluid ΔV enters the vessel at a time t = 0. Since the volume of the tank is constant, in a time interval Δt a lump of fluid ΔV will go out of the tank. The probability P_n of the "new" lump ΔV not going out of the vessel in a length of time t is

$$P_n = \left(\frac{V}{V+\Delta V} \right)^{\frac{t}{\Delta t}}$$

where $\frac{t}{\Delta t}$ is the number of increments or lumps ΔV passing through the vessel in that time t.

or $$\frac{1}{P_n} = \left(1 + \frac{\Delta V}{V}\right)^{\frac{t}{\Delta t}}$$

or $$- \operatorname{Ln} P_n = \frac{t}{\Delta t} \ln \left(1 + \frac{\Delta V}{V}\right)$$

Since ΔV and Δt are very minute increments

$$\operatorname{Ln} \left(1 + \frac{\Delta V}{V}\right) \simeq \frac{\Delta V}{V}$$

$$\therefore - \operatorname{Ln} P_n = \frac{t}{\Delta t} \cdot \frac{\Delta V}{V} = \frac{t}{V} \cdot \frac{\Delta V}{\Delta t}$$

But $\frac{\Delta V}{\Delta t}$ = the overflow rate Q

$$\therefore - \operatorname{Ln} P_n = \frac{t}{V/Q}$$

or $$P_n = e^{-t/(V/Q)} \qquad \ldots\ldots \qquad 1.4.1.$$

P_n represents the fraction of the fluid that is held in the tank longer than time t. This in fact represents the Internal age distribution function I(t) of Danckwerts (2) for a perfectly mixed vessel.

Hence $F(t) = 1 - e^{-t/(\frac{V}{Q})}$ ..... 1.4.2.

On normalisation $I(\theta) = e^{-\theta}$ ..... 1.4.3.

$F(\theta) = 1 - e^{-\theta}$ ..... 1.4.4.

The F and I diagrams for perfectly mixed vessels are illustrated in Figs. 1.4.1 and 1.4.2 respectively. I falls exponentially from 1 to 0 while F rises from 0 to 1 and becomes asymptotic at $F(\theta) = 1$.

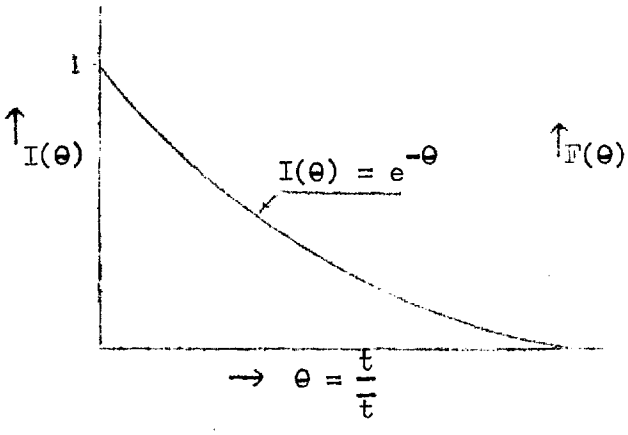

Fig.1.4.1

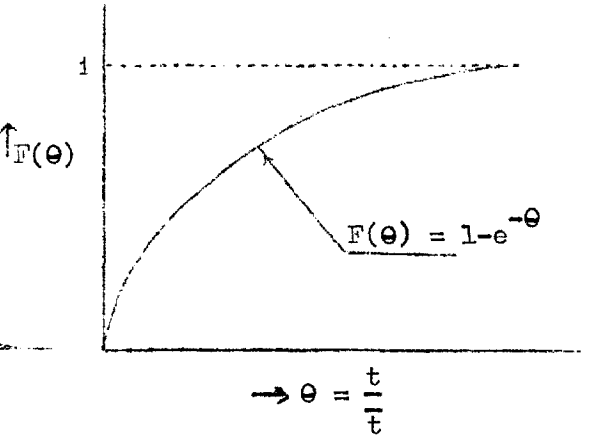

Fig. 1.4.2

Chollette and Cloutier ([11]) obtained equation 1.4.1 using a materials balance approach. Consider a vessel of volume V containing a fluid of initial concentration C_o, fed at a flow rate Q. At a time $t = 0$, a new fluid of feed composition $C_F = 0$ is introduced at the same flow rate Q into the vessel thus introducing a negative step input. At any given time t, with perfect mixing, the tank contents are of uniform composition C throughout equal to that of the effluent stream.

A material balance over a time element dt gives :-

$$Q.C_F.dt = Q.C.dt + \frac{d}{dt}(V.C)dt \qquad \text{..... 1.4.5..}$$

Since $C_F = 0$ and V = constant, equation 1.4.5 can be written :=

$$\frac{dC}{dt} + \frac{Q}{V}C = 0$$

Integrating between limits 0 and t and considering that when $t = 0$ $C = C_o$ and when $t = t$ $C = C$

$$\frac{C}{C_o} = e^{-\frac{Q}{V}t} \qquad \text{..... 1.4.6.}$$

When $\frac{C}{C_o}$ is plotted against $\frac{t}{\bar{t}}$ on semilog paper as shown in Fig.1.4.3 a straight line is obtained

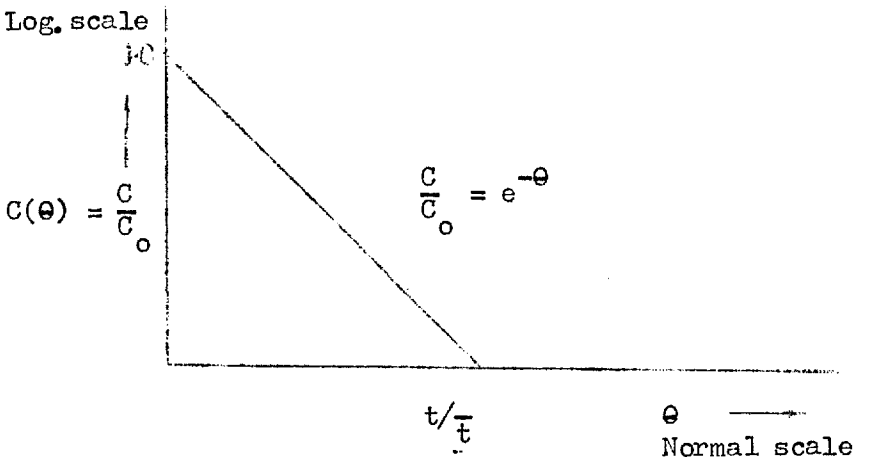

Fig. 1.4.3.

From equations 1.3.7 and 1.4.3

$$C(\theta) = -\frac{d}{d\theta} I(\theta) = e^{-\theta} \qquad \ldots\ldots 1.4.7$$

Wolf and Resnick (12) considered the function E(t) as the first derivative of F(t) so that from equations 1.4.2

$$E(t) = \frac{1}{\bar{t}} e^{-\theta} \qquad \ldots\ldots 1.4.8$$

Therefore, for the particular case of perfect mixing, normalised plots of E, I and C give the same curve as shown in Figs. (1.4.1).

The Plug Flow regime

In plug flow, all materials pass through the vessel without any mixing whatsoever; each fluid element stays in the vessel for the same length of time. In the case of a step input, the interface between the tracer and the fluid moves through the vessel like a piston. For this reason plug flow is sometimes referred to as piston flow. Under such conditions each element of the fluid remains in the vessel for a time equal to the mean residence time $\bar{t}$

In this case the F(θ) curve is a step function as shown in Fig.1.4.4.

$$F(\theta) = U(t - \bar{t}) \qquad \ldots\ldots 1.4.9$$

where

$$U(t - \bar{t}) = \begin{cases} 0, & t < \bar{t} \\ 1, & t > \bar{t} \end{cases}$$

$$I(t) = \frac{1}{\bar{t}}[1 - F(\theta)] = \frac{1}{\bar{t}}[1 - U(t - \bar{t})] \qquad \ldots\ldots 1.4.10$$

$$E(t) = \frac{dF}{dt} = \frac{d}{dt}U(t - \bar{t}) = \delta(t - \bar{t}) \qquad \ldots\ldots 1.4.11$$

$$I(\theta) = 1 - U(\theta - 1) \qquad \ldots\ldots 1.4.12$$

$$E(\theta) = \delta(\theta - 1) \qquad \ldots\ldots 1.4.13$$

where $\delta(x)$ is the Dirac Delta function or the Impulse Function defined as

$$\delta_t(x) = \begin{cases} 0, & x < t \\ +\infty, & x = t \\ 0, & x > t \end{cases}$$

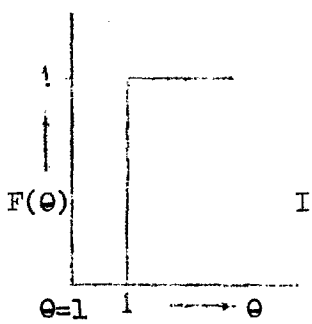

Fig.1.4.4

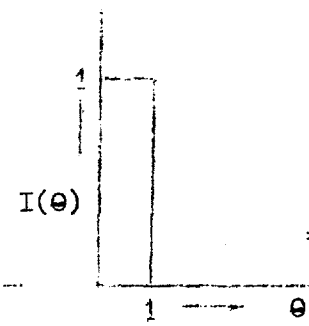

Fig.1.4.5

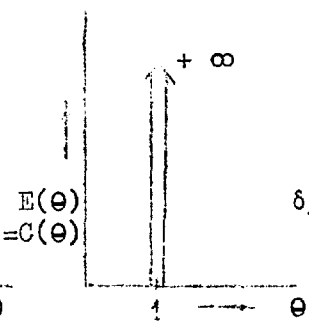

Fig.1.4.6

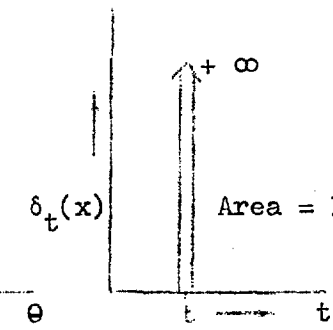

Fig.1.4.7

Fig.1.4.5 shows the I diagram, Fig.1.4.6 the E and C curves for plug flow and Fig.1.4.7 is an illustration of the Dirac Delta Function. The properties of the unit step and Dirac Delta functions will be described in detail later on.

Danckwerts (2) defined plug flow as the condition when elements of fluid which enter the vessel at the same moment, move through it with constant and equal velocity on parallel paths and leave at the same moment.

Short circuiting or Bypassing

MacMullin and Weber (1), Denbigh (13) and Weber (14) used the term "short circuiting" or "mathematical by-passing" (13) to describe conditions for which the F diagram differs from that of Fig.1.4.4. for example Figs.1.3.1 and 1.4.2. However Denbigh (13) defined "mathematical by-passing" for well agitated tanks in which the contents are substantially homogeneous, as the condition in which reactants are lost within a time shorter than is required to complete the reaction. Thus Denbigh's short circuiting was with respect to reaction time rather than theoretical detention time. MacMullin and Weber (1) considered the perfect mixing regime as an extreme case of short circuiting and argued that the occurrence of any short circuiting indicates a departure from "streamline" flow. They suggested that by dividing the system into a number of well agitated tanks in series, this problem could be solved. Since an infinite number of perfectly mixed tanks in series gives a plug flow output, the greater the number in the series the greater will be the reduction in short circuiting. Weber (14) comments that the extent of short circuiting can be quantitatively evaluated in terms of the number of reactors in the series, the vessel recirculation rate, and the volumetric overflow rate for the system. Colburn (15) defined short circuiting as the situation in a tank in which some of the feed is channelled to the outlet without being completely mixed, and later MacMullin (16) agreed that short circuiting could be interpreted as channellized flow between inlet and outlet.

Wolf and Resnick (12) regarded short circuiting as the situation in which part of the entering feed passes to the outlet with infinite velocity. Although this definition departs from reality it is commonly accepted for its ease of mathematical modelling.

A more rational definition of short circuiting can be taken from Danckwerts' (2) segregation model, although Danckwerts did not define it as such. When the contents of a vessel flow in parallel paths without being mixed with one another, the flow is said to be segregated. If the time of travel along one path is shorter than another, the flow can be considered to have shortcircuiting in a relative sense. However this model gives only a qualitative approach to the detection of short circuiting or deviations from the perfect mixing regime and therefore has limited usefulness. The method most commonly used in the literature for the detection of bypassing is the "I" curve. An initial sudden drop in the "I" curve as shown in Fig.1.4.8 indicates short-circuiting. The "E" and "C" curve also shows up short circuiting Fig.1.4.9) but the I curve is the better indicator.

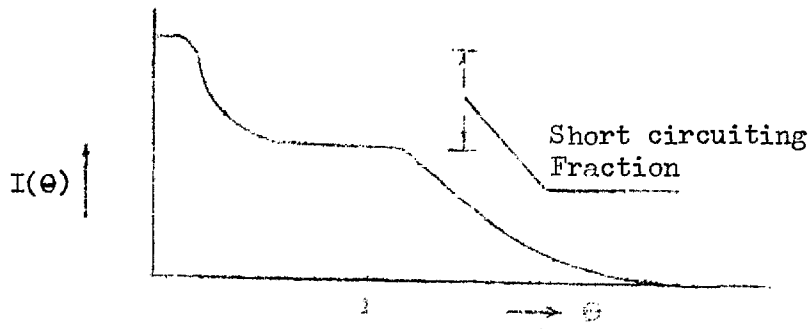

Fig. 1.4.8.

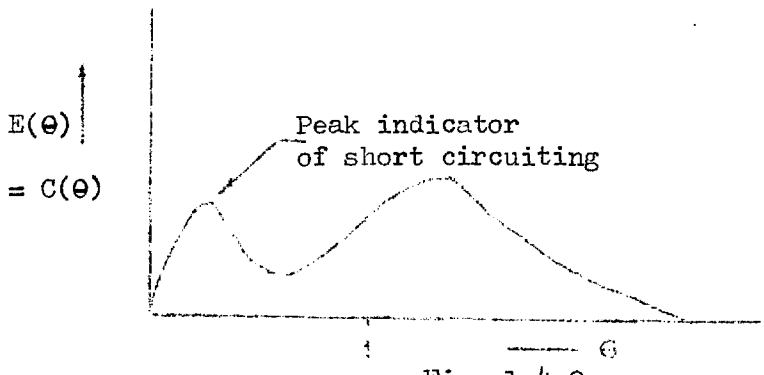

Fig. 1.4.9.

The Stagnant or Dead Water zone

A region of a vessel may retain fluid elements for a time greater than the mean residence time of the total fluid. Such a region is

called a stagnant zone. However there is a direct relationship between by-passing as defined in the last paragraph and dead water. By-passing or shortcircuiting is considered as that part of the flow which is relatively fast. Dead water was considered by Levenspiel (9), Wolf and Resnick (12), Himmelblau et al. (8) and others (3),(4) in their models as an inert region or a region of fluid at rest. Since this is physically inconceivable, it may be better defined as the flow region with relatively the slowest flow in the vessel. Thus as pointed out by Himmelblau et al. (8) from the somewhat arbitrary definitions of short circuiting and dead space, 40% short circuiting may also be called 60% dead space. Both these effects can be termed "stagnancy" (8). However in the literature "stagnancy" is generally taken to mean dead space (7).

Stagnancy may be determined qualitatively from the "E" or "C" diagram (8),(9) and the Λ function (7). Quantitative determinations were attempted by others (4),(12). Stagnancy will be discussed in some detail when dealing with combined models.

Recirculation

Recirculation is defined by Levenspiel as the pattern of flow where a portion of the fluid leaving the vessel or leaving a flow region is recirculated and returned to mix with fresh fluid. Internal recirculation is one of the most complex phenomena and is difficult to evaluate. Some statistical methods involving the use of convolution integrals have been advanced by Sinclair and McNaughton (17).

1.5. Combined Models (Qualitative Approach)

Plug flow and perfect mixing are ideal regimes which are never attained in practice. Flow patterns in a flow through system are a combination of (i) Plug flow (ii) perfect mixing (iii) by-passing (iv) stagnant zones and (v) recirculation such that the resulting outflow curve depends on the relative proportions of one or more of the above patterns of flow. The various attempts to identify these flow patterns are described below.

MacMullin and Weber were the first to investigate the "I" curve for a number of perfectly mixed vessels in series. As shown earlier they obtained the equations for $F(\Theta)$ and $I(\Theta)$ for a single perfectly mixed tank from the laws of probability. In the same way they deduced that for "n" number of equal capacity perfectly mixed vessels in series, the fraction of the total flow which has remained in the system for a time "t" or longer is equal to the probability of that event for any particle in the flow :-

$$I(\Theta) = e^{-\Theta}\left[1 + \Theta + \frac{\Theta^2}{\underline{2}} + \frac{\Theta^3}{\underline{3}} + \ldots\ldots \frac{\Theta^{n-1}}{\underline{n-1}}\right] \qquad \ldots\ldots 1.5.1$$

where $\Theta = \frac{t}{\bar{t}'}$ and $\bar{t}' = \frac{V}{nQ}$

They also deduced the equation for the "C" curve by differentiating $I(\Theta)$ w.r.t Θ and plotted a family of "I" and "C" curves for different values of n as shown in Figs. 1.5.1 and 1.5.2 respectively. McMullin and Weber did not try to interpret these curves as Denbigh (13) did but simply stated that in the "C" curve, the mode approaches the mean as the value of "n" increases, which was to be expected.

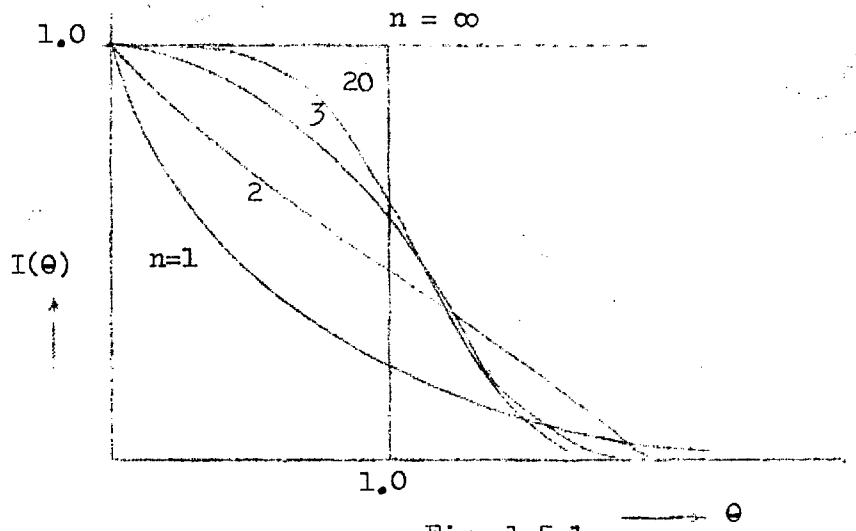

Fig. 1.5.1

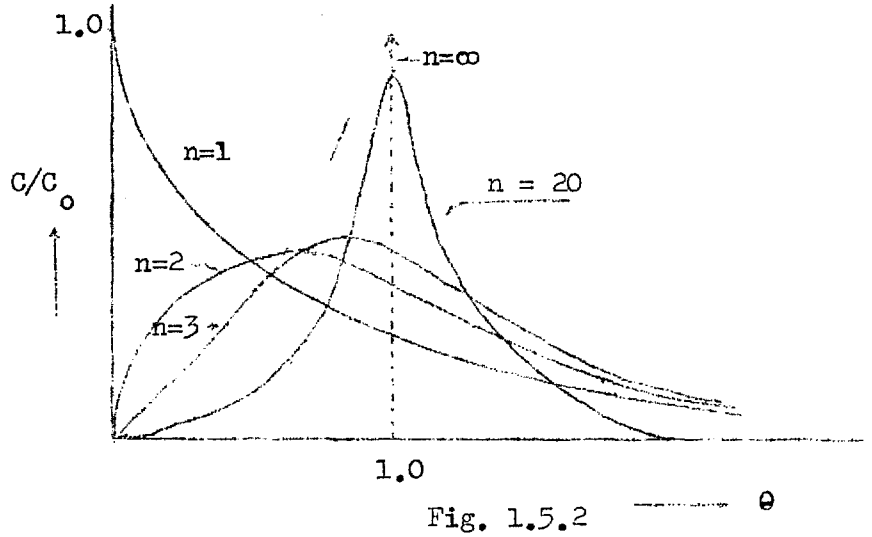

Fig. 1.5.2

Denbigh (13), considering the problem of mathematical by-passing, obtained the equation of the F function for a system of n equal volume completely mixed tanks in series from a mass balance approach

$$F(\theta) = 1 - e^{-\theta}\left[1 + \theta + \frac{\theta^2}{2!} + \frac{\theta^3}{3!} + \ldots\ldots \frac{\theta^{n-1}}{(n-1)!}\right] \quad \ldots\ldots 1.5.2$$

where θ is defined as in equation 1.5.1.

As $n \longrightarrow \infty$, $F(\theta)$ remains zero for all values of θ smaller than 1 as the term in the brackets converges to e^{θ}. For $\theta > 1$, $e^{-\theta}$ x [term in the brackets] = 0 and $F(\theta) = 1$.

Fig. 1.5.3 illustrates the "F" diagram obtained by Denbigh (13). It should be noted that as n increases, the curves shift towards the

vertical line at $\theta = 1$. As shown in Fig. 1.4.4 a vertical line at $\theta = 1$ relates to a plug flow condition. Hence the higher the number of perfectly mixed tanks in series, the more the flow through the system approaches the plug flow condition. This criterion is often used for design purposes.

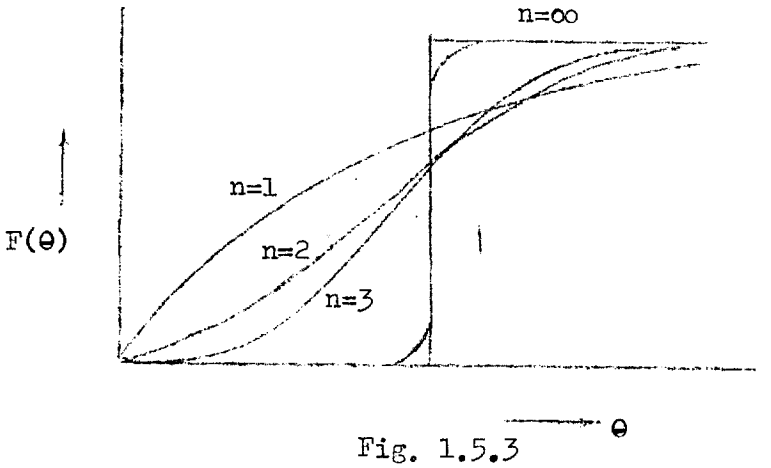

Fig. 1.5.3

Denbigh (3) explained the "C" and "F" diagrams in qualitative terms, suggesting that the more slender the peak of the "C" diagram, the more the flow approaches the plug flow conditions and that a flat peak indicates deviation from the plug flow condition. This tendency may be measured by the kurtosis of the distribution or the 4th moment of the diagram area about the mean. A low value indicates a condition approaching plug flow and a high value indicates deviation from it. Similarly the "F" diagram becomes less and less sharp at the edges as the flow deviates more and more from the plug flow condition as shown in Fig. 1.5.3.

Danckwerts (2) used the terms "hold back" and "segregation" as measures of deviation from ideal conditions. He defined "hold back" as the quantity "H" defined as the area under the F diagram between $\theta = 0$ and $\theta = 1$. This is the dotted area in Fig. 1.5.4.

$$H = \int_0^1 F(\theta)\,d\theta \qquad \ldots\ldots 1.5.3.$$

$H = 0$ for plug flow and $H = \int_0^1 (1 - e^{-\theta})\,d\theta = \frac{1}{e}$ for perfect mixing.

$H = 1$ when the entire space is completely stagnant.

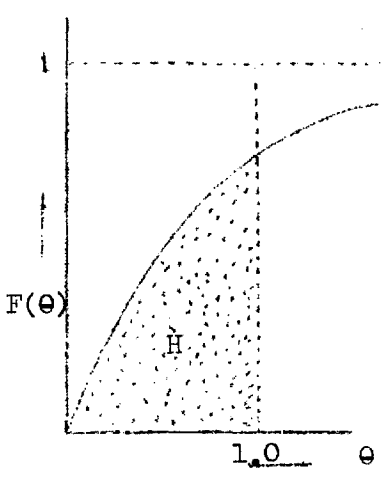

Fig.1.5.4.

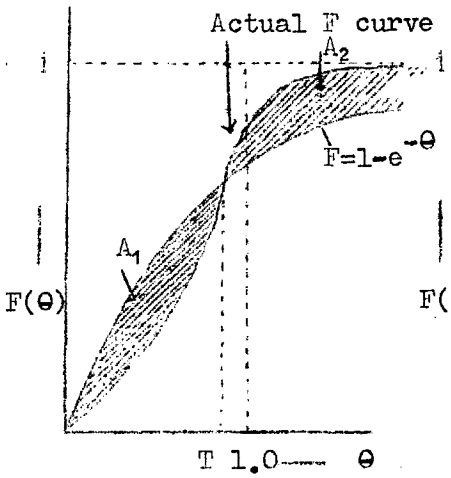

Fig. 1.5.5

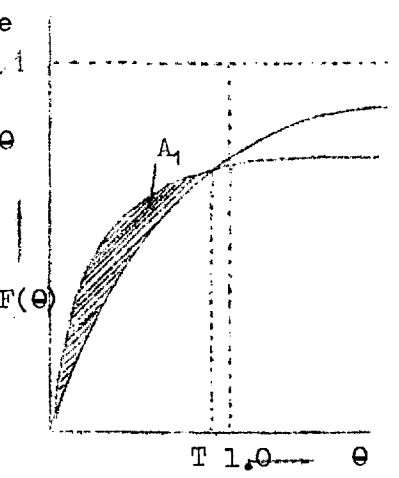

Fig. 1.5.6

Danckwerts' (2) use of the term "segregation" as a measure of the efficiency of mixing can be explained with reference to Fig. 1.5.5. If the actual diagram for a particular system is superimposed on the diagram for perfect mixing, it cuts the latter in one or more points. Areas A_1 and A_2 in Fig. 1.5.5 indicate the degree of variation from perfect mixing. Since the area between each curve and $F(\theta) = 1 - e^{-\theta}$ is the same, ($A_1 = A_2$) segregation "S" is quantitatively defined as the area A_1 between the "F" diagram of the system and the curve $F(\theta) = 1 - e^{-\theta}$ up to the point $\theta = T$ where the curves cross. When there is dead water, the diagram is like that of Fig. 1.5.6. The segregation is then $S = -A_1$. When the curves cross in two or more points as shown in Fig. 1.5.7, $A_1 + A_3 = A_2$ and segregation $= -A_2$

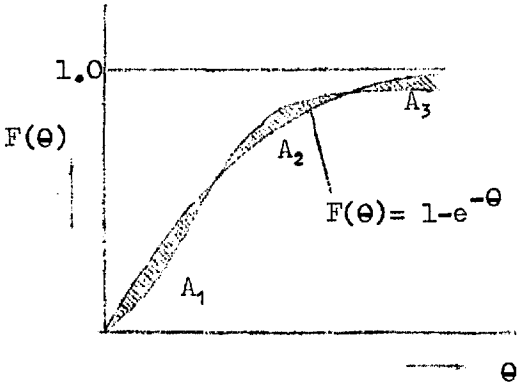

Fig. 1.5.7

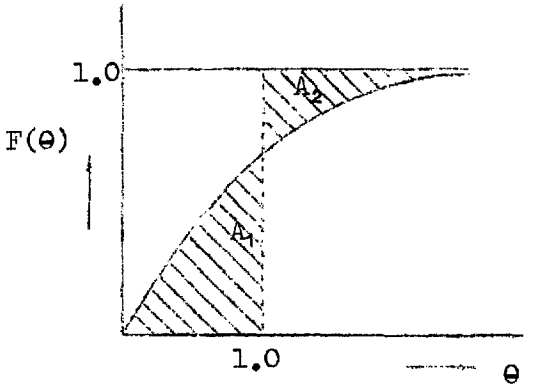

Fig. 1.5.8

Segregation for plug flow is the area A_1 in Fig.(1.5.8) = $+A_1 = \frac{1}{e}$. When most of the tank volume is dead space S $\longrightarrow$ -1, being the area between the curve $F(\theta) = 1 - e^{-\theta}$ and $F(\theta) = 1$ taken over the limits $0 \longrightarrow \infty$.

One of the most useful qualitative methods of identifying dead space is that put forward by Naor and Shinnar (7). They pointed out that the statistical parameter approach could give rise to confusion and advocated the use of the Intensity Function. They cited as an example the case of a tubular vessel filled with porous packing, through which fluid flows with near plug flow, but in which the out flow curve is affected by diffusion of the fluid into and out of the packing. In this case the porous packing modifies the plug flow curve to a J function (18). The coefficient of variation in such cases is equal to 1.0 as in the case of a completely mixed vessel, although there may be very little back mixing. Skewness or the 3rd moment of the C diagram about the mean has been considered as a measure of the amount of stagnancy. However, it is found that a system consisting of a number of ideally mixed vessels in series exhibits considerable skewness, although in the physical sense there is no stagnancy. Even recent authors (8) have indicated that skewness or the deviation from the mean is a strong indication of dead space. However Van Deemter (19) also compared the skewness of different distribution functions and concluded that it is not representative of the physical properties of the system.

The Residence Time Frequency function f(t) sometimes referred to as the Residence Time Density function (7) was mentioned in Section 1.3. It is defined as the function which gives the probability of a particle which has entered a system at time t = 0 leaving the system between times t and t + dt. Stated in another way; the

probability of a particle remaining in a system for a length of time between t and t + dt is equal to f(t)dt. Naor et al. (7) defined the Intensity Function $\Lambda(t)$ as the measure of the probability of an escape of a particle which has remained in the system for a length of time t, such that the probability of the particle leaving the system in the next time interval dt is $\Lambda(t).dt$. From Section 1.2. the probability of a particle not leaving the system before time t is I(t)dt. Therefore from the laws of probability

[Probability of remaining in the system for a length of time between t and t+dt] = [Probability of not leaving the system before time t] x [The probability of leaving the system between times t and t+dt]

$$f(t)dt = I(t)dt \times \Lambda(t)dt \qquad \ldots\ldots 1.5.4$$

$$\text{or} \quad \Lambda(t) = \frac{f(t)}{I(t)} = -\frac{d}{dt} \text{ Ln } I(t) \qquad \ldots\ldots 1.5.5$$

The function f(t) is similar to the function E(t) defined in Section 1.2. In that section the relationships between $\Lambda(t)$, E(t) and I(t) were derived. Equation 1.5.5 differs from equation 1.2.11 only in the fact that the Ln term contains $\bar{t}$. This has arisen from material balance considerations. Equation 1.5.5 was obtained from a consideration of the probabilities with respect to one particle only, without taking into consideration the volume of the tank and the overflow rate.

Naor et al. (7) showed that the relationship between f(t) and $\Lambda(t)$ is given by:-

$$f(t) = \Lambda(t).e^{-\int_o^t \Lambda(t')dt'} \qquad \ldots\ldots 1.5.6$$

From equation 1.5.4 $f(t) = \Lambda(t) \times I(t)$ 1.5.7

But $$\text{Ln } I(t) = -\int_o^t \Lambda(t')dt' \qquad \ldots\ldots 1.2.11$$

or $$I(t) = e^{-\int_o^t \Lambda(t')dt'}$$

Substituting in equation 1.5.7 gives 1.5.6.

If we regard a stagnant zone as a region for which the escape probability decreases with time, then the Intensity function may be used to indicate stagnant conditions. For a perfectly mixed vessel $\Lambda(\theta) = 1$ and for ideal plug flow a plot of $\Lambda(\theta)$ versus θ yields a vertical line at $\theta = 1$. Naor et al. (7) showed that the intensity function $\Lambda(\theta)$ does not decrease with time in the case of a number of perfectly mixed vessels in series. They also observed that a system of perfectly mixed and/or plug flow units in series does not show stagnancy. When stagnancy exists, after the main bulk of the fluid passes out of the vessel, the remaining fluid has a low probability of leaving the vessel until a time has elapsed equal to the residence time of the slow moving component. Then the $\Lambda(\theta)$ curve will no longer increase continuously but decreases at some time $t > \bar{t}$ for the system, as shown in Fig. 1.5.9.

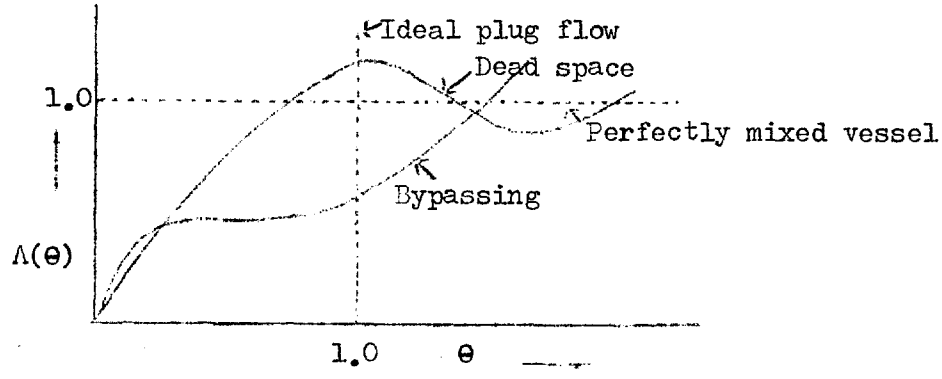

Fig. 1.5.9.

In the case of shortcircuiting or by-passing, for a time equal to the residence time of the by-passing component, the $\Lambda(\theta)$ curve increases. After this fluid has left the system, the remaining fluid will have a low probability of leaving until the mean residence time $\bar{t}$ has elapsed, when the $\Lambda(\theta)$ curve starts rising again, as shown on Fig. 1.5.9. When the deadspace and by-passing fractions are both large it is difficult to distinguish the one from the other from the $\Lambda(\theta)$ curve.

Basically the $\Lambda(\theta)$ curve does not give any further information than the $E(\theta)$ curve or the $I(\theta)$ curve. When the actual average detention time is known, the $E(\theta)$ curve can be used for quantitative determination of dead space, which the $\Lambda(\theta)$ curve cannot be used for that purpose. However it is a fairly sensitive indicator of dead space which can be applied to experimental data under different flow conditions.

Another approach to this problem of flow curve analysis has been published recently (20, 21) based on the ratios of various dimensions of the curve.

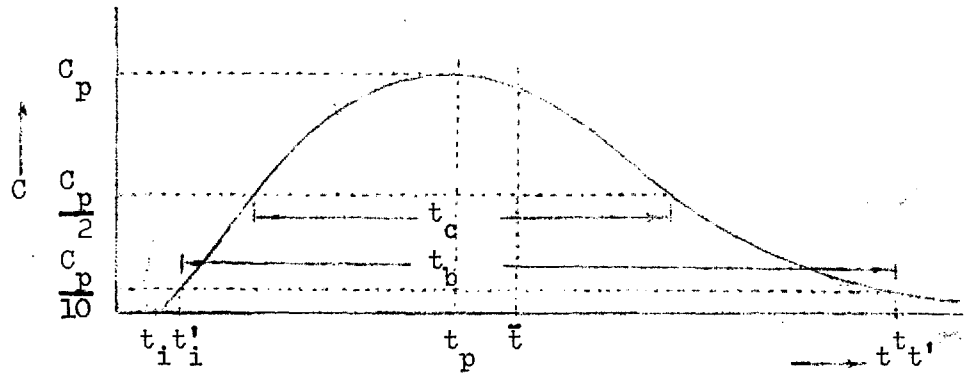

Fig. 1.5.10

$\bar{t}$ = nominal detention time = $\frac{V}{Q}$

t_p = Peak time

C_p = Peak concentration

t_c and t_b are the widths of the flow curve at $\frac{C_p}{2}$ and $\frac{C_p}{10}$ respectively.

Referring to Fig. 1.5.10 Villemonte et al. (21) proposed that :-

(i) $T_i = \frac{t_i}{\bar{t}}$ measures severe short circuiting. It has the values 1 for plug flow and 0 for perfect mixing.

(ii) $T_p = \frac{t_p}{\bar{t}}$ measures dead space and has the values 1 for plug flow and 0 for perfect mixing.

(iii) $T_c = \frac{t_c}{\bar{t}}$ measures the extent of eddy diffusion caused by turbulence and has the value $(\frac{\text{Duration of injection}}{\bar{t}})$ for plug flow and about 0.7 for perfect mixing.

(iv) $T_b = \frac{t_b}{\bar{t}}$ measures the extent of turbulent and large recirculation eddies and equals $(\frac{\text{Injection time of tracer}}{\bar{t}})$ for plug flow and 2.3 for perfect mixing.

(v) $T_e = [(t_{t'} - t_p) - (t_p - t_i)]/\bar{t}$ measures the eccentricity of the curve and thus is a function of recirculation and has the value 0 for plug flow and 2.3 for perfect mixing.

Tekkipe et al. (20) changed the term in (v) to $T_e = [(t'_t - t_p) - (t_p - t'_i)]/\bar{t}$ suggesting that it represents T_e more accurately.

It can be seen that these measures are purely qualitative and do not give any insight into the flow regimes in the system.

1.6. Combined Models (Quantitative Approach)

In this section a number of the more important attempts to analyse the flow curve quantitatively are described.

Levenspiel (9) proposed an arbitrary cut off point on the tail of the flow curve and argued that the part of the tail thus removed could be considered as representing the dead or ineffective volume of the vessel. He took this point at twice the nominal detention time. The area of the I diagram thus obtained represents the fraction of the volume which is effective and from it the dead space can be found by difference.

On the C diagram the mean can be found by computing

$$\bar{\theta} = \int_0^2 \theta . C(\theta) . d\theta \qquad \ldots\ldots 1.6.1$$

If there is no dead water $\bar{\theta} = 1$. If dead water regions are present $\bar{\theta} < 1$. If V_d is the volume of dead water and V = Volume of the system then

$$\frac{V_d}{V} = 1 - \bar{\theta} \qquad \ldots\ldots 1.6.2$$

In considering short circuiting Levenspiel assumed that it was instantaneous as shown in Fig.1.6.1(a). In such a case the I diagram shows an instantaneous drop as shown in Fig.1.6.1(b), the drop being equal to $\frac{Q_2}{Q}$ so that Q_2 can be computed. Fig.1.6.1(c) represents the C diagram for such a condition. The area of the main portion of the diagram = $\frac{Q_1}{Q}$ and the mean = $\frac{Q}{Q_1}$. From measurement of the area or the mean, the main flow can be found and hence the shortcircuiting can be determined. Levenspiel (22) gave the I and C curves for different combinations of plug flow, perfect mixing and shortcircuiting.

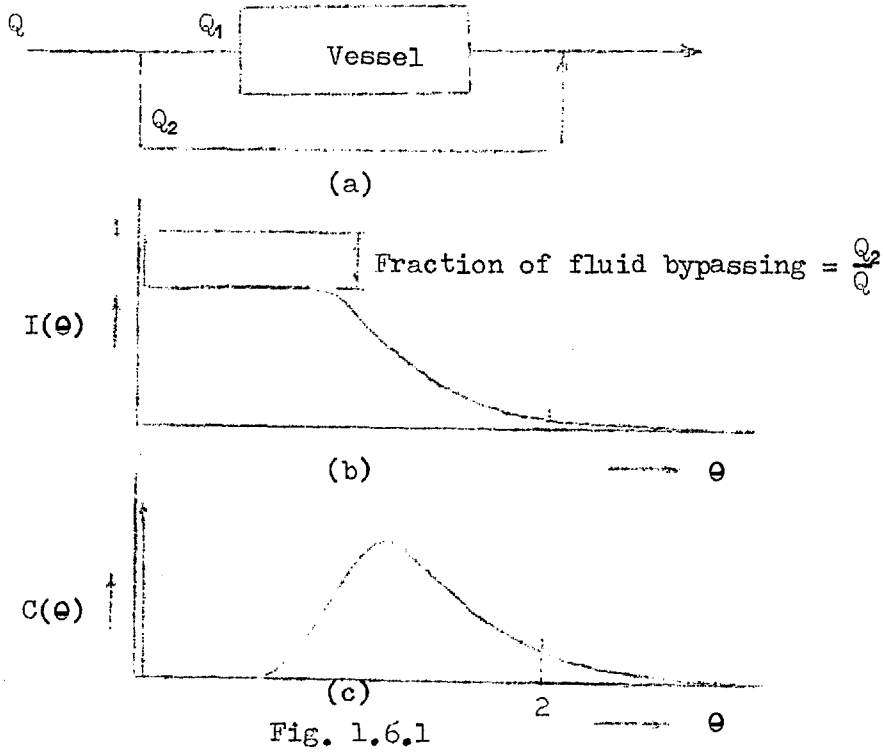

Fig. 1.6.1

Q_1 = Flow rate through the main path

Q_2 = Flow rate through the by-pass

Q = Total flow = $Q_1 + Q_2$

Although Levenspiel's (22) analysis throws new light on the formulation of mixed models, the idea of instantaneous short circuiting cannot be reconciled with reality. The determination of dead space from the I or C curve in the above manner only holds

good when the experimental data are very accurate and tracer recovery is 100%. Also although the use of the I diagram in the above manner for determining by-passing is upheld by Himmelblau et al. (8), a rough I curve or a smoothed I curve with different slopes is of no use for computing small amounts of short circuiting.

The original theoretical work of Cholette and Cloutier (11) will be illustrated by considering one of their combined models in detail. The particular model combines partial mixing and short circuiting and is illustrated in Fig.1.6.2.

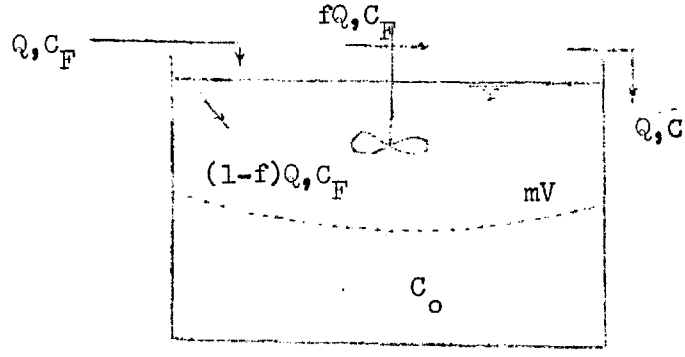

Fig. 1.6.2

A fraction m of the total volume V is assumed to be agitated (partial mixing). A fraction f is assumed to short circuit to the outlet and (1 - f) of the flow Q enters the perfect mixing zone. The initial concentration of the fluid in the vessel (which is fed continuously at the rate Q) is assumed to be uniform and equal to C_o. At a particular time t = 0, the feed composition C_F is suddenly changed from C_o to 0 (negative step change). Let the concentration in the perfect mixing zone at time t = t' be equal to c'. The material coming out of this zone mixes with the short circuiting fraction so that the combined concentration of the fluid at the outlet is C. Writing a materials balance equation for the perfect mixing zone

$$(1 - f)Q.C_F.dt = (1 - f)Q.c'.dt + mVdc'$$

or $$\frac{dc'}{dt} + \frac{(1 - f)Q}{mV} c' = 0 \qquad C_F = 0$$

Integrating between limits C_o and c'

$$\frac{c'}{C_o} = e^{\frac{-(1-f)Q}{mV}t} \qquad \ldots\ldots 1.6.3$$

Considering the outlet zone

$$f.Q.C_F.dt + (1-f)Qc'dt = Q.C.dt$$

As $C_F = 0 \quad C = (1-f)c'$

and equation 1.6.3 becomes

$$\frac{C}{C_o} = (1-f)e^{-\frac{(1-f)Q}{mV}t} \qquad \ldots\ldots 1.6.4$$

Taking logarithms on both sides

$$\text{Ln}\,\frac{C}{C_o} = \text{Ln}\,(1-f) - \frac{(1-f)Q}{mV}t \qquad \ldots\ldots 1.6.5$$

Thus plotting $\frac{C}{C_o}$ against $\frac{t}{\bar{t}}$ on semi log paper which gives a straight line, (1-f) can be obtained as the intereept on the ordinate and the slope gives $\frac{(1-f)}{m}$ from which "m" the mixing fraction of the volume can be obtained.

Note that the fraction (1-m)V in the above model is considered as completely dead, so that the concentration of the fluid remains at C_o throughout.

In a similar manner Cholette et al. (11) obtained $\frac{C}{C_o}$ functions for a number of other models.

(i) Plug flow and partial mixing in series

$$\frac{C}{C_o} = e^{\frac{1}{m}\left(\frac{t}{\bar{t}} - (1-m)\right)} \qquad \ldots\ldots 1.6.6$$

where m = the perfect mixing fraction

(1-m)= the plug flow fraction

$\bar{t} = V/Q$

(ii) Partial mixing and piston flow in parallel with a short circuit from inlet to outlet as illustrated in Fig.1.6.3.

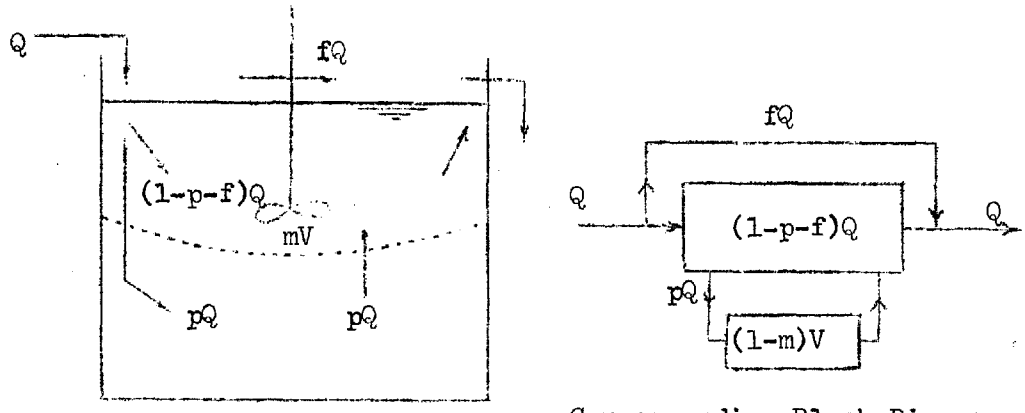

Corresponding Block Diagram

Fig. 1.6.3

$$\frac{C}{C_o} = [(1-f-p) + pe^{(1-f)(1-m)/mp}]e^{-\frac{(1-f)t}{m\bar{t}}} \qquad \ldots\ldots 1.6.7$$

where p = Fraction of the feed into the plug flow zone

m = Perfect mixing fraction

(1-m)= Plug flow fraction

f = Fraction of feed short circuiting

(1-p-f)= Fraction of feed going into the perfect mixing zone.

Equation 1.6.7 holds for $t > \frac{(1-m)\bar{t}}{p}$

For $0<t<\frac{(1-m)\bar{t}}{p}$ $C/C_o = p + (1-f-p)e^{-\frac{(1-f)t}{\bar{t}m}}$ $\ldots\ldots\ldots 1.6.8$

(iii) Plug flow and perfect mixing in parallel with a short circuit as shown in the block diagram. Fig. 1.6.4.

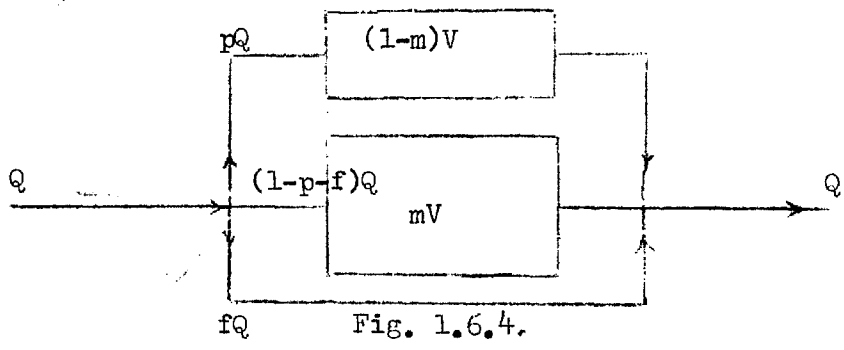

Fig. 1.6.4.

$$C/C_o = p + (1-p-f)e^{\frac{-(1-p-f)t}{\bar{t}m}} \quad \text{..... 1.6.9}$$

for $0 < t < \frac{(1-m)\bar{t}}{p}$

$$C/C_o = (1-p-f)e^{\frac{-(1-p-f)t}{\bar{t}m}} \quad \text{..... 1.6.10}$$

for $t > (1-m)\bar{t}/p$

Cholette et al. (11) produced these models with a view to determining the m fraction, or effective volume of mixing in partially mixed reactors and later (23) incorporated reaction rates into their equations for reactor design but again on a theoretical basis only. No method of fitting experimental data to these equations was reported.

Wolf and Resnick (12) made use of transfer functions (which will be discussed fully in Chapter 2) in the derivation of F(t) functions for a number of combined models. Their F(t) functions are the response curves to a unit step function input. One such model is shown in Fig.1.6.5 where plug flow, perfect mixing, and a measurement lag are combined in series, while a fraction short circuits the perfect mixing zone. The short circuit is again instantaneous.

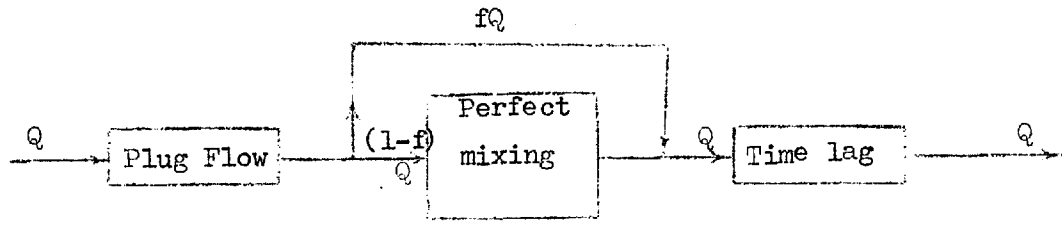

Fig. 1.6.5

The F(t) function for this model is:-

$$F(t) = 1 - \text{Exp.}\left[-\frac{(1-f)}{ar(1-d)\bar{t}} * \left\{t - L - \frac{p(1-d)r\bar{t}}{(1-f)} + mar(1-d)\bar{t}\right\}\right. \quad \text{.....1.6.11}$$

for $F(t) \geq 0$

where f = Fraction of the feed short circuiting

$r\bar{t}$ = True residence time

$\bar{t} = V/Q$

d = Fraction of the volume considered to be dead

p = Plug flow fraction

a = Perfect mixing fraction

L = Lag in measurement

m = Lag factor.

They concluded that the F(t) function for any system can be represented in the general form

$$F(t) = 1 - e^{-\eta(t-\epsilon)/\bar{t}} \quad \text{for } F(t) \geq 0$$

$$\text{and } F(t) = 0 \quad \text{for } 0 < t < \epsilon \qquad \text{..... 1.6.12}$$

For the combined model above

$$\eta = \frac{(1-f)}{ar(1-d)}. \qquad \text{..... 1.6.13}$$

$$\epsilon = [L + \frac{p(1-d)r\bar{t}}{(1-f)} - mar(1-d)\bar{t}] \qquad \text{..... 1.6.14}$$

They concluded that η was a measure of the efficiency of mixing. For perfect mixing $\eta = 1$ and for pure plug flow $\eta \rightarrow \infty$. When dead space is present $\eta > 1$ and for shortcircuiting $\eta < 1$. Thus η is a measure of deviation from perfect mixing. ϵ is a measure of the time lag in the system. It may be the result of plug flow in the system or a lag in measurement. For shortcircuiting as defined by Wolf and Resnick ϵ is negative. The authors did not explain or refer to the method by which they obtained the transfer functions or the technique by which they are combined algebraically. The idea of obtaining a negative ϵ due to an "anticipatory response" cannot be accepted. Their method of obtaining the parameters was entirely graphical, and the errors in so doing are reflected in obtaining 100%

plug flow for turbulent oil in a pipe, and 100% perfect mixing in gas fluidized beds.

Rebhun and Argaman (4) applied Wolf and Resnick's (12) technique to a model sedimentation tank in order to determine the proportions of the different flow regimes present. They assumed that the tank contained a combination of perfect mixing, plug flow and dead space. The formula they derived for F(t) is as follows.

$$F(t) = 1 - \text{Exp}\left[-\frac{1}{(1-p)(1-m)}\left\{\frac{t}{\bar{t}} - p(1-m)\right\}\right] \qquad \ldots\ldots 1.6.15$$

where m = the dead space fraction

$1-m$ = the effective fraction of the tank volume

p = the plug flow fraction

$1-p$ = the perfect mixing fraction

$\bar{t}$ = Average detention time

$$\text{or } F(t) = 1 - e^{-\eta(t-\epsilon)/\bar{t}} \qquad \ldots\ldots 1.6.16$$

where

$$\eta = \frac{1}{(1-p)(1-m)}$$

$$\epsilon = p(1-m)t$$

Re-arranging equation 1.6.15 and taking natural logs

$$\text{Ln}\,[1 - F(t)] = -\frac{1}{(1-p)(1-m)}\left\{\frac{t}{\bar{t}} - p(1-m)\right\} \qquad \ldots\ldots 1.6.17$$

A plot of $[1 - F(t)]$ versus $\frac{t}{\bar{t}}$ on semi log paper gives a straight line of slope $(\log e)/(1-m)(1-p)$.

If $F(t) = 0$ then $p(1-m) = \frac{t}{\bar{t}}$

Therefore given the slope of the straight line and the value of $t/\bar{t}$ for $[1 - F(t)] = 1$, the values of m and p can be computed.

The experiments were conducted on a model tank, with varying flow rate, depth and inlet arrangements and the results obtained by the method were correlated with the statistical parameters of the

distribution curves. The conclusions put forward by Rebhun and Argaman were that in most sedimentation basins 60% of the total volume was occupied by perfect mixing and that only 40% of the volume was occupied by the plug flow of the classical settling tank theory.

This work was strongly criticised by Wallace (24) who insisted that perfect mixing in a sedimentation tank was unrealistic, and that the fraction (1-p) should be regarded as a deviation from plug flow rather than perfect mixing. However no indication was given as to the form which this deviation might take. In analysing some of the experimental results Rebhun et al. (4) obtained some negative dead space fractions which they disregarded and attributed to experimental error.

A more constructive contribution to this discussion was that of El-Baroudi (25), who considers that plug flow is non-existent in sedimentation tanks, and estimates that such basins consist of approximately 10% complete mixing and 90% measurable turbulent mixing. Again these estimates are not backed up by any experimental verification. However turbulent shear flow approximates more closely to ideal piston flow (because of its velocity profile) than any other real flow except that of flow through porous media. El Baroudi also pointed out that ideal dead space does not exist in real systems and that in the above experiments the negative values of dead space obtained corresponded to values of $^{t}a/_{\bar{t}}$ greater than 1. El Baroudi (25) again suggested that the response function resulting from an impulse input is more amenable to graphical solution. Accordingly differentiating equation 1.6.17 we obtain

$$f(\frac{t}{\bar{t}}) = \frac{d^{F(\frac{t}{\bar{t}})}}{d(\frac{t}{\bar{t}})} = \frac{1}{(1-p)(1-m)} \text{Exp}\left[-\frac{1}{(1-p)(1-m)}\left\{\frac{t}{\bar{t}} - p(1-m)\right\}\right] \quad \ldots\ldots \quad 1.6.18$$

Thus on semilog paper a plot of $f(\frac{t}{\bar{t}})$ versus $\frac{t}{\bar{t}}$ yields a straight line with slope $-\frac{\log_e}{(1-p)(1-m)}$. The advantage of this method is that the

values of $\frac{C}{C_o}$ can be directly plotted without the need to determine the fractions $F(\theta)$. Here El Baroudi (25) proposed two approximations :-

(i) The rising limb of the plot is converted to a vertical straight line at a point midway between θ_i and θ_m as shown in Fig.1.6.6.

(ii) The falling limb is considered to be a straight line, thus representing equation 1.6.18 for $\theta \geq p(1-m)$. Thus the real curve is transformed into a right angled triangle ABC in which

$AB = \frac{1}{(1-p)(1-m)}$ and θ at $B = p(1-m)$. From these two dimensions p and m can be computed.

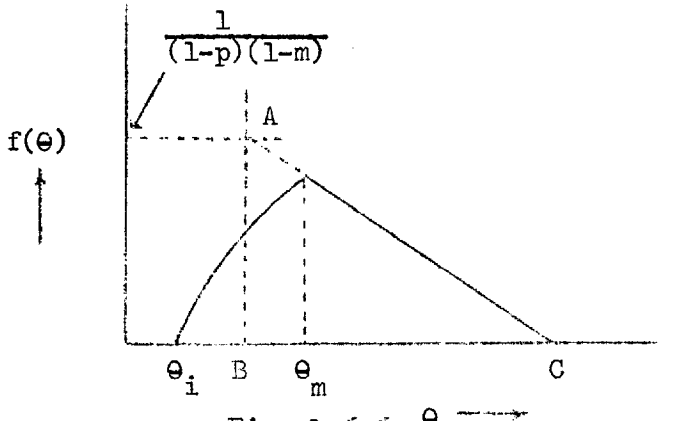

Fig. 1.6.6

El-Baroudi (25) showed that by applying this method to Rebhun et al. data, the negative dead spaces found by them could be eliminated in favour of increased values for the plug flow fractions.

He pointed out that the vertical straight line approximation to the rising limb of the curve is satisfactory when there is a relatively small amount of longitudinal mixing. For a broad rising limb, which he attributed to high longitudinal mixing he advocates Rebhun's et al's (4) original method with the modification that only the points on the falling limb or tail of the curve are used when determining the line of best fit, thus ignoring the rising limb. However as will be shown later, the rising limb of the curve is just as important as the tail and should not be ignored or approximated by a vertical straight line. Its shape

is a function, not only of longitudinal mixing, but also of short-circuiting and recirculation. Also the breadth of the curve ($\theta_i \rightarrow \theta_m$ Fig.1.6.6) will be shown to be directly proportional to the injection time of the tracer.

The use of convolution for the determination of the response of a system to any type of input is recommended by many authors (8)(17). However this can only be done when the response of the system to an impulse is known (8). An interesting account of the way in which convolution integrals may be used to determine the residence time probability density function f(t) (defined as in Levenspiel (22)) of a complex flow system is given by Sinclair and McNaughton (17). This method is described in the following paragraphs.

The rules for the addition and multiplication of continuous probability functions (26) are used. They are as follows :-

Given two continuous random variables Z_1 and Z_2 with probability density functions $f_1(j)$ and $f_2(j)$ respectively, (i.e. the probability that $j < Z_1 < j + dj = f_1(j).dj$, then, the probability density function of the variable Z is given by

$$f(j) = \int_{-\infty}^{+\infty} f_1(a).f_2(j-a)da \qquad \ldots\ldots 1.6.19$$

when $Z = Z_1 + Z_2$

and when $Z = Z_1$ or Z_2

$$f(j) = Kf_1(j) + (1-K)f_2(j) \qquad \ldots\ldots 1.6.20$$

where K is the probability that $Z = Z_1$ and (1-K) is the probability that $Z = Z_2$. The integral in equation 1.6.19 is called the Convolution integral, Falting integral, or a form of Duhamel's integral. Equation 1.6.19 is written for convenience in the following notation

$$f = f_1 * f_2 \qquad \ldots\ldots 1.6.21$$

and Eqn.1.6.20 $f = Kf_1 + (1-K)f_2$ $\ldots\ldots 1.6.22$

These rules are used in the case of two subsystems of R.T.P. (Residence Time Probability) $f_1(t)$ and $f_2(t)$ as follows. If the two subsystems are in series then the R.T.P. of the whole system :-

$$f(t) = f_1 * f_2 = \int_0^t f_1(a).f_2(t-a)da \qquad \ldots\ldots 1.6.23$$

When the two subsystems are in parallel :-

$$f(t) = Kf_1 + (1-K)f_2 \qquad \ldots\ldots 1.6.24$$

This is because a particle passing through the system has the probability of passing through either of the two subsystems, K being the probability of its passing through the first.

These two basic combinations are used in any system with a number of independent subsystems occurring in series, parallel or combination. An important contribution of Sinclair and McNaughton (17) is the equation for a system with recirculation. The block diagram of this case is shown in Fig.1.6.7 together with an analytical diagram which shows how the contributions are made to the point B by the successive recirculation fractions.

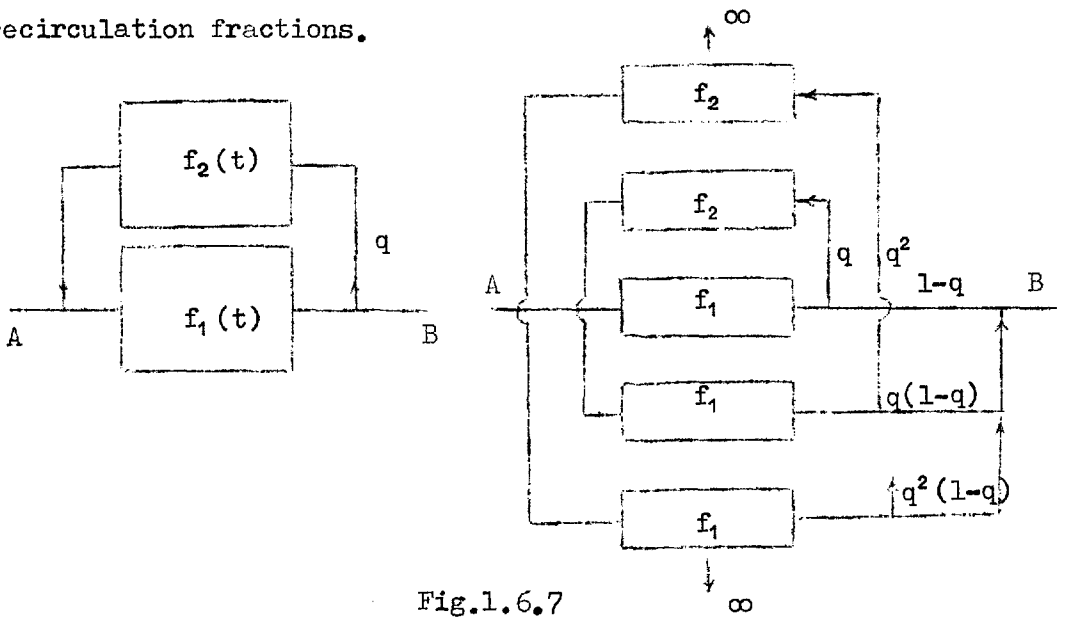

Fig.1.6.7

q = the fraction of the total flow entering at A which is recirculated as shown. A part of the flow of materials that enters the system at A makes 1,2,3,... n..... passes through the forward path with R.T.P. $f_1(t)$

and 0,1,2,3 ... (n-1) ... ∞ passes through the recycle path with R.T.P. $f_2(t)$. For unit quantity of material entering at the point A, a part (1-q) goes to the point B after the first pass. The fraction q is recycled of which q(1-q) reaches the point B after the 2nd pass etc. Then the R.T.P. for the overall system is the summation of the R.T.P.'s for each of the infinite number of fractions. The amount subscribed to the point B :-

From the 1st pass = $(1-q)f_1$

From the 2nd pass = $q(1-q)f_1 * f_2 * f_1$

From the 3rd pass = $q^2(1-q)f_1 * (f_2 * f_1) * (f_2 * f_1)$

From the nth pass = $q^{n-1}(1-a)f_1 * (f_2 * f_1) * (f_2 * f_1) * (f_2 * f_1) \ldots .(n-1)$ times

$\therefore$ the R.T.P. for the whole system f_{A-B}

$$f_{A-B} = (1-q)f_1 + q(1-q)f_1 * (f_2 * f_1) + q^2(1-q)f_1 * (f_2 * f_1) * (f_2 * f_1) + \ldots$$

Using the notation $f^{n*} = f*f*f* \ldots$ n times

$$f_{AB} = (1-q) \sum_{n=o}^{\infty} q^n f_1 * (f_1 * f_2)^{n*} \qquad \ldots\ldots 1.6.25$$

It need not be pointed out that equation 1.6.25 can only be solved on a computer and that it takes a considerable amount of time to solve the convolution integrals, even if, as suggested by Sinclair et al. (17), one of the two paths is considered to have zero residence time. Furthermore the characteristics of each subsystem that contribute to $f_1(t)$, $f_2(t)$ etc must be known in order to determine f(t) for the system. Once f(t) is known the response to any input can be determined by the convolution

$$C_o(t) = \int_o^t C_i(a).\ f(t-a)da \qquad \ldots\ldots 1.6.26$$

or

$$C_o(t) = \int_o^t C_i(t-a)\ f(t)da \qquad \ldots\ldots 1.6.27$$

Equation 1.6.27 can be obtained from material balance consideration as follows :-

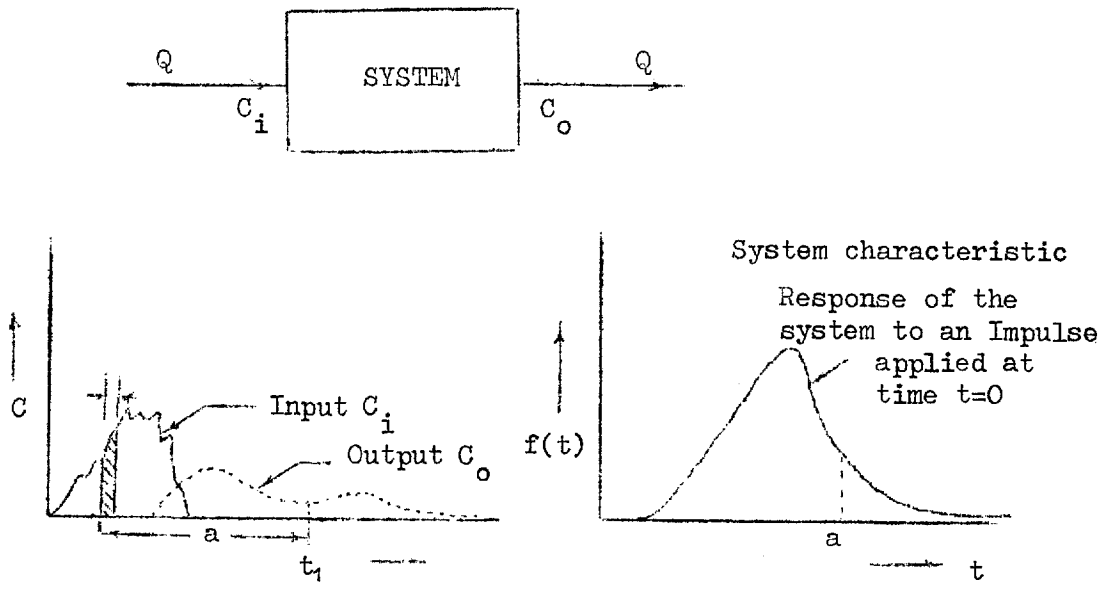

Fig.1.6.8

Suppose an arbitrary input $C_i(t)$ is fed into the system which produces a response $C_o(t)$. The steady volumetric flow rate is equal to Q. The form of the output signal will depend on the form of the input signal and the characteristics of the system.

At a time t_1, the mass rate of the tracer leaving the system is $Q.C_o(t_1)$. Some of the tracer at the outlet entered the system at a time interval a before t_1, when the rate of tracer entering the system was $QC_i(t_1-a)$. The fraction of this inlet mass contributing to the exit mass rate after a time interval a is therefore:-

$$QC_i(t_1-a).\ f(a)da.$$

This can be viewed in another way. The input can be considered to be made up of a number of impulses of width Δa. Then the quantity of **tracer** put into the system in a time interval Δa after time (t_1-a) is equal to $QC_i(t_1-a)\Delta a$. Now suppose that the response characteristic to a unit impulse of this particular system after a time a is equal to f(a). Therefore it follows that the output concentration due to this particular impulse (of width Δa) is equal to $Q.C_i(t_1-a).\Delta a.f(a)$, assuming linearity. Now considering all the elementary impulses summed to produce the input pulse, then the output concentration $C_o(t_1)$ is given by the summation

$$C_o(t_1) = \sum_{a=o}^{t_1} QC_i(t_1-a).f(a).\Delta a$$

$$\text{As } \Delta a \rightarrow 0 \quad C_o(t_1) = Q \int_o^{t_1} C_i(t_1-a).f(a).da$$

$$\text{For } Q = 1 \quad C_o(t_1) = \int_o^{t_1} C_i(t_1-a).f(a).da \qquad \ldots\ldots 1.6.28$$

Equation 1.6.28 is similar to equations 1.6.27 and 1.6.19. Thus knowing any two of the three functions $C_i(t)$, $C_o(t)$ and $f(t)$, the 3rd can be determined. Generally $C_i(t)$ and $C_o(t)$ are known and $f(t)$ is determined. In some cases $C_o(t)$ can be predicted for any input when the system characteristics are known.

1.7 Summary and purpose of present study

From the above review and discussion it is clear that theories and methods do exist on the interpretation of flow curves and on the description of flow systems in terms of combinations of idealised flow regimes. However they are in general lacking in a number of respects.

Most of the theoretical equations are concerned with the system response to an ideal impulse input, or a unit step input. No information appears to exist on the response equations of systems to thick pulses. In a practical case, when the residence time in a system is short, or when it is not desirable to force a quantity of tracer into the system inlet in a short time, thus causing an undesirable disturbance to the flow, a thick pulse is a better alternative.

The graphical methods of solution which are generally used suffer from the serious drawback that they tend to ignore the points contributed by the frontal interface of the output pulse as is evident in the case of Rebhun and Argaman (4).

The delay time implicit in any practical case of short activity, which causes a considerable amount of mathematical complexity is generally omitted on this account.

Few of the theories advanced by authors are supported by actual experimental work. Convolutions and transfer functions are readily derived but their practical use is limited because of the shortage of appropriate computer programmes.

The objects of this study are to formulate response equations corresponding to thick pulses and thus establish a technique for the determination of the different flow regimes, which add up to a flow system characteristic, on a quantitative basis. Particular attention is paid to such considerations as recirculation and shortcircuiting with delay time, as these are of particular interest to designers of large flow systems containing density gradients. A number of workable computer programmes are presented and the theory is supported by experimental data.

CHAPTER II

THEORY PART A

2.1. Analysis of flow systems

The analysis considered relates to a "flow through system". The word "flow" implies a continuous flow of any fluid through the system.

Dooge[27] defined a "system" as a structure, a device, or a procedure, real or abstract, that interrelates with reference to time an input with its corresponding output. The input or stimulus may be in the form of energy, matter or information. Schematically the situation is as shown in Fig.2.1.1.

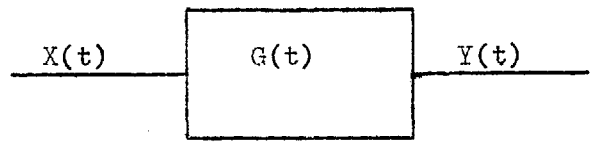

Fig.2.1.1

where X(t) = Input as a function of time

G(t) = System characteristics

Y(t) = Output as a function of time.

The relationship between Y(t) and X(t) depends on G(t) and may be linear or nonlinear. The reaction of the system to an input depends on the state of the system. This "state" may be known from past history or known features or may be a subject for determination. A system may be time dependent or time invariant depending on whether the response is related to the time of input or not.

Three different problems may arise and are shown in tabular form below.

		Type of Problem	Input	System	Output
Analysis	(1)	Prediction	Known	Known	To be determined or predicted
	(2)	Identification	Known	To be determined	Known
	(3)	Identification	Unknown	Known	Known

The present analysis is concerned wholly with problems of the second type.

A basic assumption in the deduction of the following theory is that the system concerned is linear. Linearity means that the system has the property of superposition, expressed mathematically as follows.

If $X_1(t) \longrightarrow Y_1(t)$, then for a linear system

$aX_1(t) \longrightarrow aY_1(t)$ where "a" is a constant of proportionality.

Also $aX_1(t) + bX_2(t) \longrightarrow aY_1(t) + bY_2(t)$

If the input X(t) is the synthesis of a number of simultaneous inputs $X_1(t)$, $X_2(t)$ ...., $X_{n'}(t)$ or

$$X(t) = \sum_{n=1}^{n'} C_n X_n(t)$$ where "C" is a constant of proportionality,

then from the principles of superposition

$$Y(t) = \sum_{n=1}^{n'} C_n Y_n(t)$$

The following additional assumptions are also made.

(i) The system is assumed to be a combination of independent flow zones.

(ii) The zones are interconnected in such a way that no flow changes its course from its designated forward path.

(iii) The properties of the flowing fluid do not change with time and distance. In other words their is no reaction taking place in the reactor.

2.2 Transfer functions and Block Diagrams

Bearing in mind the above assumptions the system under consideration can be compared with a servomechanism in the broader field of Automatic Control Systems, and the theory of such systems may be applied in this case.

The input and output shown in Fig.2.1.1 can be related algebraically to the system characteristic G(t) in the form of a transfer function. The latter is defined as the ratio between the Laplace transform of the output and the Laplace transform of the input.

Let

$$LY(t) = Y(S)$$

$$LX(t) = X(S)$$

$$LG(t) = G(S)$$

where L stands for Laplace Transform of and "S" is the Laplace "S".

$$\text{Then } G(S) = \frac{Y(S)}{X(S)} \qquad \ldots\ldots 2.2.1$$

$$\text{or} \quad Y(S) = G(S).X(S) \qquad \ldots\ldots 2.2.2$$

Inverting Y(S) to time domain

$$Y(t) = L^{-1}\{G(S).X(S)\} \qquad \ldots\ldots 2.2.3$$

Therefore, knowing the input function X(t) and formulating the Transfer function G(S) with assumed Transfer Elements, Y(t) can be predicted. Conversely, the assumed transfer elements can be corrected by comparing the predicted values of Y(t) with the known values of Y(t). A Transfer Element is an element with a defined Transfer Function which possesses the characteristic of unilateral transfer of signals. An element which consists of several transfer elements connected one after the other is also a transfer element[28].

The next important step is the construction of Block Diagrams. A block diagram is not a circuit diagram as in electrical engineering.

It indicates only the signal transfer, whereas a circuit diagram represents also the state of energy transfer. The three elements necessary to construct a block diagram are

(i) a transfer element to indicate received signals and their transformation into other signals,

(ii) a summing point to produce the algebraic sum of two signals, and

(iii) a pick off point to separate a signal into two paths.

The elements (ii) and (iii) are only necessary when there is more than one signal. The transfer element is indicated by a block in which the transfer function of the element is usually written. The components of a block diagram are shown in Fig.2.2.1.

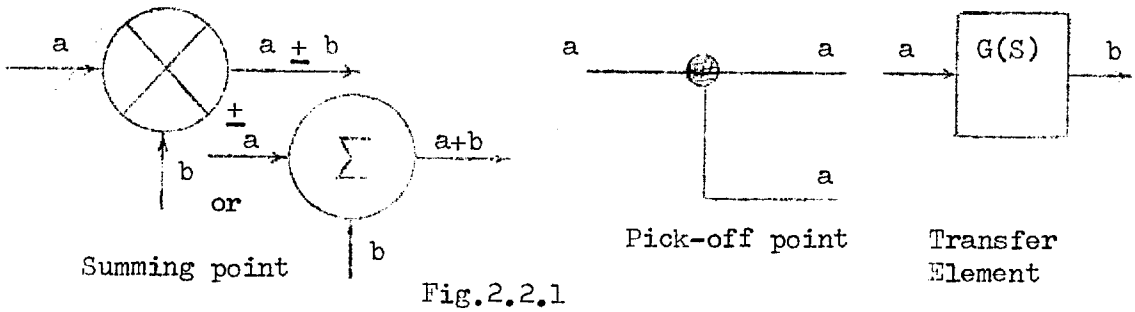

Fig.2.2.1

A system with a number of transfer elements arranged in different combinations is difficult to analyse by ordinary means. The Equivalent Transformation technique of assimilating the transfer elements into one Block Diagram makes the analysis very much easier. The following algebraic rules should be observed :

(i) The product of the transfer functions in the forward path (the signal path from input to output) is invariant, i.e. cannot be altered or replaced.

(ii) The product of the transfer functions in each loop is invariant.

(iii) Two neighbouring summing (or pick up) points can be interchanged.

(iv) A summing point cannot be interchanged for a pick off point and vice versa.

Using these rules, any combination of transfer elements can be transformed into one block diagram. Three of the most useful combinations and transformations that will be used in the construction of models are given below:

(i) Series Connection:

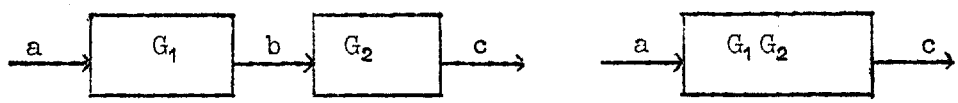

Before transformation After transformation

Fig.2.2.2

Referring to Fig.2.2.2, two transfer elements with transfer functions G_1 and G_2 are connected in series; where "a" is the input signal, "b" is the output from G_1 and "c" is the output from the whole system. Then from the properties of transfer functions (see equation 2.2.2)

$$b = aG_1$$

As b is the input to element G_2

$$c = bG_2$$

Substituting the value of b

$$c = aG_1G_2$$

Thus, the transfer function of the system is $G_1 \times G_2$ and the equivalent transformation block diagram is shown in Fig.2.2.2. In general if there are n transfer elements $n = 1, 2, \ldots \infty$, with transfer functions $G_1, G_2, \ldots G_n$ in series then the equivalent transfer function of the system is

$$G = \prod_{n=1}^{\infty} G_n \qquad \ldots\ldots 2.2.4$$

(ii) Parallel Connection:

When the two elements G_1 and G_2 are combined in parallel as shown in Fig.2.2.3 and "a" is the input and "d" is the output signal of the system, the equivalent transfer function is obtained as follows:

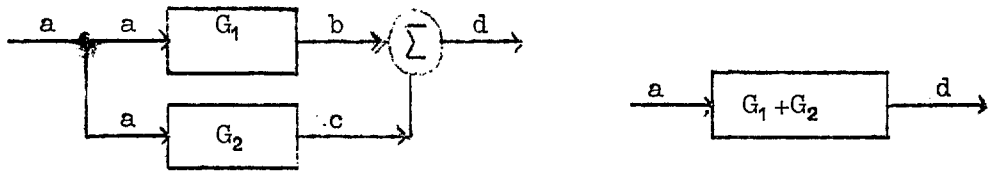

Before Transformation After Transformation

Fig.2.2.3

Let b = the output signal from the element G_1

and c = the output signal from the element G_2

Then $b = a.G_1$

$c = a.G_2$

Since $d = b + c$

by substitution $d = a(G_1 + G_2)$

Thus if a system contains $n = 1,2,3,\ldots\infty$ transfer elements in parallel, with transfer functions $G_1, G_2, \ldots G_n$, then the equivalent transfer function of the system

$$G = \sum_{n=1}^{\infty} G_n \qquad \ldots\ldots 2.2.5$$

(iii) Feed back system:

"Feed back" is a most important aspect of Automatic Control. The problem considered here is the case of a positive feed back in which the signal from the feed back element is added to the primary input so that the input to the main element is an addition, rather than a difference which is so often the case with automatic regulator.

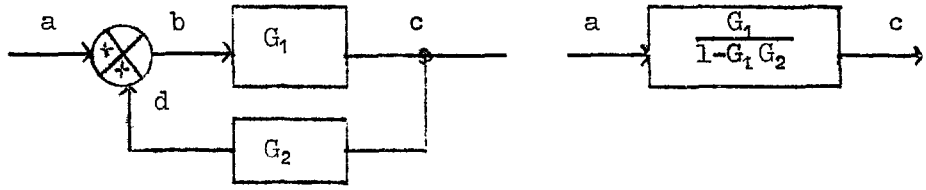

Before Transformation After Transformation

Fig.2.2.4

The transfer elements are arranged as shown in Fig.2.2.4.

Let a = The input signal into the system

c = The output signal of the system

b = Input into the element G_1

d = Output of the element G_2

Then,

$$b = a + d$$

$$c = bG_1$$

But c acts as an input in G_2

$$\therefore d = c.G_2 = bG_1 G_2$$

$$\therefore b = a + bG_1 G_2$$

$$\text{or } b(1-G_1 G_2) = a$$

$$\text{or } b = \frac{a}{1-G_1 G_2}$$

on substitution $$c = \frac{aG_1}{1-G_1 G_2}$$

Therefore the equivalent transfer function of the system is equal to

$$\frac{G_1}{1-G_1 G_2} \qquad \ldots\ldots 2.2.6$$

If the summing point in Fig.2.2.4 were an error sensing device, such that b = a-d, the equivalent transfer function in that case would be $\frac{G_1}{1+G_1 G_2}$. It is necessary that the system be a closed loop in order to obtain the above formula.

2.3 Transfer functions for perfect mixing and plug flow

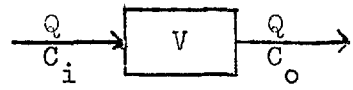

Fig.2.3.1

Let the element be perfectly mixed, of volume V with flow rate Q. If a tracer input of concentration C_i be introduced into the element at a time t = 0, and if $C_o(t)$ is the concentration of the tracer at the output end of the element at any time t, then from materials balance considerations :

Amount of tracer entering at the instant of time t	=	Amount going out of the element at the instant t	+	Amount accumulated within the element

or

$$Q.C_i(t) = Q.C_o(t) + V\frac{dC_o(t)}{dt}$$

or

$$C_i(t) = C_o(t) + \frac{V}{Q}.\frac{dC_o(t)}{dt}$$

Taking the Laplace Transform of both sides

$$C_i(S) = C_o(S) + \frac{V}{Q}.S.C_o(S)$$

and assuming that $C_o(t) = 0$ at $t = 0$

$$C_o(S)(1 + \frac{V}{Q}S) = C_i(S)$$

or

$$\frac{C_o(S)}{C_i(S)} = \frac{1}{1+\frac{V}{Q}.S} \qquad \ldots\ldots 2.3.1$$

Therefore by definition the transfer function $G(S) = \frac{1}{1+\frac{V}{Q}.S}$

Let $\frac{V}{Q} = T$ Then $G(S) = \frac{1}{1+TS}$ 2.3.2

Equation 2.3.2 is analogous to that of a 1st order system in control theory. The term T is known as the Time Constant of the

system which, in this case, is the nominal detention time. Ceaglske[28] stresses the importance of this time constant and points out that it is the only factor that determines the position of the transient response curves of 1st order systems. The time constant in general is a combination of several physical properties of the system, or in other words no single physical property is responsible for the type of response obtained. If the properties of the systems are known, the Time Constant can be calculated and the response curves drawn.

As plug flow is equivalent to a time lag, the transfer function for a plug flow element is simply a translation function. If Q is the inflow rate into a plug flow element of volume V, then the lag time is $\frac{V}{Q} = T$ and the corresponding transfer function of the element is

$$\frac{C_o(S)}{C_i(S)} = e^{-TS} \qquad \ldots\ldots 2.3.3$$

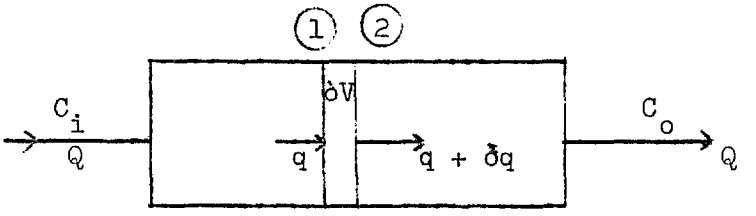

Fig.2.3.2

Consider a plug flow element of volume V. At any time t a thin block of material of volume δV between the planes (1) and (2) is assumed to be homogeneous and of the same concentration as that of the fluid entering at the plane face (1). Assume that the concentration of the ingoing tracer at the plane (1) is q and that the concentration at the plane (2) is $(q + \delta q)$. This change in concentration δq is purely imaginary and may be positive or negative. Then for a flow rate Q a mass balance for the block between planes (1) and (2) yields :

$$q(t) \times Q = (q(t) + \delta q(t) \times Q + \delta V \frac{dq(t)}{dt}$$

or $$\delta q(t) = - \frac{\delta V}{Q} \cdot \frac{dq(t)}{dt}$$

Taking the Laplace Transform of both sides

$$\delta q(S) = -\frac{\delta V}{Q} \; S \; q(S) \text{ , assuming } q(t) = 0 \text{ at } t = 0$$

or $$\frac{\delta q(S)}{q(S)} = - \frac{\delta V}{Q} \cdot S \qquad \ldots\ldots 2.3.4$$

As the plug flow element is made up of an infinite number of such blocks, equation 2.3.4 can be written for the whole element as:

$$\sum_{n=1}^{\infty} \frac{\delta q(S)}{q_n(S)} = - \frac{V}{Q} S \qquad \ldots\ldots 2.3.5$$

In the limiting case when $\delta q \longrightarrow 0$, equation 2.3.5 becomes

$$\int_{C_i(S)}^{C_o(S)} \frac{dq(S)}{q(S)} = - \frac{V}{Q} \cdot S$$

or $$\text{Ln} \frac{C_o(S)}{C_i(S)} = - \frac{V}{Q} \cdot S = - TS$$

or $$\frac{C_o(S)}{C_i(S)} = e^{-TS}$$ which is the derivation of equation 2.3.3.

Consider a system composed of two elements in series as shown in the block diagram Fig.2.3.3. The first element is a perfect mixing element of time constant K_1 and the second element is a plug flow element of lag constant K_2.

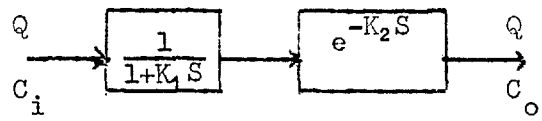

Fig.2.3.3

If the total volume of the system is V and the flow rate is Q, then let m be the fraction of the total volume occupied by the perfect mixing block and let p be the fraction occupied by the

plug flow block, so that m + p = 1. Therefore in equation 2.3.2 $T = \frac{mV}{Q} = mT$, where $T = \frac{V}{Q}$ the nominal detention time of the system. Let $K_1 = mT$ representing the time constant of the perfect mixing element. Similarly T in equation 2.3.3 $= \frac{pV}{Q} = pT = K_2$ for the plug flow element.

Then the equivalent transfer function of the system from equation 2.2.4 is

$$G(S) = \frac{e^{-K_2 S}}{1+K_1 S} \qquad \ldots\ldots 2.3.6$$

or $$\frac{C_o(S)}{C_i(S)} = \frac{e^{-K_2 S}}{1 + K_1 S}$$

or $$C_o(S) = C_i(S) \frac{e^{-K_2 S}}{1 + K_1 S} \qquad \ldots\ldots 2.3.7$$

$$\therefore C_o(t) = L^{-1}\left\{C_i(S) . \frac{e^{-K_2 S}}{(1+K_1 S)}\right\} \qquad \ldots\ldots 2.3.8$$

Thus the parameters that control the output function $C_o(t)$ are K_1 and K_2. Depending on the form of the input function $C_i(t)$ equation 2.3.8 may be used to give the direct solution of a two parameter model.

2.4. Solution of two parameter model using a thick input pulse

By a thick input pulse is meant a pulse of rectangular shape. This has all the properties of a Gate Function, a brief description of which is given below

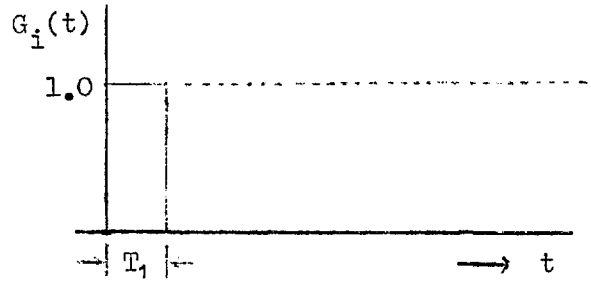

Fig.2.4.1

A rectangular pulse as shown in Fig.2.4.1 is called a Gate Function and may be regarded as the difference of two unit step functions given by

$$G_i(t) = U(t) - U(t-T_1) \qquad \ldots\ldots 2.4.1$$

where T_1 is the pulse width.

An interesting property of the Gate Function is that if any function which has non-zero values in the duration of the gate is multiplied by the gate function, the value of that function within the gate is unaffected[29]. This property can be used to invert the Laplace Transform of complex input functions.

However the gate function only is used in this study because of its simplicity of application both in analysis and experimentation compared with the unit step function, or the impulse function, or more complex functions.

$\therefore C_i(t) = U(t) - U(t-T_1)$ is used in the two parameter model. Taking Laplace Transforms

$$C_i(S) = \frac{1}{S} - \frac{e^{-ST_1}}{S} \qquad \ldots\ldots 2.4.2$$

Putting this value of $C_i(S)$ in equation 2.3.8 gives

$$C_o(t) = L^{-1}\left\{\left(\frac{1}{S} - \frac{e^{-ST_1}}{S}\right) \times e^{-K_2S}/(1+K_1S)\right\} \qquad \ldots\ldots 2.4.3$$

The right hand side of equation 2.3.11 is simplified and transformed as follows :

$$L^{-1}\left\{\frac{e^{-K_2S}}{S(1+K_1S)} - \frac{e^{-S(T_1+K_2)}}{S(1+K_1S)}\right\}$$

$$= L^{-1}\frac{e^{-K_2S}}{S(1+K_1S)} - L^{-1}\frac{e^{-S(T_1+K_2)}}{S(1+K_1S)}$$

$$\therefore C_o(t) = (1-e^{-(t-K_2)/K_1}) * U(t-K_2) - (1-e^{-(t-T_1-K_2)/K_1}) * U(t-T_1-K_2)$$

Thus equation (2.4.3) becomes

$$C_o(t) = 0 \quad \ldots\ldots\ldots\ldots\ldots \quad 0 < t < K_2$$

$$C_o(t) = 1 - e^{-(t-K_2)/K_1} \quad \ldots\ldots \quad K_2 < t < T_1 + K_2 \qquad \ldots\ldots 2.4.4$$

$$C_o(t) = e^{-(t-T_1-K_2)/K_1} - e^{-(t-K_2)/K_1} \quad \ldots\ldots \quad t > T_1 + K_2$$

This equation is illustrated graphically in Fig.2.4.2

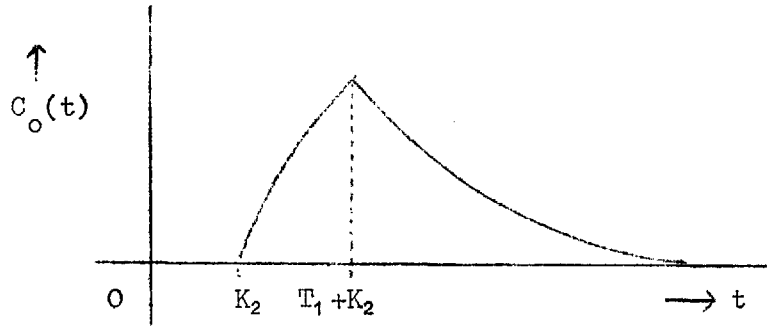

Fig. 2.4.2

Thus in the absence of any other parameters, the length of time between the first injection of tracer at the inlet and the first appearance of tracer at the outlet is equal to the lag constant K_2. Knowing K_2, the plug flow fraction p can be determined. Once p is known, the perfect mixing fraction can be obtained since m = 1-p.

The rising limb in Fig.2.4.2 represents $C_o(t) = 1 - e^{-(t-K_2)/K_1}$ which continues up to the time $(T_1 + K_2)$. This means that the rise continues for a time equal to the input pulse width. If T_1 is small, the peak becomes more sharp. For $T_1 \longrightarrow 0$, the rising limb becomes a vertical line at $t = K_2$.

The falling limb represents the exponential decay $C_o(t) = e^{-(t-T_1-K_2)/K_1} - e^{-(t-K_2)/K_1}$. As T_1 decreases, the drop after the peak becomes steeper. For a particular T_1, the rate of decay depends on the time constant K_1, which in turn is proportional to the degree of mixing.

A family of curves is drawn in Fig.2.4.3 for which m = 0.6, p = 0.4, T the theoretical detention time = 5 minutes and four values of the pulse width T_1 are taken. The curves are presented as plots

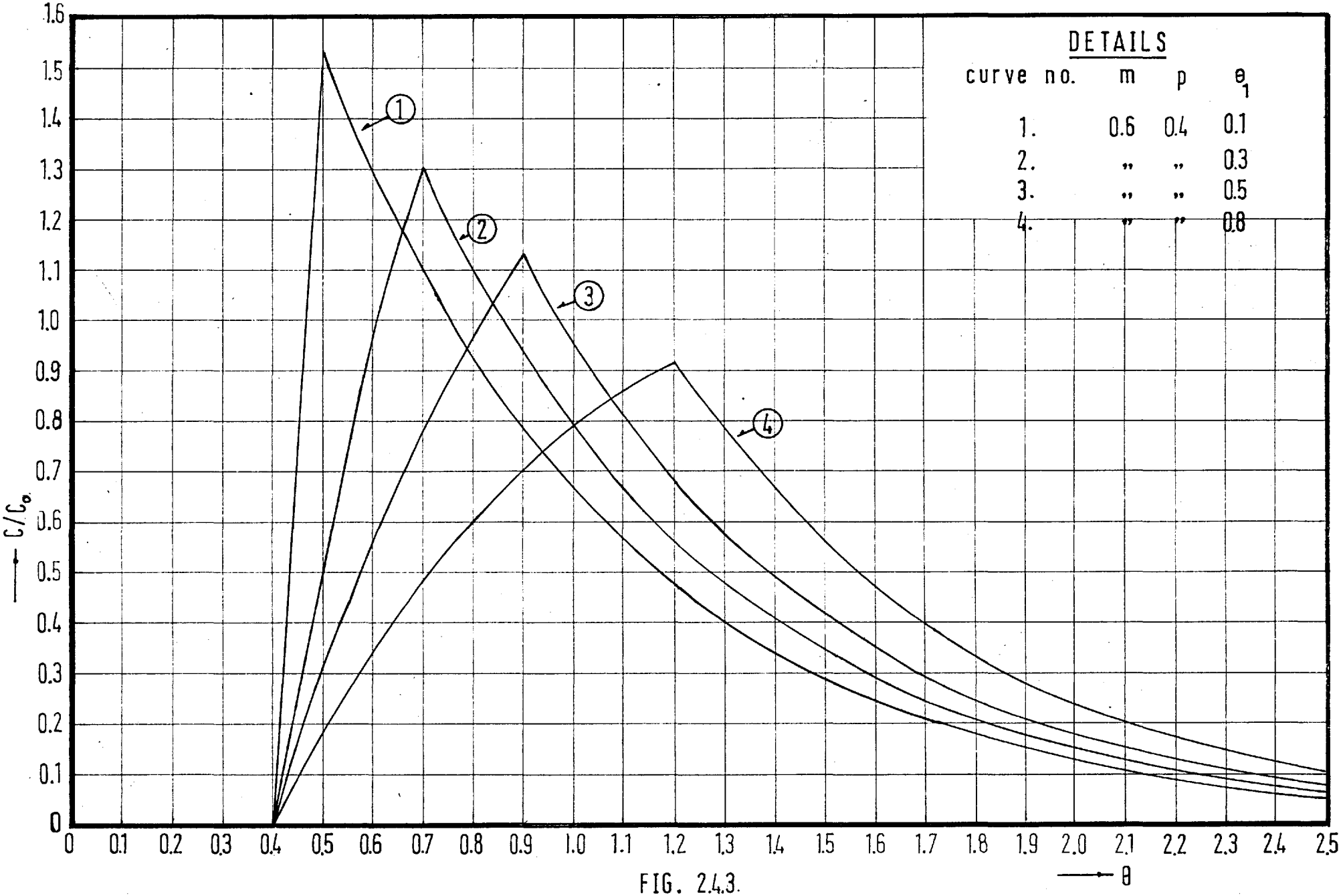
DETAILS
curve no. m p θ_1
1. 0.6 0.4 0.1
2. " " 0.3
3. " " 0.5
4. " " 0.8
1
2
3
4
C/C_0
θ
0 0.1 0.2 0.3 0.4 0.5 0.6 0.7 0.8 0.9 1.0 1.1 1.2 1.3 1.4 1.5 1.6 1.7 1.8 1.9 2.0 2.1 2.2 2.3 2.4 2.5
0 0.1 0.2 0.3 0.4 0.5 0.6 0.7 0.8 0.9 1.0 1.1 1.2 1.3 1.4 1.5 1.6

FIG. 2.4.3.

of C/C_o versus t/T (or θ) where C_o is equal to the amount of tracer added divided by the tank volume.

It can be seen clearly that the slope of the rising limb, obtained by connecting the point of first appearance of tracer to the apex of the curve, is inversely proportional to the width of the input pulse T_1 and tends to flatten out as T_1 increases. Also as the width of the input pulse increases, the tail of the curve gets longer, a fact which has been noted by a number of investigators. Therefore it is important to know the form of the input pulse, as a non-idealised input may result in a flattened peak and a long tail which may be mistaken for dead space or increased mixing.

2.5. Four parameter model with short circuiting

Real cases of perfect mixing in series with plug flow are rare, and in most practical cases there is a fraction of the flow which is comparatively slow moving or fast moving with respect to the main bulk of the flow. In this model it is assumed that such a flow occurs in parallel with the main flow. This flow is referred to henceforth as the short circuit flow.

In the first instance, it is assumed that the short circuit flow is wholly represented by a plug flow element.

Let m = Fraction of the total volume of the system which is perfectly mixed.

p = Fraction of the total volume which is plug flow in series with m.

s = Fraction of the total volume occupied by the short circuiting flow.

$m + p + s = 1$

V = Total volume of the system

f = Fraction of the total inflow Q that short circuits.

Then the time constant of the perfectly mixed element m equals $K_1 = \frac{mT}{(1-f)}$, the lag constant of the plug flow element in the main flow equals $K_2 = \frac{p.T}{(1-f)}$, and the lag constant in the short circuiting element equals $K_3 = \frac{T.s}{f}$.

The block diagram of this model is shown in Fig.2.5.1.

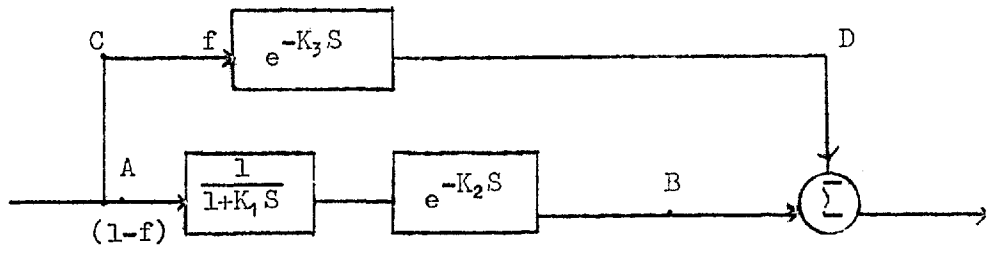

Fig.2.5.1

From equations 2.3.2 and 2.3.3 the Transfer function of the perfect mixing element is equal to $\frac{1}{1 + K_1S}$, the transfer function of the plug flow element is equal to e^{-K_2S} and the transfer function of the short circuiting element is equal to e^{-K_3S}. Referring to Fig.2.5.1 the transfer function between points C and D is equal to $f\ e^{-K_3S}$ and between points A and B is equal to $(1-f)e^{-K_2S}/(1+K_1S)$. The diagram of Fig.2.5.1 can be reduced as shown in Fig.2.5.2

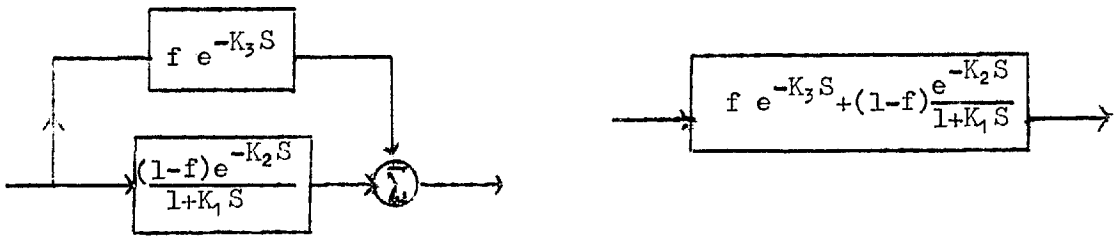

(a) (b)

Fig.2.5.2

Therefore the combined transfer function of the system is as follows:

$$G(S) = f\ e^{-K_3S} + (1-f)e^{-K_2S}/(1+K_1S) \qquad \ldots\ldots\ 2.5.1$$

Considering a rectangular input of width T_1 and height unity:-

$$C_i(t) = U(t) - U(t - T_1) \text{ and}$$

$$C_i(S) = \frac{1}{S} - \frac{e^{-ST_1}}{S} \qquad \text{See equation 2.4.2}$$

$$\therefore C_o(S) = C_i(S).G(S)$$

or $$C_o(S) = \left(\frac{1}{S} - \frac{e^{-ST_1}}{S}\right)[f\, e^{-K_3 S} + (1-f)e^{-K_2 S}/(1+K_1 S)]$$

or $$C_o(S) = \frac{f\, e^{-K_3 S}}{S} - \frac{f\, e^{-S(T_1+K_3)}}{S} + \frac{(1-f)e^{-K_2 S}}{S(1+K_1 S)} - \frac{(1-f)e^{-S(T_1+K_2)}}{S(1+K_1 S)} \qquad 2.5.2$$

Inverting the Laplace Transform,

$$C_o(t) = L^{-1}\frac{fe^{-K_3 S}}{S} - L^{-1}\frac{fe^{-S(T_1+K_3)}}{S} + L^{-1}\frac{(1-f)e^{-K_2 S}}{S(1+K_1 S)} - L^{-1}\frac{(1-f)e^{-S(T_1+K_2)}}{S(1+K_1 S)}$$

or

$$C_o(t) = f*U(t-K_3) - f*U(t-T_1-K_3) + (1-f)(1-e^{-(t-K_2)/K_1})*U(t-K_2)$$
$$-(1-f)(1 - e^{-(t-T_1-K_2)/K_1})* U(t-T_1-K_2) \qquad \text{..... ..... } 2.5.3$$

Equation 2.5.3 may be written in terms of θ where $\theta = {}^{t}/_{T}$ in which case the values of K_1, K_2 and K_3 become

$$K_1 = \frac{m}{(1-f)}, \quad K_2 = \frac{p}{(1-f)} \text{ and } K_3 = \frac{S}{f} \text{ and } \theta_1 = {}^{T_1}/_{T}$$

Four conditions may arise :-

(1) $K_3 < K_2 < (\theta_1 + K_3) < (\theta_1 + K_2)$
(2) $K_3 < (\theta_1 + K_3) < K_2 < (\theta_1 + K_2)$

} See Equation 2.5.4

(3) $K_2 < K_3 < (\theta_1 + K_2) < (\theta_1 + K_3)$
(4) $K_2 < (\theta_1 + K_2) < K_3 < (\theta_1 + K_3)$

} See Equation 2.5.5

Conditions (1) and (2) arise when $K_3 < K_2$ and in this case equation 2.5.3 has the following form.

$$
\begin{aligned}
&\text{(i)} && C_o(\theta) = 0 && 0 < \theta < K_3 \\
&\text{(ii)} && C_o(\theta) = f && (K_3 < \theta < K_2 \text{ or } K_3 < \theta < (\theta_1 + K_3) \text{ depending on whether } K_2 < (\theta_1 + K_3) \text{ or } K_2 > (\theta_1 + K_3)) \\
&\text{(iiia)} && C_o(\theta) = f + (1-f)(1-e^{-(\theta-K_2)/K_1}) && K_2 < \theta < (\theta_1 + K_3) \\
&\text{(iiib)} && C_o(\theta) = 0 && (\theta_1 + K_3) < \theta < K_2 \\
&\text{(iv)} && C_o(\theta) = (1-f)(1-e^{-(\theta-K_2)/K_1}) && \begin{cases} (\theta_1 + K_3) < \theta < (\theta_1 + K_2) \text{ or} \\ K_2 < \theta < (\theta_1 + K_2) \end{cases} \\
&\text{(v)} && C_o(\theta) = (1-f)(e^{-(\theta-\theta_1-K_2)/K_1} - e^{-(\theta-K_2)/K_1}) && \theta > (\theta_1 + K_2)
\end{aligned}
\qquad 2.5.4
$$

When $K_2 < K_3$, the function takes the following form (conditions (3) and (4))

$$
\begin{aligned}
&\text{(i)} && C_o(\theta) = 0 && 0 < \theta < K_2 \\
&\text{(ii)} && C_o(\theta) = (1-f)(1-e^{-(\theta-K_2)/K_1}) && K_2 < \theta < K_3 \text{ or } K_2 < \theta < (\theta_1 + K_2) \\
&\text{(iiia)} && C_o(\theta) = f + (1-f)(1-e^{-(\theta-K_2)/K_1}) && K_3 < \theta < (\theta_1 + K_2) \\
&\text{(iiib)} && C_o(\theta) = (1-f)(e^{-(\theta-\theta_1-K_2)/K_1} - e^{-(\theta-K_2)/K_1}) && (\theta_1 + K_2) < \theta < K_3 \\
&\text{(iv)} && C_o(\theta) = f + (1-f)(e^{-(\theta-\theta_1-K_2)/K_1} - e^{-(\theta-K_2)/K_1}) && \begin{cases} (\theta_1 + K_2) < \theta < (\theta_1 + K_3) \\ \text{(or } K_3 < \theta < (\theta_1 + K_3)) \end{cases} \\
&\text{(v)} && C_o(\theta) = (1-f)(e^{-(\theta-\theta_1-K_2)/K_1} - e^{-(\theta-K_2)/K_1}) && \theta > (\theta_1 + K_3)
\end{aligned}
\qquad 2.5.5
$$

Fig.2.5.3 shows the form of equation 2.5.4 with the various functions labelled accordingly, except part (iiib) which is excluded.

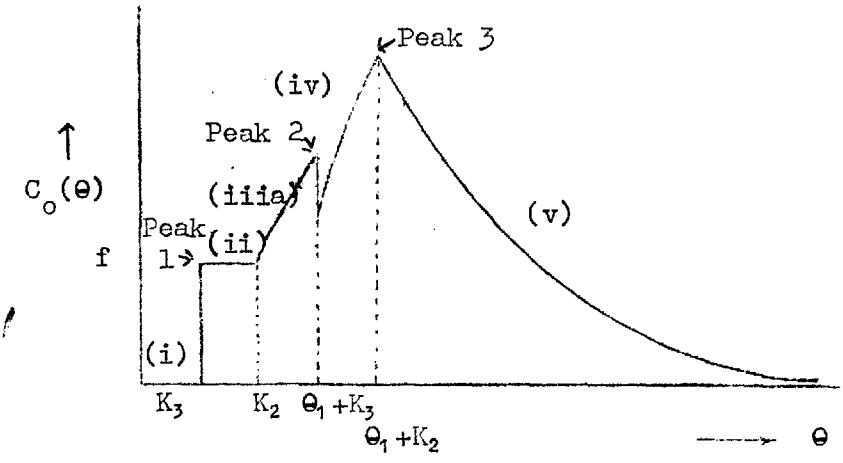

Fig. 2.5.3

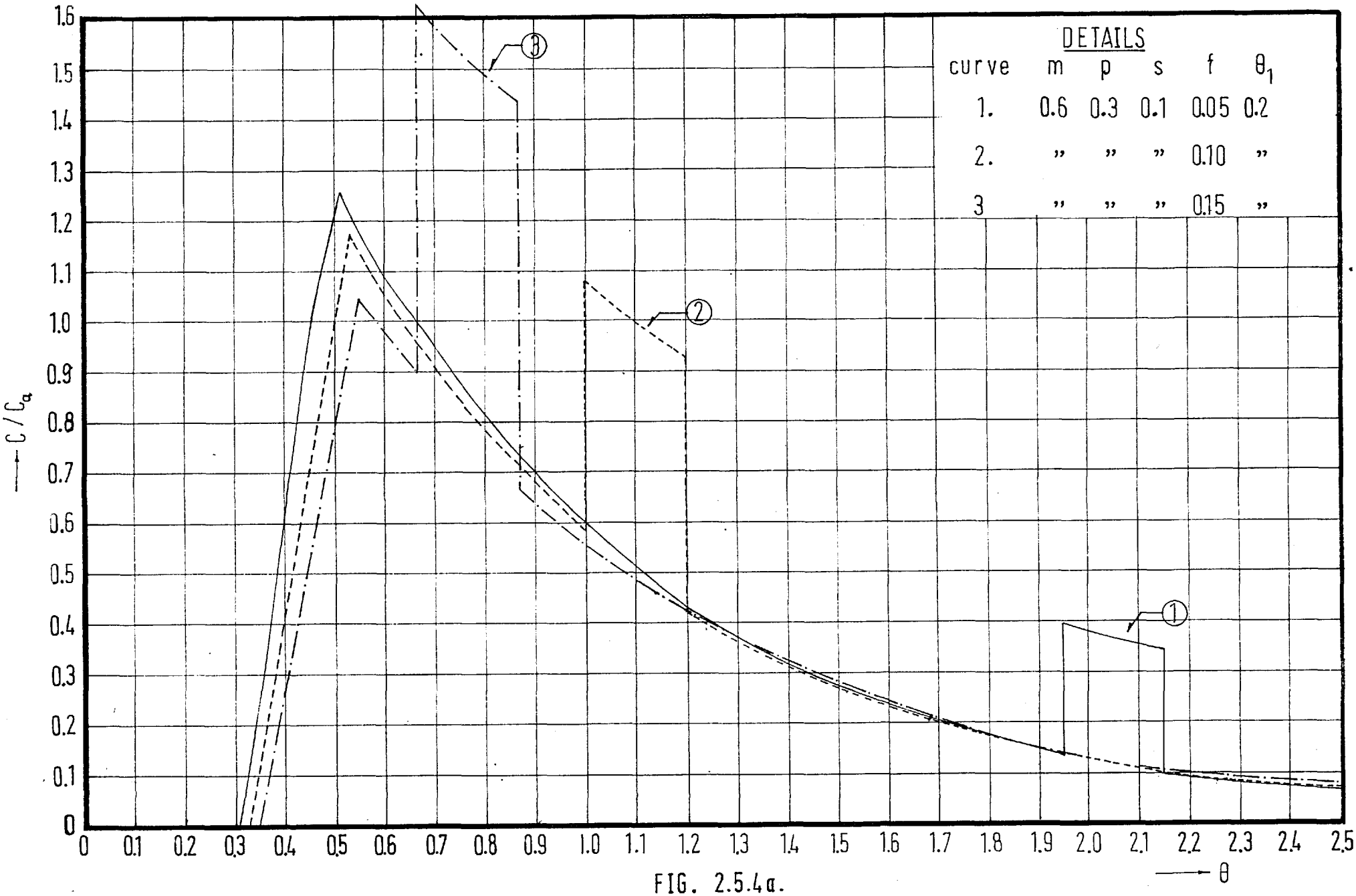
DETAILS
curve m p s f θ1
1. 0.6 0.3 0.1 0.05 0.2
2. " " " 0.10 "
3 " " " 0.15 "
C / Cα
θ
1.6
1.5
1.4
1.3
1.2
1.1
1.0
0.9
0.8
0.7
0.6
0.5
0.4
0.3
0.2
0.1
0
0 0.1 0.2 0.3 0.4 0.5 0.6 0.7 0.8 0.9 1.0 1.1 1.2 1.3 1.4 1.5 1.6 1.7 1.8 1.9 2.0 2.1 2.2 2.3 2.4 2.5
①
②
③

FIG. 2.5.4a.

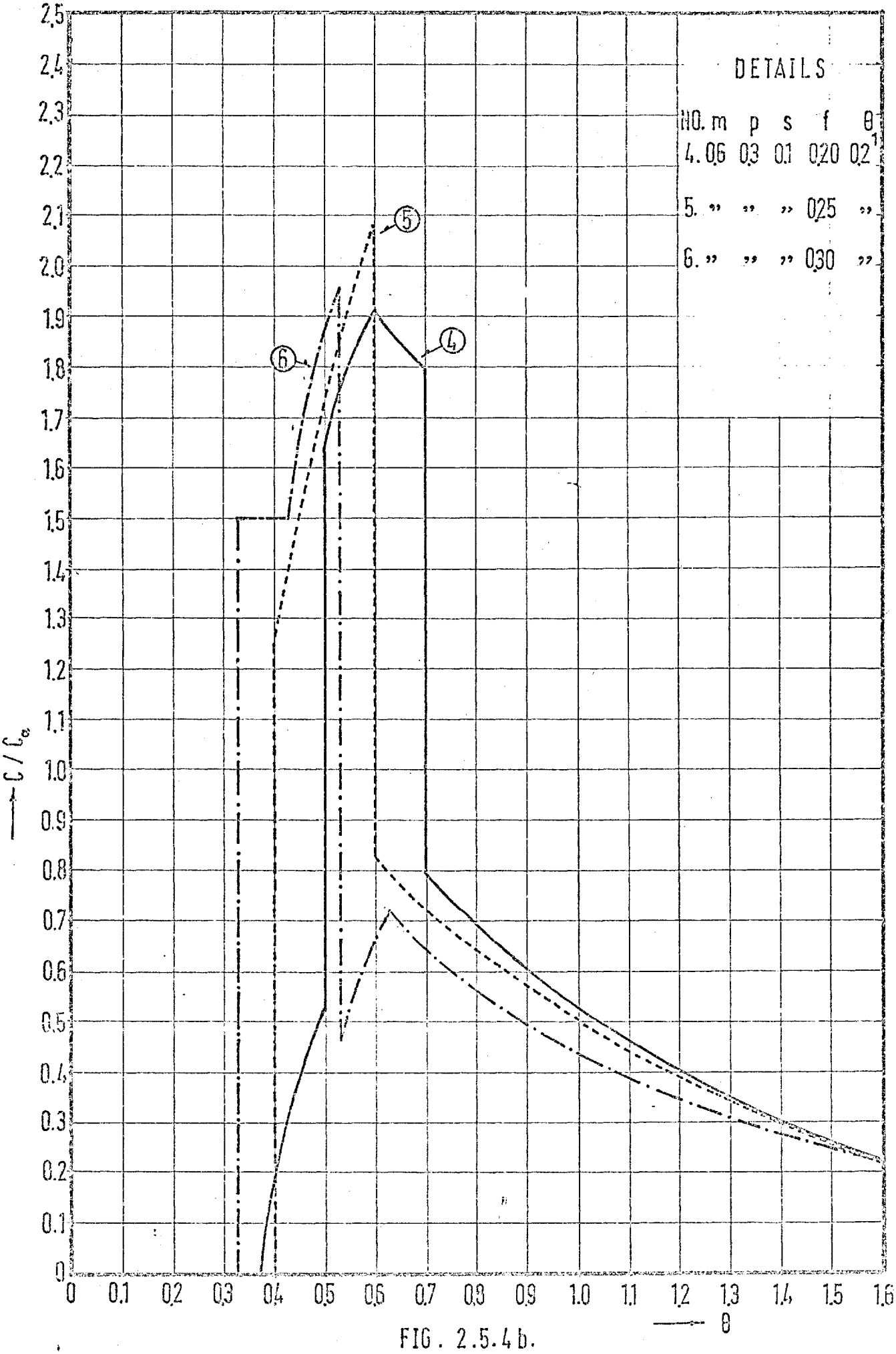
DETAILS
NO. m p s f θ
4. 0.6 0.3 0.1 0.20 0.2
5. " " " 0.25 "
6. " " " 0.30 "
⑤
④
⑥
C / C∞
θ
0 0.1 0.2 0.3 0.4 0.5 0.6 0.7 0.8 0.9 1.0 1.1 1.2 1.3 1.4 1.5 1.6
0 0.1 0.2 0.3 0.4 0.5 0.6 0.7 0.8 0.9 1.0 1.1 1.2 1.3 1.4 1.5 1.6 1.7 1.8 1.9 2.0 2.1 2.2 2.3 2.4 2.5

FIG. 2.5.4 b.

Part (i) shows the time lag required for the short circuiting flow to reach the outlet. This situation indicates that the short-circuiting part of the flow traverses the system in a shorter time than the main flow. Part (ii) shows the tracer concentration corresponding to this short circuiting flow. Part (iii) of the curve is generated when the main bulk of the flow mixes with the short circuiting flow at the outlet. Part (iv) starts when the input of tracer is stopped and the rise is entirely due to the main flow. This rise continues up to a peak at time $(\theta_1 + K_2)$. Part (v) is the exponential decay part of the curve. The above curve has three peaks. The sharpness of the first peak depends on the relative velocity of the short circuit, and it merges with part (iii) of the curve when the relative velocity is small. The second peak corresponds to the end of tracer output through the bypassing channel. The third peak indicates that the end of the tracer pulse has reached the outlet by way of the mainflow. The second peak will be higher than the third peak if the tracer injection is continued for a comparatively long time depending on the amount of short circuiting. Curve No.6 in Fig.2.5.4 is an example of such a case.

Equation 2.5.4 including part (iiib) and excluding part (iiia) represents an extreme case of short circuiting when a shooting flow across the system occurs. The flow diagram for such a case is shown in Fig.2.5.5. If the injection time θ_1 is short, the result is a discontinuous two part outflow curve as shown. The first part corresponds to the short circuit and the second part to the main flow. The time of occurrence of each change is labelled on the abscissa. Such a curve is easier to analyse than any other type as the shortcircuiting fraction is readily deduced. This will become clear in the analysis of experimental curves in Chapter 4.

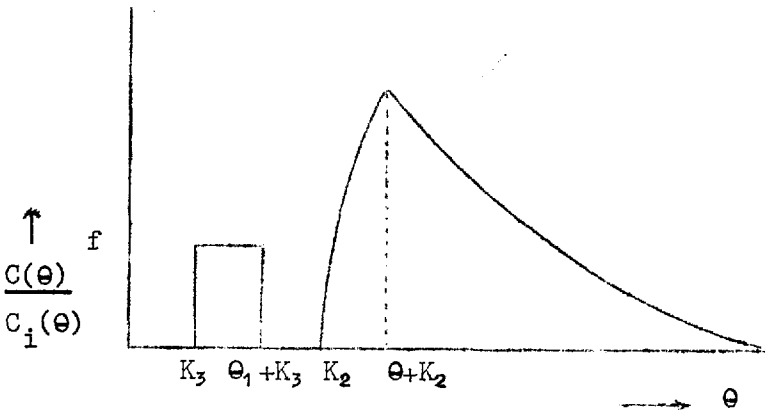

Fig.2.5.5

Equation 2.5.5 applies to the case of shortcircuiting in which the shortcarcuiting fraction is slow moving compared to the main flow. This may be regarded as a stagnant zone. Two types of curves result corresponding to conditions (3) and (4).

When $K_2 < K_3 < (\theta_1 + K_2) < (\theta_1 + K_3)$ a curve of the type shown in Fig.2.5.6 is generated. This curve has only one peak which occurs at time $(\theta_1 + K_2)$ and is disproportionately tall. This happens when the negative step of the rectangular input pulse arrives at the outlet by way of the main flow, during the time when the shortcircuited pulse is passing through. The various parts of the curve are labelled and correspond to equation 2.5.5 excluding (iiib). Curve No.4 in

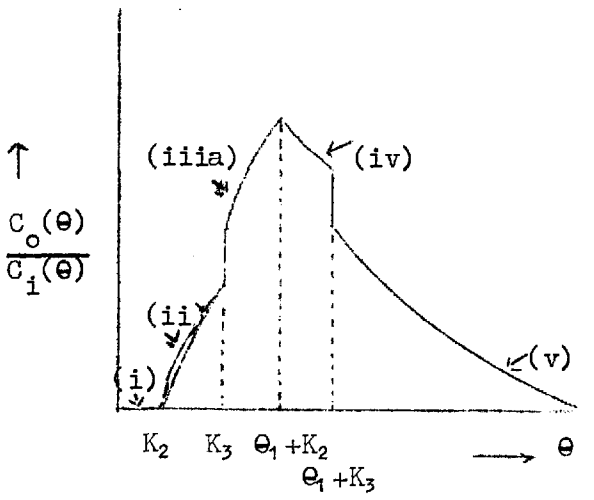

Fig.2.5.6

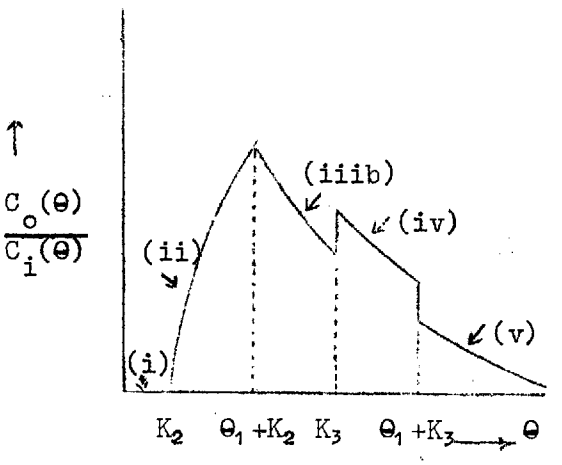

Fig.2.5.7

Fig.2.5.4 is a computer generated curve of this type with $K_2 = 0.375$, $K_3 = 0.5$, $\theta_1 = 0.2$ and $K_1 = 0.75$. It should be noted that for a very narrow input pulse, the peak becomes tall and slender, a result which might be misinterpreted as a high plug flow condition.

When $K_2 < (\theta_1 + K_2) < K_3 < (\theta_1 + K_3)$, the outflow curve takes the form of Fig.2.5.7. This curve has a second peak on the tail part of the main curve. If the stagnant region releases its contents after a long delay and is itself a plug flow region then a sudden rise in the tail occurs as illustrated in Fig.2.5.7 at $\theta = K_3$. The height of this second peak depends on f and K_3. The greater the value of f and the nearer the value of K_3 to $(\theta_1 + K_2)$, the higher will be the peak. Computer generated curve No.2 in Fig.2.5.4 with f = 10%, $K_1 = 0.66$, $K_2 = 0.33$ and $\theta_1 = 0.2$ shows the second peak to be only slightly lower than the main peak. Curve No.3 in the same figure with f = 15%, $K_3 = 0.667$, $K_1 = 0.7$, $\theta_1 + K_2 = 0.55$ and $\theta_1 = 0.2$ is an example of a large peak generated by the shortcircuiting flow, at the expense of the main peak due to the major flow. The distinguishing feature between the two peaks is that the one due to the main flow has a smooth rise and slow decay, while the one resulting from the short circuiting flow has a sharp rise and a sharp fall. The two peaks become indistinguishable when the difference between K_3 and $(\theta_1 + K_2)$ becomes very small or smaller than the sampling interval. This is illustrated by curves No.4 and 5 in Fig.2.5.4. It is important to be able to distinguish the position of the second peak in order to select an initial value of K_3 in the optimisation analysis which will be described later.

2.6. Five parameter short circuiting model

In the previous model, the assumption of plug flow in the short-circuiting element has given rise to sharp peaks or humps caused by such shortcircuiting. However, in practice the sudden increases and decreases in the output curve may not be as sharp and abrupt as the above model indicates. A better approximation to reality would be to assume a shortcircuiting path with plug flow and perfect mixing in series. The block diagram for such a model is shown in Fig.2.6.1.

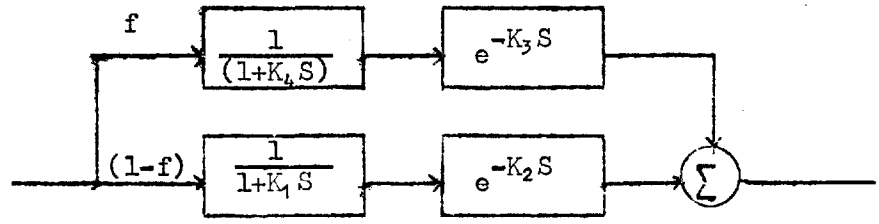

Fig.2.6.1

The equivalent block diagram is shown in Fig.2.6.2.

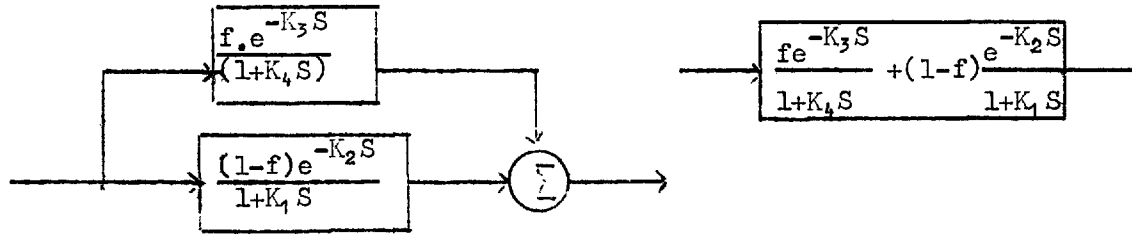

Fig.2.6.2

The transfer function for the short circuiting path is

$$G_2(S) = \frac{f.e^{-K_3S}}{1 + K_4S}$$ and for the main path is $G_1(S) = (1-f)\frac{e^{-K_2S}}{1+K_1S}$

where K_1 and K_2 are the time constant and the lag constant respectively for the main zone. K_4 and K_3 are respectively the time constant and the lag constant for the short circuiting zone. f is the fraction of the total flow that passes through the short circuiting path as before. The combined transfer function for the system is

$$G(S) = G_1(S) + G_2(S)$$

or

$$G(S) = f\frac{e^{-K_3 S}}{1+K_4 S} + (1-f)\frac{e^{-K_2 S}}{1+K_1 S} \qquad \ldots\ldots 2.6.1$$

For a rectangular input of unit height and width T_1, the Laplace transformed input to the system is

$$C_i(S) = \frac{1}{S} - \frac{e^{-ST_1}}{S}$$

If $C_o(t)$ is the output function,

Then $$C_o(S) = C_i(S).G(S)$$

or

$$C_o(S) = (\frac{1}{S} - \frac{e^{-ST_1}}{S})[f\frac{e^{-K_3 S}}{1+K_4 S} + (1-f)\frac{e^{-K_2 S}}{1+K_1 S}] \qquad \ldots\ldots 2.6.2$$

or

$$C_o(S) = \frac{f\, e^{-K_3 S}}{S(1+K_4 S)} - \frac{f\, e^{-S(T_1+K_3)}}{S(1+K_4 S)} + \frac{(1-f)e^{-K_2 S}}{S(1+K_1 S)} - \frac{(1-f)\, e^{-S(t_1+K_2)}}{S(1+K_1 S)}$$

Inversing the transform

$$C_o(t) = f \times (1-e^{-(t-K_3)/K_4}) * U(t-K_3) - f(1-e^{-(t-T_1-K_3)/K_4}) *$$
$$U(t-T_1-K_3) + (1-f)(1-e^{-(t-K_2)/K_1}) * U(t-K_2)$$
$$-(1-f)(1-e^{-(t-T_1-K_2)/K_1}) * U(t-T_1-K_2) \qquad \ldots\ldots 2.6.3$$

Equation 2.6.3 is made dimensionless by replacing t by θ and T_1 by θ_1 where $\theta = \frac{t}{T}$ and $\theta_1 = T_1/T$. As in the four parameter model described in section 2.5 two conditions may arise

(1) $K_2 > K_3$

(2) $K_3 > K_2$

(1) Equation 2.6.3 may be written as follows :

(i) $C_o(\theta) = 0$ when $0 < \theta < K_3$

(ii) $C_o(\theta) = f(1 - e^{-(\theta-K_3)/K_4})$ when $(K_3 < \theta < K_2$ or $K_3 < \theta < (\theta_1+K_3))$

(iiia) $C_o(\theta) = f(1 - e^{-(\theta-K_3)/K_4}) + (1-f)(1-e^{-(\theta-K_2)/K_1})$

when $K_2 < \theta < (\theta_1 + K_3)$

(iiib) $C_o(\theta) = f(e^{-(\theta-\theta_1-K_3)/K_4} - e^{-(\theta-K_3)/K_4})$ when $(\theta_1+K_3) < \theta < K_2$

(iv) $C_o(\theta) = f(e^{-(\theta-\theta_1-K_3)/K_4} - e^{-(\theta-K_3)/K_4}) + (1-f)(1-e^{-\frac{(\theta-K_2)}{K_1}})$ ...2.6.4

when $(\theta_1+K_3) < \theta < (\theta_1+K_2)$

or $K_2 < \theta < (\theta_1+K_2)$

(v) $C_o(\theta) = f(e^{-(\theta-\theta_1-K_3)/K_4} - e^{-\frac{(\theta-K_3)}{K_4}}) + (1-f)(e^{-\frac{(\theta-\theta_1-K_2)}{K_1}} - e^{-(\theta-K_2)/K_1}$

when $\theta > (\theta_1 + K_2)$

(2) Similarly when $K_3 > K_2$ equation 2.6.3 can be written as follows:

(i) $C_o(\theta) = 0$ when $0 < \theta < K_2$

(ii) $C_o(\theta) = (1-f)(1-e^{-(\theta-K_2)/K_1})$ when $K_2 < \theta < K_3$

or $K_2 < \theta < (\theta_1 + K_2)$

(iiia) $C_o(\theta) = (1-f)(1-e^{-(\theta-K_2)/K_1}) + f(1-e^{-(\theta-K_3)/K_4})$

when $K_3 < \theta < (\theta_1+K_2)$

(iiib) $C_o(\theta) = (1-f)(e^{-(\theta-\theta_1-K_2)/K_1} - e^{-(\theta-K_2)/K_1})$ ...2.6.5

when $(\theta_1+K_2) < \theta < K_3$

(iv) $C_o(\theta) = (1-f)(e^{-\frac{(\theta-\theta_1-K_2)}{K_1}} - e^{-\frac{(\theta-K_2)}{K_1}}) + f(1-e^{-(\theta-K_3)/K_4})$

when $(\theta_1+K_2) < \theta < (\theta_1+K_3)$

or $K_3 < \theta < (\theta_1+K_3)$

(v) $C_o(\theta) = (1-f)(e^{-\frac{(\theta-\theta_1-K_2)}{K_1}} - e^{-\frac{(\theta-K_2)}{K_1}}) + f(e^{-(\theta-\theta_1-K_3)/K_4} - e^{-(\theta-K_3)/K_4})$

when $\theta > (\theta_1 + K_2)$

Equation 2.6.4 excluding part (iiib) produces a curve as shown in Fig.2.6.3. Different parts of the curve are labelled according to equation 2.6.4.

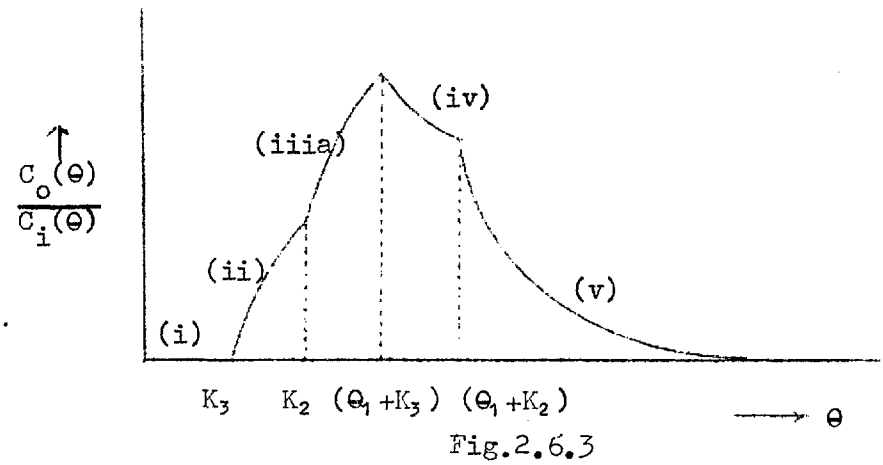

Fig.2.6.3

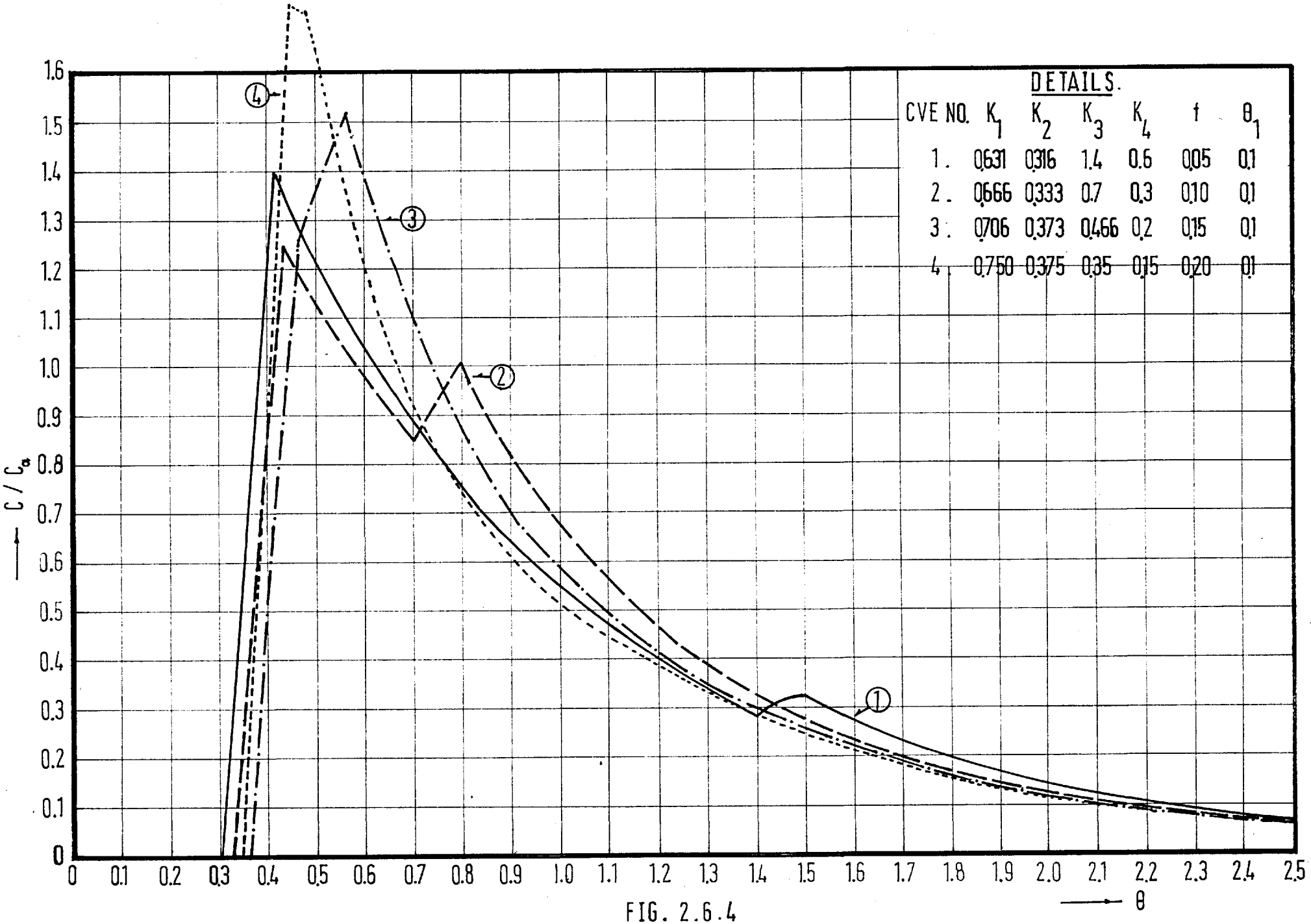
DETAILS.
CVE NO. K1 K2 K3 K4 t θ1
1. 0.631 0.316 1.4 0.6 0.05 0.1
2. 0.666 0.333 0.7 0.3 0.10 0.1
3. 0.706 0.373 0.466 0.2 0.15 0.1
4. 0.750 0.375 0.35 0.15 0.20 0.1
C / Ca
θ
1
2
3
4

FIG. 2.6.4

Curve No.4 in Fig.2.6.4 is a computer generated curve where the shortcircuiting fraction is 20% of the total flow and occupies 10% of the total volume. Of this shortcircuiting volume, 70% is plug flow and 30% is perfect mixing. In the main path of the flow 60% of the volume is occupied by perfect mixing and 30% by plug flow. The overall constants are $K_1 = 0.75$, $K_2 = 0.375$, $K_3 = 0.35$, $K_4 = 0.15$, $f = 0.20$ and $\theta_1 = 0.1$.

Equation 2.6.4 excluding part (iiia) gives rise to a curve as shown in Fig.2.6.5. The curve is correspondingly labelled and has two peaks, the first peak being due to the short circuit.

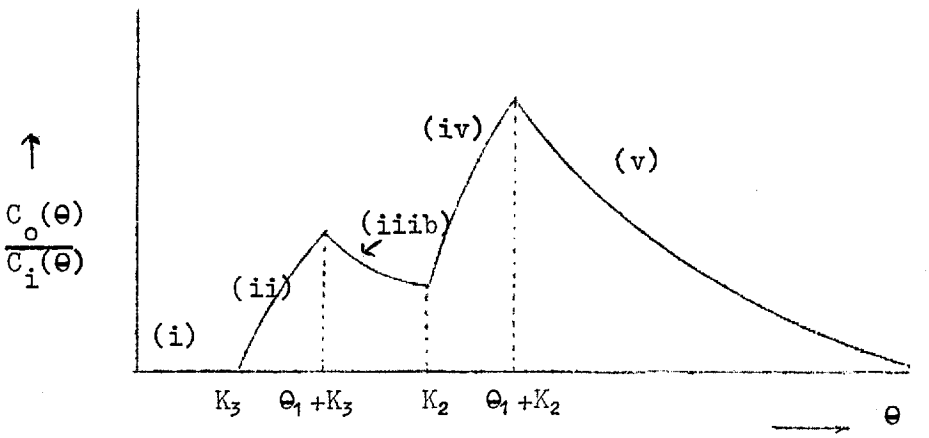

Fig.2.6.5.

Figure 2.6.3 may be compared with Fig.2.5.3 and it will be seen that the present model produces a gradual rather than a step change from phase (i) through phase (ii) and from phase (iiia) through phase (iv). Fig.2.6.3 might be confused with Fig.2.5.6 because of similarity of shape, but closer examination reveals the fundamental difference. In Fig.2.6.3 the curves of part (ii) and (iiia) are different, whereas in Fig.2.5.6 part (iiia) is a continuation of the initial exponential rise of part (ii) with a step addition equal to f. In the limiting case, in which the perfect mixing constant K_4 vanishes, this model becomes identical with the previous four parameter model of Fig.2.5.6. The selection of either model is

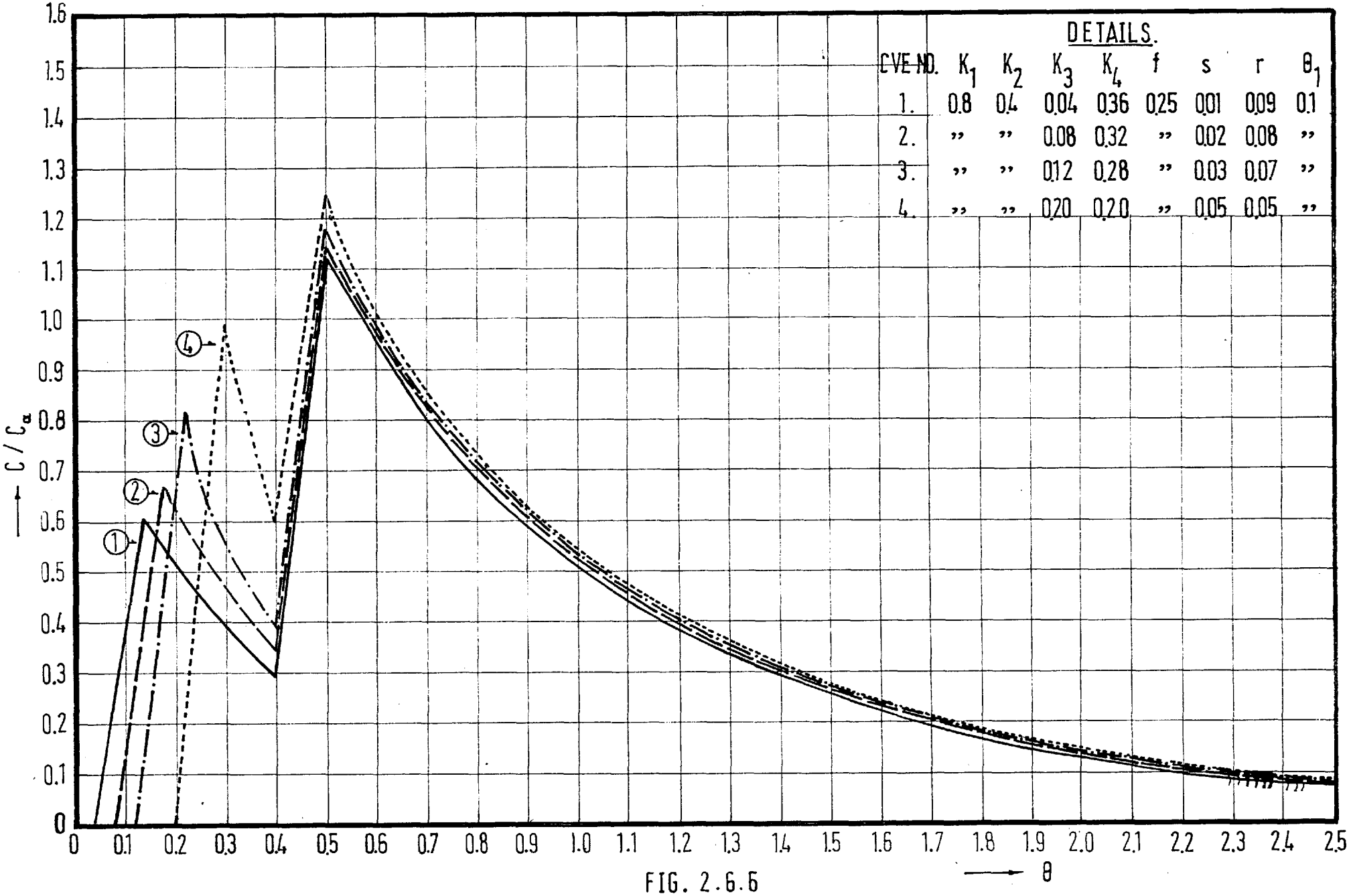
DETAILS.
CVE NO. K1 K2 K3 K4 f s r θ1
1. 0.8 0.4 0.04 0.36 0.25 0.01 0.09 0.1
2. " " 0.08 0.32 " 0.02 0.08 "
3. " " 0.12 0.28 " 0.03 0.07 "
4. " " 0.20 0.20 " 0.05 0.05 "
C / Cα
θ
1.6 1.5 1.4 1.3 1.2 1.1 1.0 0.9 0.8 0.7 0.6 0.5 0.4 0.3 0.2 0.1 0
0 0.1 0.2 0.3 0.4 0.5 0.6 0.7 0.8 0.9 1.0 1.1 1.2 1.3 1.4 1.5 1.6 1.7 1.8 1.9 2.0 2.1 2.2 2.3 2.4 2.5

FIG. 2.6.6

a matter of judgment and either will lead to results which are equal within tolerable limits.

The conditions which give rise to the curve of Fig.2.6.5 are easy to distinguish. It has two peaks of gradual rise and gradual fall. The rise and fall of the shortcircuiting peak is illustrated by the family of computer generated curves presented in Fig.2.6.6. The steepness of the rise and fall depends on the time constant K_4 of the short circuiting flow. Also if the short circuit volume is held constant and K_4 is increased, the tracer arrives at the system outlet in a shorter time. These points are illustrated by curves $1 \longrightarrow 4$ of Fig.2.6.6.

Equation 2.6.5 is valid when there is a stagnant zone (i.e. when $K_3 > K_2$). When $K_2 < (\theta_1 + K_2) < K_3 < (\theta_1 + K_3)$, a curve of the type shown by curve No.1 in Fig.2.6.4 is obtained, which is characterised by a late rise or peak in the tail of the main flow curve. Again the steepness of the rise and fall depends on the time constant K_4 of the short circuiting part of the model. As K_4 decreases, the curve approaches the pattern of Fig.2.5.7. Curve No.1 in Fig.2.6.4 is a typical case often seen in experimental results. As K_3 decreases, the second peak approaches the first one as illustrated by curve No.2 in the same figure. Curve No.3 results when $K_2 < K_3 < (\theta_1 + K_2) < (\theta_1 + K_3$ in which case the second peak follows closely on the first. Fig.2.6.3 and No.3 of Fig.2.6.4 are very difficult to distinguish from Fig.2.5.6 in cases where K_3 is very nearly equal in value to $(\theta_1 + K_2)$. The decision as to whether to use a four parameter model or a five parameter model should be based on the way in which the peak falls off. If this is gradual or the peak seems to be flat, a five parameter model is more appropriate.

2.7 Recirculation models

The mathematical solution of models containing a recirculation element is difficult and only those cases in which the transfer function of the recirculation element is taken as unity appear in the literature. Takamatsu et al.[30] attempted to fit a model consisting of a plug flow main path combined with a plug flow recirculation path, to experimental results obtained on a model sedimentation tank with induced surface recirculation. They were successful in matching the peaks, but omitted all other parts of the flow curve, so that it is clear that such a model is not completely satisfactory.

The model presented here consists of a main flow path consisting of perfect mixing and plug flow in series, combined with a plug flow recirculation path. The block diagram of this model is shown in Fig.2.7.1.

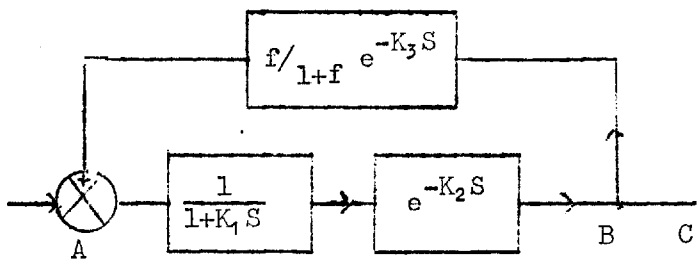

Fig.2.7.1

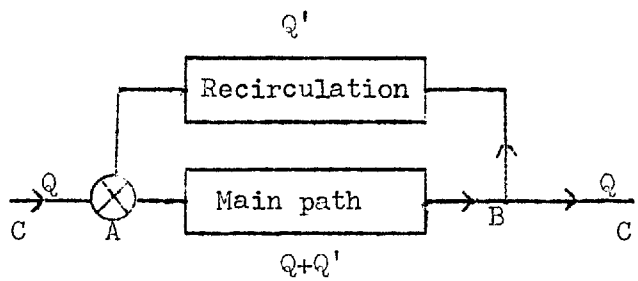

Fig.2.7.2.

Let Q be the inflow rate, and Q' the quantity recirculated as shown in Fig.2.7.2. Then (Q + Q') is the quantity flowing through the main path. Let $f = \frac{Q'}{Q}$. Then the flow through the main path

= Q(1 + f) and the recirculated flow = Qf. Therefore $\frac{f}{(1+f)}$ of the flow which comes to the point B is recirculated.

Let the fraction of the total volume occupied by the perfect mixing, plug flow, and recirculation elements be m, p, and r respectively, such that m + p + r = 1. It should be noted that the volume occupied by the main flow is less than unity and that the flow rate through this smaller volume is greater than Q. Thus the residence time of the main flow fraction decreases with increasing recirculation.

Let $K_1 = \frac{m}{1+f}$, $K_2 = \frac{p}{1+f}$ and $K_3 = \frac{r}{f}$ be the time constants of the perfect mixing, plug flow and recirculation elements respectively. Then the transfer function of the forward path $G_1(S) = \frac{e^{-K_2 S}}{1+K_1 S}$ and that of the recirculation path $G_2(S) = \frac{f}{1+f} e^{-K_3 S}$. Then the equivalent transfer function from points A to B from equation 2.2.4 is

$$G_{AB}(S) = \frac{e^{-K_2 S}/(1+K_1 S)}{1 - (\frac{f}{1+f}) \cdot \frac{e^{-S(K_2+K_3)}}{1+K_1 S}} \qquad \ldots\ldots 2.7.1.$$

But $$G_{AC}(S) = \frac{1}{1+f} G(S)_{AB} \qquad \ldots\ldots 2.7.2.$$

Therefore $$G_{AC}(S) = (\frac{1}{1+f}) \left(\frac{e^{-K_2 S}/(1+K_1 S)}{1 - (\frac{f}{1+f}) \frac{e^{-S(K_2+K_3)}}{1+K_1 S}} \right) \qquad \ldots\ldots 2.7.3.$$

Equation 2.7.3 cannot be easily inverted to the time domain. One method of solution makes use of convolution integrals but this is too complex when a rectangular input is used.

Equation 2.7.3 may be simplified by expanding the denominator using MacLaurin's series as follows:

$$G(S) = (\frac{1}{1+f}) \cdot \frac{e^{-K_2 S}}{(1+K_1 S)} \cdot \left(1 - \frac{f}{1+f} \cdot \frac{e^{-S(K_2+K_3)}}{(1 + K_1 S)}\right)^{-1}$$

or

$$G(S) = (\frac{1}{1+f}) \cdot \left(\frac{e^{-K_2 S}}{1+K_1 S}\right) \cdot \left(1 + \frac{f}{1+f} \cdot \frac{e^{-S(K_2+K_3)}}{(1 + K_1 S)}\right) \qquad \ldots\ldots 2.7.4.$$

assuming $\left\{\frac{f}{1+f} \cdot \frac{e^{-S(K_2+K_3}}{(1+K_1S)}\right\} < 1$ and truncating the series after the first two terms considering all other terms to be negligibly small.

Let $C_i(\theta)$ and $C_o(\theta)$ be the concentration of the input and output pulse with respect to the normalised time θ. Then for a rectangular input of unit height and width θ_1

$$C_i(S) = \frac{1}{S} - \frac{e^{-S\theta_1}}{S}$$

Therefore $C_o(S) = C_i(S) \times G(S)$

$$\text{or } C_o(S) = \left(\frac{1}{S} - \frac{e^{-S\theta_1}}{S}\right)\left(\frac{1}{1+f}\right)\left(\frac{e^{-K_2S}}{1+K_1S} + \frac{f}{1+f} \cdot \frac{e^{-S(2K_2+K_3)}}{(1+K_1S)^2}\right)$$

$$\text{or } C_o(S) = \frac{1}{(1+f)}\left[\frac{e^{-K_2S}}{S(1+K_1S)} - \frac{e^{-S(\theta_1+K_2)}}{S(1+K_1S)} + \frac{f}{1+f} \cdot \frac{e^{-S(2K_2+K_3)}}{S(1+K_1S)^2} - \frac{f}{1+f}\frac{e^{-S(\theta_1+2K_2+K_3)}}{S(1+K_1S)^2}\right]$$

..... 2.7.5

Inverting the Laplace transform,

$$C_o(t) = \frac{1}{1+f}\left[(1-e^{-(\theta-K_2)/K_1}) * U(\theta-K_2) - (1-e^{-(\theta-\theta_1-K_2)/K_1}) * U(\theta-\theta_1-K_2)\right.$$

$$+ \left(\frac{f}{1+f}\right)\left\{1 - \left(1+\frac{\theta-2K_2-K_3}{K_1}\right)e^{-\frac{(\theta-2K_2-K_3)}{K_1}}\right\} * U(\theta-2K_2-K_3)$$

$$\left. - \left(\frac{f}{1+f}\right)\left\{1 - \left(1+\frac{\theta-\theta_1-2K_2-K_3}{K_1}\right)e^{-\frac{(\theta-\theta_1-2K_2-K_3)}{K_1}}\right\} * U(\theta-\theta_1-2K_2-K_3)\right]$$

..... 2.7.6

Two situations may arise in solving equation 2.7.6.

(1) $K_2 < (\theta_1 + K_2) < (2K_2 + K_3) < (\theta_1 + 2K_2 + K_3)$

(2) $K_2 < (2K_2 + K_3) < (\theta_1 + K_2) < (\theta_1 + 2K_2 + K_3)$

When condition (1) applies equation 2.7.6. becomes

(i) $C_o(\theta) = 0$ when $0 < \theta < K_2$

(ii) $C_o(\theta) = \left(\frac{1}{1+f}\right)(1 - e^{-(\theta-K_2)/K_1})$ when $K_2 < \theta < (\theta_1 + K_2)$

(iii) $C_o(\theta) = \left(\frac{1}{1+f}\right)(e^{-(\theta-\theta_1-K_2)/K_1} - e^{-(\theta-K_2)/K_1})$ when $(\theta_1+K_2) < \theta < (2K_2 + K_3)$

(iv) $C_o(\theta) = \left(\frac{1}{1+f}\right)\left[e^{-\frac{(\theta-\theta_1-K_2)}{K_1}} - e^{-\frac{(\theta-K_2)}{K_1}} + \frac{f}{1+f}\left\{1-\left(1+\frac{\theta-2K_2-K_3}{K_1}\right)e^{-(\theta-2K_2-K_3)/K_1}\right\}\right]$

when $(2K_2+K_3) < \theta < (\theta_1+2K_2+K_3)$

(v) $C_o(\theta) = \left(\frac{1}{1+f}\right)\left[e^{-\frac{(\theta-\theta_1-K_2)}{K_1}} - e^{-\frac{(\theta-K_2)}{K_1}}\right.$ 2.7.7

$\left. + \frac{f}{1+f}\left\{\left(1+\frac{\theta-\theta_1-2K_2-K_3}{K_1}\right)e^{-\frac{(\theta-\theta_1-2K_2-K_3)}{K_1}} - \left(1+\frac{\theta-2K_2-K_3}{K_1}\right)e^{-(\theta-2K_2-K_3)/K_1}\right\}\right]$

when $\theta > (\theta_1+2K_2+K_3)$

For condition (2), the equation is identical to equation 2.7.8 except for the following variations.

(ii) The limits of part (ii) are $K_2 < \theta < (2K_2 + K_3)$

(iii) $C_o(\theta) = \frac{1}{1+f}\left[1 - e^{-(\theta-K_2)/K_1} + \frac{1}{1+f}\left\{1 - \left(1 + \frac{\theta-2K_2-K_3}{K_1}\right)e^{\frac{(\theta-2K_2-K_3)}{K_1}}\right\}\right]$

when $(2K_2+K_3) < \theta < (\theta_1+K_2)$

(iv) The limits of part (iv) are $(\theta_1+K_2) < \theta < (\theta_1+2K_2+K_3)$ 2.7.8

Equation 2.7.7 gives rise to curves such as that of Fig.2.7.3. This particular curve was generated by assuming $K_1 = 0.545$, $K_2 = 0.309$, $K_3 = 0.6$, $f = 0.1$ and $\theta_1 = 0.1$. AB in the figure represents part (ii) of the equation. The peak B is reached after a time $(\theta_1 + K_2)$, K_2 being the time of first appearance of the tracer at the outlet. BC represents part (III) of the equation which is in the form of an exponential decay. C is the point when the recirculated tracer begins to appear at the outlet after a time $(2K_2 + K_3)$. From C for a time equal to θ_1, the curve takes the form of part (iv) and thereafter is represented by a further exponential decay, part (v).

It can be seen that when the value of K_3 is small, the point C will be difficult to locate. One method of determining this point is to draw an exponential decay curve from the point B using constants K_1, K_2 and f determined from a best fit of the rising limb AB. The value of K_2 is given by the position of the point A, and it remains

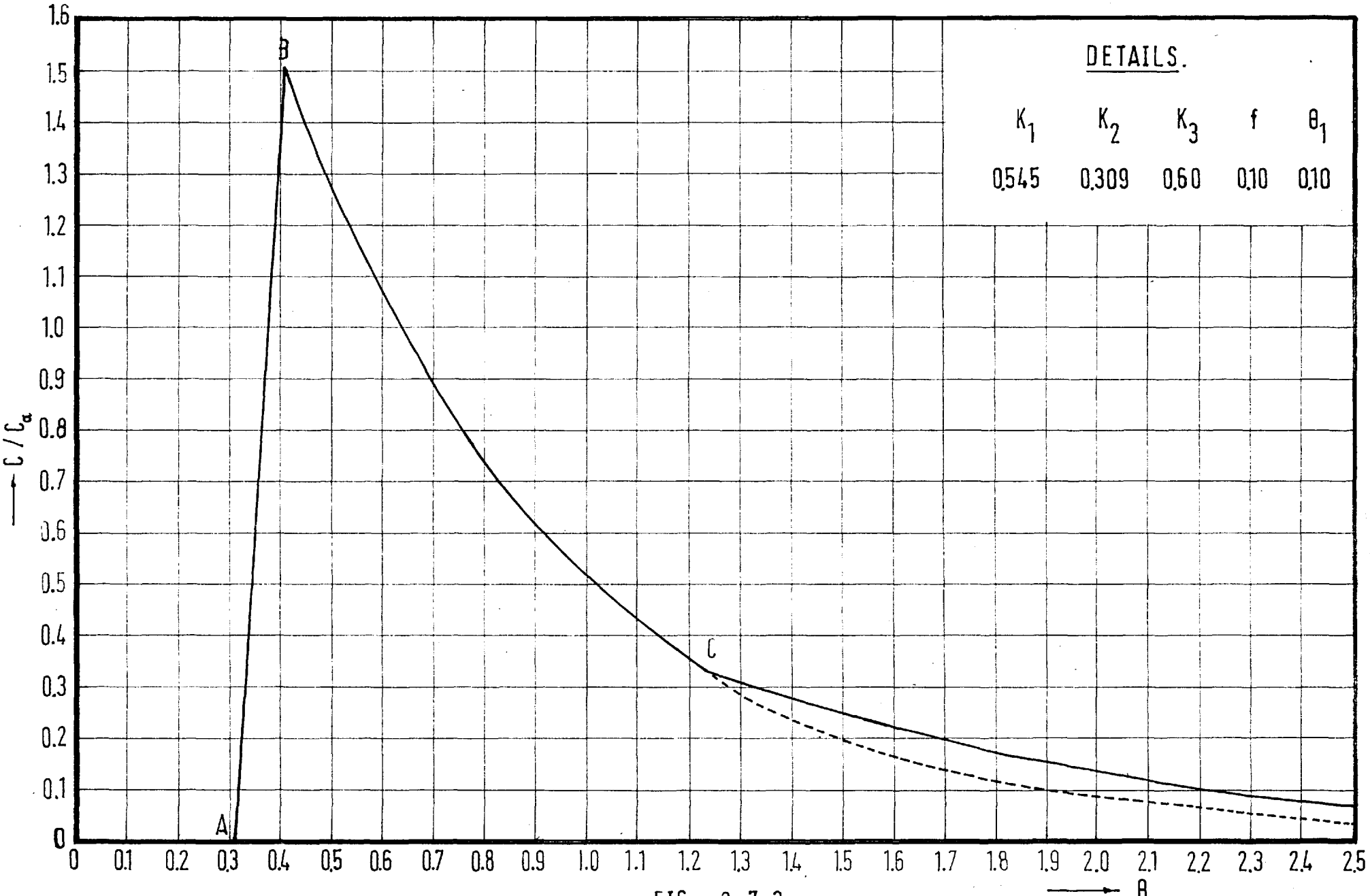
DETAILS.
K1 K2 K3 f θ1
0.545 0.309 0.60 0.10 0.10
A
B
C
C / Cα
θ
0 0.1 0.2 0.3 0.4 0.5 0.6 0.7 0.8 0.9 1.0 1.1 1.2 1.3 1.4 1.5 1.6 1.7 1.8 1.9 2.0 2.1 2.2 2.3 2.4 2.5
0 0.1 0.2 0.3 0.4 0.5 0.6 0.7 0.8 0.9 1.0 1.1 1.2 1.3 1.4 1.5 1.6

FIG. 2.7.3.

to select values of K_1 and f in equation 2.7.8 part (ii) such that it fits the curve AB. As shown by the dotted line on Fig.2.7.3, the point C is located where the exponential from B deviates from the actual flow curve, and thus an estimate of the value of K_3 is obtained. Using these initial estimates of K_1, K_2, K_3 and f, the flow curve can be fitted to equation 2.7.8 by a suitable optimisation technique, provided that this model is appropriate.

Fig.2.7.4 shows three computer generated curves with different recirculation times K_3 and constant recirculation rate f = 0.10. Since f is a constant, an increasing value of K_3 corresponds to an increase in the volume occupied by recirculation and a consequent decrease in the main path volume. This gives lower values of K_1 and K_2. Another effect of recirculation on the flow curve which is evident in Fig.2.7.4 is that as K_3 increases the tail of the curve becomes longer.

Cases in which $\theta_1 > (K_2 + K_3)$ are rare and hence equation 2.7.8 can be neglected.

The effect of increased recirculating flow with constant recirculation time constant (i.e. f increases but K_3 remains constant) is illustrated in Fig.2.7.5. With increased recirculation, the second peak of the flow curve becomes more and more prominent until the effect becomes similar to that of shortcircuiting.

The question arises as to how to distinguish a recirculation peak from a shortcircuiting peak. This problem may be tackled by examining the curve closely bearing in mind the following points.

(a) If the distance between the first and second peaks of the curve is less than the value of K_2, then the second peak is invariably due to short circuiting.

(b) If the second peak of the curve has a sharp rise and fall as

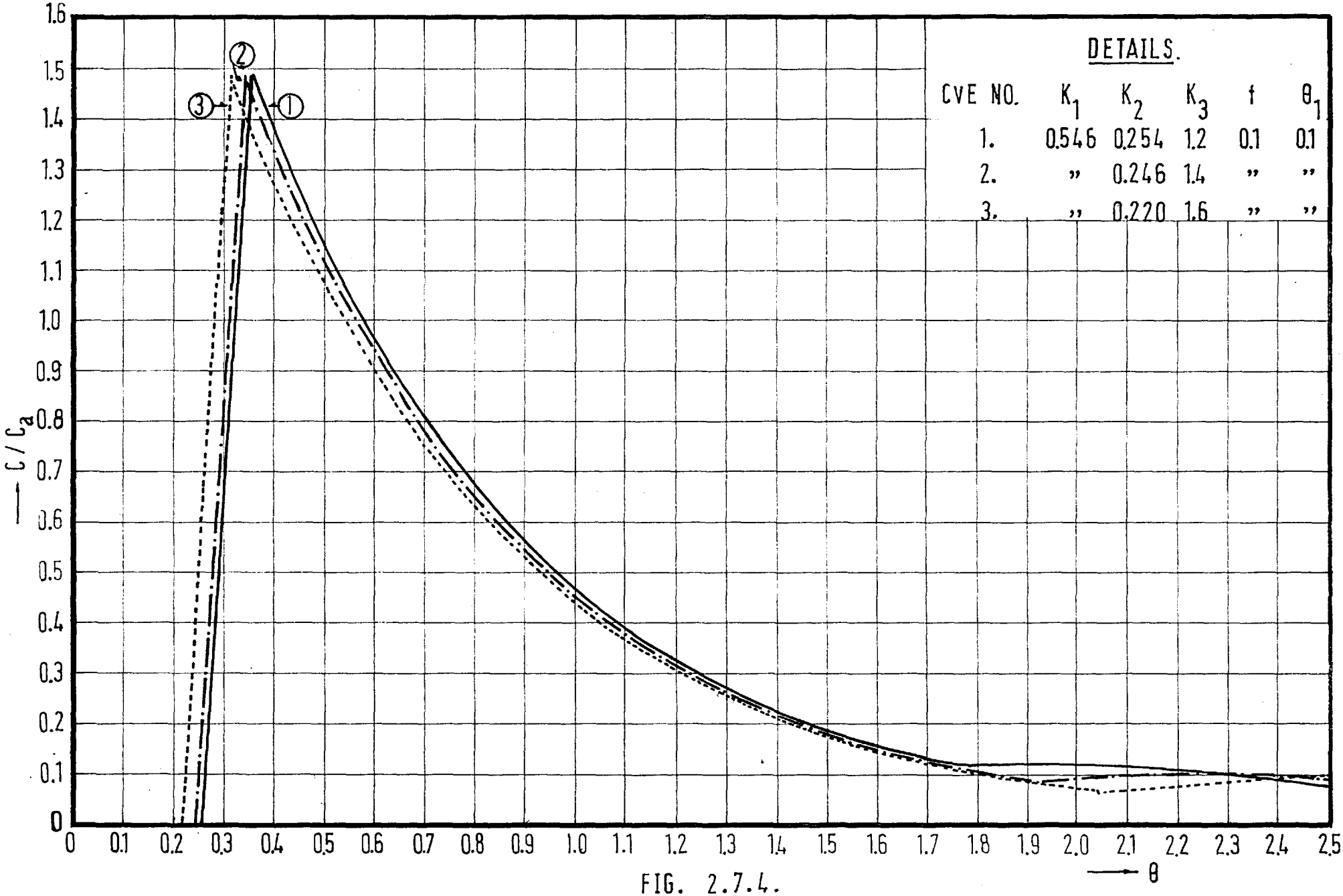
DETAILS.
CVE NO. K1 K2 K3 t θ1
1. 0.546 0.254 1.2 0.1 0.1
2. " 0.246 1.4 " "
3. " 0.220 1.6 " "
C / Ca
θ
1.6
1.5
1.4
1.3
1.2
1.1
1.0
0.9
0.8
0.7
0.6
0.5
0.4
0.3
0.2
0.1
0
0 0.1 0.2 0.3 0.4 0.5 0.6 0.7 0.8 0.9 1.0 1.1 1.2 1.3 1.4 1.5 1.6 1.7 1.8 1.9 2.0 2.1 2.2 2.3 2.4 2.5
① ② ③

FIG. 2.7.4.

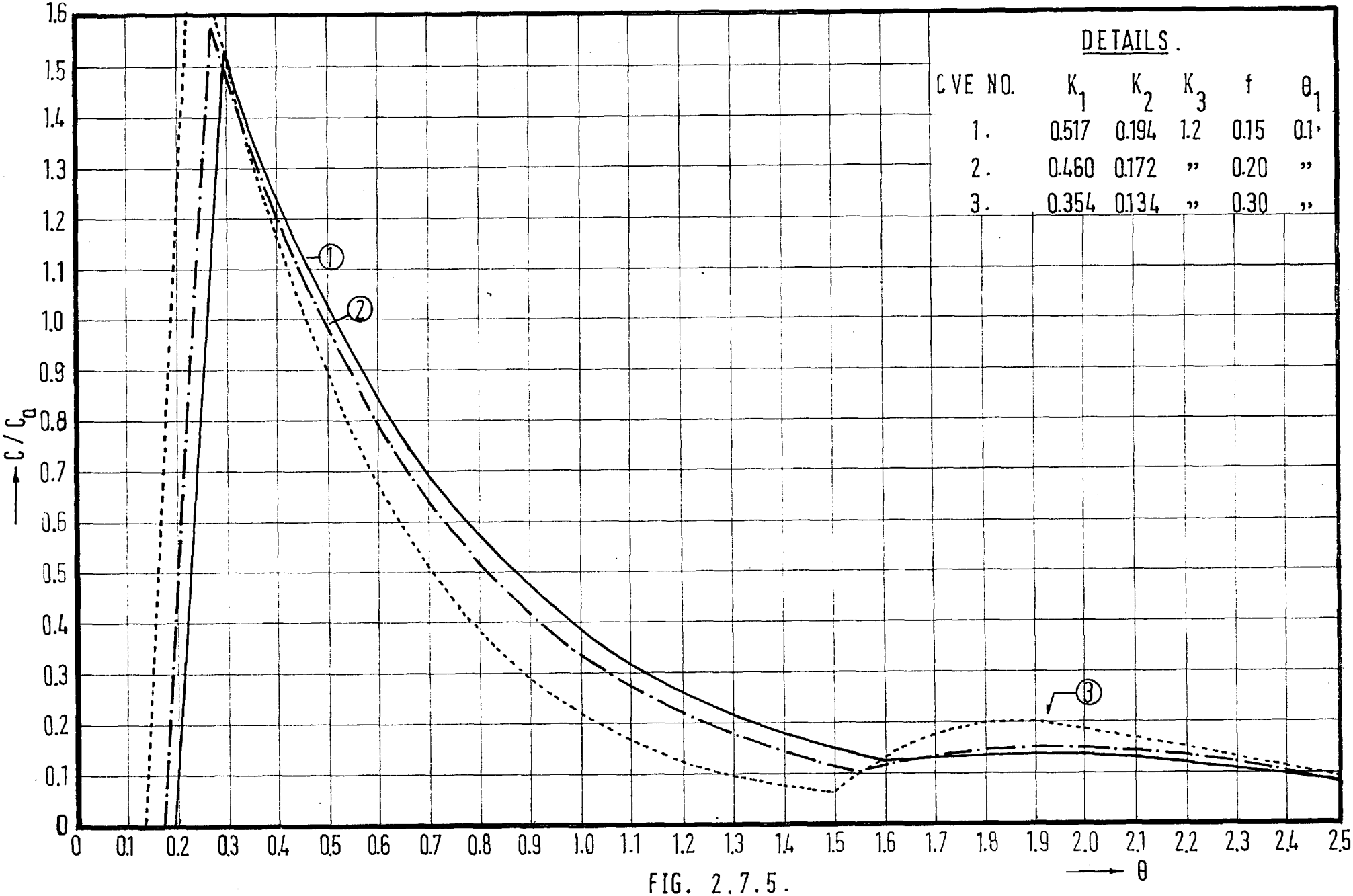
DETAILS.
CVE NO. K1 K2 K3 f θ1
1. 0.517 0.194 1.2 0.15 0.1
2. 0.460 0.172 " 0.20 "
3. 0.354 0.134 " 0.30 "
C / Ca
θ
1
2
3
0 0.1 0.2 0.3 0.4 0.5 0.6 0.7 0.8 0.9 1.0 1.1 1.2 1.3 1.4 1.5 1.6 1.7 1.8 1.9 2.0 2.1 2.2 2.3 2.4 2.5
0 0.1 0.2 0.3 0.4 0.5 0.6 0.7 0.8 0.9 1.0 1.1 1.2 1.3 1.4 1.5 1.6

FIG. 2.7.5.

shown in Fig.2.5.4 then it can only be caused by a short circuit.

(c) A gradual rise and gradual fall in the second peak as illustrated by curve No.1 in Fig.2.6.4 may be due to shortcircuiting or recirculation.

In order to determine which model is the more appropriate it is necessary first of all to determine the values of f, K_1 and K_2, by fitting the model equation to the rising limb of the first peak of the experimental curve. For the short circuiting model the equation of the rising limb is:-

$$C_o(\theta) = \frac{1}{(1+f)} \left(1 - e^{-(\theta-K_2)/K_1}\right).$$

The value of K_2 in either case is fixed by the first arrival time of the tracer, and since for small values of f, $\left(\frac{1}{1+f}\right) \simeq (1-f)$, the values of f, K_1 and K_2 obtained from a best fit of the rising limb will not differ by very much. The value of K_3 is fixed by the time at which the second peak starts to rise in either case, but the secondary peaks are different. The shortcircuiting model produces higher secondary peaks than the recirculation model and the more appropriate choice should be made accordingly.

From the above analysis, it can be concluded that systems with either short circuiting or recirculation can be quantitatively examined. When both shortcircuiting and recirculation are present, the analysis is more difficult particularly when the shortcircuit is of the slow flow type analogous to stagnancy. In the next section a model combining fast shortcircuiting with plug flow recirculation is developed which may prove useful in more complex situations.

2.8 Combined shortcircuit and recirculation model

A flow diagram showing the assumed arrangement of the flow zones is given in Fig.2.8.1.

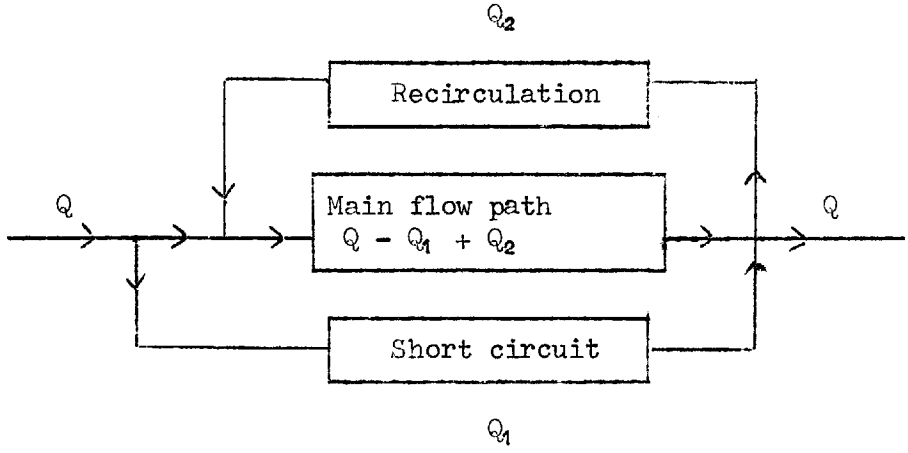

Fig.2.8.1.

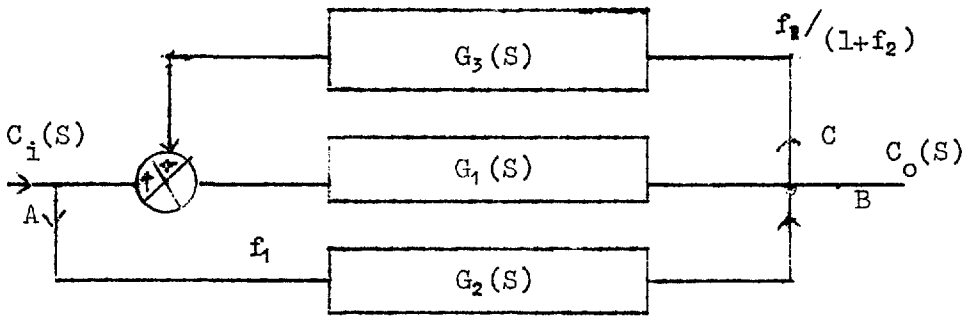

Fig.2.8.2.

where Q is the flow rate into the system

Q_1 = Flow which is shortcircuited

Q_2 = Flow which is recirculated

T = nominal detention time for the whole system

Let m, p, s and r be the fractions of the total volume occupied by the perfect mixing, plug flow, short circuiting and recirculation zones respectively.

Let $f_1 = \frac{Q_1}{Q}$ and $f_2 = \frac{Q_2}{Q}$

Then if K_1, K_2, K_3 and K_4 be the time constants of the four elements, assuming as before that the main flow consists of perfect

mixing and plug flow in series, then

$$K_1 = \frac{mT}{(1 - f_1 + f_2)}$$

$$K_2 = \frac{pT}{(1 - f_1 + f_2)}$$

$$K_3 = \frac{rT}{f_2}$$

$$K_4 = \frac{sT}{f_1}$$

If normalised with respect to time, then T becomes unity in the above constants as before.

The transfer functions for the main path, shortcircuit, and recirculation transfer elements are as follows:

$$G_1(S) = \frac{e^{-K_2 S}}{1 + K_1 S}$$

$$G_2(S) = e^{-K_4 S}$$

$$G_3(S) = e^{-K_3 S}$$

A block diagram of the system is shown in Fig.2.8.2. For simplicity in the first case it is assumed that the shortcircuit takes place at a point A before the summing point of the recirculation element, so that a fraction f_1 of what comes to the point A passes through the shortcircuiting path. Also it is assumed that the summing point C of the shortcircuiting element coincides with the pick off point of the recirculation element. Therefore the fraction of material that is recirculated from the point C is equal to $\frac{Q_2}{Q+Q_2} = \frac{f_2}{1+f_2}$ and the fraction that reaches the point B or the outlet of the system is equal to $1 - \frac{f_2}{1+f_2} = \frac{1}{1+f_2}$

$G(S)_1$ the equivalent transfer function for the system is derived from equations 2.2.5 and 2.2.6 as follows.

$$G(S) = f_1 . G_2(S) + G_1(S)/[1 - \frac{f_2}{1+f_2} . G_1(S) . G_3(S)] \quad \ldots\ldots 2.8.1$$

Substituting the values of $G_1(S)$, $G_2(S)$ and $G_3(S)$ in equation 2.8.1 and expanding the denominator of the second term as in equation 2.7.4

$$G(S) = f_1 e^{-K_4 S} + e^{-K_2 S}/(1+K_1 S) + f_2 e^{-S(2K_2+K_3)}/\{(1+f_2)(1+K_1 S)^2\} \quad \ldots\ldots 2.8.2$$

Again taking a rectangular input of width Θ_1, in dimensionless form, so that $C_i(S) = \frac{1}{S} - \frac{e^{-S\Theta_1}}{S}$,

$C_o(S) = \frac{1}{1+f_2} . \{G_c(S)\} . \{C_i(S)\}$, where C_c refers to the transfer function at the point in Fig.2.8.2. and = G(S).

$$\therefore C_o(S) = \frac{1}{(1+f_2)} \times (\frac{1}{S} - \frac{e^{-S\Theta_1}}{S}) \times [f_1 e^{-K_4 S} + e^{-K_2 S}/(1+K_1 S) + f_2 e^{-S(2K_2+K_3)}/\{(1+f_2) \times (1+K_1 S)^2\}]$$

$$\text{or } C_o(S) = [f_1 e^{-K_4 S}/S - f_1 e^{-S(K_4+\Theta_1)}/S + e^{-K_2 S}/S(1+K_1 S) - e^{-S(K_2+\Theta_1)}/S(1+K_1 S) + f_2 e^{-S(2K_2+K_3)}/S\{(1+f_2)(1+K_1 S)^2\} - f_2 e^{-S(\Theta_1+2K_2+K_3)}/S\{(1+f_2)(1+K_1 S)^2\}]/(1+f_2) \quad \ldots\ldots 2.8.3$$

Inverting the Laplace Transform,

$$C_o(\Theta) = f_1/(1+f_2) \ast U(\Theta-K_4) - f_1/(1+f_2) \ast U(\Theta-\Theta_1-K_4) + (1-e^{-(\Theta-K_2)/K_1})/(1+f_2) \ast U(\Theta-K_2) - (1-e^{-(\Theta-\Theta_1-K_2/K_1})/(1+f_2) \ast U(\Theta-\Theta_1-K_2) + f_2/(1+f_2)^2 [1-(1+\frac{\Theta-2K_2-K_3}{K_1}) e^{-(\Theta-2K_2-K_3)/K_1}] \ast U(\Theta-2K_2-K_3) - f_2/(1+f_2)^2 [1-(1+\frac{\Theta-\Theta_1-2K_2-K_3}{K_1}) e^{-(\Theta-\Theta_1-2K_2-K_3)/K_1}] \ast U(\Theta-\Theta_1-2K_2-K_3) \quad \ldots\ldots 2.8.4$$

Four situations may arise

(1) $K_4 < K_2 < (\Theta_1 + K_4) < (\Theta_1 + K_2) < (2K_2 + K_3) < (\Theta_1 + 2K_2 + K_3)$

(2) $K_4 < (\Theta_1 + K_4) < K_2 < (\Theta_1 + K_2) < (2K_2 + K_3) < (\Theta_1 + 2K_2 + K_3)$

(3) $K_2 < K_4 < (\theta_1 + K_2) < (\theta_1 + K_4) < (2K_2 + K_3) < (\theta_1 + 2K_2 + K_3)$

(4) $K_2 < (\theta_1 + K_2) < K_4 < (\theta_1 + K_4) < (2K_2 + K_3) < (\theta_1 + 2K_2 + K_3)$

Situations, when $\theta_1 \geq (K_2 + K_3)$ are not considered. When conditions (1) and (2) are applied to equation 2.8.4 the output curve has the following form:-

(i) $C_o(\theta) = 0$ $\quad 0 < \theta < K_4$

(ii) $C_o(\theta) = f_1/(1+f_2)$ $\quad K_4 < \theta < K_2$ or $K_4 < \theta < \theta_1 + K_4)$

(iiia) $C_o(\theta) = f_1(1+f_2) + 1/(1+f_2)(1-e^{-(\theta-K_2)/K_1})$ $\quad K_2 < \theta < (\theta_1 + K_4)$

(iiib) $C_o(\theta) = 0$ $\quad (\theta_1 + K_4) < \theta < K_2$

(iv) $C_o(\theta) = 1/(1+f_2)(1-e^{-(\theta-K_2)/K_1})$ $\quad (\theta_1 + K_4) < \theta < (\theta_1 + K_2)$ or

$K_2 < \theta < (\theta_1 + K_2)$

(v) $C_o(\theta) = 1/(1+f_2)(e^{-(\theta-\theta_1-K_2)/K_1} - e^{-(\theta-K_2)/K_1})$ $\quad (\theta_1 + K_2) < \theta < (2K_2 + K_3)$

(vi) $C_o(\theta) = 1/(1+f_2)[e^{-(\theta-\theta_1-K_2)/K_1} - e^{-(\theta-K_2)/K_1} + \frac{f_2}{1+f_2}\{1-(1+\frac{\theta-2K_2-K_3}{K_1})$

$e^{-(\theta-2K_2-K_3)/K_1}\}]$

$(2K_2 + K_3) < \theta < (\theta_1 + 2K_2 + K_3)$

(vii) $C_o(\theta) = 1/(1+f_2)\ [e^{-(\theta-\theta_1-K_2)/K_1} - e^{-(\theta-K_2)/K_1} + \frac{f_2}{1+f_2}\{(1+\frac{(\theta-\theta_1-2K_2-K_3)}{K_1})$

$e^{-(\theta-\theta_1-2K_2-K_3)/K_1} - (1+\frac{\theta-2K_2-K_3}{K_1})e^{-(\theta-2K_2-K_3)/K_1}\}]$

$\theta > (\theta_1 + 2K_2 + K_3)$

..... 2.8.5

Applying conditions (3) and (4) results in a curve of the following form

(i) $C_o(\theta) = 0$ $\quad 0 < \theta < K_2$

(ii) $C_o(\theta) = 1/(1+f_2)(1-e^{-(\theta-K_2)/K_1})$ $\quad K_2 < \theta < K_4$ or $K_2 < \theta < (\theta_1 + K_2)$

(iiia) $C_o(\theta) = \frac{1}{(1+f_2)}[(1-e^{-(\theta-K_2)/K_1}) + f_1]$ $\quad K_4 < \theta < (\theta_1 + K_2)$

(iiib) $C_o(\theta) = \frac{1}{(1+f_2)}(e^{-(\theta-\theta_1-K_2)/K_1} - e^{-(\theta-K_2)/K_1})$ $\quad (\theta_1 + K_2) < \theta < K_4$

(iv) $C_o(\theta) = \frac{1}{(1+f_2)}[(e^{-(\theta-\theta_1-K_2)/K_1} - e^{-(\theta-K_2)/K_1}) + f_1]$

$(\theta_1 + K_2) < \theta < (\theta_1 + K_4)$ or

$K_4 < \theta < (\theta_1 + K_4)$

(v) $$C_o(\theta) = \frac{1}{(1+f_2)} \left[\left(e^{-(\theta-\theta_1-K_2)/K_1} - e^{-(\theta-K_2)/K_1}\right)\right] \quad (\theta_1+K_4) < \theta < (2K_2+K_3)$$

(vi) Same as (vi) of equation 2.8.5.

(vii) Same as (vii) of equation 2.8.5. ..... 2.8.6.

It can be seen that equation 2.8.5. is valid when $K_4 < K_2$ and equation 2.8.6. is valid when $K_2 < K_4$.

Four curves plotted from computer data are shown in Fig.2.8.3. Curves (1) and (2) are cases in which $K_2 < K_4$. Curve (1) is the case in which $(\theta_1 + K_2) < K_4$ and has two peaks. The second peak is produced by the short circuiting flow and has a sharp rise and fall. As the recirculation time is low (= 0.333), the expected third hump is not visible and the effect of recirculation can be ascertained only by the technique mentioned in connection with the curve shown on Fig.2.7.3. Curve (2) of Fig.2.8.3 illustrates the case when $K_4 < (\theta_1+K_2)$. Curve (3) is the case when $K_4 < K_2$ and the recirculation time has the value 0.733. It is characterised by two peaks (which cannot be detected unless the sampling interval is sufficiently small) and a hump on the tail produced by recirculation. Curve (4) arises when K_2 and K_4 are almost equal. Such a case gives rise to a disproportionately high peak followed by a sharp fall.

The above model represents the case in which the inflow to the system is divided into two distinct parts. One of the parts bypasses the system directly to the outlet and consequently does not contain any recirculated flow. The case in which a fraction of the recirculated flow is also bypassed is more general and is considered below.

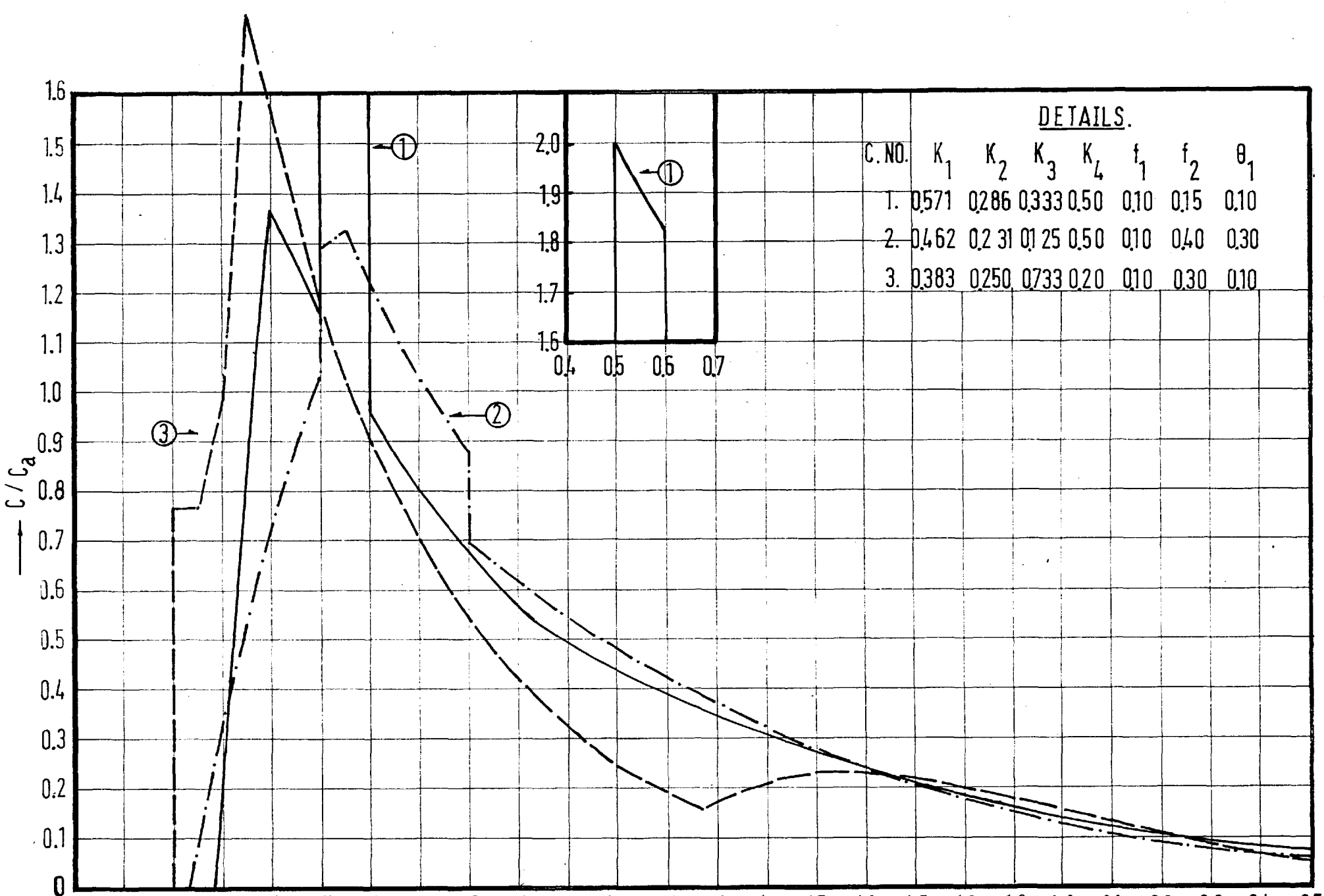
DETAILS.
C.NO. K1 K2 K3 K4 f1 f2 θ1
1. 0.571 0.286 0.333 0.50 0.10 0.15 0.10
2. 0.462 0.231 0.125 0.50 0.10 0.40 0.30
3. 0.383 0.250 0.733 0.20 0.10 0.30 0.10
C / Ca
θ
1.6
1.5
1.4
1.3
1.2
1.1
1.0
0.9
0.8
0.7
0.6
0.5
0.4
0.3
0.2
0.1
0
0 0.1 0.2 0.3 0.4 0.5 0.6 0.7 0.8 0.9 1.0 1.1 1.2 1.3 1.4 1.5 1.6 1.7 1.8 1.9 2.0 2.1 2.2 2.3 2.4 2.5
2.0
1.9
1.8
1.7
1.6
0.4 0.5 0.6 0.7
①
②
③

FIG. 2.8.3

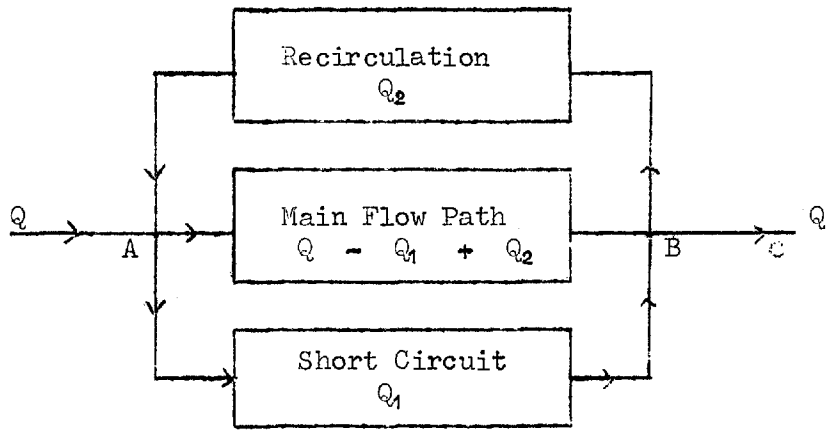

Fig.2.8.4

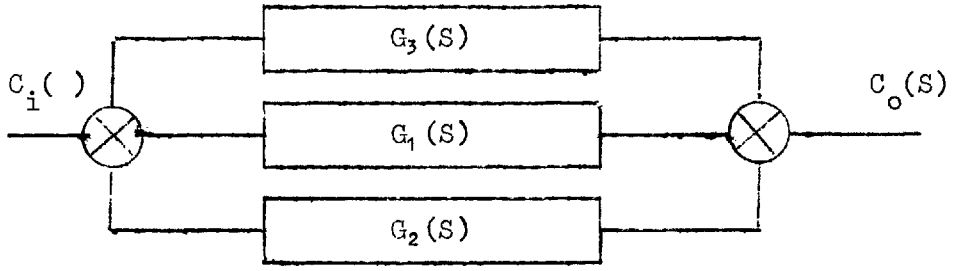

Fig.2.8.5

Again Q = the flow rate into the system

Q_1 = the flow which is shortcircuited

Q_2 = the flow which is recirculated

T = the nominal detention time for the whole system.

Let $\frac{Q_1}{Q} = f_1$ and $\frac{Q_2}{Q} = f_2$

The total flow into the point 'A' in Fig.2.8.4 is equal to $Q + Q_2$. Of this total flow the fraction that short circuits is equal to

$\frac{Q_1}{Q+Q_2} = \frac{f_1}{1+f_2}$ and the fraction that goes along the main path = $\frac{Q - Q_1 + Q_2}{Q + Q_2} = \frac{1 - f_1 + f_2}{1 + f_2}$.

As in the case of the previous treatment the fraction that recirculates from the point 'C' is equal to $\frac{Q_2}{Q_1+Q_2} = \frac{f_2}{1+f_2}$. In order to simplify the algebra the following notation is introduced at this point.

$$A_1 = \frac{1 - f_1 + f_2}{1 + f_2}$$

$$A_2 = \frac{f_1}{1 + f_2}$$

$$A_3 = \frac{f_2}{1 + f_2}$$

Let the Transfer Functions of the main path, short circuit and recirculation elements be G_1, G_2 and G_3 respectively as shown in the Block Diagram of Fig.2.8.5, where

$$G_1 = A_1 \frac{e^{-K_2 S}}{1+K_1 S}$$

$$G_2 = A_2 e^{-K_4 S}$$

and $G_3 = A_3 e^{-K_3 S}$

The constants K_1, K_2, K_3 and K_4 have the same meaning as before.

The equivalent Transfer Function of the system from the point A to the point C is $G(S) = \frac{G_1 + G_2}{1-G_3(G_1+G_2)} \left(\frac{1}{1+f_2}\right)$

Again expanding the denominator:

$$G(S) = (G_1 + G_2)\{1 + G_3(G_1+G_2)\}\left(\frac{1}{1+f_2}\right)$$

or $$G(S) = (G_1 + G_2 + G_3 G_1^2 + G_3 G_2^2 + 2G_3 G_1 G_2)\left(\frac{1}{1+f_2}\right) \quad \ldots\ldots 2.8.7$$

Putting in the values of G_1, G_2 and G_3 in Equation 2.8.7

$$G(S) = \left[A_1 \cdot \frac{e^{-K_2 S}}{1+K_1 S} + A_2 e^{-K_4 S} + A_3 A_1^2 e^{-S(2K_2+K_3)} \cdot \frac{1}{(1+K_1 S)^2}\right. \quad \ldots\ldots 2.8.8$$

$$\left. + A_3 A_2^2 e^{-S(2K_4+K_3)} + 2A_1 A_2 A_3 e^{-S(K_2+K_3+K_4)} \frac{1}{(1+K_1 S)}\right] \left(\frac{1}{1+f_2}\right)$$

With a rectangular input of width θ_1,

$$C_i(S) = \frac{1}{S} - \frac{e^{-S\theta_1}}{S}$$

Then $$C_o(S) = \left(\frac{1}{S} - \frac{e^{-S\theta_1}}{S}\right).G(S) \quad \ldots\ldots 2.8.9$$

Inverting the Laplace Transform in equation 2.8.9 term by term.

$$C_o(t) = [A_1 (1-e^{-(\theta-K_2)/K_1}) * U(\theta-K_2) - A_1 (1-e^{-(\theta-\theta_1-K_2)/K_1}) * U(\theta-\theta_1-K_2)$$

$$+ A_2 * U(\theta-K_4) - A_2 * U(\theta - \theta_1 - K_4)$$

$$+ A_3 A_1{}^2 \left\{1 - (1 + \frac{\theta-2K_2-K_3}{K_1}) e^{-(\frac{\theta-2K_2-K_3}{K_1})}\right\} * U(\theta-2K_2-K_3)$$

$$- A_3 A_1{}^2 \left\{1 - (1 + \frac{\theta-\theta_1-2K_2-K_3}{K_1}) e^{-(\frac{\theta-\theta_1-2K_2-K_3}{K_1})}\right\} * U(\theta-\theta_1-2K_2-K_3)$$

$$+ A_3 A_2{}^2 * U(\theta-2K_4-K_3) - A_3 A_2{}^2 * U(\theta-\theta_1-2K_4-K_3)$$

$$+ 2A_1 A_2 A_3 \left\{1 - e^{-(\theta-K_2-K_3-K_4)/K_1}\right\} * U(\theta-K_2-K_3-K_4)$$

$$-2A_1 A_2 A_3 \left\{1 - e^{-(\theta-K_2-K_3-K_4)/K_1}\right\} * U(\theta-\theta_1-K_2-K_3-K_4)] x \frac{1}{1+f_2}$$

..... 2.8.10

Assuming that the pulse width θ_1 is less than $2K_2$, $(K_2 + K_3)$ and $(K_3 + K_4)$, equation 2.8.10 produces eight different composite curves each comprising eleven parts, for the conditions $K_2 < K_4$ and $K_2 > K_4$. If $K_2 < K_4$ the limits of the four curves are as follows :-

(1) $K_2 < (\theta_1+K_2) < K_4 < (\theta_1+K_4) < (2K_2+K_3) < (\theta_1+2K_2+K_3) < (K_2+K_3+K_4)$
$< (\theta_1+K_2+K_3+K_4) < (2K_4+K_3) < (\theta_1+2K_4+K_3)$

(2) $K_2 < K_4 < (\theta_1+K_2) < (\theta_1+K_4) < (2K_2+K_3) < (K_2+K_3+K_4) < (\theta_1+2K_2+K_3)$
$< (2K_4+K_3) < (\theta_1+K_2+K_3+K_4) < (\theta_1+2K_4+K_3)$

(3) $K_2 < (\theta_1+K_2) < (2K_2+K_3) < (\theta_1+2K_2+K_3) < K_4 < (\theta_1+K_4) < (K_2+K_3+K_4)$
$< (\theta_1+K_2+K_3+K_4) < (2K_4+K_3) < (\theta_1+2K_4+K_3)$

(4) $K_2 < (\theta_1+K_2) < (2K_2+K_3) < K_4 < (\theta_1+2K_2+K_3) < (\theta_1+K_4) < (K_2+K_3+K_4)$
$< (\theta_1+K_2+K_3+K_4) < (2K_4+K_3) < (\theta_1+2K_4+K_3)$

If $K_2 > K_4$ the limits of the four curves are as follows :-

(5) $K_4 < (\theta_1+K_4) < (2K_4+K_3) < (\theta_1+2K_4+K_3) < K_2 < (\theta_1+K_2)$
$< (K_2+K_3+K_4) < (\theta_1+K_2+K_3+K_4) < (2K_2+K_3) < (\theta_1+2K_2+K_3)$

(6) $K_4 < (\theta_1+K_4) < (2K_4+K_3) < K_2 < (\theta_1+2K_4+K_3) < (\theta_1+K_2)$
$<$ as for (5)

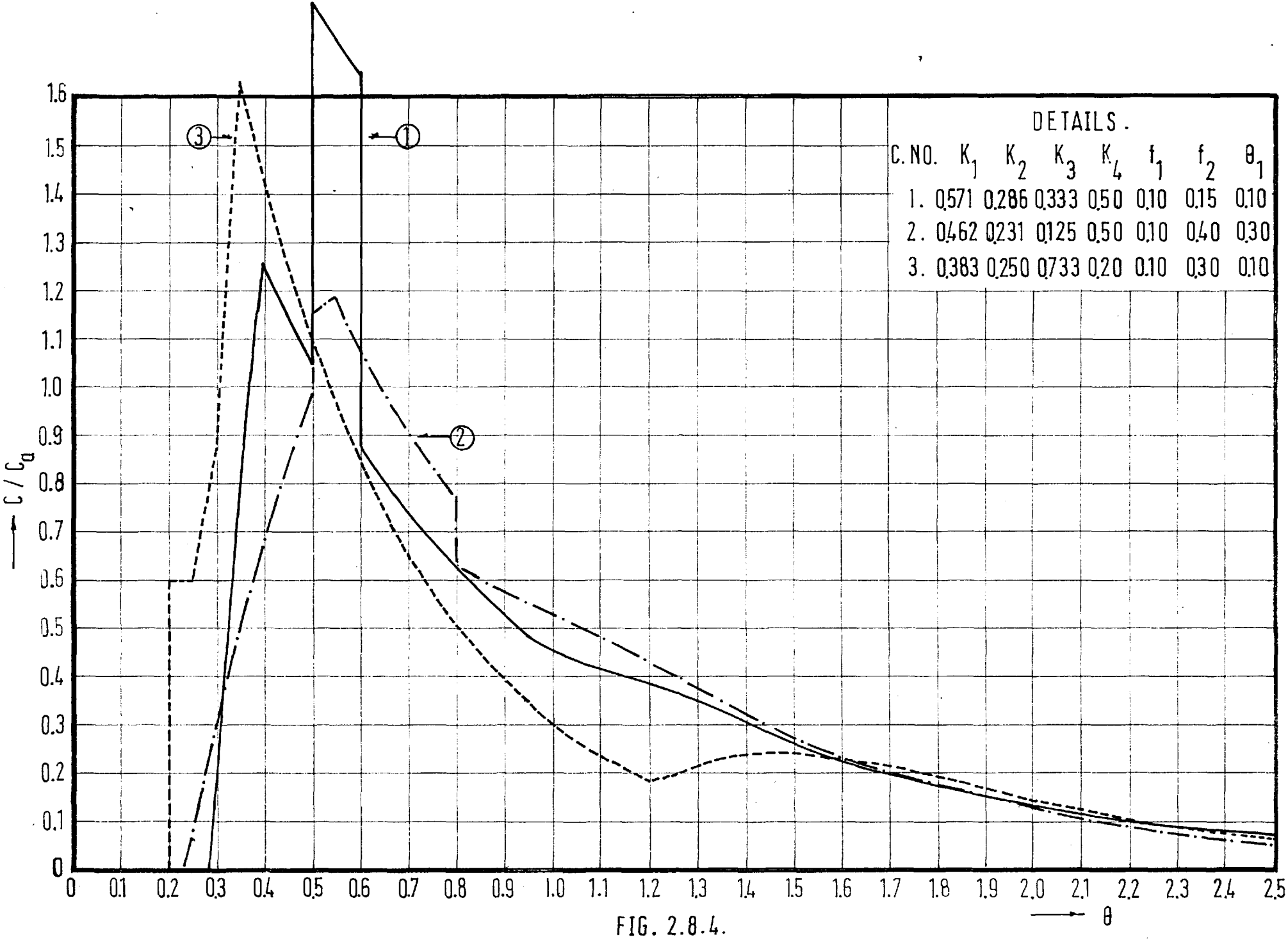
DETAILS.
C.NO. K1 K2 K3 K4 f1 f2 θ1
1. 0.571 0.286 0.333 0.50 0.10 0.15 0.10
2. 0.462 0.231 0.125 0.50 0.10 0.40 0.30
3. 0.383 0.250 0.733 0.20 0.10 0.30 0.10
C / Ca
θ
1
2
3

FIG. 2.8.4.

(7) $K_4 < (\theta_1+K_4) < K_2 < (2K_4+K_3) < (\theta_1+K_2) < (\theta_1+2K_4+K_3)$

$<$ as for (5)

(8) $K_4 < K_2 < (\theta_1+K_4) < (\theta_1+K_2) < (2K_4+K_3) < (\theta_1+2K_4+K_3)$

$< (K_2+K_3+K_4) < (2K_2+K_3) < (\theta_1+K_2+K_3+K_4) < (\theta_1+2K_2+K_3)$

Equation 2.8.10 has been computed and presented on Fig.2.8.4 as curves 1, 2, and 3 for conditions (1), (2) and (8) respectively. These may be compared with the curves on Fig.2.8.3. On comparison it can be seen that the most obvious effects of shortcircuiting part of the recirculated flow are to reduce the magnitude of the peaks of the curves. Also it is clear that peaks in the immediate vicinity of the major peak of a curve cannot be caused by recirculation unless the flow in the main path is predominantly plug flow.

2.9. Conclusion

In this chapter a number of models are suggested which might be used to study complex flow situations. In a practical case a flow test should be performed and the flow curve obtained for a known rectangular input. The output curve is then studied and a model is selected. The corresponding theoretical curve is fitted to the practical curve within acceptable limits of accuracy by varying the values of the parameters. The best model is that which gives the best fit for the minimum number of parameters. This approach is referred to hereinafter as "the direct method".

In the next chapter, another technique of analysis, known in Control Systems theory as the "Pulse Response Technique", is considered. Although "Pulse Response" or "Frequency Response" techniques are standard methods of analysis in control systems, they are seldom used in systems with long residence times. However, it has been found that this technique produces valuable information regarding the nature of such a system and may be used as a guide in selection of the initial values of the parameters, in analysis of a flow curve by the direct method.

CHAPTER III

THEORY PART B

3.1. Frequency Response

A well known technique used for testing the dynamic properties of a system in Electrical Engineering is that of frequency response. It involves the application of a sinusoidal pulse at the input end of a system under steady state conditions and the measurement of the steady state variation of the output response. The frequency of the applied input is varied over a wide range and the corresponding responses are recorded. From these frequency response data, it is possible to determine time constants, undamped natural frequencies, and damping ratios in the circuits under test.

Enough information is stored in the frequency response data to determine the output from the circuit due to any input within the limits of linear operation. However according to Clements et al.[32] this technique is not as widely used in chemical engineering as one would expect considering its many advantages.

The basic mathematical background associated with pulse spectra and frequency response information is given here. According to the well known theory of Fourier, it is possible to represent almost any periodic function as the summation of a series of sinusoidal waves of different frequencies and amplitudes[33]. A pulse form may be analysed as being composed of a d.c. component (zero frequency), a fundamental frequency, and an infinite number of harmonics, the amplitude and phase of each component depending upon the shape and characteristics of the pulse form[34]. Any repeating function of time having an angular period of 2π may be represented by the Fourier series:-

$$S_n = \frac{a_o}{2} + a_1 \cos\theta + a_2 \cos 2\theta + \ldots\ldots a_n \cos n\theta$$
$$+ b_1 \sin\theta + b_2 \sin 2\theta + \ldots\ldots b_n \sin n\theta \qquad \ldots\ldots 3.1.1.$$

where

$\theta = 2\pi f_p t = wt$

$f_p = {}^1/_{\text{Time Period}} = \text{Pulse repetition rate}$

$w = \text{Angular frequency in radians/sec.}$

$$a_n = \frac{1}{\pi} \int_{-\pi}^{+\pi} f(\theta).\cos n\theta \, d\theta$$

$$b_n = \frac{1}{\pi} \int_{-\pi}^{+\pi} f(\theta) \sin n\theta \, d\theta$$

$$a_o = \frac{1}{\pi} \int_{-\pi}^{+\pi} f(\theta) \, d\theta$$

The term $\frac{1}{2}a_o$ represents the d.c. component, the $(a_1 \cos\theta + b_1 \sin\theta)$ represents the fundamental frequency harmonic, the $(a_2 \cos 2\theta + b_2 \sin 2\theta)$ represents the second harmonic and so on up to the nth harmonic.

Equation 3.1.1. can be written as:-

$$S_n = \tfrac{1}{2}a_o + c_1 \sin(\theta+\phi_1) + c_2 \sin(2\theta+\phi_2) + \ldots\ldots$$
$$\ldots\ldots + c_n \sin(n\theta+\phi_n) \qquad \ldots\ldots 3.1.2.$$

where the c's are the coefficients of the Fourier series.

$$c_n = (a_n^2 + b_n^2)^{+\frac{1}{2}} \text{ and } \phi_n = \tan^{-1}\frac{a_n}{b_n}$$

If these coefficients c_n are plotted for n = 1,2,3 ... etc a curve is obtained. The ordinates of this curve at n = 1,2,3, etc are known as the Pulse Frequency Spectrum.

If the shape of a particular pulse remains the same, but the pulse repetition rate is decreased (see Fig.3.1.1) then more lines are added to the spectrum. The magnitudes of these lines compared

with those of the previous spectrum are reduced, but the ratios of these magnitudes to one another remain the same. Part (i) of Fig.3.1.1 shows a periodic rectangular pulse of time period T, part (ii) shows the same rectangular pulse with a time period 2T. Part (iii) shows the plot of c_n versus 'w' associated with part (i), and part (iv) shows the increased number of spectral lines and reduced magnitude associated with part (ii).

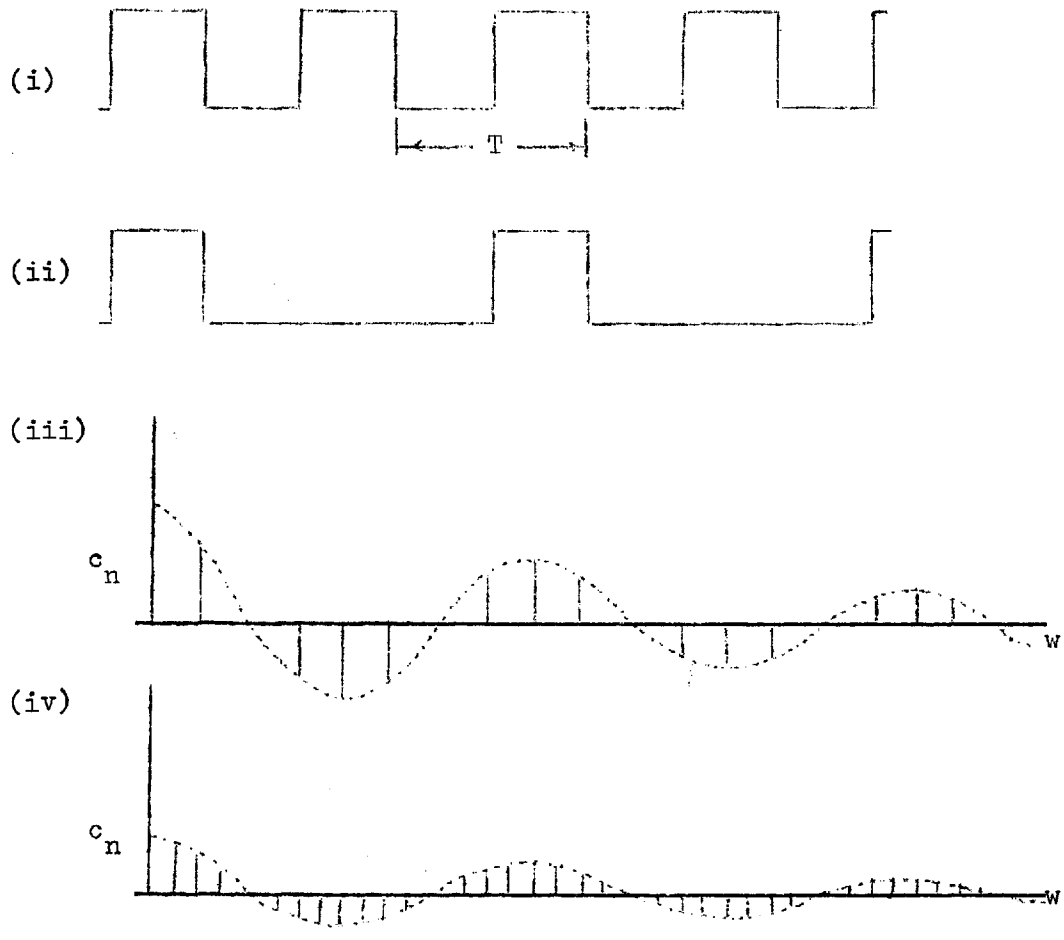

Fig.3.1.1

The sinusoidal nature of the c_n plot is due to the fact that $b_n = 0$ for a rectangular pulse and $c_n = a_n$. As the pulse occurs less and less often, the spectrum contains more and more lines, until in the limiting case, the pulse occurs only once and the spectral lines merge with each other to form a continuous envelope curve. Any individual amplitude is infinitesimal, but the envelope still retains

the same shape as before[34]. The expression which describes this envelope is the Fourier integral of the time function which represents the pulse form. This operation is known as taking the Fourier transform.

The Fourier Integral is the integral of the Fourier series described by equation 3.1.1.

If the pulse form is described by a function f(t), then the Fourier transform (hereinafter referred to as the FT) of f(t) is given by:

$$FT\ (f(t)) = \int_{-\infty}^{+\infty} f(t)e^{-jwt}dt = F(jw) \qquad \ldots\ldots\ 3.1.3$$

For a single pulse, the limits of the integral are from 0 to t_p, where t_p = pulse width. Therefore equation 3.1.3 becomes

$$FT\ (f(t)) = \int_{0}^{t_p} f(t)e^{-jwt}dt \qquad \ldots\ldots\ 3.1.4$$

where w = frequency in radians per second

and $j = \sqrt{-1}$

The Frequency Response of a system is defined as the ratio of the Fourier transform (FT) of the output pulse to the FT of the input pulse:

$$\text{Frequency Response} = \frac{\text{FT output}}{\text{FT input}} = G(jw) \qquad \ldots\ldots\ 3.1.5$$

It is also known as the "Performance Function" and it should be noted that it is defined in a manner similar to the "Transfer Function" of Chapter 2. The transfer function is expressed in terms of the Laplace "S" and is in the time domain, whereas the frequency response is in the frequency domain and may be obtained by simply writing **S** = jw. From equation 3.1.5 it follows that:-

$$FT\ output = FT\ input \times G(jw) \qquad \ldots\ldots\ 3.1.6$$

Thus if the system characteristics are known, the FT of the output

pulse can be predicted for any input pulse. If on the other hand the output pulse is known corresponding to a known input pulse, then the Frequency Response for the system can be determined.

For any particular value of w, G(jw) can be represented as

$$G(jw) = |G| \angle \phi_G \text{.....} \quad \text{..... 3.1.7}$$ (35)

The part $|G|$ refers to the magnitude or amplitude and the $\angle \phi_G$ is the angle or phase. These values of magnitude and phase angle are the ratios of the magnitudes and phase angles of corresponding input and output pulses, obtained in accordance with the rules of vector algebra. The magnitude of the quotient of two vectors is equal to the quotient of their magnitudes and the phase angle of the quotient of two vectors is equal to the phase angle of the vector in the numerator minus the phase angle of the vector in the denominator[36].

For this reason $|G|$ in equation 3.1.7 is known as the magnitude ratio or "gain" between the output and the input amplitudes:-

$$|G| = \frac{\text{Output amplitude}}{\text{Input amplitude}}$$

Referring to Fig.3.1.2 if G_i represents the amplitude of the input pulse and G_o that of the output pulse, then the magnitude ratio of the frequency response of the system is given by $|G| = G_o/G_i$, and the phase angle ϕ_g in radians by which the output lags behind the input is given by $\phi_G = \phi_{G_i} - \phi_{G_o}$ where ϕ_{G_i} represents the phase angle described by the input pulse from the origin and ϕ_{G_o} that of the output pulse. In fig.3.1.2 $\phi_{G_i} = 0$. Therefore $\phi_G = -\phi_{G_o}$ which is negative because it lags behind the input. Thus if a pure sinusoidal input is introduced into a linear system, the magnitude ratio can be easily obtained from the amplitudes of the input and output pulses. The feasibility of this technique in cases of pure plug flow is illustrated by Denbigh[3] and Krenkel[37].

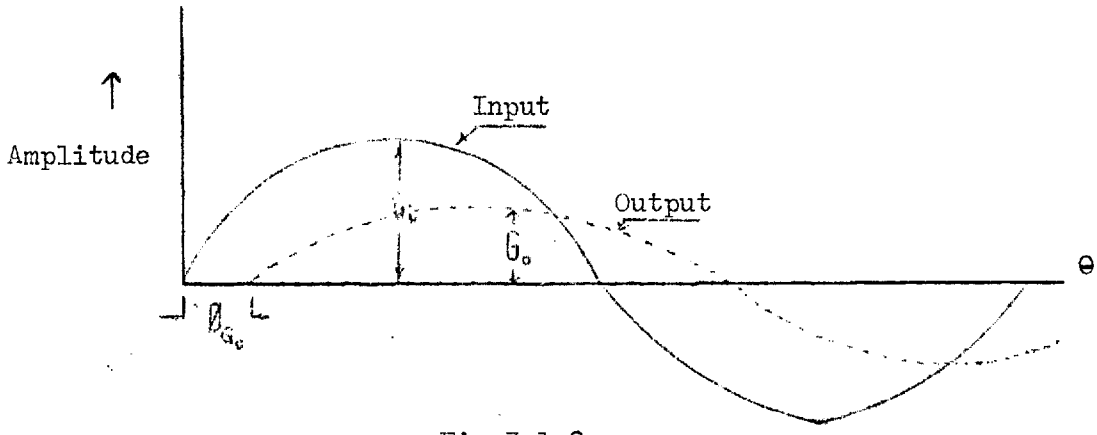

Fig.3.1.2

3.2. System characteristics from Frequency Response Functions

The problem is that of determining the system characteristics embodied in the Frequency Response Function G(jw). If the output corresponding to a particular input is known, from these data, the magnitude ratio and phase angle can be determined by a data reduction technique which will be discussed later. In Chapter 2 transfer functions corresponding to various theoretical models were derived and from each of these transfer functions the magnitude ratio and phase angle can be determined directly for the particular theoretical model. By comparing the magnitude ratio or the phase angle obtained from the mathematical model which includes the various parameters representing the system characteristics, with the magnitude ratio or phase angle obtained from the experimental data, optimum values of the parameters can be determined.

The manner in which the M.R. (magnitude ratio) is obtained from the system transfer function is illustrated by the following simple example. Let the transfer function of a system be

$$\text{T.F.} = \frac{1}{1 + ST}$$

Writing $S = jw$, $G(jw) = \dfrac{1}{1 + jwT}$ ..... 3.2.1.

In this case the numerator is simply 1. In the complex plane this is represented by a vector A as shown in Fig.3.2.1, having a magnitude of 1 and a phase angle 0 with the +ve real axis. The denominator is a complex number of which the real part is equal to 1 and the imaginary part is equal to wT. It can be represented by the vector B the magnitude of which is $(1 + w^2T^2)^{\frac{1}{2}}$ which makes an angle ϕ with the positive real axis. From Fig.3.2.1 it can be seen that $\tan \phi = wT$, so that $\phi = \tan^{-1} wT$. From the last section it follows that for this system

$$M.R. = {}^{1}/(1 + w^2T^2)^{\frac{1}{2}}$$
$$\phi = - \tan^{-1} wT$$

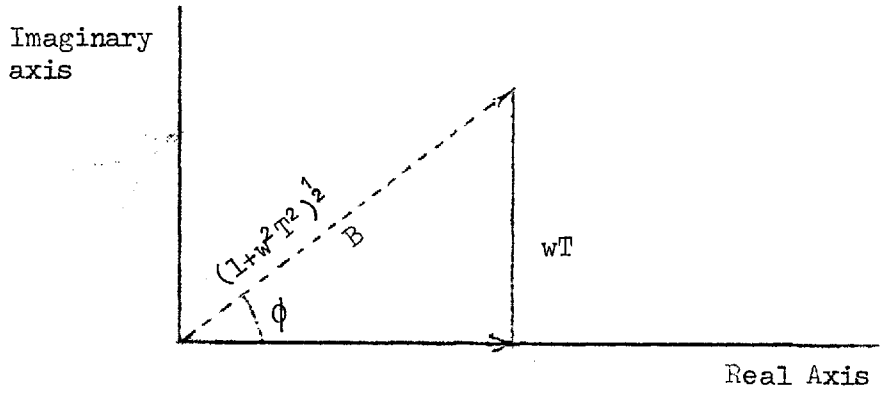

Fig.3.2.1

Considering experimental results, it is comparatively easy to determine the M.R. from a purely sinusoidal input and sinusoidal output. However in practice, a purely sinusoidal input is difficult to generate, and is not always desirable for other reasons. Such a series of pulses may interfere with the steady flow condition of a system, and from a practical viewpoint cannot be continued for a long time because of possible interruptions in the normal running of a plant. For flow systems in which changes occur very rapidly a sinusoidal input cannot be used. The use of a single pulse for these studies is more common, as it can produce the same amount of

information as a series of pulses and an input of any known pulse shape can be used. The time taken is shorter and the equipment required is less costly in the case of a single pulse. Law and Bailey[38] distinguish the use of a single pulse from the use of a train of pulses by calling the former the "Pulse Technique" and the latter the "Frequency Response Technique".

If $C_i(t)$ and $C_o(t)$ are the input and output pulse functions respectively and T_i and T_o are the corresponding pulse widths then the Frequency Response of the system from equations 3.1.4 and 3.1.5 is:-

$$G(jw) = \frac{\text{FT(Output pulse)}}{\text{FT (Input pulse)}} = \frac{\int_o^{T_o} C_o(t)e^{-jwt}dt}{\int_o^{T_i} C_i(t)e^{-jwt}dt} \qquad \ldots\ldots 3.2.2$$

Using the Euler relationship,

$$e^{-jx} = \cos x - j \sin x$$

Equation 3.2.2 becomes

$$G(jw) = \frac{\int_o^{T_o} C_o(t) \cos wt\, dt - j \int_o^{T_o} C_o(t) \sin wt\, dt}{\int_o^{T_i} C_i(t) \cos wt\, dt - j \int_o^{T_i} C_i(t) \sin wt\, dt} \qquad \ldots\ldots 3.2.3$$

Let $A = \int_o^{T_o} C_o(t) \cos wt\, dt$

$B = \int_o^{T_o} C_o(t) \sin wt\, dt$

$C = \int_o^{T_i} C_i(t) \cos wt\, dt$ and

$D = \int_o^{T_i} C_i(t) \sin wt\, dt$

Equation 3.2.3 may be written

$$G(jw) = \frac{A - jB}{C - jD} \qquad \ldots\ldots 3.2.4$$

It follows therefore from section 3.1 that the magnitude ratio and phase angle are given by:-

$$\left.\begin{aligned} M.R. &= \left[\frac{A^2 + B^2}{C^2 + D^2}\right]^{\frac{1}{2}} \quad \text{and} \\ \phi &= \tan^{-1}\left[\frac{A.D - B.C}{C^2 + D^2}\right] \end{aligned}\right] \qquad \ldots\ldots 3.2.5$$

For a particular frequency, the values of A, B, C and D can be obtained with the aid of a digital computer, using a technique known as a data reduction technique. The key to the successful use of this technique is the accurate evaluation of the integrals represented by A, B, C and D, and this in turn depends upon the accuracy with which the input and output pulses are recorded. Various methods have been proposed in the literature [32][38][39] for evaluating these integrals. The trapezoidal approximation technique of Dreifke et al.[40] which is a modification of earlier techniques has been used in this study and is described below.

If the pulse to be integrated is as shown in Fig.3.2.2

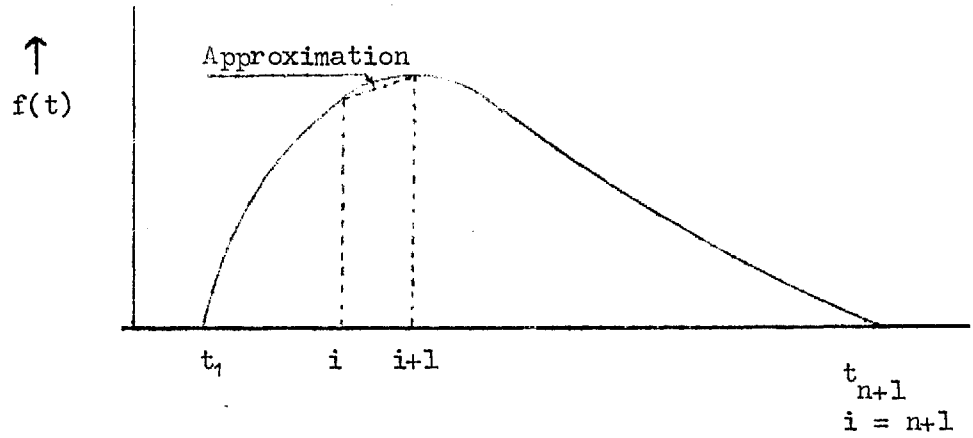

Fig.3.2.2

Let f_i be the ordinates of the pulse i = 1,2,3,...n+1 and consider two such ordinates f_i and f_{i+1}. The tops of the ordinates are joined by a straight line which approximates the curve connecting them as shown. The interval between the two ordinates is taken as Δt.

Therefore the equation of the straight line which approximates the curve is given by

$$f(t) = f_i + [(f_{i+1}-f_i)/\Delta t](t - t_i) \qquad \ldots\ldots 3.2.6$$

where t_i is the time at the i_{th} ordinate. Re-arranging equation 3.2.6

$$f(t) = f_i(1 - \frac{t}{\Delta t} + \frac{t_i}{\Delta t}) + f_{i+1}(\frac{t}{\Delta t} - \frac{t_i}{\Delta t}) \qquad \ldots\ldots 3.2.7$$

The Fourier Transform of the function f(t) considered at the i_{th} interval can be evaluated from its definition as

$$F.T._i\ (f(t)) = \int_{t_i}^{t_{i+1}} f(t)e^{-jwt}dt \qquad \ldots\ldots 3.2.8$$

Therefore from equation 3.2.7

$$F.T._i\ \ f(t) = \int_{t_i}^{t_{i+1}} \left\{ f_i(1+\frac{t_i}{\Delta t} - \frac{t}{\Delta t}) + f_{i+1}(\frac{t}{\Delta t} - \frac{t_i}{\Delta t}) \right\} e^{-jwt}dt \qquad \ldots\ldots 3.2.9$$

It can be shown (see Appendix) that equation 3.2.9 on integration yields

$$F.T._i \left\{f(t)\right\} = \frac{f_i.j}{w}\left[\frac{j}{w\Delta t}e^{-jwt_{i+1}} - (\frac{j}{w\Delta t} + 1)e^{-jwt_i}\right]$$

$$+\frac{f_{i+1}}{w}\left[1 - \frac{j}{w\Delta t}e^{-jwt_{i+1}} + \frac{j}{w\Delta t}e^{-jwt_i}\right] \ldots\ldots 3.2.10$$

The integrals for the trapezoidal intervals can now be summed over the whole pulse width from t_1 to t_{n+1}

$$\therefore FT_{t_1-t_{n+1}} \left\{f(t)\right\} = \sum_{i=1}^{i=n} FT_i \left\{f(t)\right\} \qquad \ldots\ldots 3.2.11$$

For convenience equation 3.2.11 can be written as

$$FT_{t_1-t_{n+1}}\{f(t)\} = \frac{f_1 \cdot j}{w}\left[\frac{j}{w\Delta t}e^{-jwt_2} - \left(1+\frac{j}{w\Delta t}\right)e^{-jwt_1}\right]$$

$$+\sum_{i=2}^{i=n}\frac{f_1 \cdot j}{w}e^{-jwt_i}\left[\frac{j}{w\Delta t}e^{-jw\Delta t} - \left(\frac{j}{w\Delta t}+1\right)+\left(1-\frac{j}{w\Delta t}\right)+\frac{j}{w\Delta t}e^{jw\Delta t}\right]$$

$$+ f_{n+1}\cdot\frac{j}{w}e^{-jwt_{n+1}}\left[\left(1-\frac{j}{w\Delta t}\right)+\frac{j}{w\Delta t}e^{jw\Delta t}\right] \quad \ldots\ldots 3.2.12$$

Note that the first and last segments under the curve are integrated separately by Dreifke et al.[40]. Separating the real and imaginary parts of equation 3.2.12 it can be written as follows (see Appendix)

$$FT_{t_1-t_{n+1}}\{f(t)\} = \left[\Delta t f_1\left\{\frac{1}{2}\left(\frac{\sin w\frac{\Delta t}{2}}{w\frac{\Delta t}{2}}\right)^2\cos wt_1 - \frac{1}{w\Delta t}\left(1-\frac{\sin w\Delta t}{w\Delta t}\right)\sin wt_1\right\}\right.$$

$$+\Delta t\left(\frac{\sin w\frac{\Delta t}{2}}{w\frac{\Delta t}{2}}\right)^2 x\sum_{i=2}^{n} f_i\cos wt_i$$

$$\left.+\Delta t.f_{n+1}\left\{\frac{1}{2}\left(\frac{\sin w\frac{\Delta t}{2}}{w\frac{\Delta t}{2}}\right)^2\cos wt_{n+1}+\frac{1}{w\Delta t}\left(1-\frac{\sin w\Delta t}{w\Delta t}\right)\sin wt_{n+1}\right\}\right]$$

$$+j\left[\Delta t f_1\left\{-\frac{1}{2}\left(\frac{\sin w\frac{\Delta t}{2}}{w\frac{\Delta t}{2}}\right)^2\sin wt_1 - \frac{1}{w\Delta t}\left(1-\frac{\sin w\Delta t}{w\Delta t}\right)\cos wt_1\right\}\right.$$

$$+\Delta t\left(\frac{\sin w\frac{\Delta t}{2}}{w\frac{\Delta t}{2}}\right)^2 x\sum_{i=2}^{n} f_i\,(-\sin wt_i)$$

$$\left.+\Delta t.f_{n+1}\left\{-\frac{1}{2}\left(\frac{\sin w\frac{\Delta t}{2}}{w\frac{\Delta t}{2}}\right)^2\sin wt_{n+1}+\frac{1}{w\Delta t}\left(1-\frac{\sin w\Delta t}{w\Delta t}\right)\cos wt_{n+1}\right\}\right] \quad \ldots\ldots 3.2.13$$

Equation 3.2.13 is used in the data reduction technique in this study and a computer programme has been written by the author in which

two different interval values Δt_1 and Δt_2 are used for the steep and the flat portions of the curves respectively.

If the function f(t) above represents the output function, then the real part of equation 3.2.13 gives the term A of equations 3.2.4 and 3.2.5 and the imaginary part of equation 3.2.13 gives the term B. If the function f(t) represents the input pulse, then the real and imaginary parts of equation 3.2.13 give the terms C and D respectively in equations 3.2.4 and 3.2.5.

Using equation 3.2.5 it is now possible to compute the magnitude ratio M.R. and the phase angle ϕ for various values of the frequency w. This computation is made from experimental data. From the transfer function of the proposed theoretical model, the magnitude ratios and phase angles are also computed for the same values of frequency. The parameters that control the theoretical transfer function are optimised so that the magnitude ratio and phase angle obtained from the theory fit those obtained from the experimental data.

The optimisation method known also as the regression technique[38] consists of matching magnitude ratios and phase angles in Bode form. The plots of M.R. versus w and ϕ versus w on log.log paper are known as Bode plots. This is a standard method of analysis[35,38,40] and typical Bode plots are shown in Fig.3.2.3.

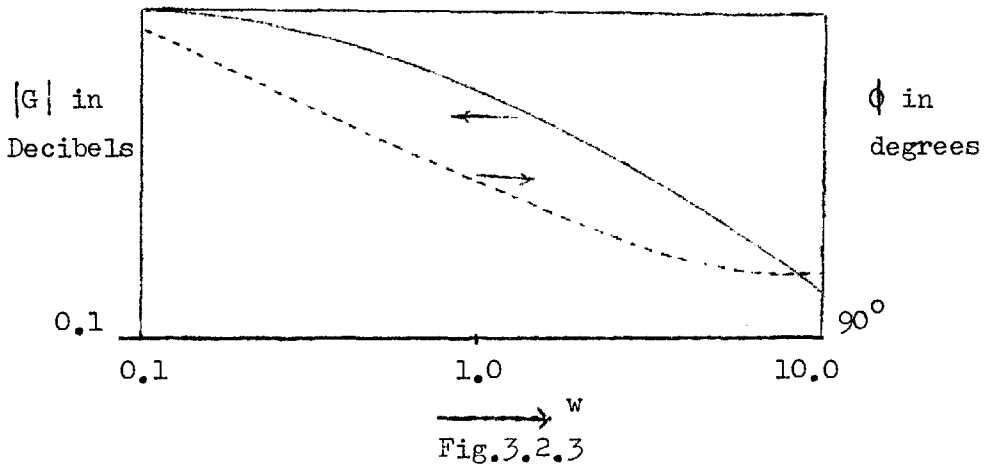

Fig.3.2.3

The magnitude ratio at zero frequency is known as the system gain. In the Bode representation, the magnitude ratio data are normalised before plotting by dividing all values by the system gain. Also in the data reduction technique, the time lag (known also as dead time) for the first arrival of tracer at the output should be removed from the output pulse test data by shifting the time origin to the first arrival point.

The optimisation of model parameters can be achieved by matching either magnitude ratios or phase angles for the appropriate frequency range. Either is sufficient and in this study magnitude ratio has been used, because of the difficulty of determining in which quadrant ϕ lies when using a digital computer.

3.3. Magnitude ratios and Phase angles for the Transfer functions of theoretical models

A. The transfer function of the two parameter model of section 2.3 is given by equation 2.3.6.

$$G(S) = \frac{e^{-K_2 S}}{1+K_1 S}$$

Converting to frequency domain by writing $S = jw$

$$G(jw) = \frac{e^{-jwK_2}}{1+jwK_1}$$

or

$$G(jw) = \frac{\cos wK_2 - j \sin wK_2}{1 - j(-wK_1)}$$

Using equation 3.2.5

$$M.R. = \left[\frac{1}{1 + K_1^2 w^2}\right]^{\frac{1}{2}} \qquad \ldots\ldots 3.3.1$$

and

$$\phi = - \tan^{-1} K_1 w \qquad \ldots\ldots 3.3.2$$

B. The transfer function of the four parameter short circuiting model of section 2.5 is given by equation 2.5.1.

$$G(S) = fe^{-K_3 S} + (1-f)e^{-K_2 S}/(1+K_1 S)$$

or

$$G(S) = \left\{fe^{-K_3 S}(1+K_1 S) + (1-f)e^{-K_2 S}\right\}/(1+K_1 S)$$

Converting to frequency domain :-

$$G(jw) = [\{f(\cos K_3 w - j \sin K_3 w)(1+jK_1 w)+(1-f)(\cos K_2 w - j \sin K_2 w)\}/(1+jK_1 w)]$$

or

$$G(jw) = [\{f \cos K_3 w + jfK_1 w \cos K_3 w - jf \sin K_3 w + fK_1 w \sin K_3 w + (1-f) \cos K_2 w - j(1-f) \sin K_2 w\}/(1+jK_1 w)]$$

or

$$G(jw) = [\{f(\cos K_3 w + K_1 w \sin K_3 w)+(1-f) \cos K_2 w\} - j\{f(\sin K_3 w - K_1 w \cos K_3 w)+(1-f) \sin K_2 w\}] / \{1-j(-K_1 w)\}$$

Using equation 3.2.5

$$M.R. = \left[[\{f(\cos K_3 w + K_1 w \sin K_3 w)+(1-f) \cos K_2 w\}^2 + \{f(\sin K_3 w - K_1 w \cos K_3 w + (1-f) \sin K_2 w\}^2] / (1+K_1^2 w^2)\right]^{\frac{1}{2}} \quad \ldots\ldots 3.3.3$$

$$\phi = \tan^{-1}\left[[\{f(\cos K_3 w + K_1 w \sin K_3 w)+(1-f) \cos K_2 w\}K_1 w - \{f(\sin K_3 w - K_1 w \cos K_3 w)+(1-f) \sin K_2 w\}] / (1+K_1^2 w^2)\right] \quad \ldots\ldots 3.3.4$$

Note that the system gain in this model is 1, which is obtained by putting w = 0 in equation 3.3.3.

C. The transfer function for the five parameter short circuiting model of section 2.6 is given by equation 2.6.1.

$$G(S) = f.\frac{e^{-K_3 S}}{1 + K_4 S} + (1-f)\frac{e^{-K_2 S}}{1 + K_1 S}$$

Converting to Frequency domain,

$$G(jw) = \frac{f\, e^{-jwK_3}}{1 + jwK_4} + \frac{(1-f)\, e^{-jwK_2}}{1 + jwK_1}$$

or

$$G(jw) = \frac{f\{(\cos wK_3 - j \sin wK_3)(1+jwK_1)+(1-f)(\cos K_2 w - j \sin K_2 w)(1+jwK_4)\}}{(1+jwK_4)(1+jwK_1)}$$

or

$$G(jw) = \{f(\cos wK_3 - j \sin wK_3 + jwK_1 \cos wK_3 + wK_1 \sin wK_3) + (1-f)(\cos wK_2 - j \sin wK_2 + jwK_4 \cos K_2 w + wK_4 \sin K_2 w)\} / (1+jwK_1 + jwK_4 - K_1 K_4 w^2)$$

or

$$G(jw) = [\{f(\cos wK_3 + wK_1 \sin wK_3)+(1-f)(\cos wK_2 + wK_4 \sin K_2 w)\} - j\{f(\sin wK_3 - wK_1 \sin wK_2)+(1-f)(\sin wK_2 - wK_4 \cos K_2 w)\}] / [(1-K_1 K_4 w^2) - j\{-w(K_1 + K_4)\}]$$

..... 3.3.5

Defining $A = f(\cos wK_3 + wK_1 \sin wK_3)+(1-f)(\cos wK_2 + wK_4 \sin K_2 w)$

$B = f(\sin wK_3 - wK_1 \sin wK_3)+(1-f)(\sin wK_2 - wK_4 \cos K_2 w)$

$C = (1 - K_1 K_4 w^2)$

$D = -w(K_1 + K_4)$

Equation 3.3.5 becomes

$$G(jw) = \frac{A - jB}{C - jD}$$

Using equation 3.2.5

$$M.R. = \left[\frac{A^2 + B^2}{C^2 + D^2}\right]^{\frac{1}{2}} \qquad \text{..... 3.3.6}$$

$$\phi = \tan^{-1}\left[\frac{AD - BC}{C^2 + D^2}\right]^{\frac{1}{2}} \qquad \text{..... 3.3.7}$$

D. The transfer function for the recirculation model of section 2.7 is given by equation 2.7.1.

$$G(S) = \frac{1}{(1+f)} \cdot \frac{e^{-K_2 S}}{(1+K_1 S)} \cdot \frac{}{\left\{1 - \left(\frac{f}{1+f}\right) \frac{e^{-S(K_2+K_3)}}{1 + K_1 S}\right\}}$$

Converting to frequency domain.

$$G(jw) = \frac{1}{(1+f)} \cdot \frac{(\cos K_2 w - j \sin K_2 w)}{(1+jK_1 w - K\{\cos (K_2+K_3)w - j \sin (K_2+K_3)w\})}$$

$$= \frac{1}{(1+f)} \left[\frac{\cos K_2 w - j \sin K_2 w}{\{1 - K \cos (K_2+K_3)w\} - j\{-K_1 w - K \sin (K_2+K_3)w\}} \right]$$

..... 3.3.8

where $K = \frac{f}{1+f}$

Therefore the Magnitude Ratio

$$M.R. = \frac{1}{1+f} \left[1/[\{1 - K \cos (K_2+K_3)w\}^2 + \{-K_1 w - K \sin (K_2+K_3)w\}^2] \right]^{\frac{1}{2}}$$

..... 3.3.9

and

$$\phi = \tan^{-1} \left[\frac{\cos K_2 w\{-K_1 w - K \sin (K_2+K_3)w\} - \sin K_2 w\{1-K \cos (K_2+K_3)w\}}{\{1-K \cos (K_2+K_3)w\}^2 + \{- K_1 w - K \sin (K_2+K_3)w\}^2} \right]$$

..... 3.3.10

Note that the gain of all the system models given above at zero frequency is unity. This can be used as a check on the experimental transfer function gain at zero frequency.

3.4. System Sensitivity

By increasing the number of parameters in a mathematical model, the model can be made to fit experimental data better and better. However a large number of parameters will cause overloading in optimisation and also the significance of important parameters in the model will tend to become reduced. Sensitivity analysis or the determination of the effect on the overall transfer function of the system by a small change in only one of the parameters, is useful in deciding on the number of parameters that should be included.

Himmelblau et al.[8] have defined system sensitivity as the change in the output variable due to a change in any one of the system, coefficients or in some cases system inputs. It enables an engineer to predict possible changes in

a system output quantitatively based on proposed or actual changes in the system parameters.

Horowitz[41] has defined sensitivity in Laplace Transform space in what he terms "Conventional Form" as S_x^T where

$$S_x^T = \frac{\partial T(S)}{T(S)} \Big/ \frac{\partial x}{x} \qquad \ldots\ldots 3.4.1$$

where T(S) = the transfer function of the system of which x is a parameter the sensitivity of which is to be determined. This is the inverse of Bode's original definition. Horowitz[41] specifies two conditions for the use of equation 3.4.1.

(i) The change "∂x" in the parameter should be infinitesimally small.

(ii) The parameter "x" should be independent of the other parameters in the system transfer function T(S).

The usual way of writing equation 3.4.1 is as follows:

$$S_x^T = \frac{x}{T(S)} \ast \frac{\partial T(S)}{\partial x} \qquad \ldots\ldots 3.4.2$$

If the parameter change is finite but small then

$$S_x^T = \frac{\Delta T(S)}{T(S)} \ast \frac{x}{\Delta x} \qquad \ldots\ldots 3.4.3$$

Then in a given system if there is a small change in a parameter x from x_o to x_f, and the system transfer function changes from $T_o(S)$ to $T_f(S)$, by using equation 3.4.3 and an Argand diagram S_x^T can be determined.

In the following paragraphs sensitivity analysis is applied to three of the models of Chapter 2.

(i) Consider the four parameter short circuiting model of section 2.5 in which $G_1(S) = \frac{1}{1+K_1 S}$, $G_2(S) = e^{-K_2 S}$ and $G_3(S) = e^{-K_3 S}$ and the transfer function $T = fG_3 + (1-f)G_1 . G_2$. The S within parenthesis

is omitted for simplicity.

Consider a small change in the parameter K_1.

Let the subscripts (or superscripts) o and f denote the values before and after the change. For example $G_1^{\,o}$ changes to $G_1^{\,f}$ when $K_1^{\,o}$ changes by a small increment to $K_1^{\,f}$, and the initial and final values of the transfer function are T_o and T_f respectively.

Then $T_o = fG_3 + (1-f)G_1^{\,o}G_2$

$T_f = fG_3 + (1-f)G_1^{\,f}G_2$

$\Delta G_1 = (G_1^{\,f} - G_1^{\,o})$

$\Delta T = T_f - T_o = (1-f)(G_1^{\,f} - G_1^{\,o})G_2$

$= (1-f)\Delta G_1 . G_2$

From equation 3.4.3

$$S_{K_1}^{T} \text{ or } S_{G_1}^{T} = \frac{\Delta T/T_o}{\Delta G_1/G_1^{\,o}} = \frac{(1-f)\Delta G_1 . G_2 . G_1^{\,o}}{T_o . \Delta G_1} = \frac{(1-f)G_1^{\,o}G_2}{T_o}$$

$$= \frac{(1-f)G_1^{\,o}.G_2}{fG_3 + (1-f)G_1^{\,o}G_2} = \frac{1}{1 + \dfrac{fG_3}{(1-f)G_1^{\,o}G_2}} = \frac{1}{1+L_o} \quad \ldots\ldots 3.4.4$$

where $L_o = \dfrac{fG_3}{(1-f)G_1^{\,o}G_2}$

The ratio T_o/T_f is obtained as follows :

$$\frac{T_o}{T_f} = \frac{fG_3 + (1-f)G_1^{\,o}.G_2}{fG_3 + (1-f)G_1^{\,f}.G_2} = \frac{\dfrac{fG_3}{(1-f)G_1^{\,o}G_2} + 1}{\dfrac{fG_3}{(1-f)G_1^{\,o}G_2} + \dfrac{G_1^{\,f}}{G_1^{\,o}}}$$

$$= \frac{L_o + 1}{L_o + \dfrac{G_1^{\,f}}{G_1^{\,o}}} \quad \ldots\ldots 3.4.5$$

Note that L_o, $G_1^{\,o}$ and $G_1^{\,f}$ are all functions of $S(jw)$. Hence $S_{G_1}^{T}$ and T_o/T_f are also functions of $S(jw)$. By plotting the locus of $L_o(jw)$ and $\dfrac{G_1^{\,f}}{G_1^{\,o}}(jw)$ for different values of w on an Argand

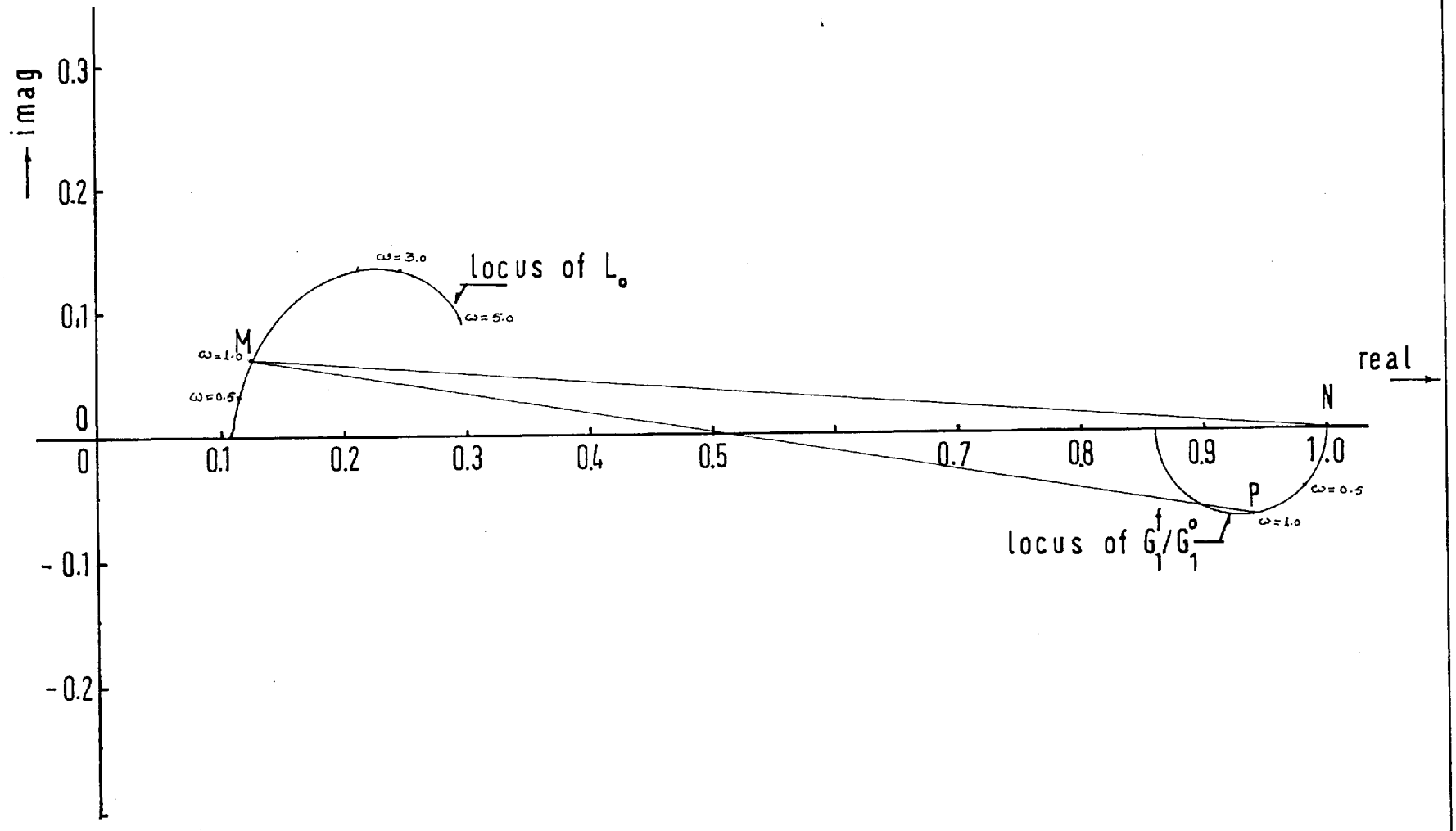
imag
0.3
0.2
0.1
0
0
-0.1
-0.2
0.1
0.2
0.3
0.4
0.5
0.7
0.8
0.9
1.0
real
ω=3.0
locus of L_o
ω=5.0
M
ω=1.0
ω=0.5
N
P
ω=0.5
ω=1.0
locus of G_1^f/G_1^o

FIG. 3.4.1

diagram, $S^{T}_{G_1}$ and T_o/T_f can be determined.

The method is illustrated by an example.

Let the values of K_1, K_2, K_3 and f in the above system be 0.778, 0.278, 0.5 and 0.1 respectively and let the time constant K_1 be changed from 0.778 to 0.90. Then the values of the parameters G_1, G_2 and G_3 are

$$G_1{}^o = \frac{1}{1+0.778S} \quad \text{and} \quad G_1{}^f = \frac{1}{1+0.90S}$$

$$G_2 = e^{-0.278S}$$

$$G_3 = e^{-0.5S}$$

Then $$L_o = \frac{fG_3}{(1-f)G_1{}^oG_2}$$

$$= \frac{1}{9}\left\{\cos(0.222w) + 0.778w \sin(0.222w)\right\}$$

$$+ j \times \frac{1}{9}\left\{0.778\ w \cos(0.222w) - \sin(0.222w)\right\} \qquad \ldots\ldots 3.4.6$$

and

$$\frac{G_1{}^f}{G_1{}^o} = \frac{1 + 0.778\ wj}{1 + 0.9\ wj} = \frac{1 + 0.7002w^2 - 0.122\ wj}{1 + 0.81\ w^2} \qquad \ldots\ldots 3.4.7$$

The loci of $L_o(jw)$ and $\left[\frac{G_1{}^f}{G_1{}^o}\right]_{jw}$ are plotted in Fig.3.4.1 from equations 3.4.6 and 3.4.7.

Considering the sensitivity of the system at w = 1 and referring to the figure, OM = L_o where M is the point on the locus of $L_o(jw)$ at w = 1 and O is the origin of the complex plane. The point N corresponds to 1.0 on the real axis. If P is the point on the locus of $G_1{}^f/G_1{}^o$ corresponding to a frequency w = 1 then the vector MN = OM + ON = L_o + 1 and the vector MP = OM + OP = $L_o + \frac{G_1{}^f}{G_1{}^o}$. From the equations 3.4.4 and 3.4.5 and Fig.3.4.1 $S^{T}_{G_1} = 1.175$ and $\frac{T_o}{T_f} = 1.06$. These two values show that the system is sensitive to changes in K_1. When a system is completely insensitive the values obtained for S^{T}_{G} tend towards 0.

It can be seen from Fig.3.4.1 that the locus of $L_o(jw)$ droops downwards for values of w greater than 3 approx., $S^T_{G_1} < 1$ and the sensitivity to change in G_1 decreases rapidly.

The effective frequency bandwidth should be determined by a stability analysis before a test for sensitivity is made, but since stability is not a problem in this type of model, this aspect of the problem is ignored in this analysis.

For comparison the sensitivity obtained from equation 3.4.2 is

$$S^T_{G_1} = \frac{G_1}{T_o} \times \frac{\partial T}{\partial G_1} = \frac{G_1 G_2 (1-f)}{fG_3 + (1-f)G_1 G_2} = \frac{1}{1 + \dfrac{fG_3}{(1-f)G_1 G_2}}$$

The result is the same as that obtained from equation 3.4.4. However the value given for $S^T_{G_1}$ by the above when $w = 0$ is $(1-f) = 0.9$ whereas the result obtained from Fig.3.4.1 is $S^T_{G_1\ w=o} = 1.12$ and $\frac{T_o}{T_f} = 1$. This discrepancy is due to the fact that the change in the value of G_1 is not infinitesimal.

Consider now the sensitivity of T for the same model to a small change in G_3. Let the value of K_3 change from 0.5 to 0.6. Then

$$T_o = fG_3{}^o + (1-f)G_1 G_2$$

$$T_f = fG_3{}^f + (1-f)G_1 G_2$$

$$\Delta T = T_f - T_o = f(G_3{}^f - G_3{}^o) = f\Delta G_3$$

From equation 3.4.3

$$S^T_{G_3} = \frac{fG_3{}^o}{T_o} = \frac{fG_3{}^o}{fG_3{}^o + (1-f)G_1 G_2} = \frac{1}{1 + \dfrac{(1-f)G_1 G_2}{fG_3{}^o}}$$

$$= \frac{1}{1 + L_o} \qquad \ldots\ldots 3.4.8$$

where L_o in this case is equal to

$$L_o = \frac{(1-f)G_1 G_2}{fG_3} = \frac{0.9}{0.1} \cdot \frac{e^{-S(.278-0.5)}}{1 + 0.778S} \qquad \ldots\ldots 3.4.9.$$

and $$\frac{T_o}{T_f} = \frac{1 + L_o}{L_o + {G_3}^f/{G_3}^o} \qquad \ldots\ldots 3.4.10$$

$${G_3}^f/{G_3}^o = \frac{e^{-K_3 {}^f S}}{e^{-K_3 {}^o S}} = e^{-S({K_3}^f - {K_3}^o)} = e^{-0.1wj} \qquad \ldots\ldots 3.4.11$$

The loci of $L_o(jw)$ and $\left[\frac{{G_3}^f}{{G_3}^o}\right]_{(jw)}$ are plotted in Fig.3.4.2. The sensitivity in this case is found to vary widely with the frequency w. At low values of w the sensitivity is quite small, e.g.

$w = 1 \qquad S^T_{G_3} = 0.16$

$w = 0 \qquad S^T_{G_3} = 0.11$

But at high frequencies the system becomes more sensitive to variations in K_3, e.g.

$w = 3 \qquad S^T_{G_3} = 0.37$

$w = 5 \qquad S^T_{G_3} = 0.77$

However the value of ${}^T o/T_f$ does not vary very much, its value being approximately 1.0.

(ii) Sensitivity analysis is now applied to the five parameter short circuiting model of Chapter 2, section 2.6, and the method is illustrated with an example in which the value of K_1 and K_2 and f are numerically equal to those in the four parameter model above. The values of the parameters in this case are:-

$K_1 = 0.778$, $K_2 = 0.278$, $K_3 = 0.278$, $K_4 = 0.222$ and $f = 0.1$.

At first this model will be analysed to see if a change in K_1, (again from 0.778 to 0.9) changes the system sensitivity differently from the four parameter model. In this case, $G_1 = \frac{1}{1+K_1 S}$, $G_2 = e^{-K_2 S}$, $G_3 = e^{-K_3 S}$ and $G_4 = \frac{1}{1+K_4 S}$.

The initial value of the transfer function

$$T_o = fG_3G_4 + (1-f){G_1}^o.G_2$$

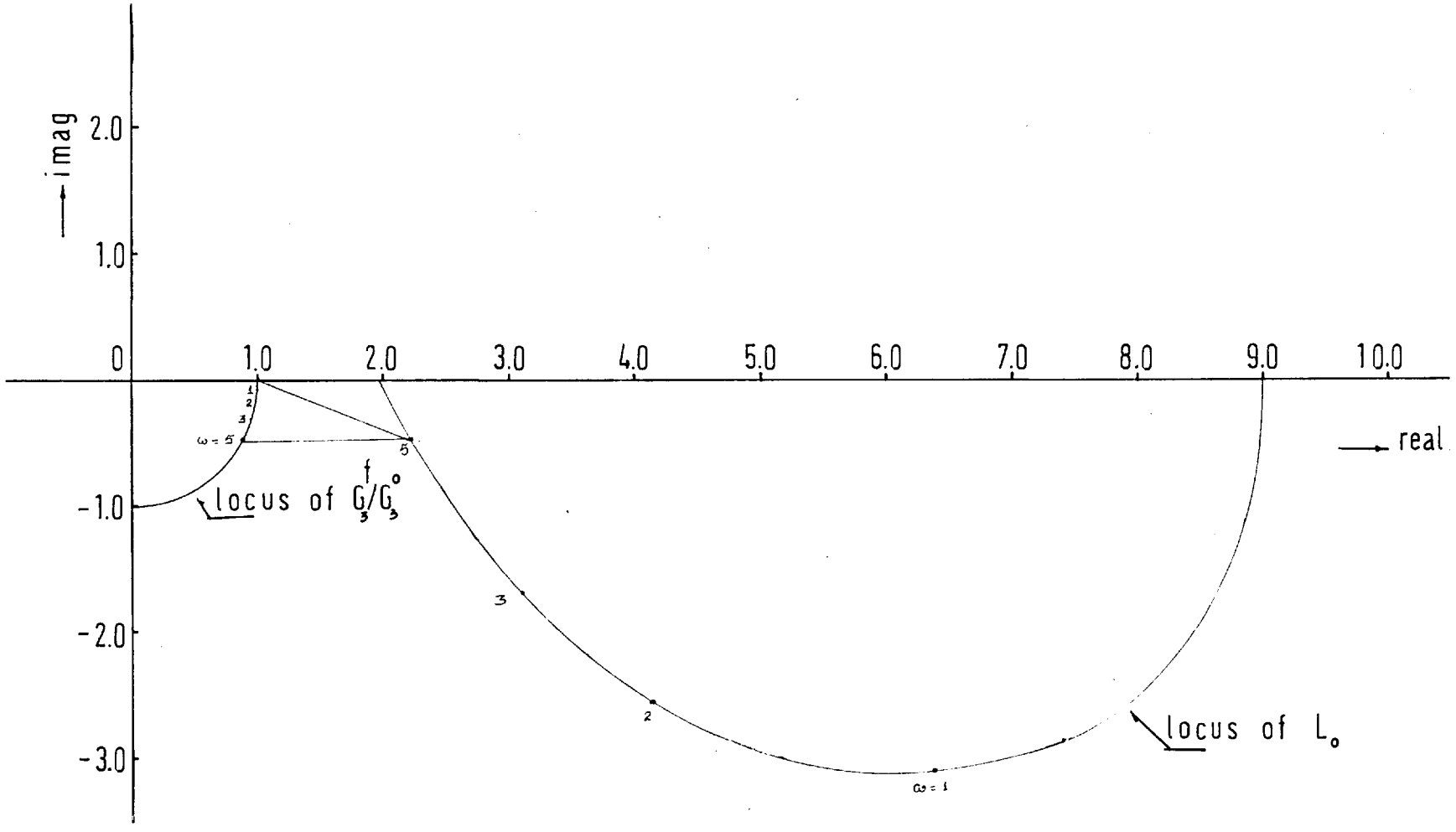
imag
2.0
1.0
0
1.0
2.0
3.0
4.0
5.0
6.0
7.0
8.0
9.0
10.0
real
-1.0
-2.0
-3.0
locus of G_3/G_3^0
locus of L_o

FIG. 3.4.2

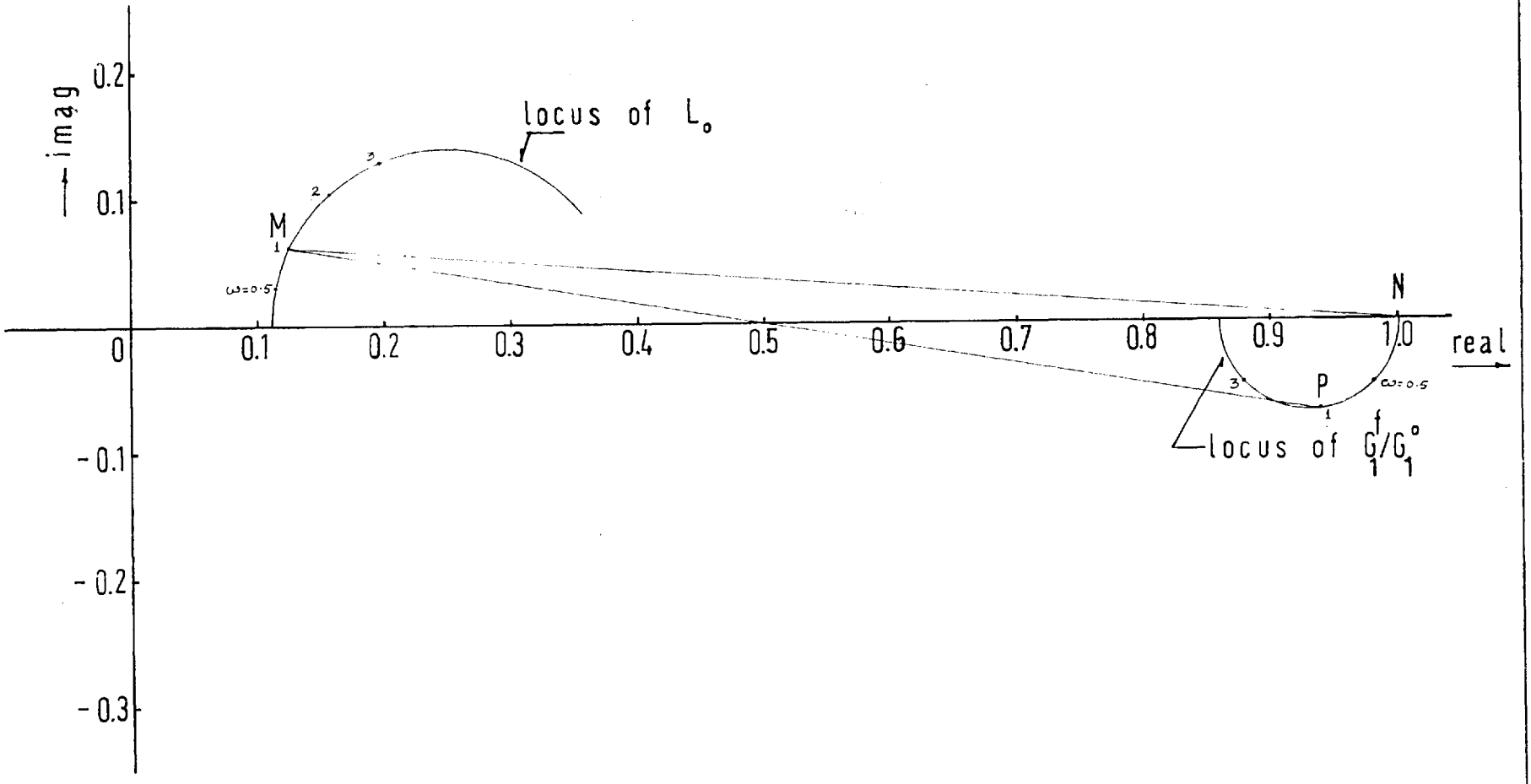
imag
0.2
0.1
0
-0.1
-0.2
-0.3
locus of L_o
M
1
2
3
ω=0.5
N
P
0.1
0.2
0.3
0.4
0.5
0.6
0.7
0.8
0.9
1.0
real
locus of G_1^f/G_1^o

FIG. 3.4.3

where $G_1{}^o$ is the value of the parameter G_1 for $K_1 = 0.778$ and $G_1{}^f$ is the new parameter value for $K_1 = 0.90$.

Therefore $T_f = fG_3G_4 + (1-f)G_1{}^f.G_2$.

Using equation 3.4.3 and procedures similar to those used in the previous model

$$S^T_{G_1} = \frac{1}{1+L_o} \quad \text{where } L_o = \frac{fG_3G_4}{(1-f)G_1{}^oG_2} = \frac{fe^{-S(K_3+K_2)}(1+K_1{}^oS)}{(1-f)(1+K_4S)} \qquad \ldots\ldots 3.4.12$$

and

$$\frac{T_o}{T_f} = \frac{1+L_o}{\frac{G_1{}^f}{G_1{}^o}+L_o} \qquad \ldots\ldots 3.4.13$$

Putting the values of K_1, K_2, K_3, K_4 and f in equation 3.4.12

$$L_o = \frac{1}{9}\,\frac{1+0.173\,w^2}{1+0.049284\,w^2} + j.\frac{1}{9}\,\frac{0.556\,w}{1+0.049284\,w^2} \qquad \ldots\ldots 3.4.14$$

and

$$\frac{G_1{}^f}{G_1{}^o} = \frac{1+j(0.778w)}{1+j(0.9\,w)} \qquad \ldots\ldots 3.4.15$$

By plotting $L_o(jw)$ and $\left[\frac{G_1{}^f}{G_1{}^o}\right]_{(jw)}$ as shown in Fig.3.4.3 the values $S^T_{G_1} = 1.14$ and $\frac{T_o}{T_f}_{w=1} = 1.06$ are obtained. When these are compared with the values $S^T_{G_1}{}_{w=1} = 1.175$ and $\frac{T_o}{T_f}_{w=1} = 1.06$, of the four parameter model it is seen that the inclusion of an additional parameter does not affect the sensitivity of the model to changes of the parameter G_1.

Now considering the effect on the sensitivity of the model caused by the change in G_3 made by increasing K_3 from 0.278 to 0.30. The sensitivity of the system is given by

$$S^T_{G_3} = \frac{1}{1+L_o} \quad \text{where } L_o = \frac{(1-f)G_1G_2}{fG_3{}^o.G_4}$$

and

$$\frac{T_o}{T_f} = \frac{L_o+1}{G_3{}^f/G_3{}^o+1}$$

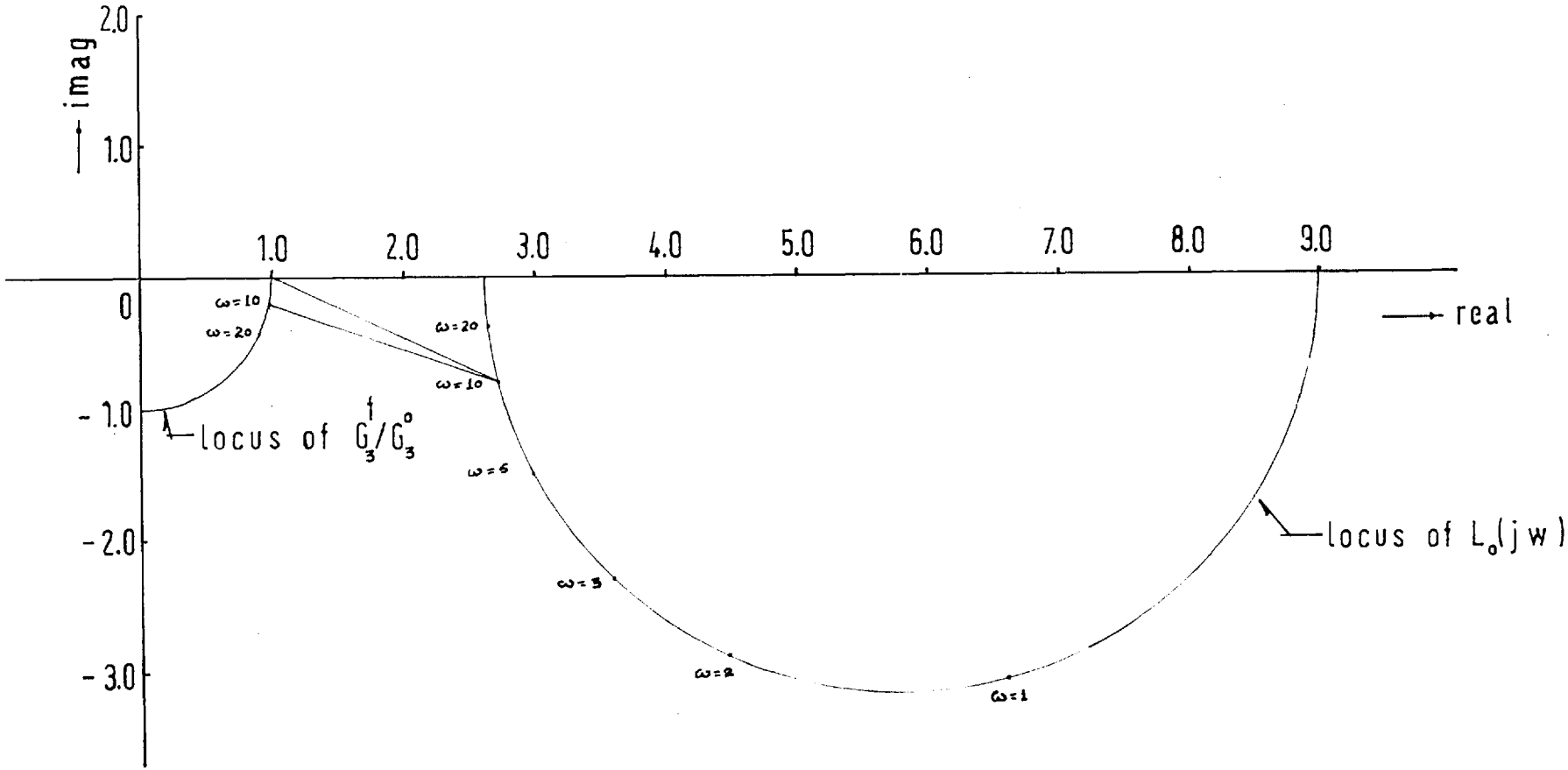
imag
2.0
1.0
0
- 1.0
- 2.0
- 3.0
1.0
2.0
3.0
4.0
5.0
6.0
7.0
8.0
9.0
real
ω=10
ω=20
ω=20
ω=10
ω=6
ω=3
ω=2
ω=1
locus of G_3^f/G_3^o
locus of $L_o(jw)$

FIG. 3.4.4

Substituting the values for K_1, K_2, $K_3{}^o$, K_4 and f in the expressions for L_o and $\frac{G_3{}^f}{G_3{}^o}$,

$$L_o = 9\left(\frac{1+0.222S}{1+0.778S}\right) = \frac{9\{1+0.173\ w^2\}}{1+0.605\ w^2} - j\,\frac{9\{0.556\ w\}}{1+0.605w^2}$$

and

$$\frac{G_3{}^f}{G_3{}^o} = e^{-j(0.022\ w)} = \cos\ (0.022\ w) - j\ \sin\ (0.022\ w)$$

Plotting the loci of $L_{o(jw)}$ and $\frac{G_3{}^f}{G_3{}^o(jw)}$ as shown in Fig.3.4.4 values of $S^T_{G_3}$ and $\frac{T_o}{T_f}$ for various values of w are determined. As in the four parameter system, this model is found to be less sensitive at low frequencies:-

$w = 1 \qquad S^T_{G_3} = 0.158$

$w = 5 \qquad S^T_{G_3} = 0.403$

whereas at $w = 10 \qquad S^T_{G_3} = 0.575$

On comparison with the four parameter model it can be seen that the sensitivity of this system to changes in K_3 is appreciably decreased by the introduction of the parameter K_4, e.g.

$w = 5 \qquad S^T_{G_3} = 0.77 \qquad$ 4 parameter case

$w = 5 \qquad S^T_{G_3} = 0.403 \qquad$ 5 parameter case

However at low frequencies, the results are very similar

(iii) In the case of recirculation models which are analogous to electrical systems with feedback, the effect of all such feedbacks is to reduce the sensitivity of the system to changes in its parameters.[8,41] Applying this analysis to the recirculation model of Chapter 2.7 in which the initial values of K_1, K_2, K_3 and f are 0.778, 0.278, 0.5, and 0.1 respectively

$$T_o = \frac{1}{(1+f)} \cdot \frac{G_1{}^o G_2}{\left\{1 - \left(\frac{f}{1+f}\right).G_1{}^o G_2 G_3\right\}}$$

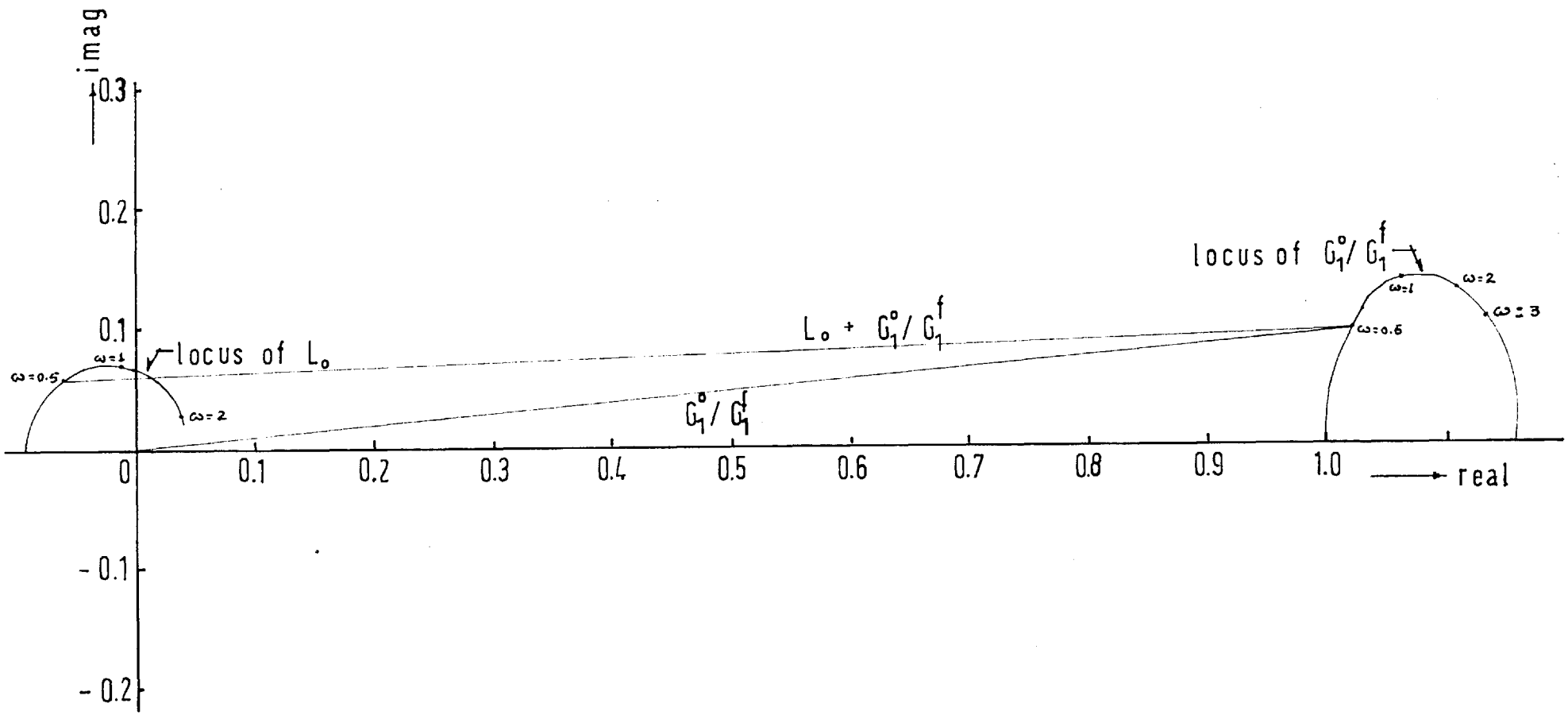
imag
0.3
0.2
0.1
- 0.1
- 0.2
0
0.1
0.2
0.3
0.4
0.5
0.6
0.7
0.8
0.9
1.0
real
locus of L_o
$L_o + G_1^o / G_1^f$
G_1^o / G_1^f
locus of G_1^o / G_1^f
ω=0.5
ω=1
ω=2
ω=0.6
ω=1
ω=2
ω=3

FIG. 3.4.5

where $G_1 = \frac{1}{1+K_1 S}$, $G_2 = e^{-K_2 S}$, $G_3 = e^{-K_3 S}$ and $G_1^{\,o}$ is the initial value corresponding to $K_1 = K_1^{\,o} = 0.778$. If $G_1^{\,f}$ is the value of G_1 when $K_1 = K_1^{\,f} = 0.90$ then

$$T_f = \frac{1}{(1+f)} \cdot \frac{G_1^{\,f} . G_2}{\left\{1 - \frac{f}{(1+f)} G_1^{\,f} . G_2 . G_3\right\}}$$

$$\Delta T = A G_2 \, \Delta G_1 \Big/ \left\{(1 - B G_1^{\,f} . G_2 . G_3)(1 - B G_1^{\,o} . G_2 . G_3)\right\}$$

where $\Delta T = (T_f - T_o)$, $\Delta G_1 = G_1^{\,f} - G_1^{\,o}$, $A = \frac{1}{(1+f)}$ and $B = \frac{f}{(1+f)}$

Then using equation 3.4.3

$$S_{G_1}^{T} = \frac{G_1^{\,o}/G_1^{\,f}}{G_1^{\,o}/G_1^{\,f} - B G_1^{\,o} G_2 G_3} = \frac{G_1^{\,o}/G_1^{\,f}}{G_1^{\,o}/G_1^{\,f} + L_o} \qquad \ldots\ldots 3.4.16$$

where $L_o = - B G_1^{\,o} . G_2 . G_3 = - \frac{f}{(1+f)} \cdot \frac{e^{-S(K_2+K_3)}}{(1 + K_1^{\,o} S)}$ 3.4.17

and $$\frac{G_1^{\,o}}{G_1^{\,f}} = \frac{1 + K_1^{\,f} S}{1 + K_1^{\,o} S} \qquad \ldots\ldots 3.4.18$$

Putting the values of the constants in equations (3.4.17) and (3.4.18)

$$L_o(jw) = - \frac{1}{11} \left\{\frac{\cos(0.778w) - 0.778\, w \sin(0.778w)}{(1 + 0.605\, w^2}\right\}$$

$$+ j \frac{1}{11} \left\{\frac{0.778w \cos(0.778w) + \sin(0.778w)}{1 + 0.605\, w^2}\right\}$$

and $$\left[\frac{G_1^{\,o}}{G_1^{\,f}}\right]_{(jw)} = \left(\frac{1 + 0.7002\, w^2}{1 + 0.605\, w^2}\right) + j\left(\frac{0.222\, w}{1 + 0.605\, w^2}\right)$$

Plotting the loci of $L_o(jw)$ and $\left[\frac{G_1^{\,o}}{G_1^{\,f}}\right]_{(jw)}$ as shown in Fig.3.4.5, the sensitivity of the system can be determined vectorially using equation 3.4.16, when

$w = 0.5$ $\qquad S_{G_1}^{T} = 0.947$

$w = 1$ $\qquad S_{G_1}^{T} = 1.0$

$$w = 2 \qquad S^{T}_{G_1} = 1.035$$

On comparison with the values obtained for the four parameter short circuiting model it can be seen that the sensitivity of the system to changes in K_1 has been decreased, as it to be expected for a system with recirculation. In a similar way the model sensitivity to changes in other parameters can be examined.

3.5. Conclusion

In this chapter various aspects of the pulse technique have been presented. It is a good method and can produce good results provided that the input and output pulses are accurately measured. Sensitivity analysis gives a guide to the range of frequencies in which the magnitude ratios and phase angles should be calculated and matched. This range of frequencies is primarily dependent on the input pulse. Hougen and Walsh[42] and Clements et al.[32] have discussed the merits of various pulse shapes. They found that an impulse can excite the highest range of frequencies and a rectangular pulse the lowest. However an impulse is difficult to measure and rarely used in practice. A narrow pulse with a sharp peak is most suitable for dynamic system analysis from experimental data.

CHAPTER IV

EXPERIMENTAL VERIFICATION OF THEORETICAL MODELS

4.1. Object of Experiments

In this chapter the experiments carried out are described. The object of these experiments was twofold, firstly to verify by direct simulation the mathematical models outlined in Chapter 2, and secondly to analyse the flow in a continuous flow rectangular model tank with the help of such mathematical techniques. In the direct simulation part of the work, 79 experiments were performed under different conditions, each one being repeated as a check on reproducibility. In the analysis of tank flow, 40 sets of experiments were performed at different flow rates, and using different input pulse shapes. Again each individual experiment was repeated once as a check on reproducibility.

4.2. Input pulse

In all these experiments an input pulse of rectangular shape was used. Various values of θ_1 in the range $0.09 \longrightarrow 4.0$ were used (where θ_1 = the dimensionless pulse width). The pulse height can also be varied and should be selected so that the pulse and its corresponding output can be measured with an accuracy which is acceptable.

In these experiments the input pulse was produced by injecting a tracer, aqueous sodium chloride, into the inflow to the system at a point sufficiently far upstream for the tracer to be completely mixed with the inflow on arrival at the input measuring point. The tracer concentration was measured in situ in the flow in terms of conductivity. Sodium chloride was used for its high solubility in water and high ionic dissociation which make it detectable in low concentrations using a sensitive bridge.

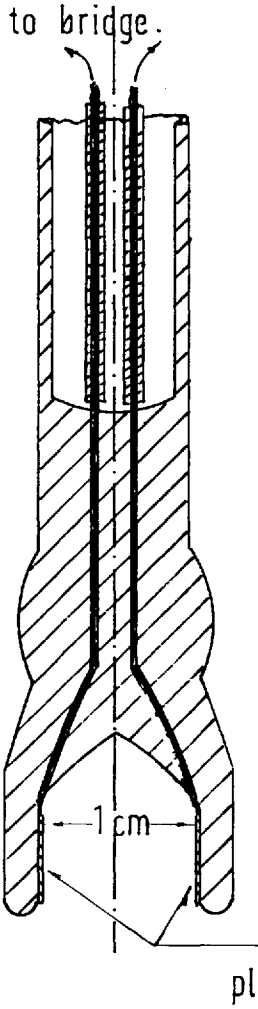

SCALE :
double size.

FIG. 4.2.1.

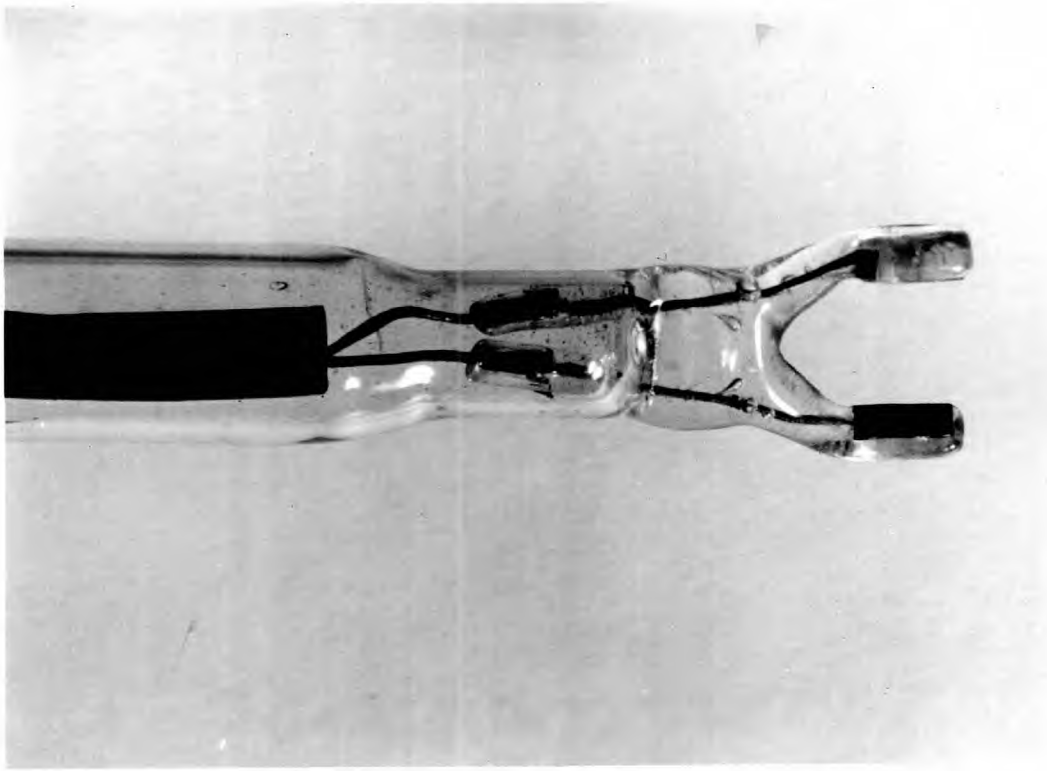

The platinum electrode cell .

PLATE 4.2.1.

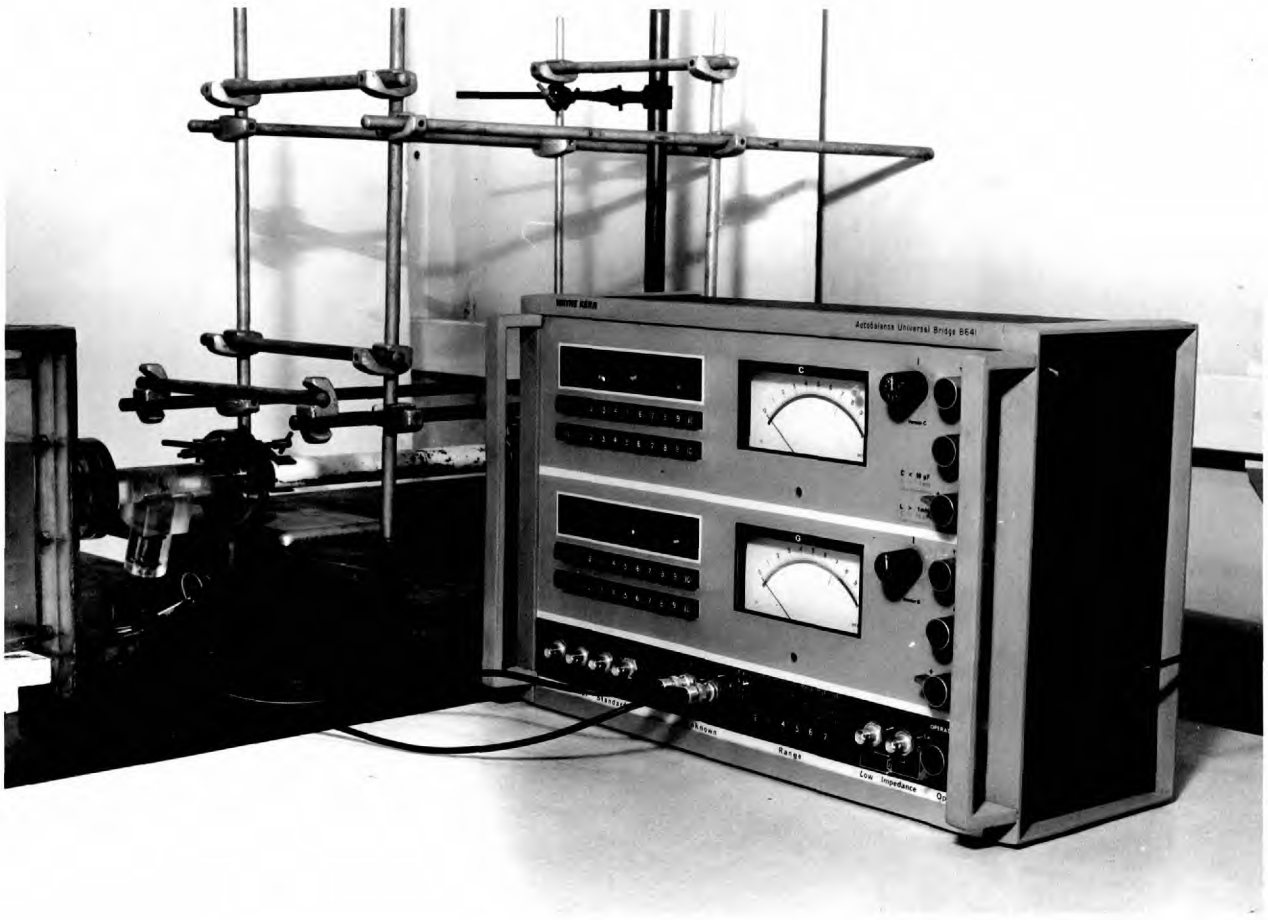

The Universal Bridge used for measuring conductivity .

PLATE 4.2.2.

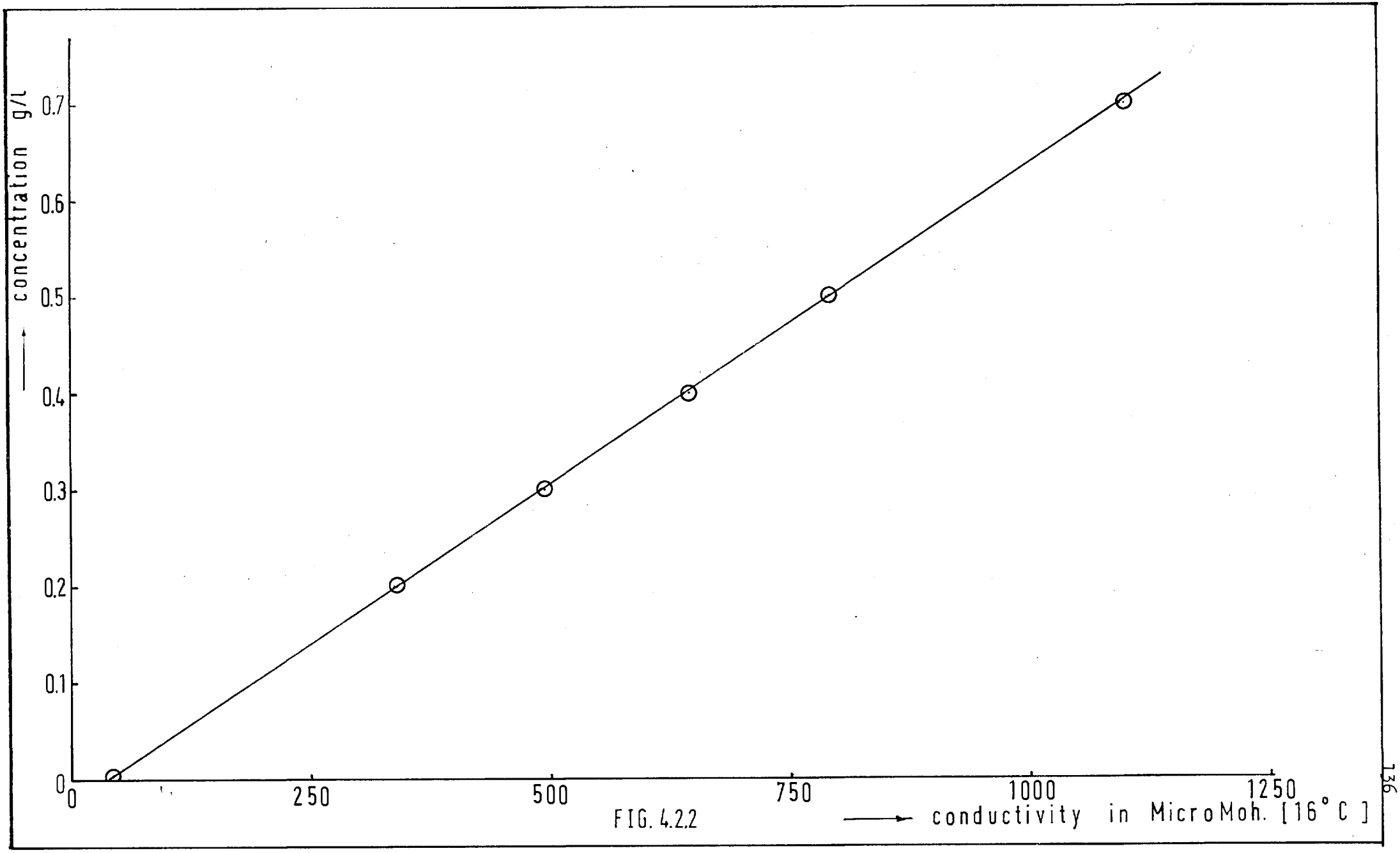
concentration g/l
0.7
0.6
0.5
0.4
0.3
0.2
0.1
0
0
250
500
750
1000
1250
conductivity in MicroMoh. [16° C]

FIG. 4.2.2

MAKE AND BREAK SWITCH .

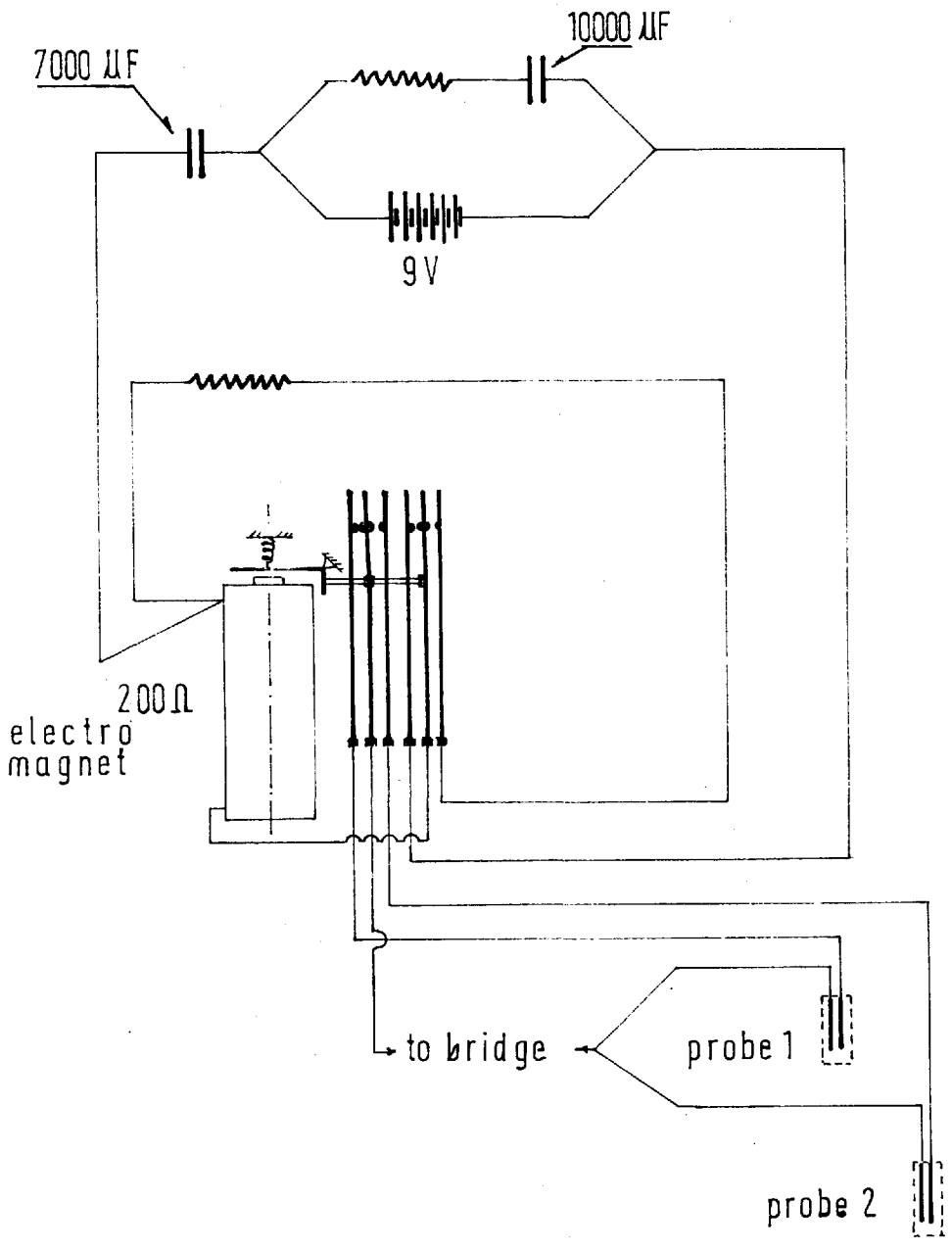

FIG. 4.2.3.

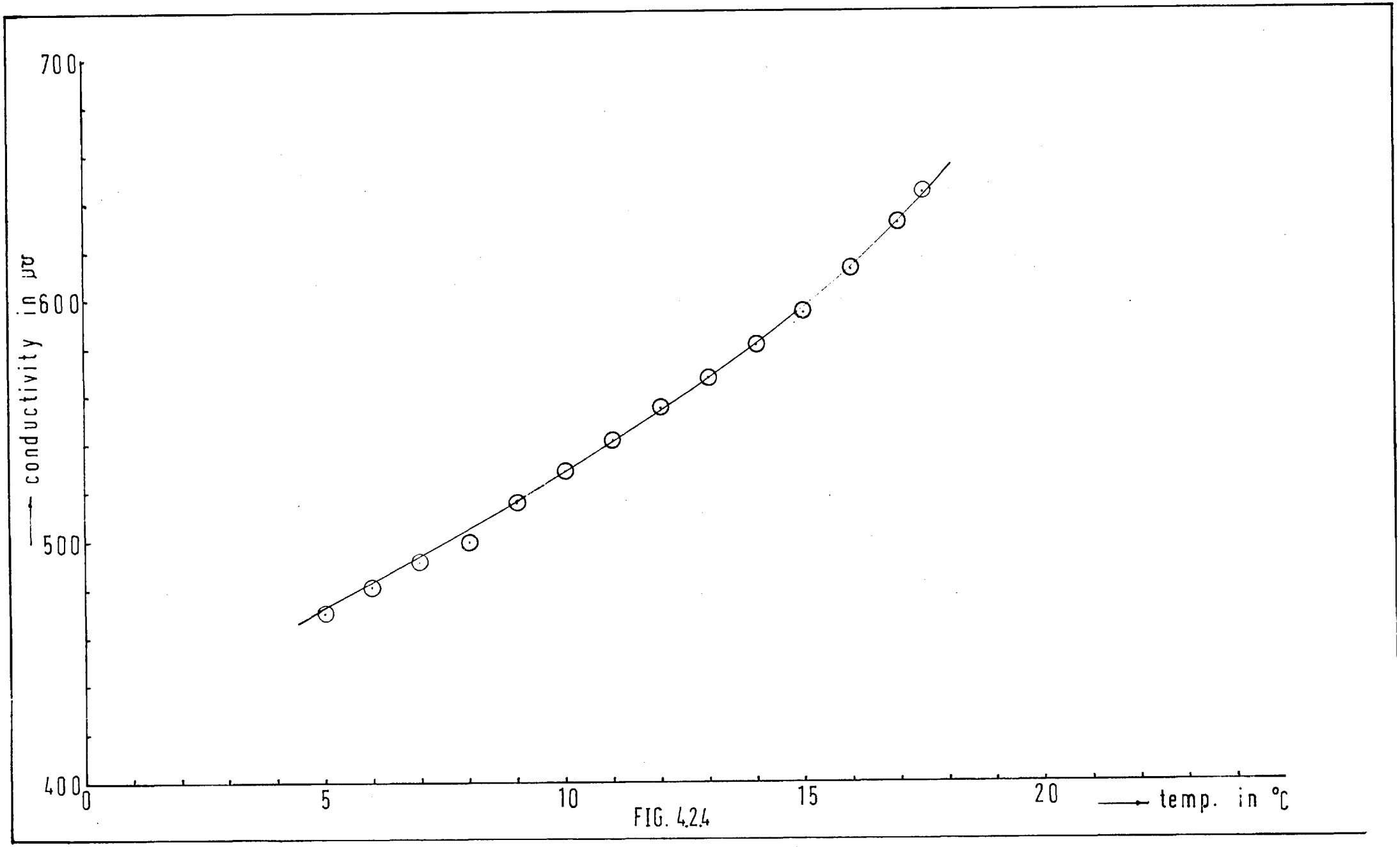

FIG. 4.24

Conductivity was measured by means of a platinum electrode cell (No.C521, Wayne Kerr) shown diagrammatically in Fig.4.2.1 and illustrated in Plate 4.2.1. The electrodes are platinized and the cell constant is 1.0 ± 1% so that when used in conjunction with a bridge, values of specific conductivity in absolute units are given directly in Mhos. The bridge used in this case was an "Autobalance Universal Bridge" (No.B641 Wayne Kerr) illustrated in Plate No.4.2.2 and the overall accuracy of the cell and bridge is ± 2%.

At low concentrations, the relationship between concentration and conductivity is linear for sodium chloride in solution (see Fig.4.2.2) so that for these experiments, the concentrations were kept within the linear range and pulse shapes could therefore be plotted directly from bridge readings. It is also sufficient that results be precise rather than accurate, as for these experiments relative values of conductivity are adequate. Absolute values of conductivity are not necessary.

In order to facilitate the measurement of pulse ordinates at short time intervals, the bridge was coupled to a digital voltmeter (Dynamco DM 2006) which gave an accuracy of 0.01% of full scale deflection. With these instruments values of conductivity could be recorded to three decimal places of a μmho. However considering that a change in temperature of 1°C results in a change in conductivity of approximately 10 μmhos or more it was decided to record values to the nearest μmho.

Two conductivity cells were used, at the inlet and outlet end of the system, each immersed in the flow, for the purpose of recording the input and output pulses. An electro-mechanical switch was used to connect the probes alternately to the bridge. The time between consecutive readings was approximately 3 seconds. The circuit

diagram of this switch is shown in Fig.4.2.3.

The principal objection to the use of sodium chloride is its high density in solution (43, 44, 45). However it is still widely used (4, 9, 46) and in this particular case, considering the lowest throughput of the rectangular tank (4.0 litres per minute) and the maximum flow of tracer (0.1 litres per minute) of concentration not greater than 10 gr/ℓ, the specific gravity of the fully mixed tracer reaching the tank inlet was found to be 0.9990 (at 20°C) compared with the specific gravity of the tapwater in the tank which was found to be 0.9989. All the experimental runs were carried out at a temperature of 7 - 8°C and the temperature was found not to vary during any experiment by more than one degree. This is important because of the non-linear relation between temperature and conductivity shown in Fig.4.2.4.

4.3. Experimental Set-up for direct simulation

Plug flow and perfect mixing are theoretical concepts which cannot be achieved in the laboratory. However plug flow can be approximated by turbulent flow in pipes[9,12] and perfect mixing can be simulated by intense agitation of the liquid in a suitable vessel using diffused air. Using appropriate combinations of these two, experimental models were built up corresponding to the theoretical models of Chapter 2.

General views of the apparatus used are illustrated in Plates 4.3.1, 4.3.2 and 4.3.3. A flow diagram is given in Fig.4.3.1. Steady flow through the system was maintained from a constant head tank of capacity 0.33 m^3, controlled by a needle valve V_1, and measured by means of a rotameter which was calibrated volumetrically a number of times.

LAYOUT OF THE DIRECT VERIFICATION APPARATUS.

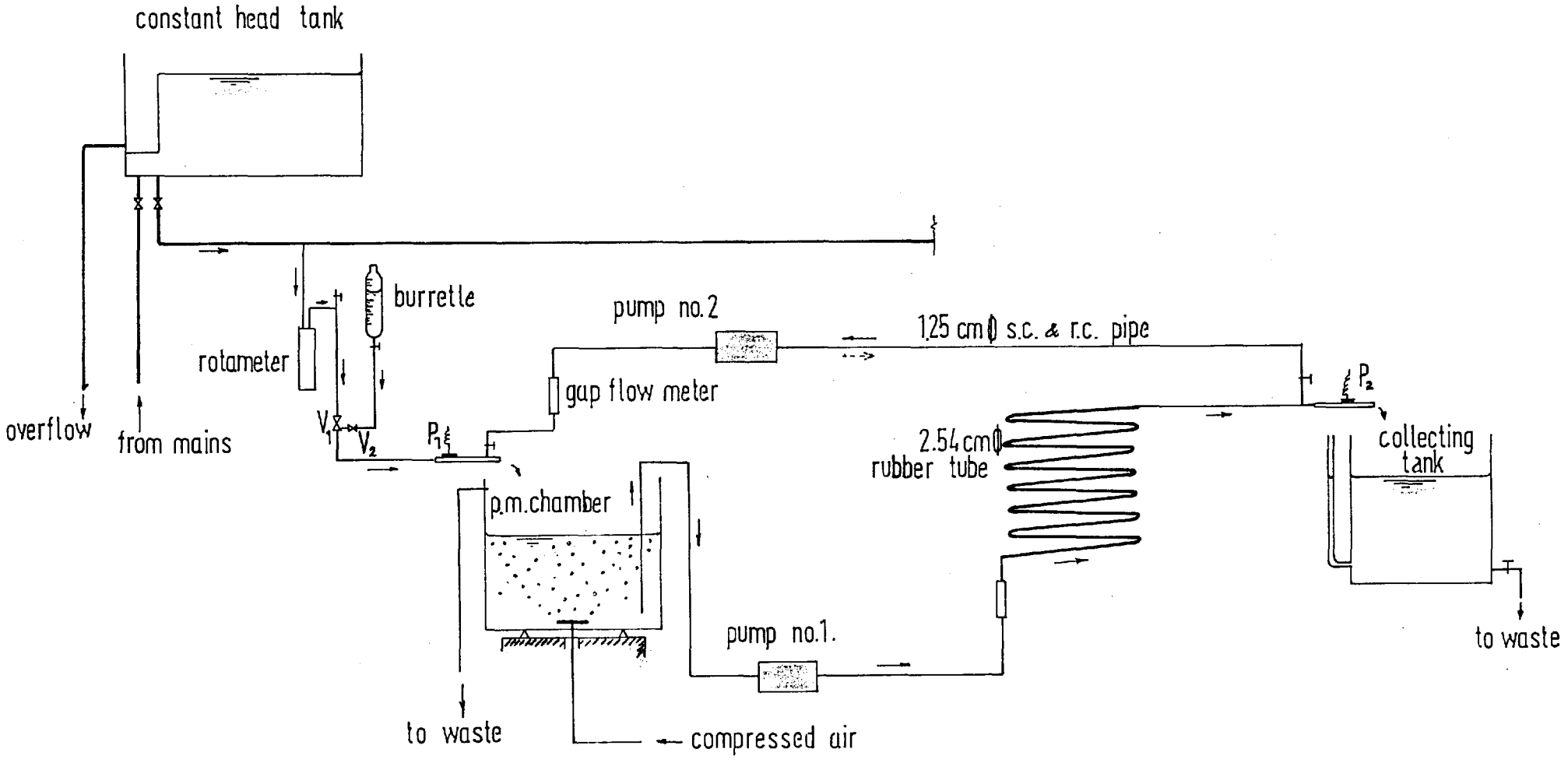

FIG. 4.3.1.

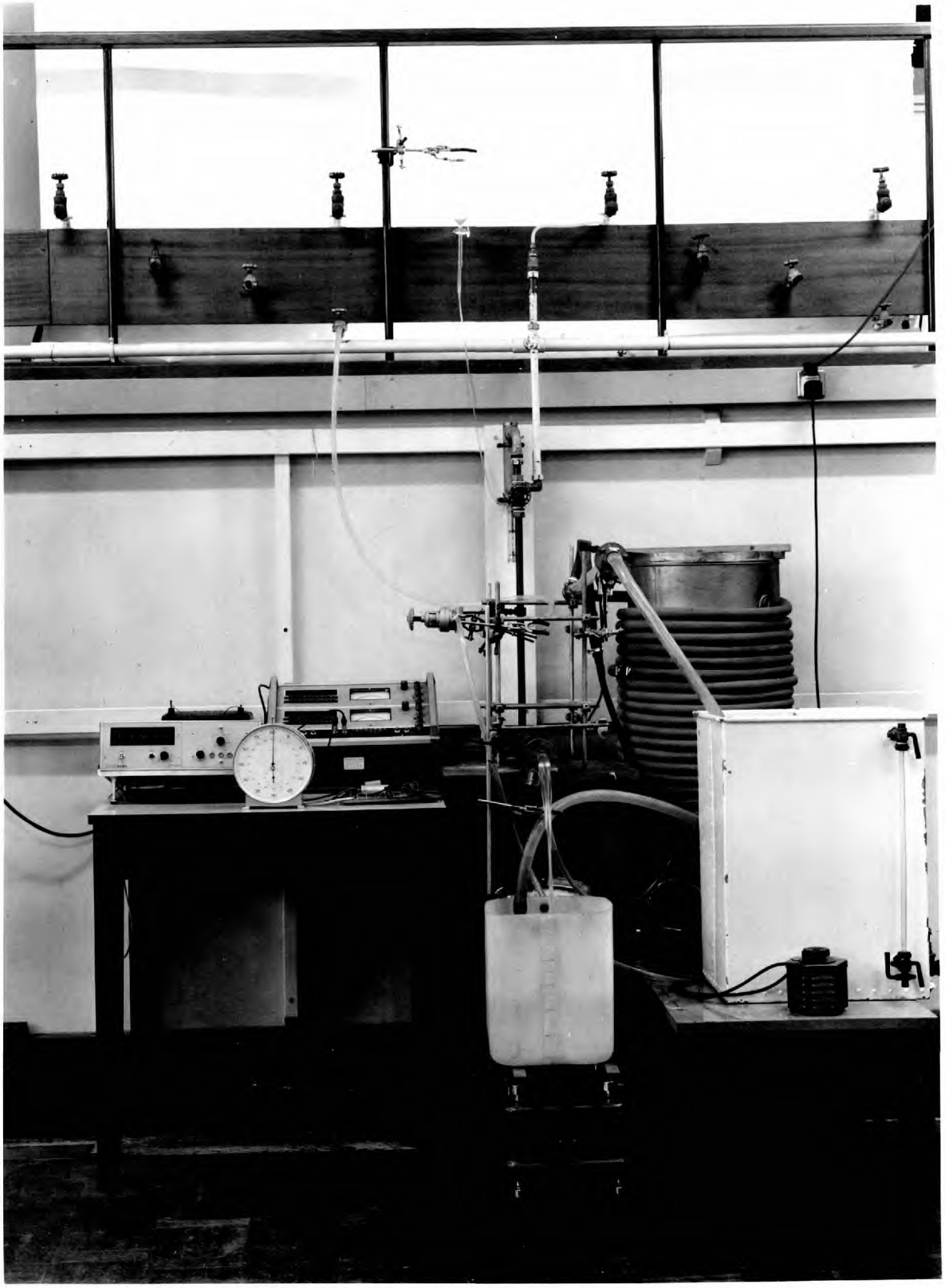

General view of the "Direct verification" set-up .

PLATE 4.3.1.

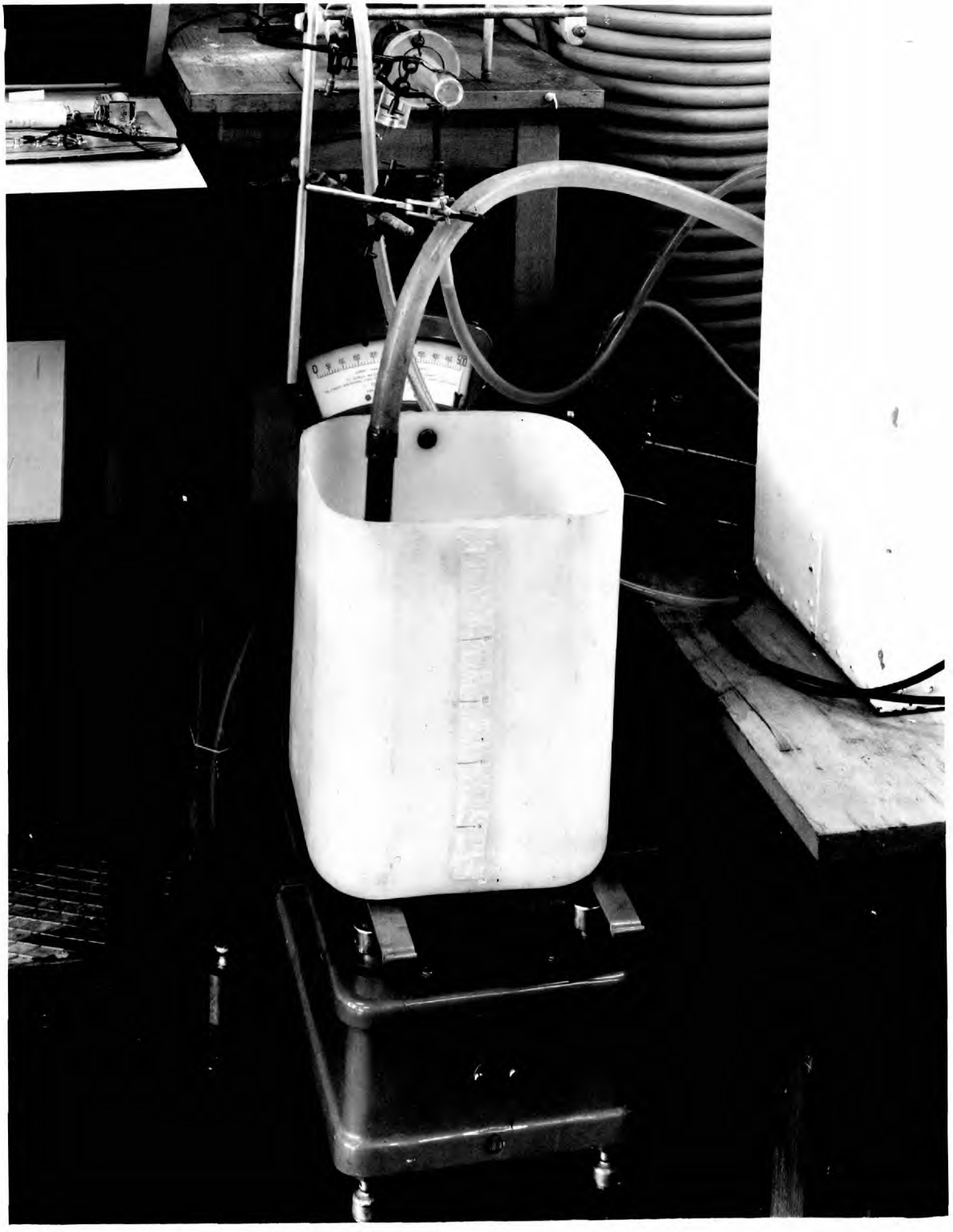

The "Perfect mixing" tank .

PLATE 4.3.2.

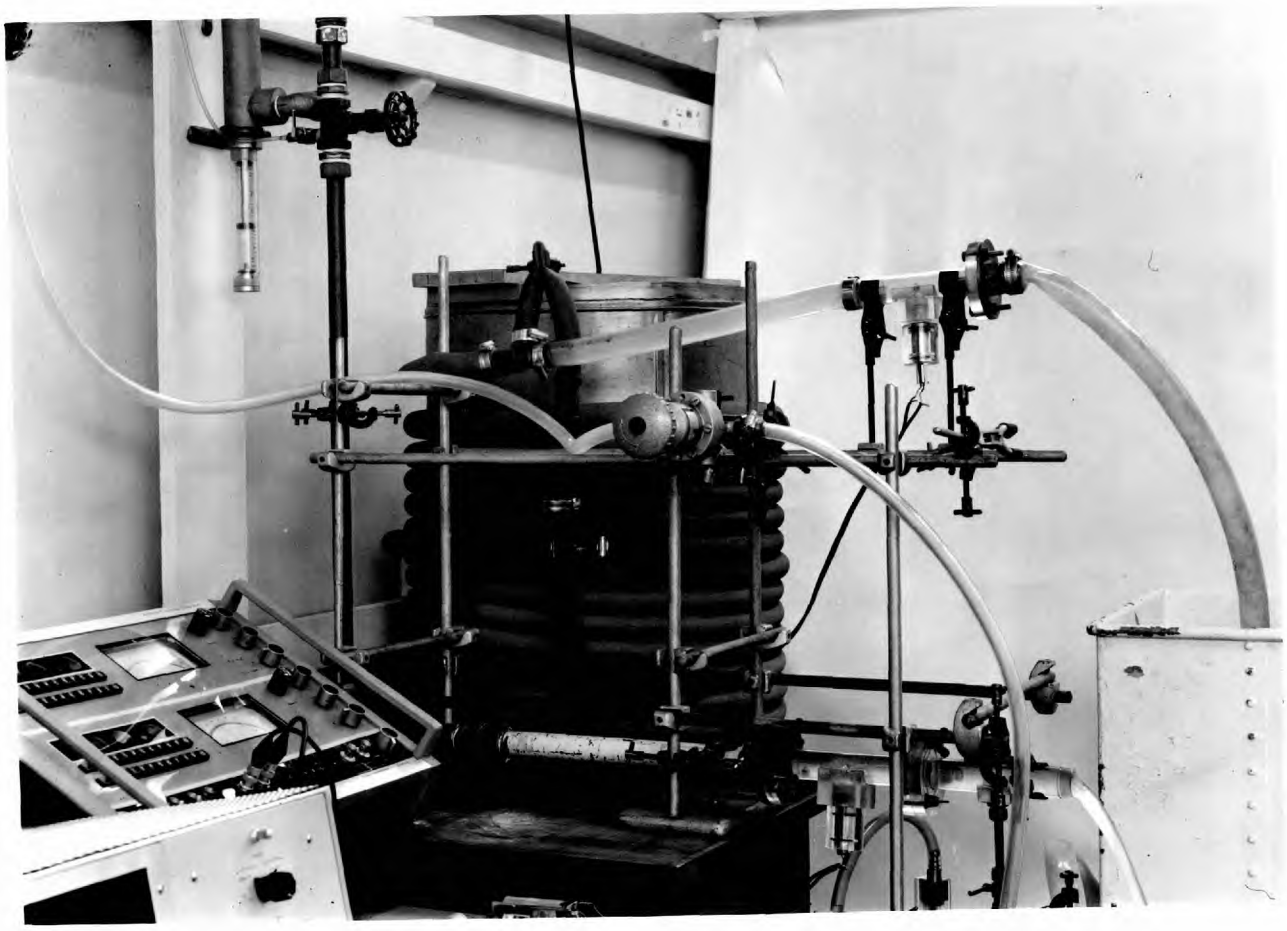

The "Plug flow" tubing .

PLATE 4.3.3.

The tracer solution was stored in a graduated vessel of capacity 1 litre fixed at a height of approximately 1 metre above the injection point. The rate of tracer flow was controlled by a valve at the base of this vessel, the vessel being connected to the tracer injection point by a 3mm bore polythene tube. At the injection point an on - off instrument toggle valve V_2, which opens and closes instantaneously gave the effect of a step rise or step fall as required in the tracer flow. To ensure good mixing the tracer was introduced into the centre of the flow through a piece of stainless steel 1 mm bore tubing inserted in the outlet of the toggle valve, and this valve was screwed into the body of the flow control valve V_1 just downstream of the valve gate.

The conductivity probes P_1 and P_2 were mounted centrally in 2.54 cm diameter perspex tubing in such a way that the electrodes were parallel to the direction of flow and equidistant from the pipe centre line.

The inflow from the tube containing P_1 discharged freely into the perfect mixing chamber, which consisted of a polythene vessel 29 cm x 30 cm x 37 cm of capacity 30 litres. Mixing was accomplished by blowing compressed air at a pressure of 0.07 Kgf/cm^2 approximately through a diffuser dome 8.75 cm diameter placed centrally at the bottom of the vessel. Mixing with compressed air was found to give better results than mechanical mixing with a stirrer. The volume of water in the perfect mixing vessel was determined directly by weighing the vessel during operation on a semi-automatic self indicating balance (Avery).

The plug flow volume consisted of 45.7 metres of 2.54 cm diameter rubber tubing wound around a 31 cm diameter drum. The tubing was subdivided into five lengths, so that a variable length could be

used, thus varying the ratio of the plug flow volume to the perfect mixing volume.

The flow from the perfect mixing chamber through the plug flow tube was maintained by a variable speed pump (No.1 of Fig.4.3.1, Stuart Turner Ltd. No.12). Steady conditions were maintained by regulating the speed of the pump in order to keep the weight of the perfect mixing chamber constant at the desired value. In this way the volume of perfect mixing was controlled to within $\pm$ 0.25 litres of the desired value. The outlet of the plug flow tube was connected to a 30 cm length of 2.54 cm dia. perspex pipe containing probe P_2 from which the flow discharged freely to the volumetric tank and hence to waste.

In order to incorporate a shortcircuiting element in the system a 7' long 1.25 cm dia. tube was connected between the downstream side of probe P_1 and the upstream side of probe P_2. The flow through this path was maintained by a variable speed pump, No.2 in Fig.4.3.1 (Charles Austen Co. type C-15) and was measured by a flow meter. This same length of tube could be used to represent recirculation by simply reversing the direction of pumping.

4.4. Objects of direct simulation experiments

The apparatus described in 4.3 was used to test the following mathematical models.

(i) The two parameter model containing perfect mixing and plug flow in series, in which the ratio of the perfect mixing to plug flow volumes could be varied.

(ii) The four parameter short circuiting model, in which the fraction of the flow which shortcircuits is varied, thus varying the shortcircuiting time and altering all the other time constants.

(iii) The recirculation model, in which the recirculation rate of flow is varied, and also the perfect mixing and plug flow fractions.

4.5. Experimental procedure for direct simulation experiments

Before conducting a flow test, the water was turned on for a considerable time at the approximate flow rate, in order to ensure that conditions reached equilibrium and temperatures and conductivity readings became steady at inlet and outlet. Then the flow was adjusted to the appropriate value by adjusting the valve V_1, and steady conditions were established throughout the system by adjusting the speed of pump No.1. If shortcircuiting or recirculation was incorporated in the model, this flow was regulated by adjusting the speed of pump No.2. Otherwise this flow path was isolated from the system.

The tracer used in these tests was prepared by dissolving sodium chloride (99.9% AnalaR) in distilled water in the desired concentration. For these tests the concentration used was 5 gr/ℓ This was thoroughly mixed in the tracer reservoir by bubbling air through before injection.

The tracer was introduced by opening valve V_2 for a predetermined length of time, and the conductivity of the flow stream was recorded at inlet and outlet at intervals of 15 seconds. It was found that the input pulse was approximately rectangular and the transition from background concentration to platform concentration required approximately 2 seconds. Recording of conductivity at P_1 and P_2 continued until the values at P_2 returned to within 1 μ℧ of the value at P_1. A record of temperature changes was also kept and any changes in background conductivity or conductivity response due to temperature changes were noted and corrections applied to the output pulse ordinates where appropriate.

4.6. Determination of mixing efficiency for the Perfect Mixing Chamber and the Plug Flow Tubing

Various experiments were conducted in order to determine the degree of mixing that could be achieved in the perfect mixing vessel at three system flow rates 5, 10 and 15 litres/minute using diffused air, and at a system flow rate of 5 ℓ/m using mechanical mixing by means of a 10 cm dia. propeller. These experiments were carried out with three different volumes of water in the mixing vessel. The outlet end of pump No.1 was directly connected to the perspex tubing housing the probe P_2.

The curves were analysed using the two parameter model and the results are tabulated in Table 4.6.1. Each result in this table is the mean of the results of three experiments, as each test was repeated three times to ensure reproducibility. It was found, other conditions being equal, that better mixing was achieved using diffused air. In the case of set 8 the diffuser was inverted. The volume of the tubing between the perfect mixing chamber and P_2 was 0.076 litres.

The volume of the plug flow in the plug flow tubing was determined by doing similar tests and again applying the two parameter model. The data are presented in Table 4.6.2.

To demonstrate the types of input and output curves obtained from these tests, the results of set Nos. 7 and 20 are plotted in Fig. 4.6.1. and 4.6.2 respectively. On these plots C refers to the concentration recorded in terms of conductivity.

From these tests it was found that approximately 90% perfect mixing could be obtained under the best conditions in the perfect mixing chamber. The higher the throughput the better the mixing obtained. It was also found that the smaller the volume of water in the vessel, the lower the value of m the perfect mixing fraction

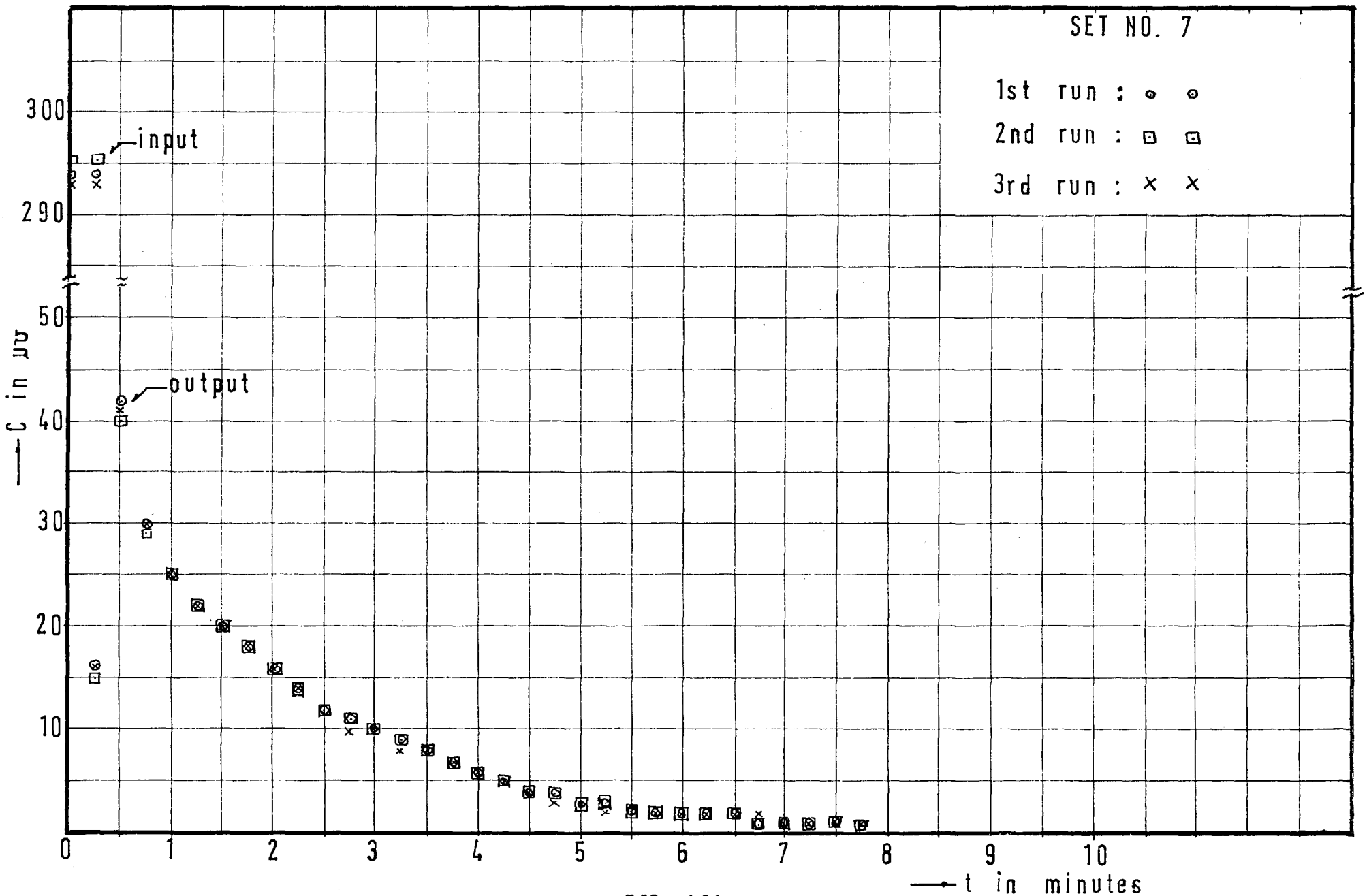
SET NO. 7
1st run : ⊙ ⊙
2nd run : ⊡ ⊡
3rd run : × ×
input
output
C in μg
t in minutes
300
290
50
40
30
20
10
0
1
2
3
4
5
6
7
8
9
10

FIG. 4.6.1

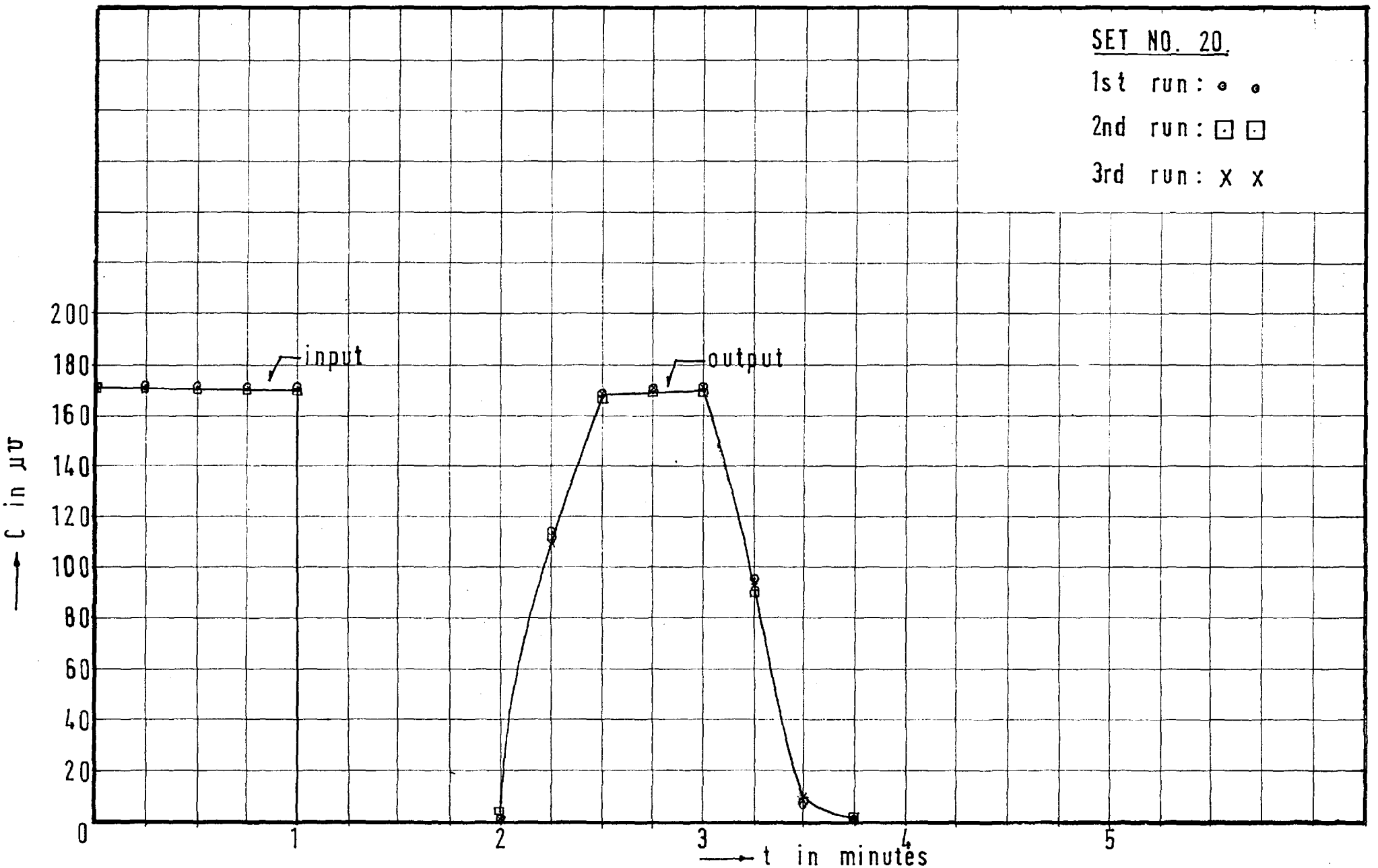
SET NO. 20.
1st run : o o
2nd run : ⊡ ⊡
3rd run : X X
input
output
200
180
160
140
120
100
80
60
40
20
0
1
2
3
4
5
C in μv
t in minutes

FIG. 4.6.2

and this was because of the fact that smaller volumes resulted in shallower depths and the diffuser dome was mounted 3.5 cm above the bottom of the vessel. The plug flow tube gave values of p, the plug flow fraction, of approximately 95% and it was found that the shorter the tube the better the result, as was to be expected. The above information was used below in assigning real rather than theoretical values to the parameters p and m in direct simulation.

Table 4.6.2

Set No.	Conc. of tracer gr/ℓ	Quantity of tracer in pulse ℓ	θ_1	Tracer recovery %	Vol. in system ℓ	Flow rate ℓ/min	Model Parameters	
							m	p
14	5	0.14	2.23	99	4.488	10	0.03	0.97
15	5	0.28	4.46	100	4.488	10	0.04	0.96
16	5	0.14	1.11	100	4.488	5	0.05	0.95
17	5	0.28	2.22	99	4.488	5	0.05	0.95
18	5	0.14	1.11	100	8.977	10	0.05	0.95
19	5	0.27	2.23	100	8.977	10	0.06	0.94
20	5	0.14	0.448	105	22.440	10	0.05	0.95
21	5	0.28	0.896	101	22.440	10	0.05	0.95

Table 4.6.1

Set Test No.	Conc. of tracer gr/ℓ	Quantity of tracer in pulse ℓ	θ_1	Tracer recovery %	Vol. in system ℓ	Flow rate ℓ/min.	Stirrer speed r.p.m.	Vol. of air diffused ℓ/m at 0.07 Kgf/cm^2	Model Parameters	
									m	p
1	5	0.04	0.125	96	10	5	350		0.79	0.21
2	5	0.04	0.083	95	15	5	280		0.83	0.17
3	5	0.14	0.330	105	15	5	350		0.86	0.14
4	5	0.04	0.063	106	20	5	560		0.87	0.13
5	5	0.04	0.125	104	10	5		35	0.88	0.12
6	5	0.04	0.083	97	15	5		35	0.90	0.10
7	5	0.04	0.125	98	20	10		35	0.89	0.11
8	5	0.04	0.125	107	20	10		35	0.85	0.15
9	5	0.04	0.167	90	15	10		35	0.86	0.14
10	5	0.04	0.250	95	10	10		35	0.83	0.17
11	5	0.04	0.375	97	10	15		35	0.82	0.18
12	5	0.04	0.250	95	15	15		35	0.86	0.14
13	5	0.04	0.187	102	20	15		35	0.90	0.10

4.7. Verification of the two parameter model

The perfect mixing chamber and plug flow tube were connected in series and operated under a variety of conditions with the total system volume varying from 15 litres to 45 litres approximately. Two values of flow through were used, 10 and 15 litres per minute. Lower values of flow were not used as it was clear that good simulation of plug flow required highly turbulent flow in the tubing. Good mixing in the perfect mixing chamber was achieved by supplying 35 litres/minute of air through the diffuser at a pressure of 0.07 Kgf/cm^2. A total of 46 experiments was performed (each experiment was repeated once, making a total of 92 runs in all) and the ratio of perfect mixing to plug flow was varied from 0.3:0.7 to 0.8:0.2 approximately. The data are shown in table 4.7.1. Each result shown in this table is obtained from the mean of a pair of experimental output curves. Typical pairs of such curves are shown in Fig.4.7.1 and 4.7.2.

The purpose of these tests was to determine whether the values for perfect mixing and plug flow, obtained by matching the two parameter model to the output curves obtained in these experiments, agreed with the known values. The "known" values were measured and corrected by applying the information obtained from the experiments of section 4.6 which process in itself assumes the validity of the model. However this was felt to be a logical approach.

The experimental values of 'm' were plotted against the optimised values in Fig.4.7.3. It has been found that the plotted points were slightly below the optimum 45° line through the origin. This can be accounted for by the approximation in calculating the corrected values of 'm'.

From these experiments it can be seen that a system such as the above can be represented by the two parameter model and that this

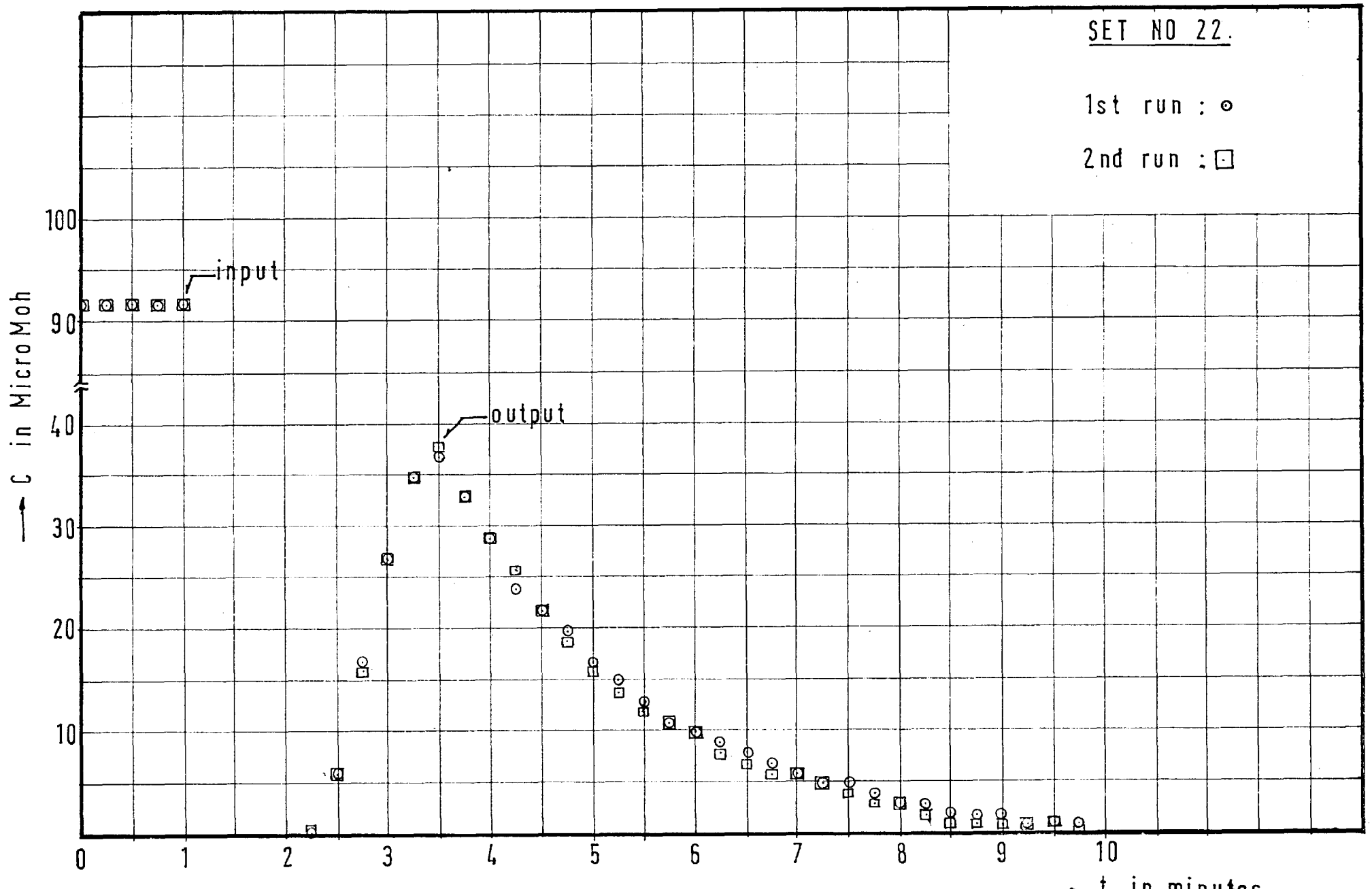
SET NO 22.
1st run : ⊙
2nd run : ⊡
input
output
C in MicroMoh
100
90
40
30
20
10
0
1
2
3
4
5
6
7
8
9
10
t in minutes

FIG. 4.7.1

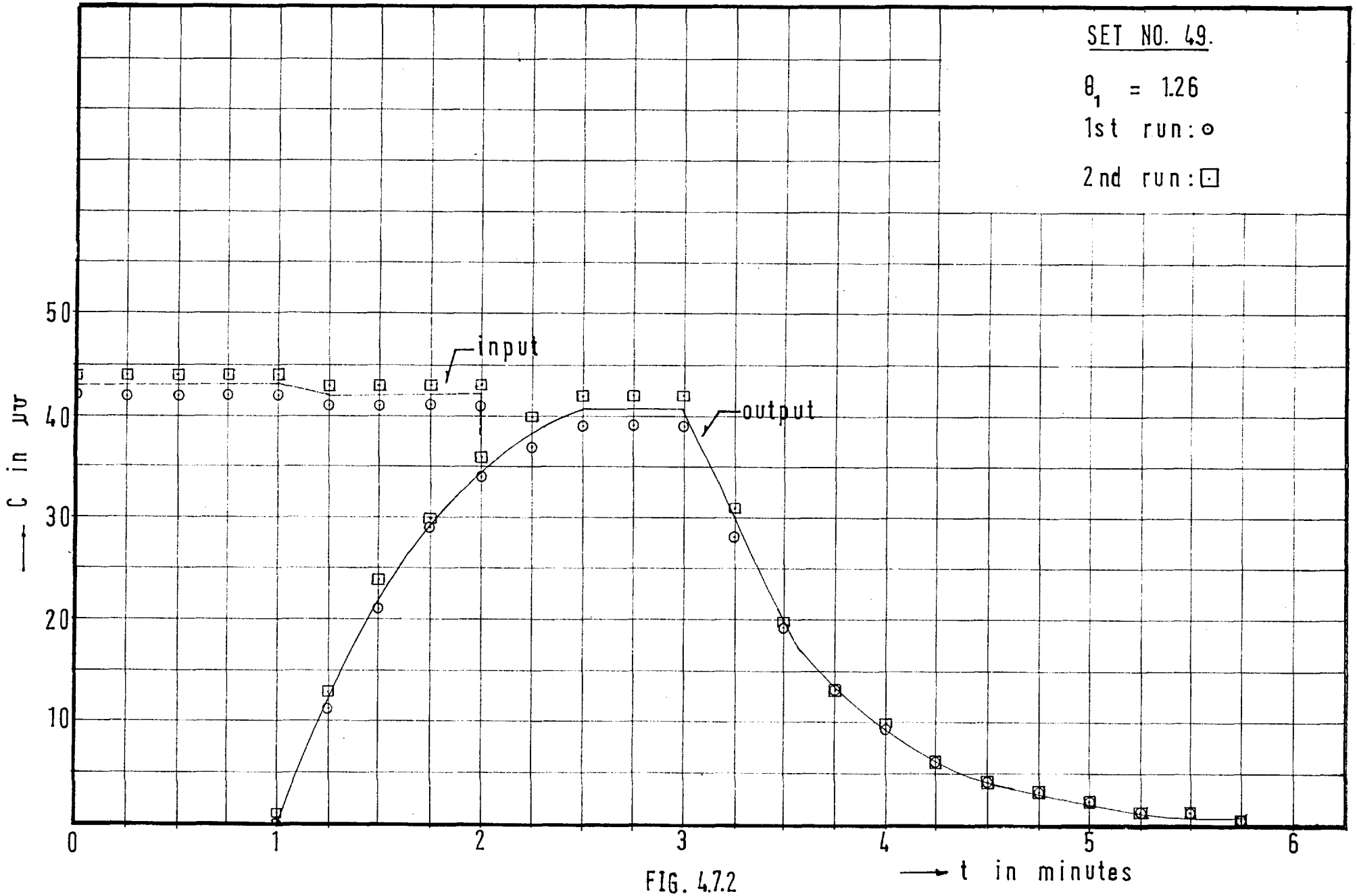
SET NO. 49.
θ_1 = 1.26
1st run: ⊙
2nd run: ⊡
input
output
50
40
30
20
10
0
1
2
3
4
5
6
C in μF
t in minutes

FIG. 4.7.2

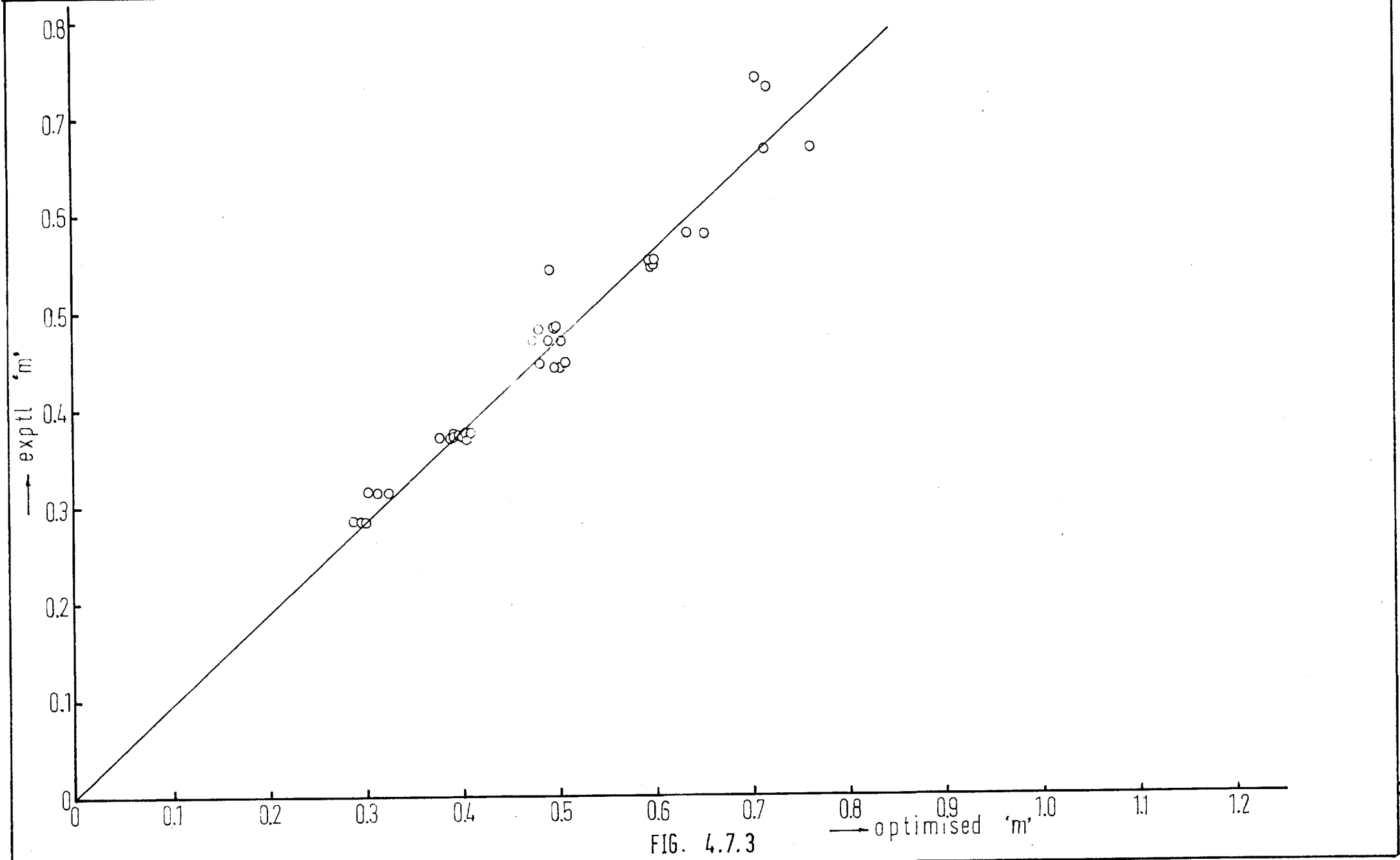
0.8
0.7
0.6
0.5
0.4
0.3
0.2
0.1
0
exptl 'm'
0
0.1
0.2
0.3
0.4
0.5
0.6
0.7
0.8
0.9
1.0
1.1
1.2
optimised 'm'

FIG. 4.7.3

Table 4.7.1

Set No.	Q litres per minute	V Total volume of system Litres	T Mean detention time mins.	θ_1 Pulse width	Input pulse step change $\mu\Omega$	Actual m	Actual p	Corr. m	Corr. p	Optimised m	Optimised p	% Tracer recov.	Stand. Error
30	10	33.24	3.32	0.30	84	0.30	0.70	0.284	0.716	0.288	0.712	99	0.021
31	10	33.24	3.32	0.60	86	0.30	0.70	0.284	0.716	0.300	0.700	101	0.009
32	15	33.24	2.22	0.45	54	0.30	0.70	0.284	0.716	0.294	0.706	100	0.029
33	15	33.24	2.22	0.91	55	0.30	0.70	0.284	0.716	0.300	0.700	106	0.008
42	10	28.70	2.87	0.35	50	0.34	0.66	0.315	0.685	0.324	0.676	104	0.018
43	10	28.70	2.87	0.70	59	0.34	0.66	0.315	0.685	0.305	0.695	106	0.030
44	15	28.70	1.91	0.52	37	0.34	0.66	0.315	0.685	0.313	0.687	106	0.011
45	15	28.70	1.91	1.05	33	0.34	0.66	0.315	0.685	0.314	0.686	104	0.024
26	10	38.24	3.82	0.26	85	0.392	0.608	0.370	0.630	0.396	0.604	104	0.009
27	10	38.24	3.82	0.53	85	0.392	0.608	0.370	0.630	0.393	0.607	106	0.005
28	15	38.24	2.55	0.39	55	0.392	0.608	0.370	0.630	0.378	0.622	104	0.005
29	15	38.24	2.55	0.78	55	0.392	0.608	0.370	0.630	0.391	0.609	98	0.01
46	10	23.89	2.39	0.42	46	0.41	0.59	0.370	0.630	0.409	0.591	99	0.013
47	10	23.89	2.39	0.84	45	0.41	0.59	0.370	0.630	0.407	0.593	102	0.017
48	15	23.89	1.59	0.63	28	0.41	0.59	0.370	0.630	0.401	0.599	105	0.018
49	15	23.89	1.59	1.26	43	0.41	0.59	0.370	0.630	0.400	0.600	98	0.019
38	10	33.70	3.37	0.296	56	0.40	0.60	0.374	0.626	0.391	0.609	98	0.030
39	10	33.70	3.37	0.59	57	0.40	0.60	0.374	0.626	0.393	0.607	101	0.016

Set No.	Q litres per minute	V Total volume of system Litres	T Mean detention time mins.	θ_1 Pulse width	Input pulse step change $\mu\Omega$	Actual m	Actual p	Corr. m	Corr. p	Optimised m	Optimised p	% Tracer recov.	Stand. Error
40	15	33.70	2.24	0.44	40	0.40	0.60	0.374	0.626	0.407	0.593	102	0.022
41	15	33.70	2.24	0.89	41	0.40	0.60	0.374	0.626	0.410	0.590	107	0.021
22	10	43.24	4.32	0.23	92	0.462	0.538	0.443	0.567	0.500	0.500	102	0.029
23	10	43.24	4.32	0.46	92	0.462	0.538	0.443	0.567	0.505	0.495	101	0.042
24	15	43.24	2.88	0.35	56	0.462	0.538	0.443	0.567	0.505	0.495	96	0.024
25	15	43.24	2.88	0.70	54	0.462	0.538	0.443	0.567	0.502	0.497	108	0.017
58	10	19.35	1.94	0.51	53	0.51	0.49	0.448	0.552	0.483	0.517	102	0.010
59	15	19.35	1.29	0.77	34	0.51	0.49	0.448	0.552	0.509	0.491	103	0.040
50	10	28.89	2.89	0.35	50	0.52	0.48	0.471	0.529	0.475	0.525	93	0.013
51	10	28.89	2.89	0.69	69	0.52	0.48	0.471	0.529	0.491	0.509	96	0.015
52	15	28.89	1.93	0.52	43	0.52	0.48	0.471	0.529	0.503	0.497	97	0.080
52	15	28.89	1.93	1.04	42	0.52	0.48	0.471	0.529	0.502	0.498	100	0.017
34	10	38.70	3.87	0.26	86	0.51	0.49	0.484	0.516	0.496	0.504	99	0.013
35	10	38.70	3.87	0.52	85	0.51	0.49	0.484	0.516	0.499	0.501	100	0.009
36	15	38.70	2.58	0.39	55	0.51	0.49	0.484	0.516	0.500	0.500	109	0.020
37	15	38.70	2.58	0.77	43	0.51	0.49	0.484	0.516	0.480	0.520	98	0.023
60	10	24.35	2.44	0.41	56	0.61	0.39	0.544	0.456	0.598	0.402	97	0.015
61	15	24.35	1.62	0.62	40	0.61	0.39	0.544	0.456	0.493	0.507	105	0.019

Set No.	Q litres per minute	V Total volume of system Litres	T Mean detention time mins.	θ_1 Pulse Width	Input pulse step change $\mu\Omega$	Actual m	Actual p	Corr. m	Corr. p	Optimised m	Optimised p	% Tracer recov.	Stand. Error
54	10	33.89	3.39	0.59	55	0.59	0.41	0.546	0.454	0.600	0.400	103	0.065
55	10	33.89	3.39	0.59	56	0.59	0.41	0.546	0.454	0.600	0.400	98	0.016
56	15	33.89	2.26	0.44	41	0.59	0.41	0.551	0.449	0.597	0.403	105	0.066
57	15	33.89	2.26	0.88	42	0.59	0.41	0.551	0.449	0.601	0.399	99	0.095
64	10	14.54	1.45	0.69	46	0.68	0.32	0.58	0.42	0.636	0.364	105	0.011
65	15	14.54	0.97	1.03	30	0.68	0.32	0.58	0.42	0.655	0.345	106	0.045
66	10	19.54	1.95	0.51	46	0.76	0.24	0.666	0.334	0.765	0.235	107	0.016
67	15	19.54	1.30	0.77	24	0.76	0.24	0.666	0.334	0.716	0.284	105	0.053
68	10	24.54	2.45	0.41	47	0.81	0.19	0.731	0.269	0.720	0.280	105	0.024
69	15	24.54	1.63	0.61	27	0.81	0.19	0.739	0.261	0.708	0.292	101	0.014

model could be used for simulation or prediction in this case with reasonable accuracy.

4.8. Verification of the 4 parameter shortcircuiting model

In order to verify this model, five experiments were performed each of which was repeated three times making a total of fifteen tests in all. A typical set (71) of three output curves is plotted in Fig.4.8.1. Shortcircuiting was achieved by the bypass pipe shown in Fig.4.3.1, controlled by Pump No.2 and measured by means of a flow meter. The experimental conditions are tabulated in Table 4.8.1, from which it can be seen that the perfect mixing, plug flow and shortcircuiting volumes are kept constant, and that the flow through the system is constant, but the fraction of this flow that shortcircuits to the outlet is varied. Thus the emphasis was put on the fraction of the flow being shortcircuited rather than on the shortcircuiting volume as this was easier from the practical point of view. The same range of shortcircuiting time constant could have been examined by keeping the shortcircuiting flow rate constant and varying the shortcircuiting volume. The shortcircuit volume was deliberately kept small to ensure good plug flow and to determine the ability of the optimisation techniques to identify small "dead space".

The experimental results were verified in three different ways. (i) To the known values of m, p, s and f corrections were made in accordance with section 4.6. These values were then used in the mathematical model to predict the output curve from the known input pulse. The output curve obtained in this way was compared with the actual experimental output curve. These curves are plotted in dimensionless form in Fig.4.8.2 for set 71.

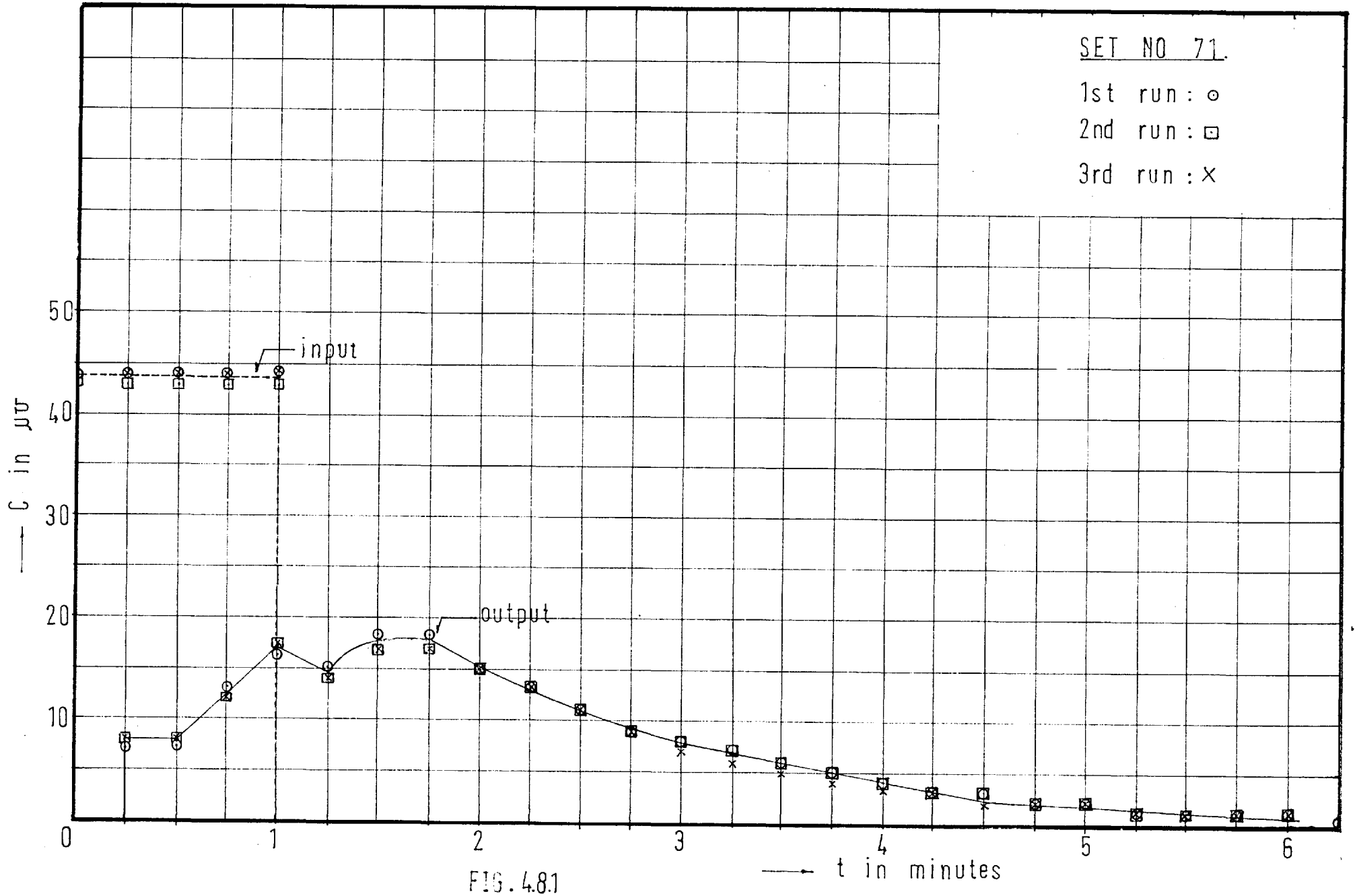
SET NO 71.
1st run : ⊙
2nd run : ⊡
3rd run : ×
input
output
50
40
30
20
10
0
1
2
3
4
5
6
C in μτ
t in minutes

FIG. 4.8.1

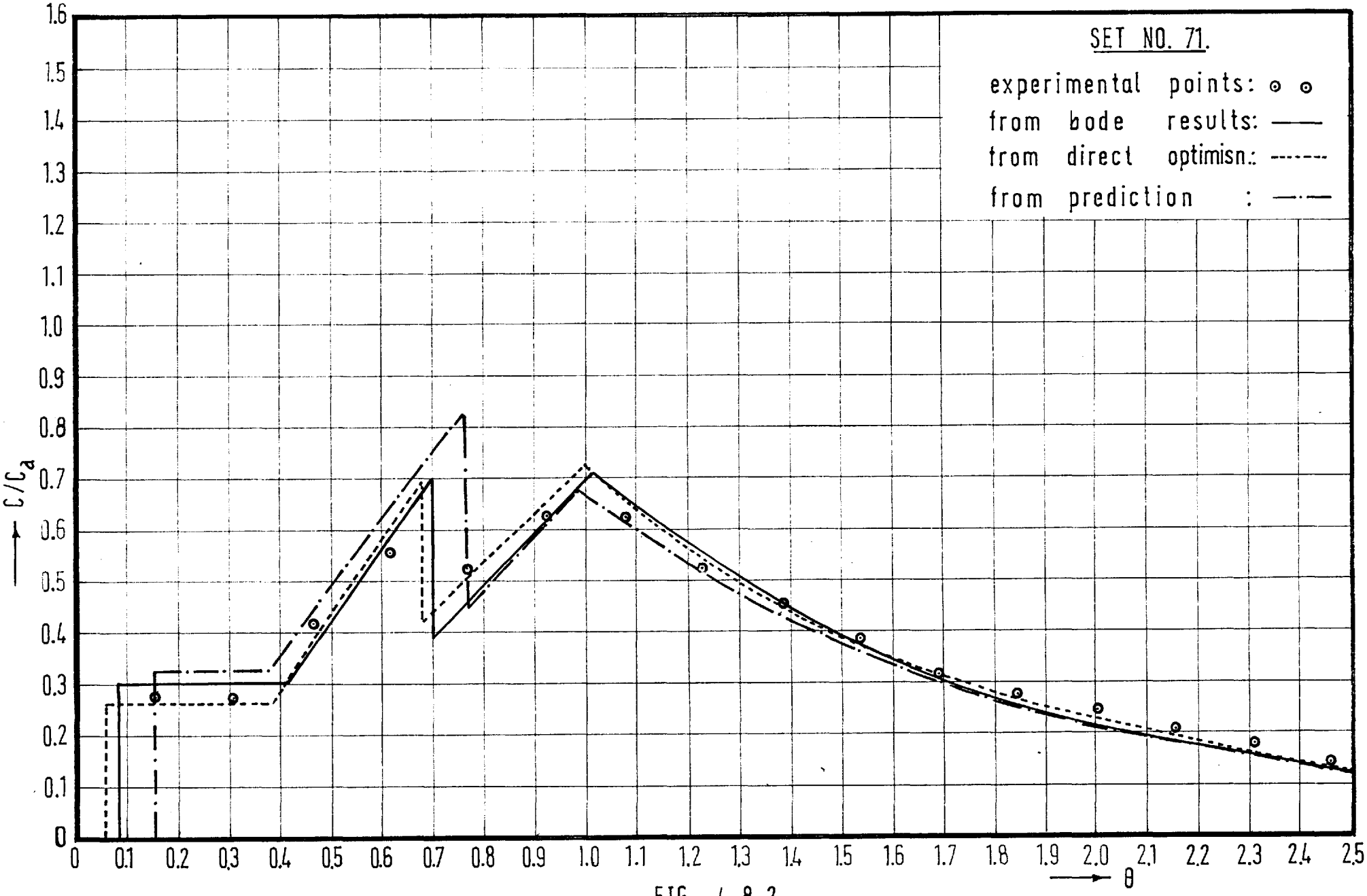
SET NO. 71.
experimental points: ⊙ ⊙
from bode results: ——
from direct optimisn.: -------
from prediction : —·—
C/C_d
θ
0
0.1
0.2
0.3
0.4
0.5
0.6
0.7
0.8
0.9
1.0
1.1
1.2
1.3
1.4
1.5
1.6
1.7
1.8
1.9
2.0
2.1
2.2
2.3
2.4
2.5

FIG. 4.8.2.

BODE PLOT.

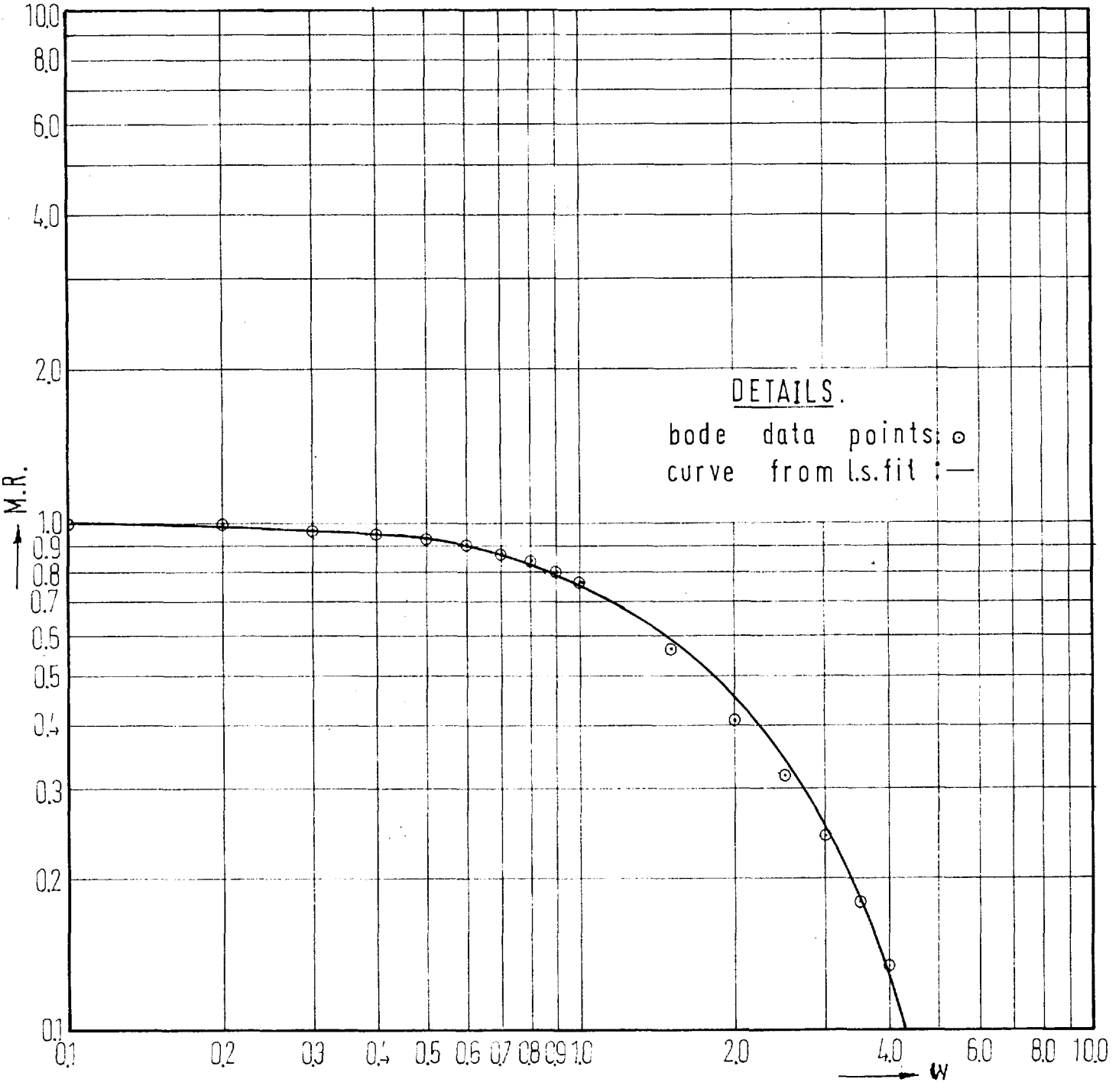

FIG. 4.8.3.

(ii) The values of the parameters in the model were optimised to give a Least Squares fit of the experimental curve. The output curve obtained in this way was also plotted on Fig.4.8.2. for set 71.
(iii) The indirect pulse response technique was applied as described in Chapter 3 using the data regression method. The Bode plot obtained for Experiment 71 is shown in Fig.4.8.3 and the curve obtained by this method is plotted in Fig.4.8.2.

4.9. Verification of the Recirculation Model

Five sets of experiments were performed on the system re-arranged so as to contain an element of recirculation. The data for these tests are shown in Table 4.9.1. It can be seen that the recirculation volume was kept constant and the recirculation rate was varied from one tenth to one quarter of the main flow. Again each experiment was repeated three times and a typical set of tests is shown in Fig.4.9.1.

The recirculation model was tested and the optimised values of the four parameters are shown in Table 4.9.2 together with the standard errors of estimate. The curve obtained in this way from set 77 is shown in Fig.4.9.2 for comparison with the experimental curve.

As a check on the combined short circuiting and recirculation model of Chapter 2 Fig.2.8.1 p. values of the six parameters were inserted in the transfer function and the output curves computed from the known inputs. These were then compared with the experimental output curves. Nominal values for S and f_1 were adopted as the experimental set up did not contain any element of shortcircuiting. An example of such a "predicted" output curve is given in Fig.4.9.2 again from set 77. This model appears to be satisfactory and produces a good fit.

Table 4.8.1.

Set No.	Flow Q litres/ min.	System vol. V litres	Mean detention time T	Pulse width θ_1	Conc. of tracer gr/ℓ	Tracer recov. %	Input step change μΩ	Perfect mix vol. ℓ	Plug flow vol. ℓ	Short-circuiting volume ℓ	Short circuit flow rate ℓ/m
70	12.0	19.80	1.65	0.613	5	110	40	15.0	4.54	0.26	3.0
71	12.0	19.80	1.65	0.613	5	105	44	15.0	4.54	0.26	2.25
72	12.0	19.80	1.65	0.613	5	102	44	15.0	4.54	0.26	1.75
73	12.0	19.80	1.65	0.613	5	104	46	15.0	4.54	0.26	1.25
74	12.0	19.54	1.628	0.615	5	104	49	15.0	4.54	-	-

Table 4.8.2.

	Initial values of Parameters assumed					Values obtained by direct optimisation					Values obtained from pulse technique				
	m	p	s	f	stand. error	m	p	s	f	stand. error	m	p	s	f	stand. error
70	0.73	0.23	0.04	0.25	0.09	0.68	0.31	0.01	0.22	0.02	0.5	0.44	0.06	0.31	0.017
71	0.66	0.30	0.04	0.188	0.08	0.68	0.31	0.01	0.17	0.02	0.647	0.337	0.016	0.19	0.014
72	0.68	0.28	0.04	0.145	0.05	0.678	0.31	0.012	0.13	0.04	0.724	0.265	0.01	0.12	0.014
73	0.66	0.30	0.04	0.104	0.04	0.64	0.34	0.02	0.12	0.03	0.742	0.248	0.01	0.08	0.006
74	0.66	0.30	0.04	0.01	0.04	0.65	0.34	0.01	0.02	0.02	0.675	0.315	0.01	0.02	0.01

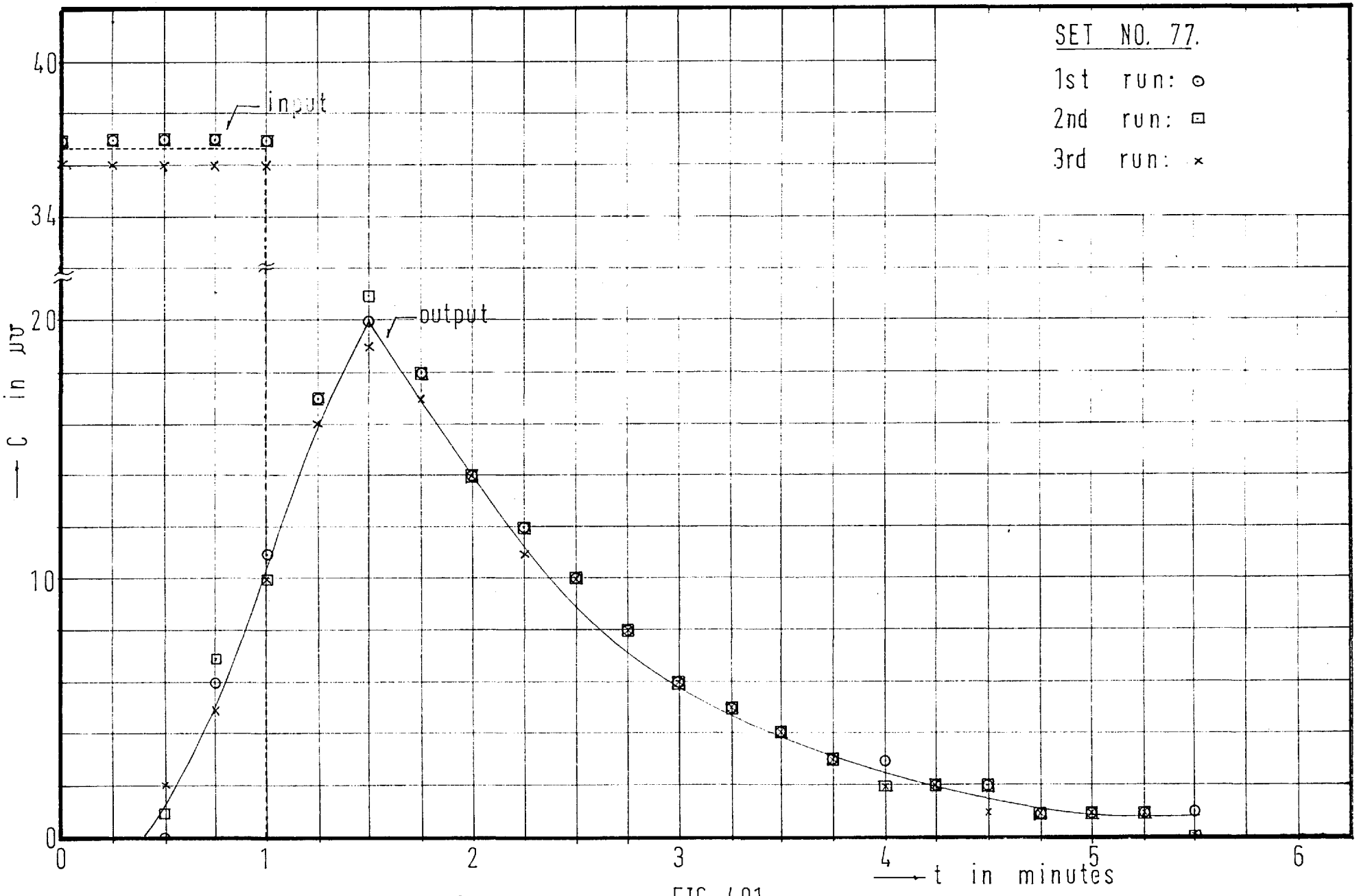
SET NO. 77.
1st run: ⊙
2nd run: ⊡
3rd run: ×
input
output
C in μg
t in minutes
0
10
20
34
40
0
1
2
3
4
5
6

FIG 4.9.1

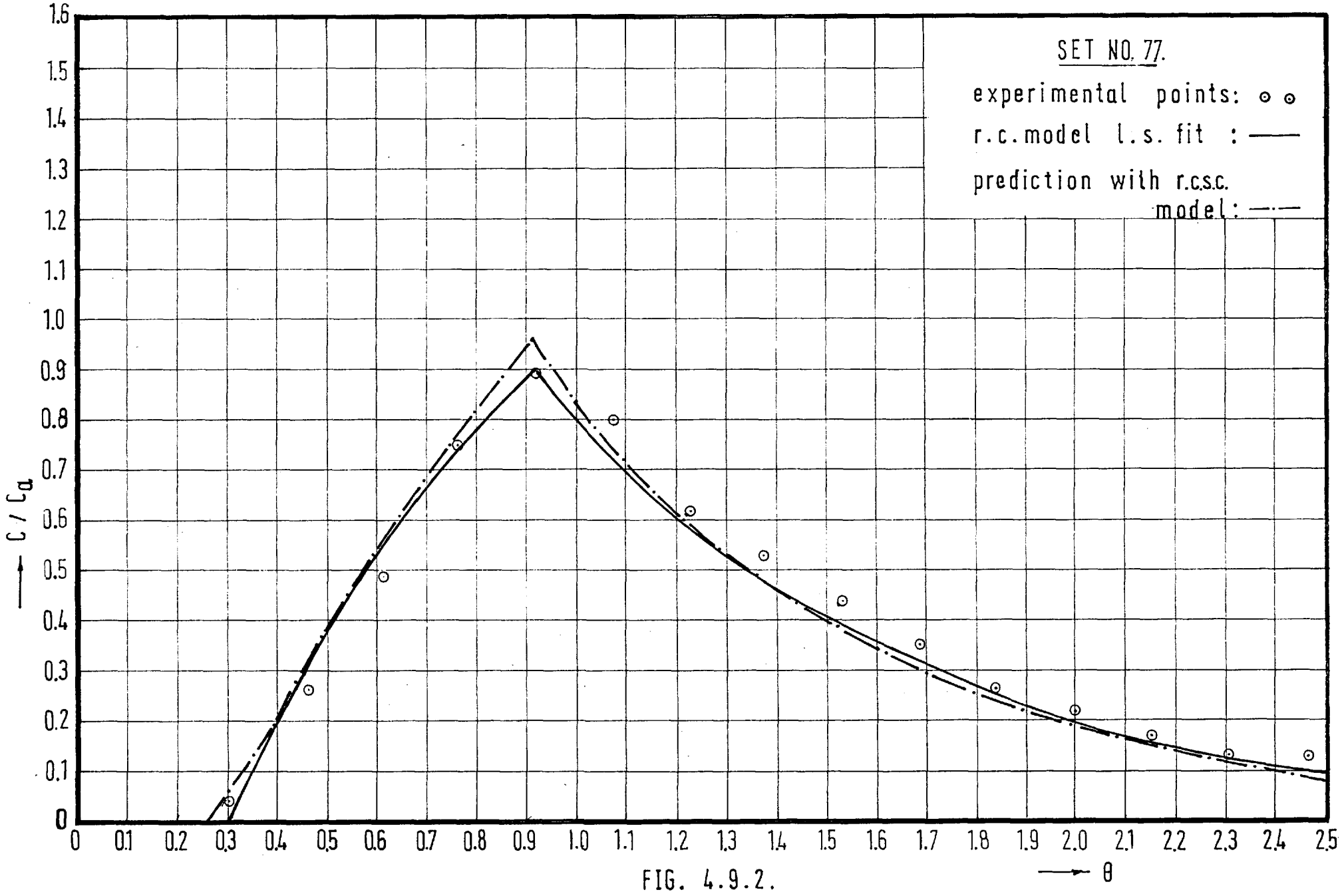
SET NO. 77.
experimental points: ⊙ ⊙
r.c.model l.s. fit : ——
prediction with r.c.s.c. model: —·—
C / Cd
θ
0 0.1 0.2 0.3 0.4 0.5 0.6 0.7 0.8 0.9 1.0 1.1 1.2 1.3 1.4 1.5 1.6 1.7 1.8 1.9 2.0 2.1 2.2 2.3 2.4 2.5
0 0.1 0.2 0.3 0.4 0.5 0.6 0.7 0.8 0.9 1.0 1.1 1.2 1.3 1.4 1.5 1.6

FIG. 4.9.2.

Table 4.9.1

Set No.	Flow Q litres/ min.	System vol. V litres	Mean detention time mins.	Pulse width θ_1	Conc. of tracer gr/ℓ	Input step change μΩ	Tracer recov. %	Perfect mixing volume ℓ	Plug flow vol. ℓ	Recirculation volume ℓ	Recirculation rate ℓ/m
75	12.0	19.80	1.65	0.606	5	43	98	15.0	4.54	0.26	3.0
76	12.0	19.80	1.65	0.606	5	40	98	15.0	4.54	0.26	2.10
77	12.0	19.80	1.65	0.606	5	37	102	15.0	4.54	0.26	1.74
78	12.0	19.80	1.65	0.606	5	37	103	15.0	4.54	0.26	1.20
79	12.0	19.80	1.65	0.606	5	49	102	15.0	4.54	0.26	-

Table 4.9.2

Set No.	Assumed initial values of parameters used in short-circuiting and recirculation model							Optimised values obtained from recirculation model				
	m	p	s	r	f_1	f_2	stand. error	m	p	r	f	stand. error
75	0.610	0.380	0.002	0.01	0.01	0.250	0.05	0.650	0.344	0.010	0.181	0.020
76	0.619	0.366	0.005	0.01	0.01	0.175	0.05	0.667	0.321	0.011	0.180	0.015
77	0.635	0.350	0.005	0.01	0.01	0.145	0.05	0.640	0.350	0.010	0.150	0.020
78	0.651	0.334	0.005	0.01	0.01	0.100	0.04	0.648	0.349	0.003	0.08	0.015
79	0.65	0.350	0	0	0	0	-	0.646	0.353	0.001	0.010	0.004

The simple recirculation model also fits the experimental curve well and the optimised values of the four parameters agree reasonably well with the actual values except in the case of Set No.75 in which the value of f is low. This is probably because of the approximations involved in the derivation of the model formula, in which only two terms of MacLaurin's series were included. This approximation is valid only if the recirculation rate is low.

One difficulty observed in the analysis of flow curves from these recirculation experiments by the optimisation technique is that with a very short recirculation time, the optimised values of r and f tend to diminish and merge with the perfect mixing fraction. This is logical since perfect mixing is in effect micro and macro recirculation. If a strong optimisation technique were available, the values of r and f in each of the above cases would have approached zero. However in cases where plug flow is dominant, a plug flow recirculation will probably not have this tendency to diminish.

4.10 Analysis of Flow curves obtained from a model tank

Having established the usefulness of the models of Chapter 2 in the interpretation of flow curves, a series of these curves was obtained from a continuous flow model tank and analysed by using these methods.

The model tank is shown in Fig.4.10.1. The dimensions of this model were 138 x 46 x 23 cm. The inlet was a single 2.54 cm dia. pipe mounted in the centre of one end and fitted with a baffle of diameter 7.6 cm fixed at a distance of 5 cm from the inlet end for the purpose of distributing the inflow. The outlet consisted of a single weir directly opposite the inlet fixed at a height of 15 cm

MODEL TANK

SCALE 1cm = 10 cm

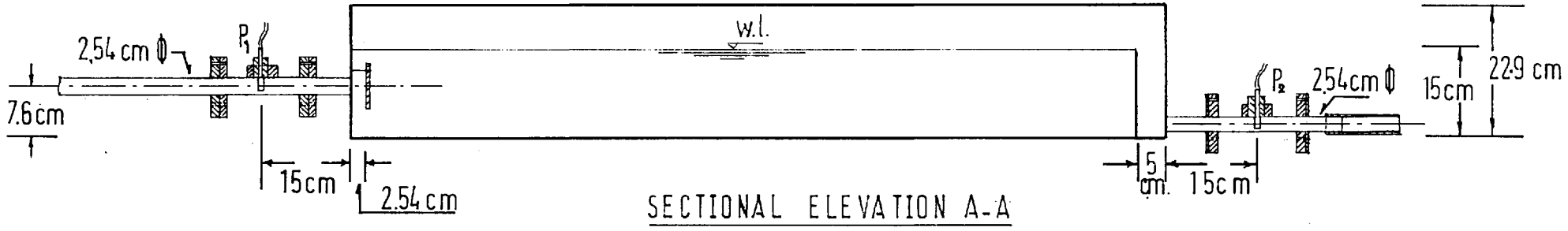

SECTIONAL ELEVATION A-A

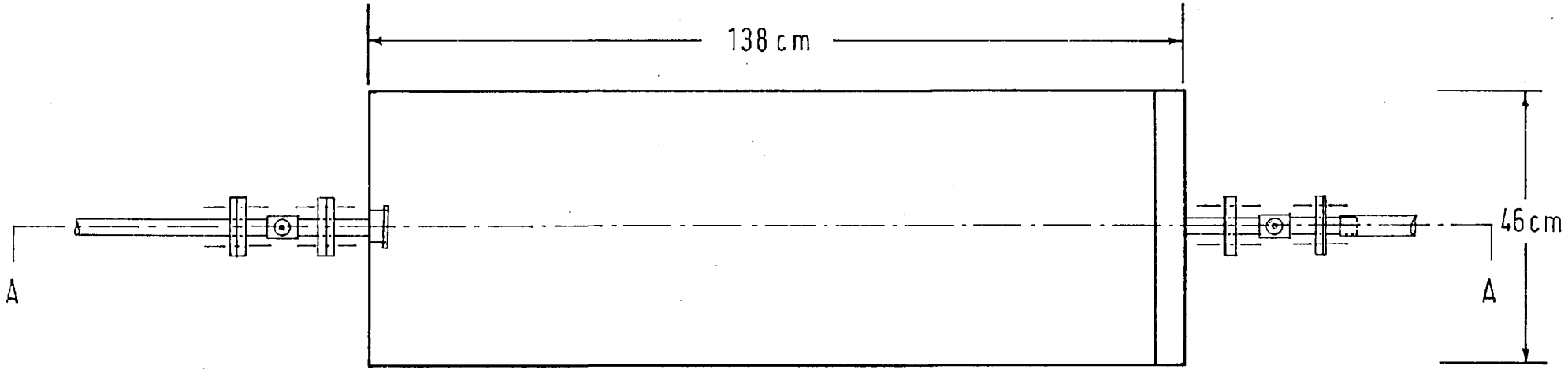

FIG. 4.10.1

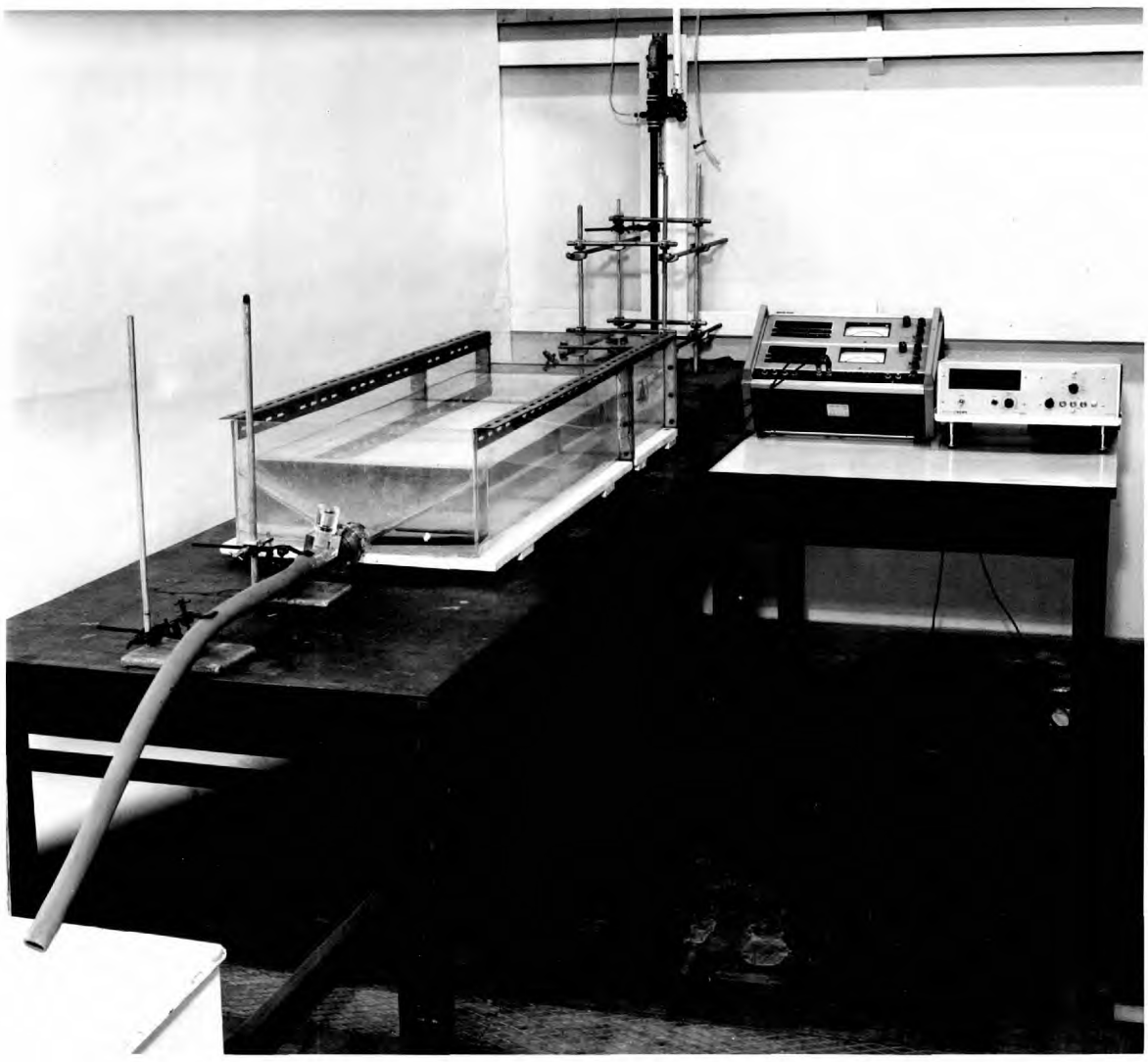

General view of the model tank set-up .

PLATE 4.10.1.

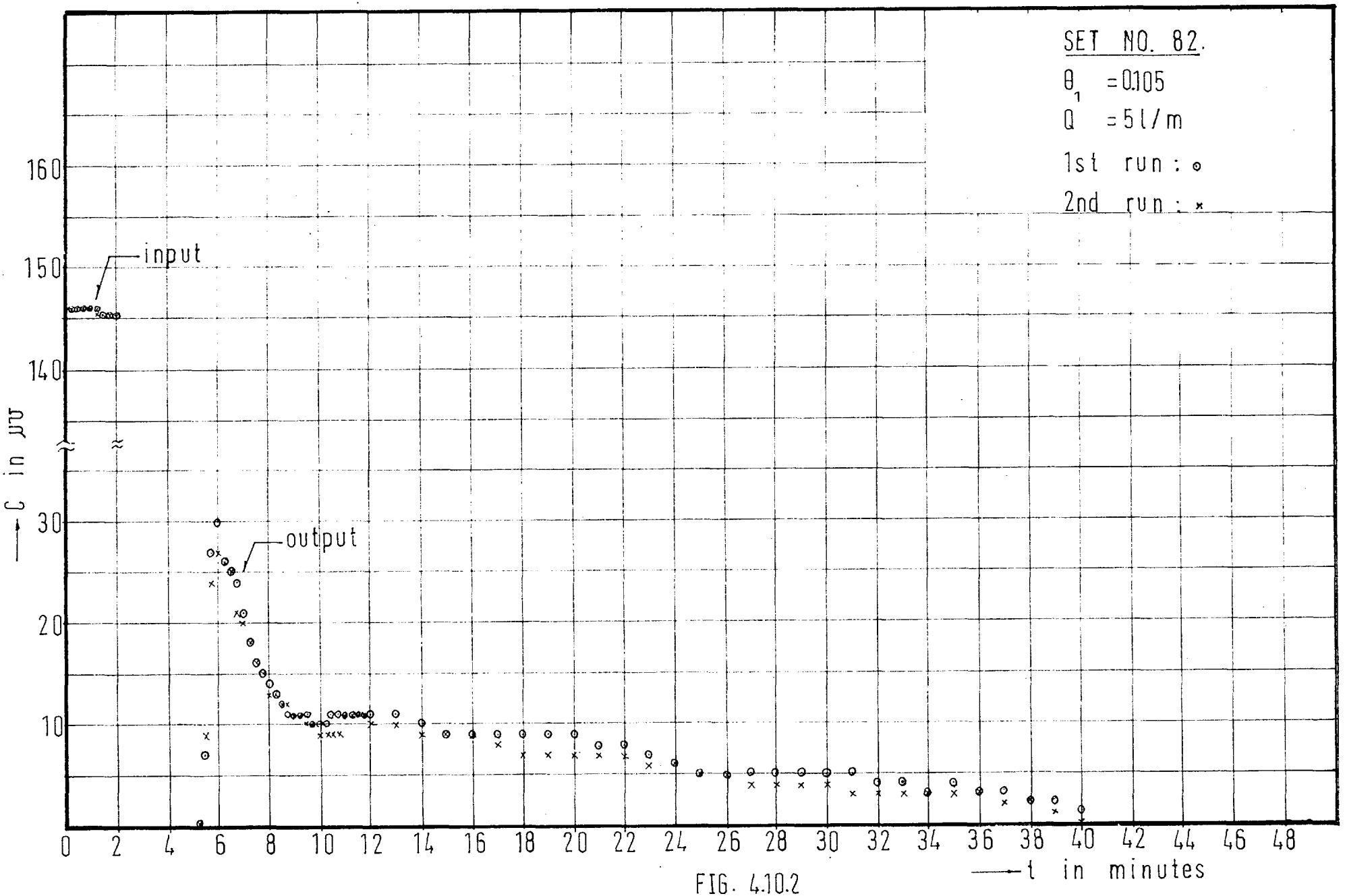
SET NO. 82.
θ1 = 0.105
Q = 5 l/m
1st run : ⊙
2nd run : ×
input
output
C in μg
t in minutes
160
150
140
30
20
10
0
2
4
6
8
10
12
14
16
18
20
22
24
26
28
30
32
34
36
38
40
42
44
46
48

FIG. 4.10.2

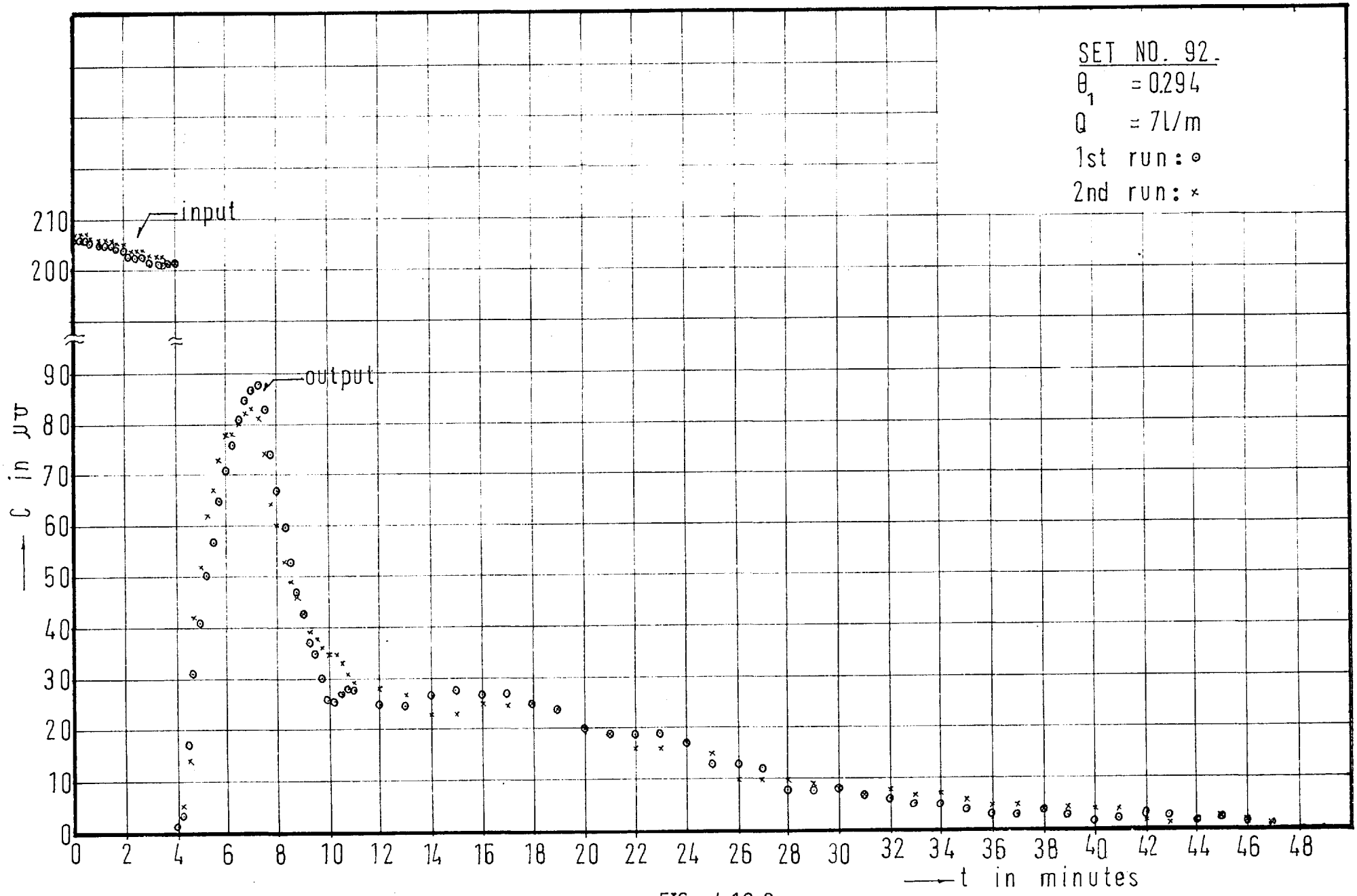
SET NO. 92.
θ1 = 0.294
Q = 7l/m
1st run: ⊙
2nd run: ×
input
output
C in μv
t in minutes
0
10
20
30
40
50
60
70
80
90
200
210
0 2 4 6 8 10 12 14 16 18 20 22 24 26 28 30 32 34 36 38 40 42 44 46 48

FIG. 4.10.3

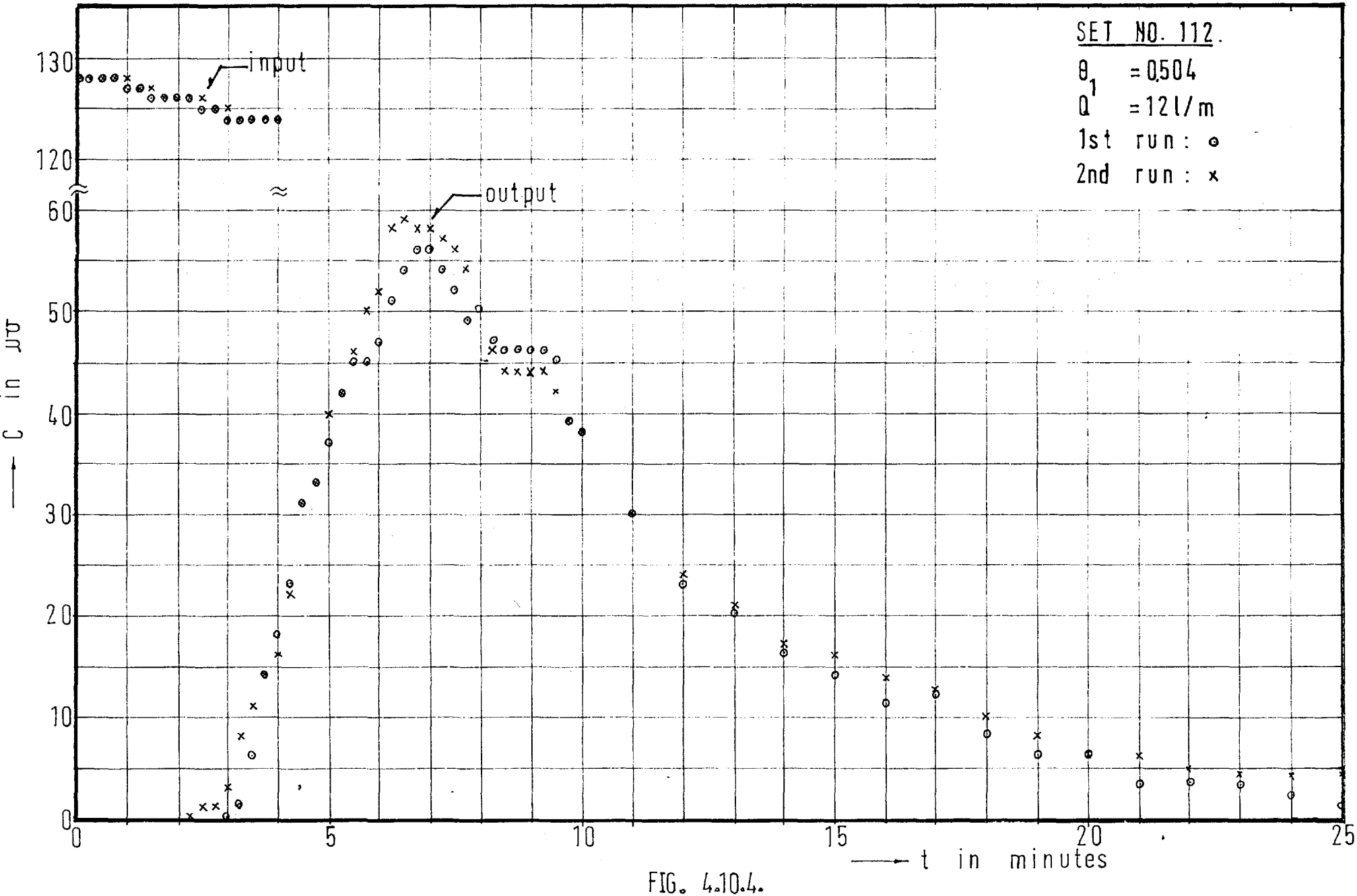
SET NO. 112.
θ_1 = 0.504
Q^1 = 12 l/m
1st run : o
2nd run : x
input
output
C in μU
t in minutes
0
5
10
15
20
25
10
20
30
40
50
60
120
130

FIG. 4.10.4.

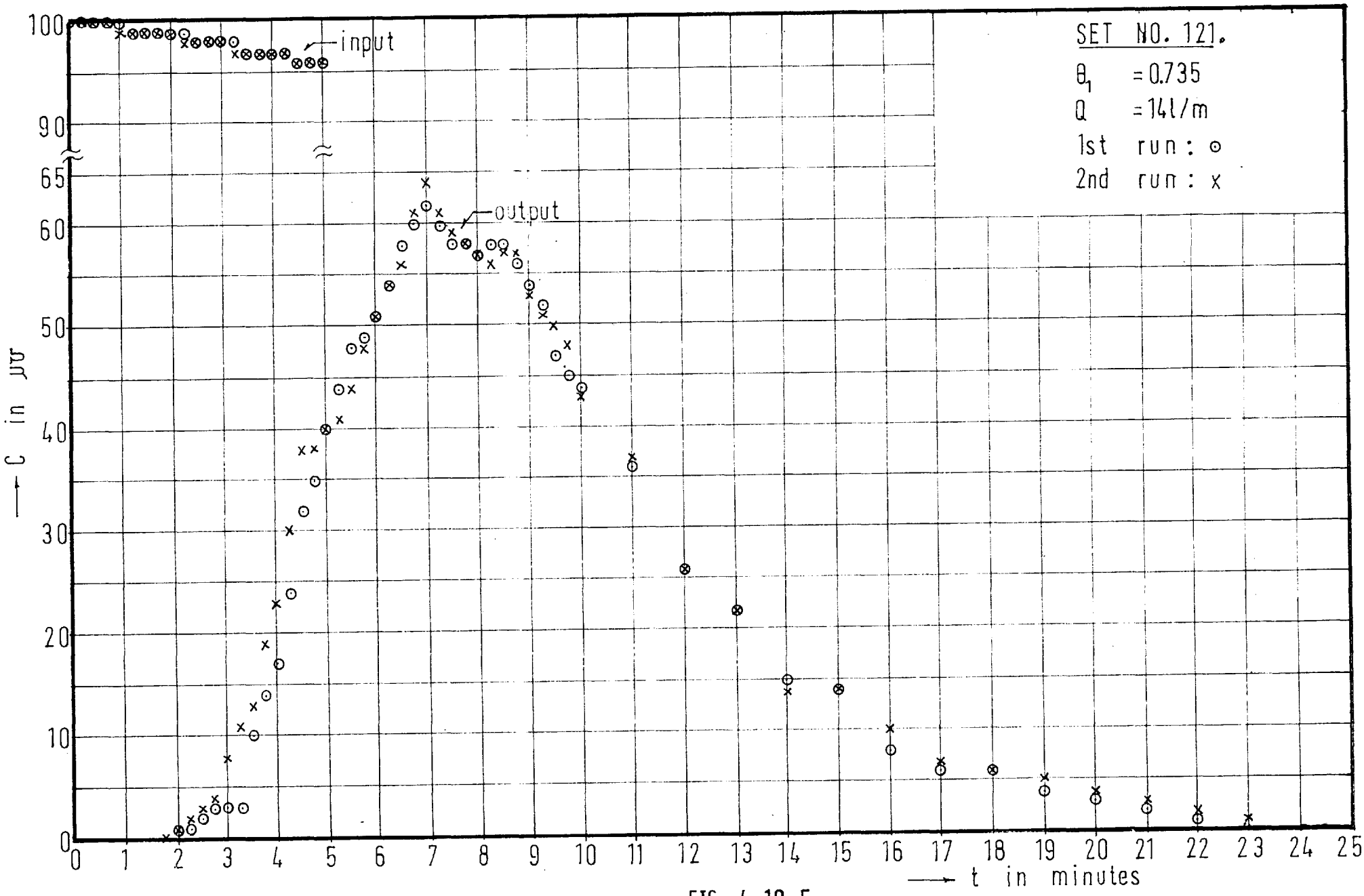
SET NO. 121.
θ_1 = 0.735
Q = 14 l/m
1st run : ⊙
2nd run : x
input
output
C in μg
t in minutes
100
90
65
60
50
40
30
20
10
0
0 1 2 3 4 5 6 7 8 9 10 11 12 13 14 15 16 17 18 19 20 21 22 23 24 25

FIG. 4.10.5

from the tank bottom thus determining the depth of flow. Downstream of this weir a collecting chamber passed the flow to a 2.54 cm diameter outlet pipe and hence through a measuring tank to waste. The probes P_1 and P_2 were mounted 15 cm upstream of the inlet and 1 5 cm downstream of the collecting chamber respectively. The tube downstream of P_2 could be throttled in order to ensure sufficient depth in the collecting chamber to maintain full pipe flow past the probe P_2 and prevent air entrainment.

The flow rate was varied from 5 litres/minute to 14 litres/minute (average tank velocity 0.12 cm/sec. to 0.338 cm/sec.) and responses were recorded for input pulses of 2, 3, 4 and 5 minutes duration. Each experiment was repeated once as a check on reproducibility and typical pairs of response curves are shown in Fig.4.10.2 - 5.

The tracer technique used was similar to that used in the direct verification experiments. Readings were taken at intervals of 15 secs for at least one nominal tank detention time. After this, readings were taken at 1 minute intervals as the rate of change of concentration was low. The temperature of the flowing water was recorded by a thermometer placed upstream of the tank outlet weir. Temperature corrections were made to the observations where necessary as before.

Tracer recovery was checked in each case and was found to lie between 95% and 105%, except in a few cases at low velocity where values less than 95% were obtained. It is thought that this was due to density currents and the consequent long tail to the output curve.

The two parameter, four parameter, and five parameter models were fitted to the curves using the optimisation techniques described in Chapter 5. The details of the experiments and the results of

the analysis are given in Tables 4.10.1

From the two parameter model data it can be seen that the flow regime consisted of approximately 71% perfect mixing and 29% plug flow. Also it can be seen that as the flow through the system was increased the perfect mixing volume tended to decrease and the plug flow volume tended to increase which is logical. However with this model the standard error of estimate was of average value 0.24 indicating a poor fit of the experimental curves.

By introducing the four parameter shortcircuiting model which includes a plug flow shortcircuit in parallel with the above, a better fit was obtained as indicated by standard errors of estimate of the order of 0.1. The average perfect mixing fraction was found to be 0.75, plug flow 0.20 and shortcircuiting 0.05.

The next step was to introduce a fifth parameter in the form of a perfect mixing element in the shortcircuit branch of the last model. This model can now be regarded as two two parameter models in parallel. As can be seen from Table 4.10.3 the standard errors of estimate were further reduced particularly for the higher flow rates. This model is more flexible than the previous model as can be seen when it is applied to set No.81 as shown in Fig.4.10.6. The outflow curve in this case has two distinct peaks, the first of which is sharp and narrow indicating a shortcircuit. The second peak has a gradual rise and a gradual fall, representing the mainflow. In this case the time constants for the shortcircuiting flow and the mainflow are widely different. Where this is not the case as in sets Nos. 90, 91, 92, 93 the two peaks merge to form a single fall peak (see Figs. 4.10.7, 8, 9 and 10). With the five parameter model, when there are two peaks it is possible to consider either peak as the shortcircuiting peak. For instance referring to Fig.4.10.6

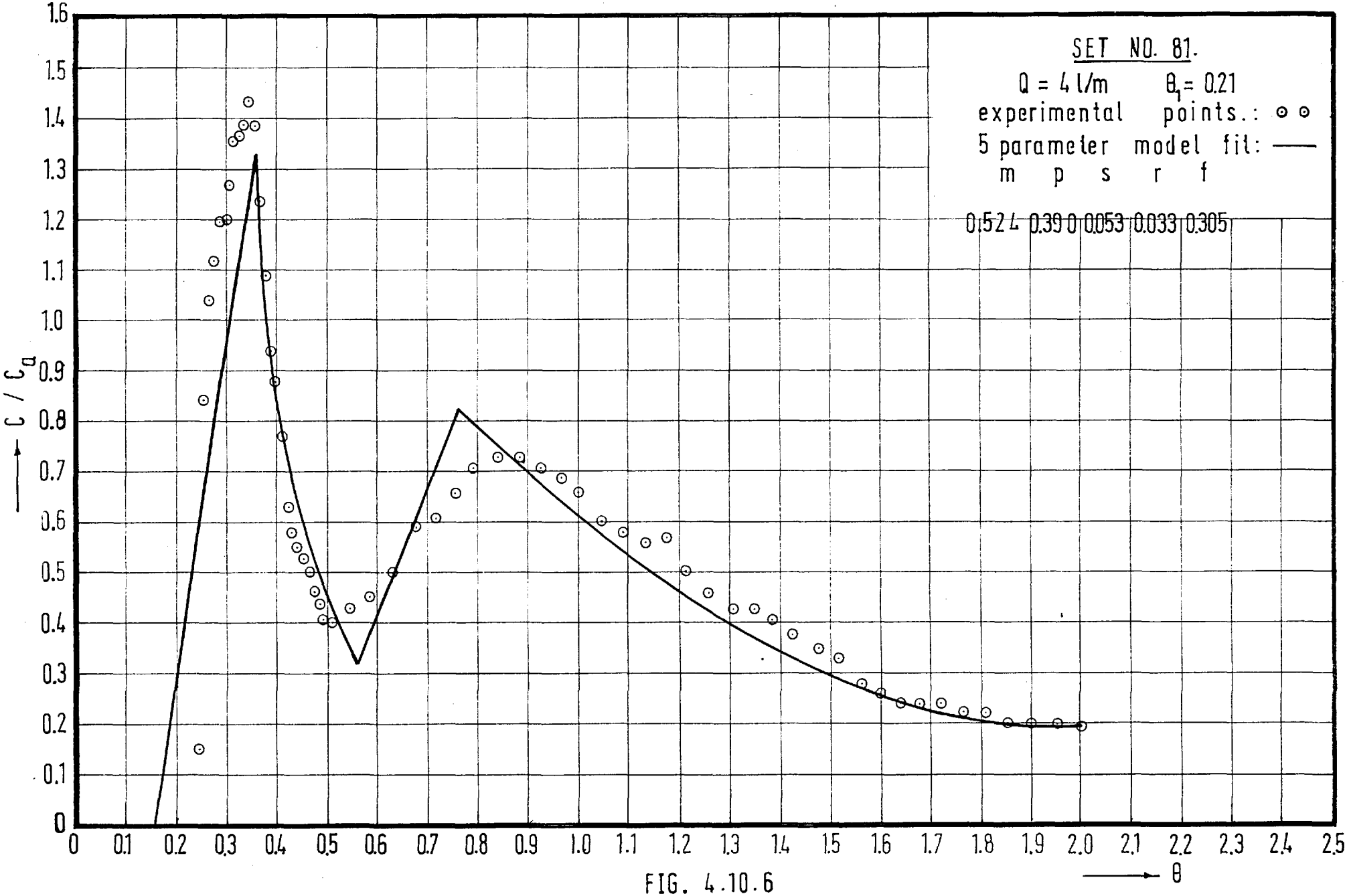
SET NO. 81.
Q = 4 l/m θ1 = 0.21
experimental points.: ⊙ ⊙
5 parameter model fit: ——
m p s r f
0.524 0.390 0.053 0.033 0.305
C / Ca
θ
0 0.1 0.2 0.3 0.4 0.5 0.6 0.7 0.8 0.9 1.0 1.1 1.2 1.3 1.4 1.5 1.6 1.7 1.8 1.9 2.0 2.1 2.2 2.3 2.4 2.5
0 0.1 0.2 0.3 0.4 0.5 0.6 0.7 0.8 0.9 1.0 1.1 1.2 1.3 1.4 1.5 1.6

FIG. 4.10.6

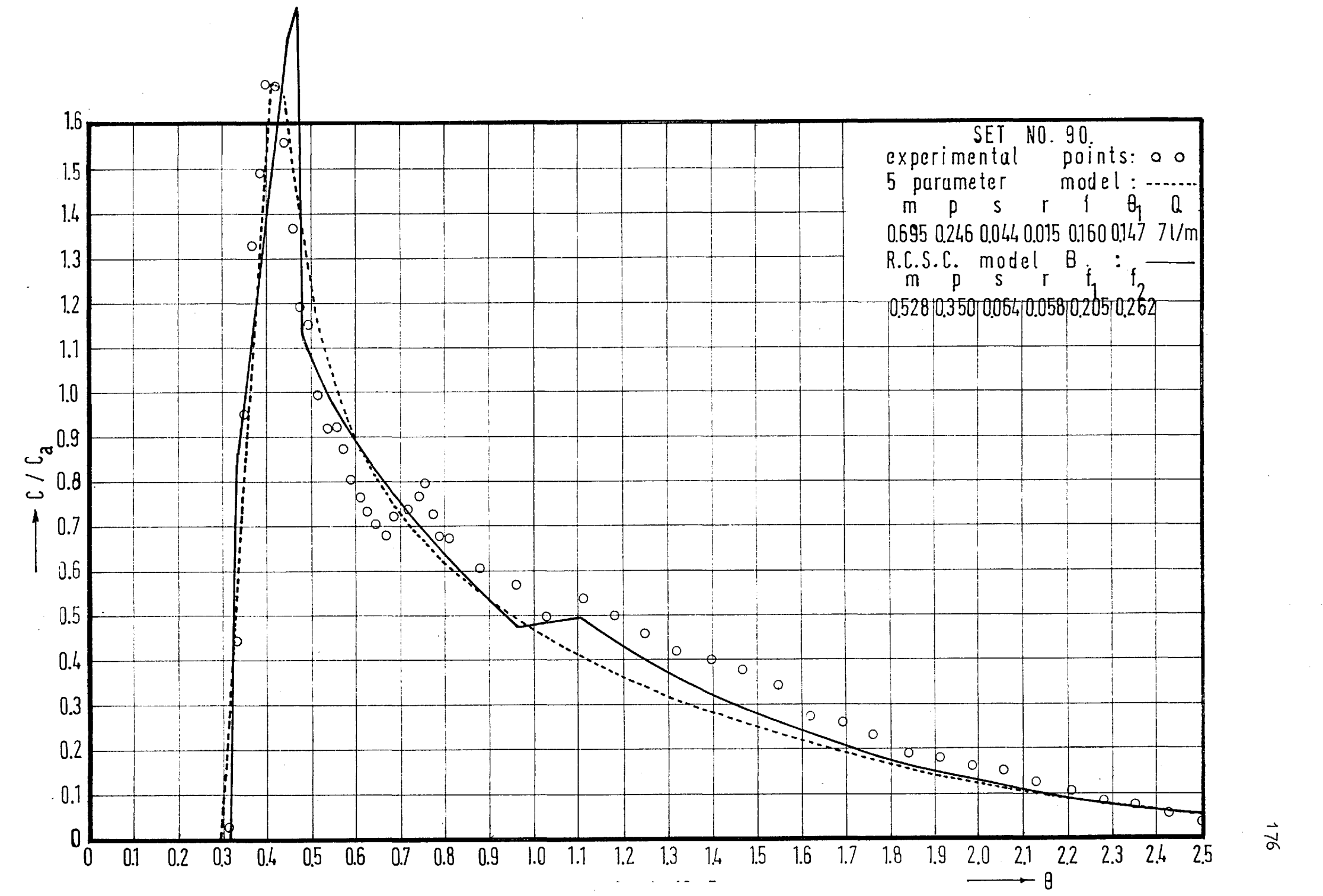
SET NO. 90.
experimental points: o o
5 parameter model : ------
m p s r f θ1 Q
0.695 0.246 0.044 0.015 0.160 0.147 7 l/m
R.C.S.C. model B : ——
m p s r f1 f2
0.528 0.350 0.064 0.058 0.205 0.262
C / Ca
θ
0 0.1 0.2 0.3 0.4 0.5 0.6 0.7 0.8 0.9 1.0 1.1 1.2 1.3 1.4 1.5 1.6 1.7 1.8 1.9 2.0 2.1 2.2 2.3 2.4 2.5
0 0.1 0.2 0.3 0.4 0.5 0.6 0.7 0.8 0.9 1.0 1.1 1.2 1.3 1.4 1.5 1.6

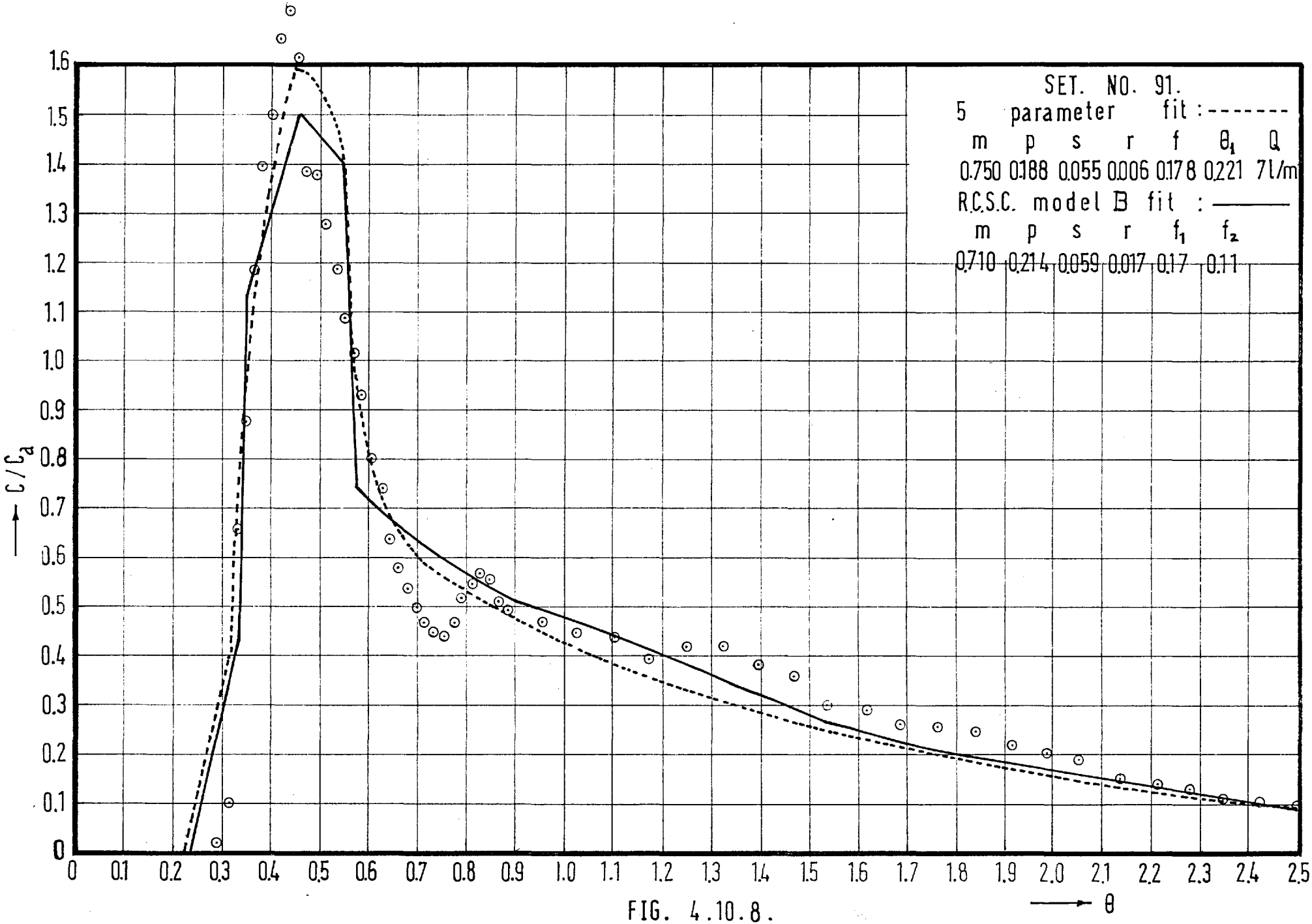
SET. NO. 91.
5 parameter fit : -------
m p s r f θ1 Q
0.750 0.188 0.055 0.006 0.178 0.221 7 l/m
R.C.S.C. model B fit : ———
m p s r f1 f2
0.710 0.214 0.059 0.017 0.17 0.11
C / Cd
θ

FIG. 4.10.8.

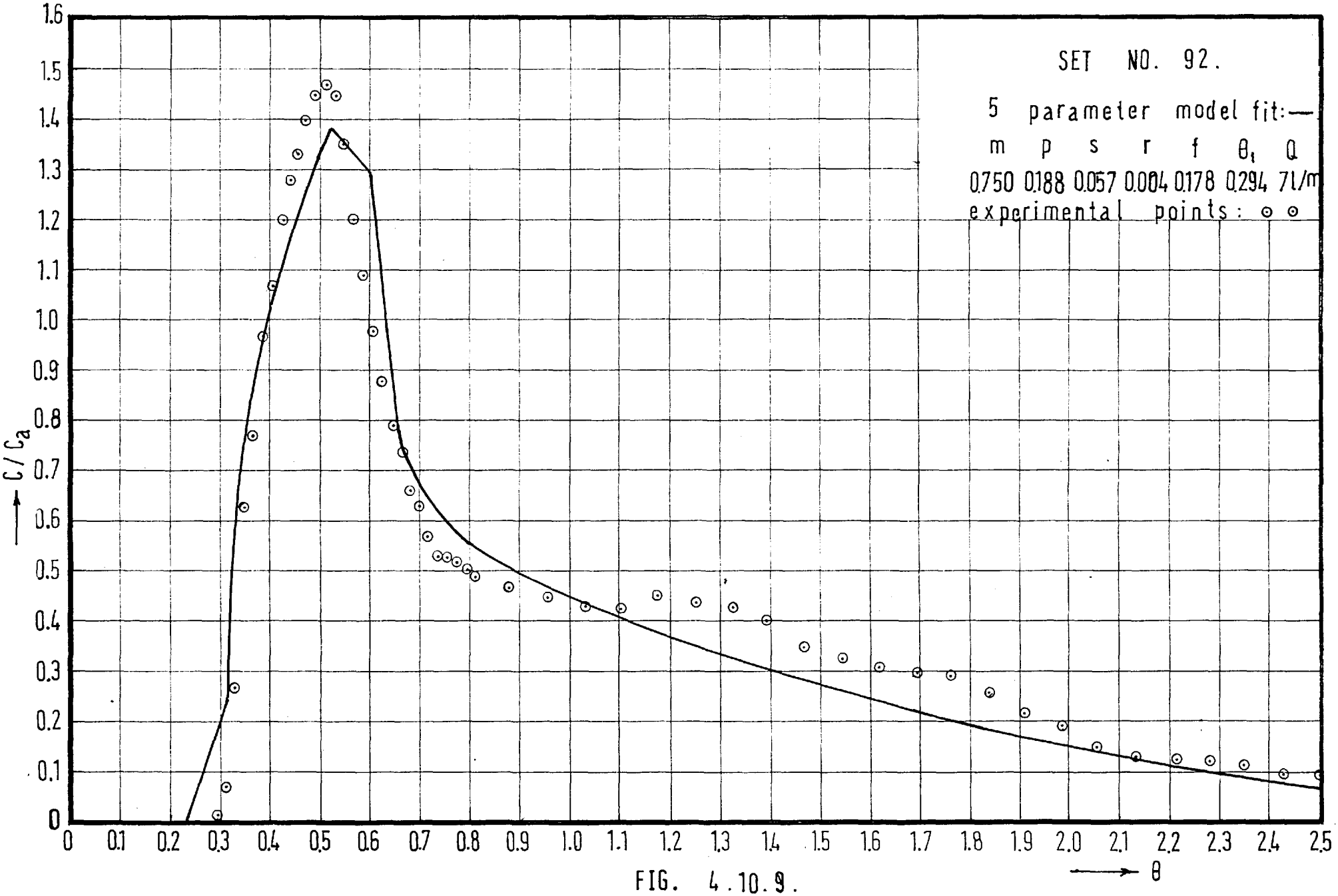
SET NO. 92.
5 parameter model fit:—
m p s r f θ1 Q
0.750 0.188 0.057 0.004 0.178 0.294 7l/m
experimental points: ⊙ ⊙
C / Ca
θ
0 0.1 0.2 0.3 0.4 0.5 0.6 0.7 0.8 0.9 1.0 1.1 1.2 1.3 1.4 1.5 1.6 1.7 1.8 1.9 2.0 2.1 2.2 2.3 2.4 2.5
0 0.1 0.2 0.3 0.4 0.5 0.6 0.7 0.8 0.9 1.0 1.1 1.2 1.3 1.4 1.5 1.6

FIG. 4.10.9.

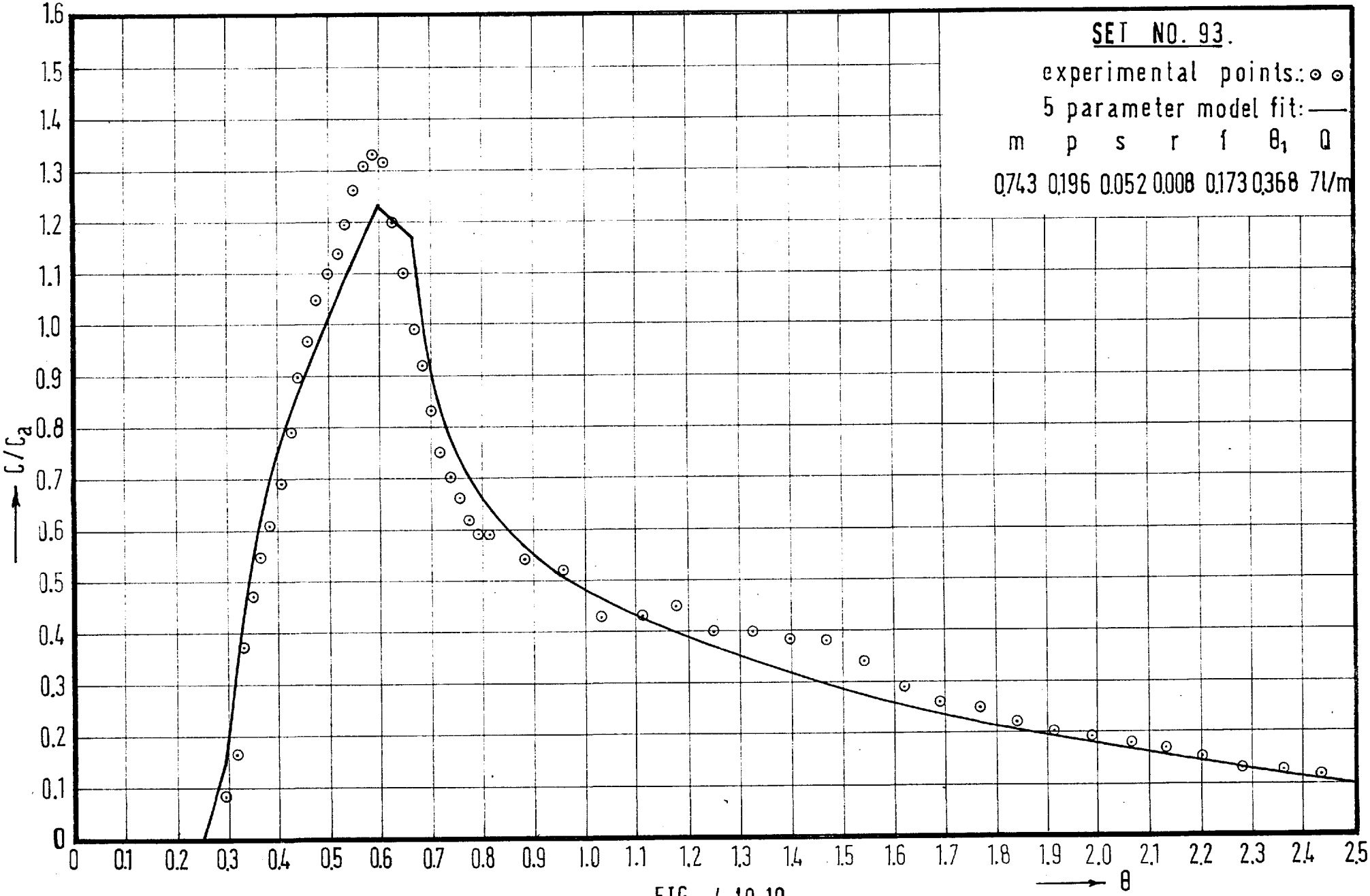
SET NO. 93.
experimental points: ⊙ ⊙
5 parameter model fit: ——
m p s r f θ1 Q
0.743 0.196 0.052 0.008 0.173 0.368 7l/m
C/Ca
θ
0 0.1 0.2 0.3 0.4 0.5 0.6 0.7 0.8 0.9 1.0 1.1 1.2 1.3 1.4 1.5 1.6 1.7 1.8 1.9 2.0 2.1 2.2 2.3 2.4 2.5
0 0.1 0.2 0.3 0.4 0.5 0.6 0.7 0.8 0.9 1.0 1.1 1.2 1.3 1.4 1.5 1.6

FIG. 4.10.10.

Table 4.10.1

Two Parameter Model

Set No.	Q ℓ/min.	θ_1	% tracer recovery	m	p	Standard Error
80	4	0.084	85	0.75	0.25	0.43
81	4	0.21	90	0.76	0.24	0.33
82	5	0.105	92	0.71	0.29	0.36
83	5	0.158	100	0.75	0.25	0.34
84	5	0.210	98	0.73	0.27	0.35
85	5	0.263	99	0.82	0.18	0.18
86	6	0.126	92	0.68	0.32	0.38
87	6	0.189	96	0.70	0.30	0.36
88	6	0.252	90	0.73	0.27	0.30
89	6	0.315	95	0.73	0.27	0.27
90	7	0.147	95	0.69	0.31	0.24
91	7	0.221	96	0.71	0.29	0.28
92	7	0.294	97	0.71	0.29	0.24
93	7	6.368	95	0.71	0.29	0.19
94	8	0.168	103	0.66	0.34	0.20
95	8	0.252	96	0.64	0.36	0.22
96	8	0.336	95	0.68	0.32	0.17
97	8	0.420	94	0.68	0.32	0.15
98	9	0.189	95	0.67	0.33	0.08
99	9	0.284	97	0.67	0.33	0.10
100	9	0.378	105	0.69	0.31	0.09
101	9	0.473	99	0.69	0.31	0.08
102	10	0.210	102	0.63	0.37	0.10
103	10	0.315	96	0.66	0.34	0.07
104	10	0.421	97	0.66	0.34	0.06
105	10	0.525	96	0.68	0.32	0.06
106	11	0.231	102	0.62	0.38	0.11
107	11	0.347	98	0.65	0.35	0.07
108	11	0.462	98	0.65	0.35	0.04
109	11	0.578	98	0.68	0.32	0.04
110	12	0.252	98	0.62	0.38	0.09
111	12	0.378	96	0.65	0.35	0.07
112	12	0.504	98	0.62	0.38	0.07
113	12	0.630	95	0.65	0.35	0.04

Table 4.10.1 (continued)

Set No.	Q ℓ/min	θ_1	% tracer recovery	m	p	Standard Error
114	13	0.273	98	0.59	0.41	0.12
115	13	0.410	97	0.66	0.34	0.10
116	13	0.546	95	0.66	0.34	0.08
117	13	0.673	99	0.66	0.34	0.06
118	14	0.294	95	0.67	0.33	0.12
119	14	0.441	99	0.67	0.33	0.13
120	14	0.588	95	0.63	0.37	0.08
121	14	0.735	95	0.67	0.33	0.08

Table 4.10.2.

Four Parameter S.C. Model

Set No.	Q ℓ/min	θ_1	% tracer recovery	m	p	s	f	Standard Error
80	4	0.084	85	0.536	0.456	0.008	0.03	0.37
81	4	0.21	90					
82	5	0.105	92	0.759	0.220	0.021	0.015	0.25
83	5	0.158	100	0.727	0.233	0.040	0.170	0.19
84	5	0.210	98	0.843	0.126	0.031	0.130	0.19
85	5	0.263	99	0.779	0.193	0.028	0.140	0.12
86	6	0.126	92	0.751	0.222	0.027	0.09	0.13
87	6	0.189	96	0.785	0.174	0.041	0.14	0.15
88	6	0.282	90	0.788	0.152	0.060	0.20	0.14
89	6	0.315	95	0.777	0.192	0.031	0.18	0.15
90	7	0.147	95	0.679	0.284	0.037	0.12	0.10
91	7	0.221	96	0.749	0.200	0.051	0.16	0.12
92	7	0.294	97	0.756	0.191	0.053	0.16	0.10
93	7	0.368	95	0.748	0.206	0.046	0.14	0.08
94	8	0.168	103	0.692	0.280	0.028	0.080	0.07
95	8	0.252	96	0.716	0.271	0.013	0.033	0.10
96	8	0.336	95	0.714	0.218	0.068	0.170	0.09
97	8	0.420	94	0.727	0.215	0.058	0.140	0.08

Table 4.10.2 (continued)

Set No.	Q ℓ/min	θ_1	% tracer recovery	m	p	s	f	Standard Error
98	9	0.181	95	0.589	0.311	0.10	0.080	0.08
99	9	0.284	97	0.675	0.291	0.034	0.074	0.07
100	9	0.378	105	0.702	0.250	0.048	0.100	0.07
101	9	0.473	99	0.704	0.259	0.037	0.090	0.05
102	10	0.210	102	0.631	0.360	0.009	0.010	0.05
103	10	0.315	96	0.648	0.333	0.019	0.038	0.04
104	10	0.421	97	0.657	0.311	0.031	0.074	0.04
105	10	0.525	96	0.676	0.286	0.038	0.073	0.05
106	11	0.231	102	0.542	0.349	0.109	0.096	0.10
107	11	0.347	98	0.579	0.332	0.089	0.079	0.06
108	11	0.462	98	0.576	0.331	0.093	0.078	0.04
109	11	0.578	98	0.662	0.280	0.058	0.094	0.05
110	12	0.252	98	0.541	0.367	0.092	0.076	0.07
111	12	0.378	96	0.617	0.328	0.055	0.056	0.04
112	12	0.504	98	0.589	0.350	0.061	0.055	0.03
113	12	0.630	95	0.636	0.306	0.058	0.076	0.04
114	13	0.273	98	0.548	0.407	0.045	0.05	0.07
115	13	0.410	97	0.588	0.395	0.017	0.02	0.03
116	13	0.546	95	0.596	0.352	0.052	0.05	0.03
117	13	0.673	99	0.600	0.360	0.040	0.05	0.05
118	14	0.294	95	0.552	0.391	0.057	0.06	0.06
119	14	0.441	99	0.558	0.367	0.074	0.075	0.06
120	14	0.588	95	0.539	0.378	0.083	0.075	0.03
121	14	0.735	95	0.576	0.352	0.072	0.078	0.04

Table 4.10.3

Five Parameter - S.C. Model

Set No.	Q ℓ/min	θ_1	% tracer recovery	m	p	s	r	f	Stand. Error
80	4	0.084	85	0.42268	0.3945	0.00002	0.18281	0.2174	0.16
81	4	0.21	90	0.52403	0.38978	0.05288	0.03331	0.30536	0.16
82	5	0.105	92	0.730	0.245	0.00001	0.025	0.150	0.18
83	5	0.158	100	0.778	0.190	0.025	0.007	0.140	0.18
84	5	0.210	98	0.760	0.200	0.020	0.020	0.150	0.17
85	5	0.263	99	0.800	0.170	0.017	0.008	0.140	0.11
86	6	0.126	92	0.721	0.243	0.034	0.002	0.120	0.15
87	6	0.189	96	0.768	0.176	0.053	0.003	0.180	0.16
88	6	0.252	90	0.778	0.150	0.065	0.007	0.230	0.11
89	6	0.315	95	0.745	0.232	0.022	0.001	0.200	0.16
90	7	0.147	95	0.695	0.246	0.044	0.015	0.160	0.134
91	7	0.221	96	0.750	0.188	0.055	0.007	0.178	0.160
92	7	0.294	97	0.750	0.188	0.057	0.004	0.178	0.100
93	7	0.368	95	0.743	0.196	0.052	0.008	0.173	0.066
94	8	0.168	103	0.667	0.290	0.010	0.032	0.140	0.090
95	8	0.252	96	0.680	0.260	0.050	0.010	0.147	0.060
96	8	0.336	95	0.705	0.207	0.076	0.012	0.217	0.060
97	8	0.420	94	0.696	0.190	0.083	0.031	0.256	0.070
98	9	0.189	95	0.581	0.303	0.062	0.054	0.092	0.030
99	9	0.284	97	0.652	0.264	0.059	0.025	0.168	0.060
100	9	0.378	105	0.702	0.256	0.035	0.007	0.090	0.070
101	9	0.473	99	0.694	0.260	0.041	0.005	0.110	0.050
102	10	0.210	102	0.550	0.332	0.062	0.056	0.085	0.040
103	10	0.315	96	0.613	0.325	0.033	0.029	0.113	0.040
104	10	0.421	97	0.649	0.312	0.028	0.011	0.085	0.040
105	10	0.525	96	0.672	0.281	0.042	0.005	0.090	0.040
106	11	0.231	102	0.491	0.330	0.124	0.054	0.137	0.080
107	11	0.347	98	0.531	0.323	0.095	0.051	0.110	0.040
108	11	0.462	98	0.406	0.299	0.170	0.125	0.180	0.030
109	11	0.578	98	0.592	0.291	0.048	0.069	0.110	0.030
110	12	0.252	98	0.544	0.364	0.077	0.014	0.080	0.050
111	12	0.378	96	0.582	0.322	0.069	0.027	0.080	0.030
112	12	0.504	98	0.491	0.321	0.122	0.066	0.130	0.030
113	12	0.630	95	0.605	0.333	0.031	0.031	0.050	0.030

it is possible for the second peak to represent bypassing of a slow nature through a relatively stagnant zone.

Closer observation of the curves in Fig. 90 - 93 reveals a gradual rise and fall in the tail of each curve which can be attributable only to the presence of a recirculation element. The curve of Fig.4.10.7 and 4.10.8 are fitted with the recirculation model of Fig.2.8.5. A batter fit was obtained as a result of introducing an extra parameter. However the result was not as good as expected, due to the fact that the shortcircuiting element contained plug flow only.

In view of the complications involved when extra parameters are introduced it would appear that four parameter model describes these curves reasonably well. Where the actual system contains macro-recirculation it will be necessary to use a more complex model. In general in any given case the best model is that which fits the curve adequately and contains the least number of parameters.

Table 4.10.3 (continued)

Set No.	Q ℓ/min	θ_1	% tracer recovery	m	p	s	r	f	Standard Error
114	13	0.273	98	0.273	0.326	0.175	0.108	0.230	0.040
115	13	0.410	97	0.546	0.384	0.042	0.027	0.050	0.030
116	13	0.546	95	0.582	0.345	0.066	0.007	0.070	0.030
117	13	0.673	99	0.556	0.373	0.063	0.008	0.050	0.030
118	14	0.294	95	0.422	0.300	0.154	0.124	0.236	0.030
119	14	0.441	99	0.418	0.309	0.168	0.105	0.212	0.040
120	14	0.588	95	0.527	0.376	0.082	0.015	0.080	0.020
121	14	0.735	95	0.539	0.387	0.073	0.001	0.060	0.030

4.11 Statistical Analysis

In the literature on longitudinal mixing various conclusions have been inferred from the statistical parameters of dispersion curves, and for comparison a statistical analysis of the above experimental data was carried out. The mean, median and modal times of flow and the standard deviation of the input and output pulses for each set of experiments were determined using the following formulae.

(i) The mean time of flow is given by the centroid of the pulse shape and was calculated as follows:

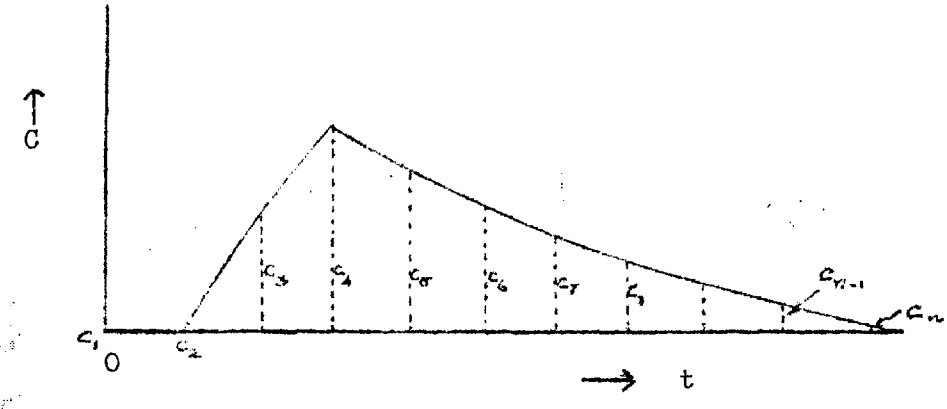

Fig.4.11.1.

Figure 4.11.1 shows a typical pulse as a plot of C against t. Readings are assumed to be taken at a uniform time intergal Δt. The distance of the centroid of the area under the pulse curve from the origin O is given by

$$\bar{t} = \frac{\sum_{i=1}^{n} \frac{\Delta t}{2}(C_i + C_{i+1}) \left\{ \frac{\Delta t}{3} \left(\frac{2C_{i+1} + C_i}{C_{i+1} + C_i} \right) + (i-1)\Delta t \right\}}{\sum_{i=1}^{n} \frac{1}{2}\Delta t(C_i + C_{i+1})} \qquad \ldots\ldots 4.11.1$$

(ii) The modal time is the time from the origin at which the maximum value of C occurs.

(iii) The median time is the time from the origin to that ordinate which bisects the area under the curve.

(iv) The standard deviation is the square root of the second moment about the mean value and is given from Fig.4.11.1 by

$$\sigma = \sqrt{\frac{\sum_{i=1}^{n} \frac{\Delta t}{2}(C_i + C_{i+1}) \left\{ \frac{\Delta t}{3} \left(\frac{2C_{i+1} + C_i}{C_{i+1} + C_i} \right) + (i-1)\Delta t - \bar{t} \right\}^2}{\sum_{i=1}^{n} \frac{\Delta t}{2}(C_i + C_{i+1})}} \qquad \ldots\ldots 4.11.2$$

In analysing the experimental results, equations 4.11.1 and 4.11.2 were modified to include two different time intervals Δt_1 in the vicinity of the peak and Δt_2 for the remainder of the curve.

There is much controversy in the literature with regard to the calculation of average detention time. Theoretically the average detention time is equal to the mean time $\bar{t}$. obtained from equation 4.11.1 which is also equal to the volume of the system divided by the flow rate. In the case of a thick input pulse the average detention time is theoretically equal to the distance between the mean of input pulse and the mean of the output pulse.

In flow systems which contain any element or region in which the flow is very slow in comparison with the main flow, often referred to

in the literature as "dead space", tracer which enters these regions is released very slowly, and at low concentrations which are difficult to measure accurately. Consequently the flow curve may have a long tail, which makes the determination of the first moment about the origin inaccurate. This difficulty has been referred to by Thackston et al.[47], Krenkel[48] and Spalding[49].

Thackston et al.[47] introduced a mathematical model to describe the flow curve in terms of the longitudinal diffusion coefficient D_L, average velocity and time of flow. This model is based on the diffusion equation

$$\frac{\partial C}{\partial t} = D_L \frac{\partial^2 C}{\partial x^2} - \bar{u} \frac{\partial C}{\partial t} \qquad \ldots\ldots 4.11.3$$

where C = the average concentration of the tracer over the cross-section of the flow

$\bar{u}$ = the mean velocity of the flow.

If the tracer is initially uniformly distributed across a plane perpendicular to the flow x = 0 at time t = 0, then the solution of equation 4.11.3 is given by Thackston et al.[47] as

$$C = \frac{M}{A\sqrt{4\pi D_L t}} e^{-(x-\bar{u}t)^2/4D_L t} \qquad \ldots\ldots 4.11.4$$

where M = total mass of the tracer

x = distance from the origin in the direction of the flow

A = cross-sectional area of flow normal to x

In dimensionless form equation 4.11.4 is written as

$$\frac{C}{M/A\bar{u}} = \sqrt{\frac{P}{4\pi t.\bar{t}}} e^{\frac{-P(1-t/\bar{t})}{4t/\bar{t}}} \qquad \ldots\ldots 4.11.5$$

where P = Peclet number = $\frac{\bar{u}x}{D_L}$ and

$\bar{t}$ = average detention time = $\frac{x}{\bar{u}}$ where

x = the distance from the injection point to the measuring point at the outlet.

$M/A\bar{u}$ = the total concentration and is given by the area under the flow curve.

Thackston et al.[47] recommend that this equation should be fitted to the flow curve by least squares taking P and $\bar{t}$ as variable parameters. From the optimum values of P and $\bar{t}$ thus obtained, the actual diffusion coefficient D_L and the average detention time $\bar{t}$ are computed.

As initial values $\bar{t}$ is taken as the nominal detention time and $\bar{u} = \frac{x}{\bar{t}}$. D_L is calculated using Levenspiel's[9] formula given below.

If σ_1 and σ_2 are the standard deviations of the input and output pulses respectively, then the change in variance between the input and output points is given by $\Delta\sigma^2 = \sigma_2^2 - \sigma_1^2$. In dimensionless form this difference is related to the Peclet number P as follows

$$\frac{\Delta\sigma^2}{\bar{t}^2} = 2/P + \frac{1}{P^2}\left(e^{-2P} + 4e^{-P} + 4Pe^{-P} - 5\right) \qquad \ldots\ldots 4.11.6$$

Calculating $\Delta\sigma^2$ and taking $\bar{t}$ as the nominal detention time P is computed and D_L is obtained. The value of P obtained from equation 4.11.6 is directly introduced into equation 4.12.5 as a first approximation in the optimisation procedure.

From the optimised average detention time, the fraction of stagnant volume, referred to here as dead space is given by

$$\frac{\text{Nominal Detention time - Optimised Detention time}}{\text{Nominal Detention Time}}$$

In Table 4.11.1 Peclet numbers, diffusion coefficients and dead space values are calculated using the time from the centroid of the input pulse to the centroid of the output pulse as the mean time $\bar{t}$ and applying equation 4.11.6. In many cases the results indicate negative dead space which is impossible.

Table 4.11.1

Set No.	Q ℓ/min	θ_1	% tracer recovery	T_p mins.	Mean of input pulse	Mean of output pulse	$\bar{t}$ mins.	% dead space	σ_i in mins.	σ_o in mins.	D_L cm²/min.	Peclet No.
80	4	0.084	85									
81	4	0.21	90									
82	5	0.105	92	2	1.00	17.01	16.01	16	0.644	8.560	235	3.22
83	5	0.158	100	3	1.49	18.79	17.30	9	0.934	9.206	307	2.99
84	5	0.210	98	4	1.99	18.00	16.01	16	1.223	9.892	322	3.13
85	5	0.263	99	5	2.48	17.91	15.43	19	1.511	7.940	298	4.10
86	6	0.126	92	2	0.99	15.20	14.21	10	0.645	7.16	296	3.90
87	6	0.189	96	3	1.49	16.84	15.35	3	0.934	8.633	376	3.07
88	6	0.252	90	4	1.99	15.60	13.61	14	1.223	7.812	394	2.93
89	6	0.315	95	5	2.48	16.58	14.10	11	1.513	8.370	400	2.78
90	7	0.147	95	2	0.99	13.24	12.25	9	0.644	5.753	296	4.55
91	7	0.221	96	3	1.49	14.12	12.62	7	0.934	6.465	367	3.67
92	7	0.294	97	4	1.99	14.90	12.91	5	1.223	7.094	420	3.21
93	7	0.368	95	5	2.48	15.13	12.65	7	1.512	7.032	423	3.19
94	8	0.168	103	2	0.998	11.97	10.97	7	0.645	5.126	332	4.64
95	8	0.252	96	3	1.490	12.26	10.77	9	0.934	5.165	346	4.45
96	8	0.336	95	4	1.990	12.19	10.20	14	1.223	5.075	373	4.13
97	8	0.420	94	5	2.480	12.62	10.14	15	1.512	4.922	330	4.67
98	9	0.189	95	2	0.998	11.01	10.01	5	0.645	4.299	291	5.94
99	9	0.284	97	3	1.490	10.87	9.37	11	0.934	4.180	315	5.50
100	9	0.378	105	4	1.990	11.43	9.44	10	1.223	4.468	361	4.79
101	9	0.473	99	5	2.480	13.50	11.02	-4	1.512	5.886	485	3.57

Table 4.11.1 (continued)

Set No.	Q ℓ/min	θ_1	% tracer recovery	T_p mins.	Mean of input pulse	Mean of output pulse	$\bar{t}$ mins.	% dead space	σ_i in mins.	σ_o in mins.	D_L $cm^2/min.$	Peclet No.
102	10	0.210	102	2	0.997	10.06	9.06	5	0.645	3.646	266	7.24
103	10	0.315	96	3	1.490	10.32	8.82	7	0.934	3.821	315	6.11
104	10	0.421	97	4	1.990	11.56	9.57	-0.5	1.223	4.707	438	4.39
105	10	0.525	96	5	2.480	11.48	8.999	5	1.512	4.411	417	4.62
106	11	0.231	102	2	0.996	10.57	9.57	-10	0.645	4.107	355	5.97
107	11	0.347	98	3	1.490	10.77	9.28	-7	0.935	4.296	419	5.05
108	11	0.462	98	4	1.980	10.92	8.94	-3	1.224	4.110	384	5.52
109	11	0.578	98	5	2.480	11.61	9.13	-5	1.512	4.676	517	4.10
110	12	0.252	98	2	0.995	8.885	7.89	0.5	0.545	3.053	268	8.60
111	12	0.378	96	3	1.492	9.553	8.06	-1	0.935	3.503	364	6.34
112	12	0.504	98	4	1.986	10.232	8.245	-4	1.224	3.780	412	5.61
113	12	0.630	95	5	2.476	10.409	7.932	0.03	1.513	3.676	380	6.08
114	13	0.273	98	2	0.998	8.416	7.418	-1	0.645	2.787	254	9.84
115	13	0.410	97	3	1.491	8.491	7.000	4	0.935	2.776	274	9.12
116	13	0.546	95	4	1.990	9.355	7.365	-0.5	1.224	3.220	362	6.91
117	13	0.673	99	5	2.481	10.329	7.847	-7	1.513	3.784	479	5.23
118	14	0.294	95	2	0.997	7.719	6.721	1	0.645	2.634	284	9.48
119	14	0.441	99	3	1.493	8.534	7.040	-3	0.935	2.852	316	8.53
120	14	0.588	95	4	1.988	8.699	6.711	1	1.224	2.835	320	8.43
121	14	0.735	95	5	2.482	9.209	6.727	1	1.512	3.021	361	7.47

Table 4.11.2

Set No.	Q ℓ/min	θ_1	% tracer recovery	T_p mins.	D_L cm^2/min.	P Peclet No.	$\bar{t}$ min.	Dead Space %	Mean % Dead Space	Mean D_L cm^2/sec	Mean P	Mean $\bar{t}$ min.
80	4	0.084	85									
81	4	0.21	90									
82	5	0.105	92	2	551	2.17	15.945	21				
83	5	0.158	100	3	477	2.51	13.538	37	35	476	2.53	13.97
84	5	0.210	98	4	445	2.68	12.699	43				
85	5	0.263	99	5	433	2.75	13.693	41				
86	6	0.126	92	2	512	2.80	12.411	27				
87	6	0.189	96	3	484	2.96	11.756	35	37	439	3.35	11.7
88	6	0.252	90	4	412	3.48	11.288	42				
89	6	0.315	95	5	347	4.14	11.344	44				
90	7	0.147	95	2	489	3.42	10.794	27				
91	7	0.221	96	3	508	3.29	10.216	35	36	415	4.23	10.39
92	7	0.294	97	4	372	4.50	10.195	40				
93	7	0.368	95	5	293	5.72	10.369	41				
94	8	0.168	103	2	443	4.31	9.481	27				
95	8	0.252	96	3	350	5.45	9.504	33	34	356	5.48	9.57
96	8	0.336	95	4	325	5.88	9.445	37				
97	8	0.420	94	5	305	6.26	9.833	38				
98	9	0.189	95	2	361	5.96	8.953	24				
99	9	0.284	97	3	356	6.05	9.013	26	29	330	6.57	9.13
100	9	0.378	105	4	314	6.84	9.061	33				
101	9	0.473	99	5	289	7.42	9.477	33				

Table 4.11.2 (continued)

Set No.	Q ℓ/min	θ_1	% tracer recovery	T_p mins.	D_L cm^2/min.	P Peclet No.	$\bar{t}$ min.	Dead Space %	% Mean Dead Space	Mean D_L cm^2/sec	Mean P	Mean $\bar{t}$ min.
102	10	0.210	102	2	392	6.10	8.573	20				
103	10	0.315	96	3	346	6.90	8.596	26	26	335	7.24	8.82
104	10	0.421	97	4	313	7.63	8.833	28				
105	10	0.525	96	5	289	8.27	9.274	29				
106	11	0.231	102	2	390	6.73	8.129	18				
107	11	0.347	98	3	358	7.35	8.250	22	22	341	7.78	8.46
108	11	0.462	98	4	326	8.06	8.539	24				
109	11	0.578	98	5	292	8.98	8.908	23				
110	12	0.252	98	2	387	7.41	7.388	19				
111	12	0.378	96	3	395	7.26	7.679	22	21	364	7.90	8.00
112	12	0.504	98	4	353	8.12	8.387	20				
113	12	0.630	95	5	324	8.84	8.559	23				
114	13	0.273	98	2	346	8.98	7.101	17				
115	13	0.410	97	3	398	7.80	7.443	19	19	351	8.91	7.72
116	13	0.546	95	4	361	8.60	7.941	19				
117	13	0.673	99	5	302	10.27	8.381	20				
118	14	0.294	95	2	431	7.76	6.532	18				
119	14	0.441	99	3	365	9.17	7.106	18	18	342	9.28	7.31
120	14	0.588	95	4	335	9.97	7.549	17				
121	14	0.735	95	5	326	10.25	8.07	19				

Table 4.11.3

Set No.	Q ℓ/min	θ_1	% tracer recovery	Nominal detention time "T" mins.	T_p min.	$\bar{t}/T$	$T_p/4T$	Corr. $\bar{t}/T$	Corr. Dead Space %	Mean Dead Space %	Mean f from 5 par.model	Mean of S.C. Vol. model 5 par. %
80	4	0.084	85									
81	4	0.21	90									
82	5	0.105	92		2	0.84	0.026	0.81	19			
83	5	0.158	100	19.04	3	0.71	0.039	0.67	33	35	0.15	3
84	5	0.210	98		4	0.67	0.052	0.62	38			
85	5	0.263	99		5	0.72	0.065	0.66	34			
86	6	0.126	92		2	0.79	0.031	0.76	24			
87	6	0.189	96	15.87	3	0.74	0.046	0.69	31	34	0.18	6
88	6	0.252	90		4	0.71	0.063	0.65	35			
89	6	0.315	95		5	0.72	0.078	0.64	36			
90	7	0.147	95		2	0.80	0.037	0.76	24			
91	7	0.221	96	13.60	3	0.76	0.055	0.71	29	29	0.17	6
92	7	0.294	97		4	0.75	0.074	0.68	32			
93	7	0.368	95		5	0.77	0.091	0.68	32			
94	8	0.168	103		2	0.80	0.042	0.76	24			
95	8	0.252	96	11.90	3	0.80	0.063	0.74	26	26	0.19	9
96	8	0.336	95		4	0.80	0.084	0.72	28			
97	8	0.420	94		5	0.83	0.105	0.72	28			
98	9	0.189	95		2	0.85	0.047	0.80	20			
99	9	0.284	97	10.58	3	0.88	0.070	0.81	19	21	0.12	7
100	9	0.378	105		4	0.86	0.094	0.77	23			
101	9	0.473	99		5	0.90	0.118	0.78	22			

Table 4.11.3 (continued)

Set No.	Q ℓ/min	θ_1	% tracer recovery	Nominal detention time "T" mins.	T_p min.	$\bar{t}/T$	$T_p/4T$	Corr. $\bar{t}/T$	Corr. Dead Space %	Mean Dead Space %	Mean f from 5 par. model	Mean of S.C. Vol. Model 5 par. %
102	10	0.210	102		2	0.90	0.053	0.85	15			
103	10	0.315	96	9.52	3	0.90	0.079	0.82	18	16	0.09	8
104	10	0.421	97		4	0.93	0.105	0.83	17			
105	10	0.525	96		5	0.97	0.131	0.84	16			
106	11	0.231	102		2	0.94	0.058	0.88	12			
107	11	0.347	98	8.65	3	0.95	0.086	0.86	14	12	0.13	18
108	11	0.462	98		4	0.99	0.115	0.87	13			
109	11	0.578	98		5	1.03	0.144	0.89	11			
110	12	0.252	98		2	0.93	0.063	0.87	13			
111	12	0.378	96	7.93	3	0.97	0.094	0.88	12	10	0.08	11
112	12	0.504	98		4	1.05	0.126	0.92	8			
113	12	0.630	95		5	1.08	0.157	0.92	8			
114	13	0.273	98		2	0.97	0.068	0.90	10			
115	13	0.410	97	7.32	3	1.01	0.102	0.91	9	7	0.06	7
116	13	0.546	95		4	1.08	0.136	0.94	6			
117	13	0.673	99		5	1.14	0.170	0.97	3			
118	14	0.294	95		2	0.96	0.074	0.89	11			
119	14	0.441	99	6.80	3	1.04	0.110	0.93	7	5	0.07	8
120	14	0.588	95		4	1.11	0.148	0.96	4			
121	14	0.735	95		5	1.18	0.184	1.00	0.4			

Table 4.11.4

Set No.	Q ℓ/min	θ_1	% tracer recovery	Nominal hor. velocity cm/s	T_p	$t_{a/T}$	$t_{m/T}$	$t_{50/T}$	$t_{10/T}$	t_{90}/t_{90}
80	4	0.084	85							
81	4	0.21	90							
82	5	0.105	92	0.1207	2	0.84	0.31	0.79	1.63	0.21
83	5	0.158	100	0.1207	3	0.90	0.31	0.94	1.78	0.18
84	5	0.210	98	0.1207	4	0.84	0.37	0.89	1.68	0.19
85	5	0.263	99	0.1207	5	0.81	0.41	0.89	1.63	0.21
86	6	0.126	92	0.1449	2	0.89	0.36	0.82	1.70	0.21
87	6	0.189	96	0.1449	3	0.96	0.38	0.88	2.02	0.18
88	6	0.252	90	0.1449	4	0.86	0.44	0.76	1.95	0.19
89	6	0.315	95	0.1449	5	0.88	0.49	0.82	2.02	0.20
90	7	0.147	95	0.1691	2	0.90	0.42	0.81	1.69	0.24
91	7	0.221	96	0.1691	3	0.93	0.44	0.86	1.91	0.21
92	7	0.294	97	0.1691	4	0.95	0.51	0.88	1.98	0.21
93	7	0.368	95	0.1691	5	0.93	0.59	0.88	2.06	0.22
94	8	0.168	103	0.1932	2	0.92	0.46	0.84	1.85	0.24
95	8	0.252	96	0.1932	3	0.90	0.53	0.84	1.85	0.25
96	8	0.336	95	0.1932	4	0.86	0.59	0.82	1.85	0.25
97	8	0.420	94	0.1932	5	0.86	0.65	0.88	1.85	0.27
98	9	0.184	95	0.2174	2	0.95	0.57	0.89	1.79	0.28
99	9	0.284	97	0.2174	3	0.89	0.57	0.87	1.70	0.29
100	9	0.378	105	0.2174	4	0.90	0.64	0.92	1.89	0.28
101	9	0.473	99	0.2174	5	1.04	0.73	1.02	2.36	0.24
102	10	0.210	102	0.2415	2	0.95	0.60	0.92	1.79	0.29
103	10	0.315	96	0.2415	3	0.93	0.64	0.92	1.70	0.31
104	10	0.421	97	0.2415	4	1.00	0.72	1.02	1.89	0.28
105	10	0.525	96	0.2415	5	0.95	0.80	1.05	2.36	0.30
106	11	0.231	102	0.2657	2	1.10	0.61	1.04	1.79	0.28
107	11	0.347	98	0.2657	3	1.07	0.69	1.04	1.79	0.26
108	11	0.462	98	0.2657	4	1.03	0.80	1.07	2.10	0.28
109	11	6.578	98	0.2657	5	1.05	0.87	1.13	2.00	0.28
110	12	0.252	98	0.2898	2	1.00	0.66	1.01	2.08	0.32
111	12	0.378	96	0.2898	3	1.02	0.72	1.04	2.19	0.30
112	12	0.504	98	0.2898	4	1.04	0.87	1.10	2.19	0.29
113	12	0.630	95	0.2898	5	1.00	0.96	1.13	2.31	0.31
114	13	0.273	98	0.3140	2	1.01	0.75	1.02	1.76	0.35
115	13	0.410	97	0.3140	3	0.96	0.78	1.02	2.01	0.35
116	13	0.546	95	0.3140	4	1.00	0.85	1.13	2.14	0.32
117	13	0.673	99	0.3140	5	1.07	1.04	1.23	2.14	0.31
118	14	0.294	95	0.3381	2	0.99	0.77	0.99	1.77	0.36
119	14	0.444	99	0.3381	3	1.04	0.84	1.10	1.77	0.37
120	14	0.588	95	0.3381	4	0.99	0.97	1.14	2.05	0.32
121	14	0.735	95	0.3381	5	0.99	1.03	1.25	2.32	0.33

In Table 4.11.2 the experimental results are fitted to the model equation 4.11.5 using the values of P and $\bar{t}$ in Table 4.11.1 as initial values. Optimum values of P and $\bar{t}$ were thus obtained, and dead space values recalculated. In this analysis the ordinates of the flow curve are made dimensionless by dividing them by the area of the curve. The time scale is not dimensionless. The dead space volumes in this case were computed by subtracting the mean time of the input pulse from the optimised mean time $\bar{t}$ of the output pulse and dividing it by the nominal detention time. Although the results shown in Table 4.11.2 now show no negative values for dead space, the values obtained are rather high. It must be remembered that the model is based on an impulse input at time t = 0 at a flow cross-section x = 0 whereas for these experiments the input was a pulse of considerable width such that the model is not strictly applicable. The fact that lower values of θ_1 (or T_p) give rise to lower values of dead space tends to support this argument. Also if dead space does exist then the longer the input pulse, or the greater the mass of tracer injected, the longer will be the tail of the dispersion curve. It appears from these experiments that if the input pulse width is increased by a length x so also is the tail of the output curve. This in itself should not give rise to any inaccuracy in estimation of $\bar{t}$ from the distance between the centroids, but when dead space exists then excessively long tails are produced which tend to give large values of $\bar{t}$.

In order to obtain a more realistic average time of flow an empirical correction factor is proposed here. It is assumed that the width of the output pulse is equal to 4T where T is the nominal detention time. The remainder of the tail if any is ignored. Then the shift in the mean time of flow of the output curve due to

a duration of injection time $T_p = T_{p/4}$. On this empirical assumption, the corrected average time of flow $\bar{t}$ = the optimised $\bar{t}$ for the output pulse - $T_{p/4}$.

The corrected $\bar{t}$ and the dead space values computed from these corrected mean times are shown in Table 4.11.3. The dead space values thus obtained are more realistic. For comparison the short circuit volumes and fractions of flow bypassing through these volumes obtained from the five parameter model are also given. It can be seen that for high flows the agreement between dead space and short-circuiting volume is reasonable. The differences between the values at the low flows might be attributable to the fact that the five parameter model includes only one element of shortcircuiting, whereas at low flows it is probable that the system contains bypassing of both the fast and slow types. The model parameter values obtained suggest that a fast shortcircuiting flow through a small volume is prominent, and consequently the possible presence of a stagnant zone has been indicated.

In Table 4.11.4 the results of the tank tests are analysed qualitatively in the manner described in Chapter 1. The mean time "t_a", modal time "t_m", 50 percentile "t_{50}", 10 percentile "t_{10}", and Morril Index i.e. 90 percentile/10 percentile, are all computed for each set. It can be seen the normalised values of mean, median and mode approach 1.0 as the flow through increases which is to be expected since higher velocities and increased turbulence tend to produce plug flow. It appears that no further information can be gained from such analysis.

CHAPTER V

OPTIMISATION TECHNIQUES

5.1. Curve Fitting

Having obtained experimental input and output data for a flow system and having proposed a mathematical model for the system, it is necessary to find the values of the parameters in the model such that it gives as nearly as possible the same relationship between input and output as does the real system. These values of the parameters are known as the optimum values, and the technique for evaluating them used in this study is curve fitting.

When the experimental data are accurate or of equal reliability, it is frequently considered that the best approximation of the parameters is that for which the sum of the squares of the differences between the fitted curve and the data over the whole domain is the least. This is known as Legendre's principle of Least Squares[50].

Mathematically, let the model to be fitted to the data be

$$E(Y) = f(x, \beta) \qquad \ldots\ldots 5.1.1$$

where x and β are in Matrix Notation, x donating the independent variables $x_1, x_2, x_3 \ldots x_m$ and $\beta_1, \beta_2, \beta_3 \ldots \beta_k$ are the values of k parameters. E(Y) is the expected value of the dependent variable Y.

Let the data points be denoted by y_i; $i = 1, 2, 3 \ldots n$ corresponding to $x_{1i}, x_{2i}, x_{3i} \ldots x_{mi}$ where n is the number of data points. Then the least squares error is given by

$$\phi = \sum_{i=1}^{n} (y_i - Y_i)^2 \qquad \ldots\ldots 5.1.2$$

where Y_i are the values of Y predicted by equation 5.1.1. The problem now is to compute those values of the parameters that will minimise ϕ.

The function $f(x, \beta)$ given by equation 5.1.1 can be linear or non-linear depending on whether the β's are linearly or non-linearly

related to the independent variables $x_{1 \to m}$. Also the function ϕ given by equation 5.1.2 will be linear or non-linear depending on whether the function E(Y) is linear or non-linear. No completely satisfactory solution exists for this problem if these functions are non-linear.

5.2. Types of Error Profile

In all non-linear curve fitting it is essential to know the variations of ϕ with respect to changes in the values of the β's. This may be visualised by plotting the values of ϕ corresponding to a particular parameter, say β_1, as shown in Fig.5.2.1 keeping the other parameters constant.

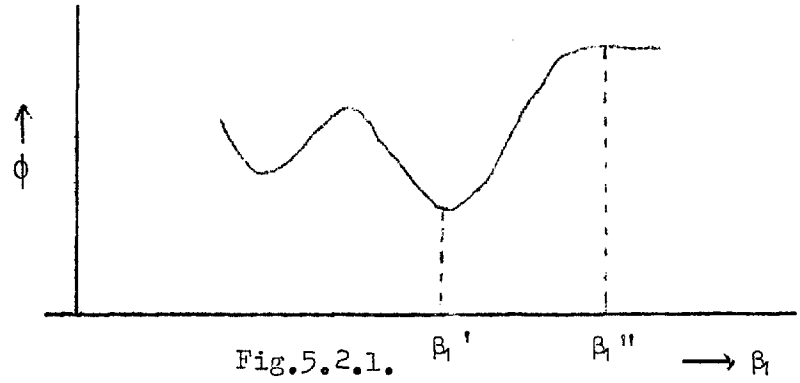

Fig.5.2.1.

If ϕ is linearly related to β_1, the error profile will be elliptical. If it is non linearly related, the profile will be distorted according to the severity of the non linearity. It is found however, that even in the most severe case of non-linearity, the error profile is nearly elliptical in the immediate vicinity of the minimum ϕ. As observed by many numerical analysts, the contour surface of ϕ is generally attenuated in some directions (left portion of the profile in Fig.5.2.1) and elongated in other directions so that the minimum lies at the bottom of a trough. If there is more than one trough, then it is essential that the

initial values of the β's be chosen on the inside slopes of the trough containing the minimum.

5.3. Available methods of solution

In this section various available methods and their respective merits and demerits will be discussed.

(i) The Newton-Raphson Method This method involves the expansion of the function ϕ given by equation 5.1.2 in the Taylor's series through the linear terms. For simplicity let equation 5.1.2 be written in a different form as follows

$$\phi = \sum_{i=1}^{n} [f_i(x,b)]^2 \qquad \ldots\ldots \quad 5.3.1$$

where $f_i(x,b) = y_i - f(x,\beta)$

For a minimum $\frac{\partial \phi}{\partial \beta} = 0$ or $\frac{\partial \phi}{\partial b} = 0$

Therefore

$$\sum_{i=1}^{n} f_i(x,b) = 0 \qquad \ldots\ldots \quad 5.3.2$$

Now a change in a parameter "β" will cause a change in "b" in equation 5.3.2. Suppose"b" changes by δb. Then, expanding $f(x,b+\delta b)$ by Taylor's series in the linear terms,

$$f(x_i,b+\delta b) = f(x_i,b) + \sum_{j=1}^{k} \frac{\partial f_i}{\partial b_j} \cdot \delta b_j$$

$$i = 1,2,3,\ldots n \qquad \ldots\ldots \quad 5.3.3$$

In equation 5.3.2 β is replaced notationally by "b", values of "b" being the least squares estimates of β. It is assumed that the vector δb is a small correction to "b". When ultimate convergence of the series of small corrections or steps is achieved, $f(x_i,b+\delta b) = 0$

$$\therefore \sum_{j=1}^{k} \frac{\partial f_i}{\partial b_j} \times \delta b_j = - f_i(x_*, b) \qquad \ldots\ldots 5.3.4$$

$$i = 1, 2, 3, \ldots n$$

In matrix form equation 5.3.4. can be written as

$$B . \delta B = f \qquad \ldots\ldots 5.3.5$$

where the matrix $B = - \frac{\partial f_i}{\partial b_j}$

Since B is not generally symmetric, multiplying both sides of equation 5.3.5. by B^T, the transpose of B

$$B^T . B . \delta B = B^T . f \qquad \ldots\ldots 5.3.6$$

Writing $B^T . B = A$ and $B^T . f = G$ equation 5.3.6 becomes

$$A . \delta B = G \qquad \ldots\ldots 5.3.7$$

Then $$\delta B = A^{-1} . G \qquad \ldots\ldots 5.3.8$$

The corrected values of the B's are given by $B + \delta B$ and the process of correction is repeated until a minimum value of ϕ is obtained. This method is also known as the Gauss method or the Gauss-Newton method. If the initial values of the parameters assumed are very near to the optimum values, this method can give a rapid convergence, but in non-linear cases sometimes divergence occurs after successive iterations and no minimum value of ϕ can be obtained.

(ii) <u>The Method of Steepest Descent</u> This method makes corrections to the trial vectors "b" by moving in the direction of the negative gradient of ϕ given by

$$\delta b = - a \frac{\partial \phi}{\partial b} = - a \cdot 2 \sum_{i=1}^{n} \frac{\partial f_i(x,b)}{\partial b} . f_i(x,b) \qquad \ldots\ldots 5.3.9$$

where "a" is a suitably selected constant. In matrix notation, the correction vector δb in the r^{th} iteration can be written as :-

$$(\frac{1}{a} I) \delta b^r = G^r \qquad \ldots\ldots 5.3.10$$

where G has the same meaning as before and I is a unit matrix. The values of the b's in the $(r+1)^{th}$ iteration are given by

$$b^{r+1} = b^{r} + \delta b^{r} \qquad \ldots\ldots 5.3.11$$

δb^{r} is obtained by solving equation 5.3.10 and the process is repeated until a minimum is obtained for the value of ϕ. The method of steepest descent always converges if the initial values of the parameters are close to the optimum values but has the disadvantage of very slow progress after the first few iterations.

(iii) Marquardt's Method Marquardt[51] modified the above methods and proposed a new method which he described as the "Maximum Neighbourhood method". This method again is based on the assumption that the truncated Taylor series can adequately represent a non linear function. Marquardt rewrote equation 5.3.7. as

$$(A + \lambda I)\delta b = G \qquad \ldots\ldots 5.3.12$$

Comparing equations 5.3.7 and 5.3.10 it is evident that methods (i) and (ii) are incorporated in this formula where λ replaces $\frac{1}{a}$ in equation 5.3.10. Equation 5.3.12 can be described more clearly as follows. Let "f" denote the function f(x,b). Then the matrix A will represent

$$A = \begin{bmatrix} \sum_{i=1}^{n} \frac{\partial f_i}{\partial b_1} \\ \sum_{i=1}^{n} \frac{\partial f_i}{\partial b_2} \\ \vdots \\ \sum_{i=1}^{n} \frac{\partial f_i}{\partial b_k} \end{bmatrix} x \begin{bmatrix} \sum_{i=1}^{n} \frac{\partial f_i}{\partial b_1} & \cdots & \sum_{i=1}^{n} \frac{\partial f_i}{\partial b_2} & \cdots & \sum_{i=1}^{n} \frac{\partial f_i}{\partial b_k} \end{bmatrix}$$

$\therefore$ A is a symmetric k x k matrix.

If the elements of the matrix "A" are written as

$$A = \begin{bmatrix} a_{11} & a_{12} & a_{13} & \cdots & a_{1k} \\ a_{21} & a_{22} & a_{23} & \cdots & a_{2k} \\ \vdots & \vdots & \vdots & & \vdots \\ a_{k1} & a_{k2} & a_{k3} & & a_{kk} \end{bmatrix}$$

Then $(A + \lambda I)$ is obtained by adding λ to the diagonal of the matrix A. δb is a vector of k elements and G is obtained as follows:-

$$G = \begin{bmatrix} \sum_{i=1}^{n} \frac{\partial f_i}{\partial b_1} \\ \vdots \\ \sum_{i=1}^{n} \frac{\partial f_i}{\partial b_k} \end{bmatrix} x \sum_{i=1}^{n} f_i$$

Thus G is a column vector of k elements. For convenience Marquardt[51] proposed that "A" and "G" should be scaled as follows:-

$$A^{*} = (a^{*}_{jj}) = \frac{a_{jj'}}{\sqrt{a_{jj}} \times \sqrt{a_{j'j'}}}$$

$$G^{*} = (g^{*}_{j}) = \frac{g_j}{\sqrt{a_{jj}}}$$

On solution the corrections δb_j are obtained by dividing δb^{*}_{j} by $\sqrt{a_{jj}}$. The asterisks denote the scaled quantities. The g's are the elements of the G vector.

Therefore after scaling equation 5.3.12 becomes

$$(A^{*} + \lambda I) \times \delta b^{*} = G^{*} \qquad \ldots\ldots 5.3.13$$

and $$\delta b^{*} = (A^{*} + \lambda I)^{-1} . G^{*} \qquad \ldots\ldots 5.3.14$$

Having obtained the corrections to the b vectors in the r^{th} iteration by solving equation 5.3.14, the zero trial vectors for

the $(r+1)^{th}$ iteration are obtained as $b^{(r+1)} = b^r + \delta b^r$. After each iteration the Least Squares value ϕ is computed. The constant λ is selected by trial and error such that $\phi^{r+1} < \phi^r$. Convergence of the step lengths is said to have been achieved if $|\delta b_j^{(r)}|/(\tau + |b_j^{(r)}|) < \epsilon$ for all j, (j = 1 $\longrightarrow$ k) for some suitable value of ϵ, say 10^{-5} and some appropriate value of τ, say 10^{-3}. Marquardt[51] proposed a procedure by which λ is varied after each iteration. In this procedure equation 5.3.14 is solved for two different values of λ in each iteration.

Marquardt's method has been used successfully by a number of authors. Krenkel[37] found it to be the most appropriate method of curve fitting in his application of a diffusion model.

In this study it has been used for obtaining mean detention values "$\bar{t}$" and Peclet numbers in Chapter 4. If the correct values of λ can be chosen, convergence is obtained rapidly. Rapid convergence is the best feature of the technique.

The major drawback of the method is that for each iteration equation 5.3.14 has to be solved twice for two different values of λ, unless the values of λ become the same in the course of the iterations. Furthermore for more than three parameters the process of calculation of the partial derivatives and inversion of the $(A + \lambda I)$ matrix becomes lengthy. Also this process cannot be used to handle constraints satisfactorily. If some of the parameters are very small when compared with others, overflowing in computer analysis becomes frequent.

(iv) <u>The Method of Law and Bailey</u> Law and Bailey[38] proposed a regression technique which is claimed by them to converge rapidly if a unique solution exists. Using the same notation, equation 5.3.7 of the Newton Raphson method is modified as follows:-

Let $D_j = \delta b_j \times g_j$ $\quad j = 1,2,3...k$ 5.3.15

and $D_T = \sum_{j=1}^{k} D_j$ 5.3.16

In equation 5.3.8 the values of the δB are unrestricted. In this method they are restricted, by multiplying the δb_j by α

$$(\delta b_j)_R = \alpha \times \delta b_j \qquad \text{..... 5.3.17}$$

where $(\delta b_j)_R$ are the restricted corrections in the parameters and α is the fraction by which the corrections are restricted. $\Delta \phi_{LR}$, the cange in ϕ for a linear function over the restricted range, can be shown to be equal to

$$\Delta\phi_{LR} = (2\alpha - \alpha^2) \times D_T \qquad \text{..... 5.3.18}$$

Let $\Delta\phi_a = \phi_a^{(r)} - \phi_a^{(r+1)}$ 5.3.19

and $\Delta\phi_{aR} = \phi_a^{(r)} - \phi_{aR}^{(r+1)}$ 5.3.20

where "r" refers to the r^{th} iteration and (r+1), the $(r+1)^{th}$ iteration. $\Delta\phi_a$ is equal to the actual change in the ϕ function over the unrestricted range. $\phi_a = \phi$ calculated from equation 5.3.1. $\Delta\phi_{aR}$ is equal to the actual change in ϕ over the restricted range and ϕ_{aR} is equal to ϕ calculated from equation 5.3.1 using restricted changes in the parameters "b". Using the terms defined above, if the following criteria are adhered to, convergence is assumed.

(a) D_T obtained from equation 5.3.16 must be positive if the direction is towards a minimum. If a minimum is required and D_T is found to be -ve, the sign of all the δb_j must be changed.

(b) If $\Delta\phi_a$ is +ve, the unrestricted calculation is converging and if negative it is diverging and the present values of the corrections must be restricted by multiplying them by a factor α.

(c) If $\Delta\phi_a$ is positive, the calculation is converging but the convergence may be slow. The criterion $\Delta\phi_{aR} - \beta\Delta\phi_{LR} \geq 0$ ensures rapid convergence. A value of β between 0.1 and 0.25 is found

suitable for a maximum rate of convergence.

Law and Bailey's method is very useful when dealing with unrestricted parameters. In the author's experience this method is better than Marquardt's method in terms of ease of operation. The trial and error involved in obtaining the initial values of λ, and the need to make computations twice are avoided in this method.

(v) Rosenbrock's Method When the parameters are constrained, or more so if they interact, it is virtually impossible to obtain a convergence using the methods outlined above. Rosenbrock's[52] method eliminates the necessity of finding derivatives and gives an easier method of optimisation. However this method requires a large number of computations and iterations, for which a computer is essential. Rosenbrock's program is used extensively at present and is readily available in computer libraries. The only task required of the user is that of estimating the initial values of the parameters.

Without going into the complexities of the technique, it may be visualised in the following simple manner. It is essentially a modification of the method of Steepest Descent, in which the increments in the parameters "b" are of arbitrary length while their direction is fixed by the negative gradient of "ϕ".

The components of a unit vector ξ^{o} in the required direction are given by equation 5.3.21.

$$\xi_j = - \frac{\partial \phi}{\partial b_j} \Big/ \left[\sum_{j=1}^{k} \left(\frac{\partial \phi}{\partial b_j} \right)^2 \right]^{\frac{1}{2}} \qquad \ldots\ldots 5.3.21$$

To illustrate, consider a case in which there are two parameters b_1 and b_2. If the value of the function "ϕ" is plotted for various values of b_1 and b_2, contours of ϕ are obtained as shown in Fig.5.3.1.

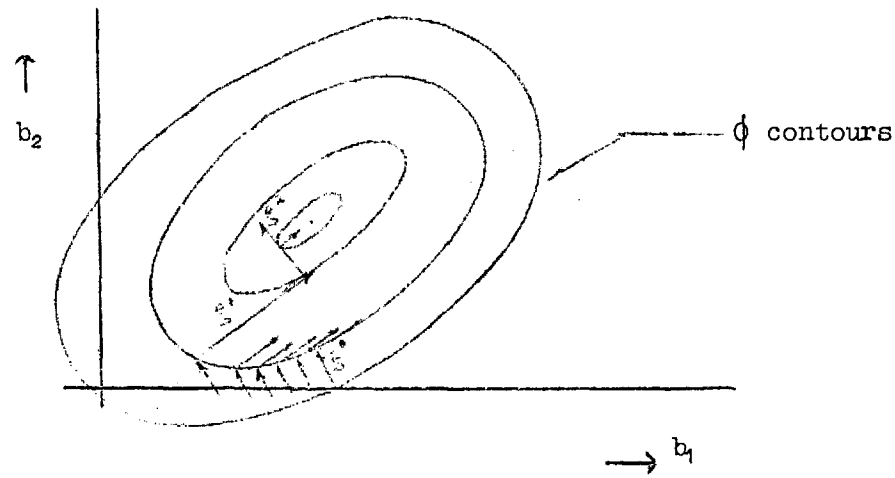

Fig. 5.3.1.

The direction of ξ^o is given by the initial estimates of b_1 and b_2. A correction is then made to b_1 or b_2 by an amount αe along a direction parallel to ξ^o, where e is a suitable step size. It is customary to make e very small to begin with. If it is found that e causes practically no change in the value of ϕ it is multiplied by a factor α where $\alpha > 1$. On the other hand if "e" causes divergence, the value of ϕ is set between 0 and 1. The process of correction in this direction is continued until the least value of ϕ is obtained for both the parameters b_1 and b_2. Then the second unit vector ξ^1 is calculated from equation 5.3.21. The $\frac{\delta\phi}{\delta b_j}$ are computed from the two adjacent points at the end of the ξ^o vector. Note that the vector ξ^o is perpendicular to the contour passing through the starting points and that when a minimum is reached along ξ^o it becomes parallel to the local contour at that minimum point. ξ^1 is therefore perpendicular to the local contour and hence perpendicular to ξ^o. The next vector ξ^2 is perpendicular to ξ^1 and parallel to ξ^o. Thus the procedure is continued until a minimum is reached.

When there are K parameters, ϕ is computed along all directions of ζ at each point and the direction along which ϕ is a minimum is chosen at each point in the process. Essentially one parameter is

varied at a time, keeping all other parameters constant. The process is continued until no further improvement is obtained in ϕ, after which a new trial vector $\underset{\sim}{\xi}$ is calculated by a method given in Rosenbrock[52] which however is omitted from this outline. In this way all the parameters are dealt with until an absolute minimum is obtained.

(vi) Powell's Method A further technique available for optimisation is that of Powell[53]. It is essentially an improvement on Rosenbrock's method in the calculation of $\underset{\sim}{\xi}$. However the author has experienced difficulty with this method in situations where the contours of ϕ are flat, or form a plateau, such as that shown in Fig.5.2.1 (two dimensional case) when the value of b_1 is equal to β_1'' for instance. This condition arises frequently with the models used in this study so that Powell's method is not considered suitable.

5.4. Optimisation of the proposed model parameters

The parameters to be optimised in the models proposed in Chapter 2 are m, p, s, r, f_1, f_2 etc depending upon the complexity of the particular model. However they do not occur explicitly in the model, but appear in the time constants K_1, K_2, K_3 etc and in conjunction with f_1 and f_2. They are also subject to the following constraints.

(i) The value of each parameter lies between the limits of 0 and 1.

(ii) The sum of all the parameters which represent fractions of tank volume is equal to 1.

(iii) Any change in the flow fractions f causes a change in all the constants K_1, K_2, K_3 etc, although the values m, p, s, etc remain constant.

(iv) If the value of one of the tank volume parameters is fixed, the range of operation of the other parameters is reduced by that amount. For example if the optimised value of "m" is found to be equal to "a" say then the range of values available to the next parameter "p" is $0 < p < (1-a)$. For the next parameter the range is still smaller and so on.

In the case of the more complex models such as the shortcircuiting and recirculation model of Fig.2.8.5, the model curve consists of eleven segments, for each of eight possible conditions, the different conditions being given by the relative values of the time constants and θ_1. During the course of optimisation, a small change in one of the parameters may change these relative values, and thus change the model from one condition where one set of eleven equations applies to another condition where a different set of equations applies. It has been found that with most of the above mentioned methods of optimisation, such a change results in divergence rather than convergence.

In the author's experience Rosenbrock's method[52] was found to be the most suited to the conditions and restraints described above. The manner in which the restraints were handled is explained here, using the four parameter model as an example.

m, p and f are replaced by m', p' and f' where

$$m' = \text{Arc sin } (\sqrt{m})$$

$$p' = \text{Arc sin } \{\sqrt{p/(1-m)}\}$$

$$f' = \text{Arc sin } (\sqrt{f})$$

The values of m', p' and f' were optimised and the optimum values of m, p, s and f were calculated after each iteration as

$$m = \sin^2 m'$$

$$p = (1-m) \sin^2 p'$$

$$s = 1 - m - p$$

$$f = \sin^2 f'$$

In this way all the constraints are satisfied although the value of s is not optimised directly. An alternative method is to optimise all four parameters and then calculate m, p and s values by dividing the optimised values by $(m + p + s)$. However it was found that this makes the optimisation more difficult as there are four parameters to be optimised instead of three. Indirect optimisation of s is more satisfactory.

5.5 A typical flow diagram

In order to illustrate the process of optimisation, a flow chart of the four parameter model computer program is given below, showing only the main blocks.

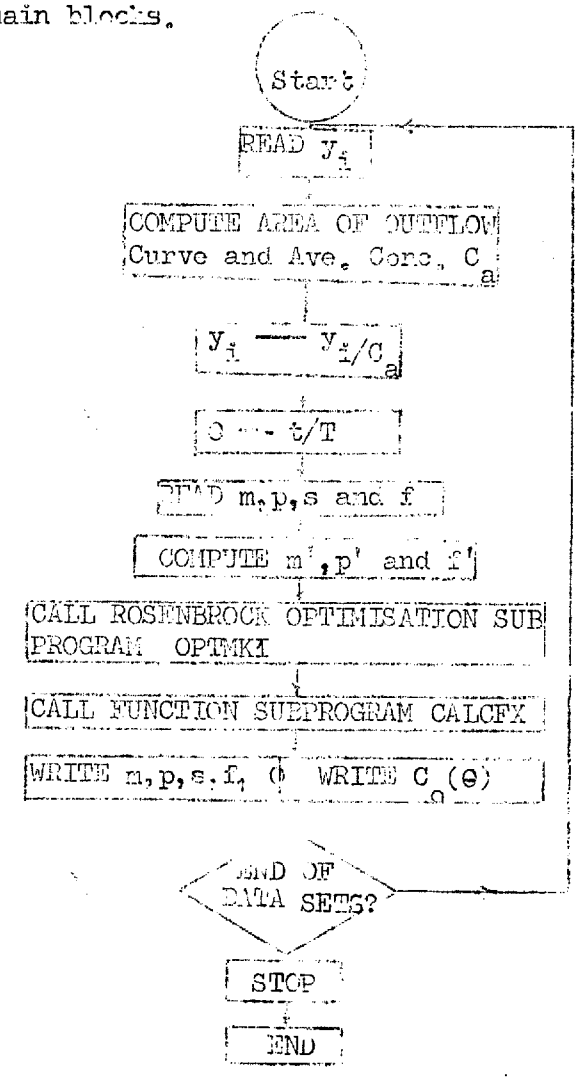

Fig.5.5.1

SUBROUTINE CALCFX

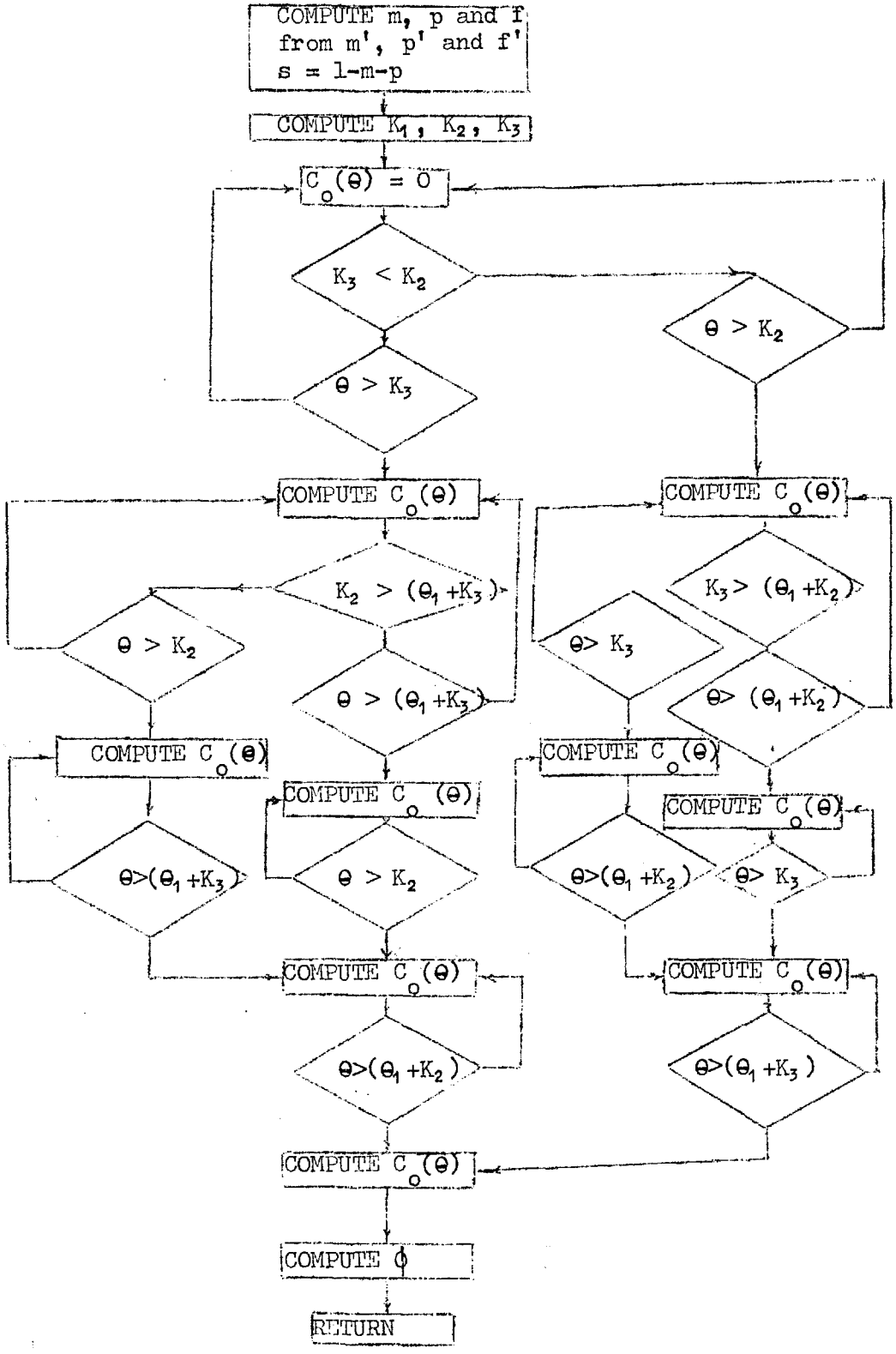

Fig.5.5.2

$C_o(\theta)$ in subroutine CALCFX is computed from the equations given in the deduction of the four parameter short circuiting model. Initial values of the parameters m, p, s and f are estimated by close observation of the output curve as discussed in Chapter 2. It is very important that realistic initial values of the parameters are selected as values chosen at random may result in a false convergence. Except in the case of the five parameter model, the absolute minimum of ϕ is unique for a particular set of values of the parameters.

5.6. Regression method for the pulse technique

An account of the method by which the Bode plot obtained from a mathematical model is matched to the Bode data obtained by experiment, thus finding optimum values of the parameters in another way.

Experimental data obtained from the Pulse Technique may take the form of a continuous record of the input and output pulses, or discrete values taken at time intervals which may be uniform or random. In the case of the direct simulation experiments in this study the time interval was a constant, but in the case of the model tank values at two different time intervals were recorded as mentioned earlier and the computer program was written accordingly.

Again the success of this technique depends on the accuracy with which the input and output data are recorded. Tracer recovery should be as close as possible to 100%. In these experiments this was difficult to achieve and in most cases the output curve was taken to represent 100% recovery and the input pulse ordinates were adjusted accordingly. This deviates from reality but was considered to be the best way of dealing with the results under the circumstances. The remaining steps in the analysis were as follows:

(i) The input and output data were normalised by dividing them by the average concentration C_a where $C_a \cdot T$ is equal to the area of the output curve. The time t was also normalised to θ. These normalisations were not necessary but were made for the sake of consistency.

(ii) As recommended by Law and Bailey[38], the origin for the time scale of the output curve was shifted to the point when the tracer first appeared at the outlet.

(iii) Magnitude ratios for the data were then obtained for values of "w" from 0 to "w_1" where "w_1" was a value such that the corresponding M.R. was less than 0.1 or increased again for further increase in w. The w values used were as follows:-

Steps of 0.01 from w = 0 to w = 0.1

Steps of 0.1 from w = 0.1 to w = 1.0

and Steps of 0.5 from w = 1.0 to w = w_1

This procedure was adopted because it was considered that at low frequencies, the system dynamics were not adequately reflected by the magnitude ratio.

(iv) The magnitude ratios thus obtained were then normalised by dividing them by the value of the magnitude ratio at w = 0.

(v) For the particular mathematical model being fitted, the values of the magnitude ratios corresponding to the same values of w were computed. The parameters of the model were then optimised to give the best fit of the magnitude ratios thus obtained to those of step (iv) using the techniques of section 5.4.

5.7 Analysis by means of Analogue Computation

So far, analysis of flow curves by digital computer has been presented. Curve fitting is also possible using an analogue computer,

in which the mathematical models are simulated by appropriate analogue programming. This method is generally quicker and easier, although it can be said that the results obtained are not as accurate as those obtained from digital computation.

(1) Analogue programming of the two parameter model.

For ease of reference, the basic equations of the two parameter model are reproduced below. It may be recalled that these equations correspond to a unit input of duration θ_1.

$$\left.\begin{array}{lll} \text{(i)} & C_o(\theta) = 0 \quad \ldots\ldots\ldots\ldots\ldots & 0 < \theta < K_2 \\ \text{(ii)} & C_o(\theta) = 1 - e^{-(\theta - K_2)/K_1} \ldots\ldots & K_2 < \theta < (\theta_1 + K_2) \\ \text{(iii)} & C_o(\theta) = e^{-(\theta-\theta_1-K_2)/K_1} - e^{-(\theta-K_2)/K_1} \ldots & \theta > (\theta_1 + K_2) \end{array}\right\} \quad 5.6.1$$

Equation 5.6.1(ii) above on differentiation yields :-

$$\frac{dY}{d\theta} = \frac{1}{K_1} e^{-(\theta-K_2)/K_1} \quad \text{where } Y = C_o(\theta)$$

Adopting the notation $\frac{dY}{d\theta} = \dot{Y}$ it may be written

$$\dot{Y} = -\frac{1}{K_1}(1 - e^{-(\theta-K_2)/K_1}) + \frac{1}{K_1}$$

or
$$\dot{Y} = -\frac{1}{K_1} \cdot Y + \frac{1}{K_1} \quad \ldots\ldots\ldots \quad 5.6.2$$

Equation 5.6.1(iii) on differentiation yields :-

$$\frac{dY}{d\theta} = \frac{1}{K_1}(e^{-(\theta-K_2)/K_1} - e^{-(\theta-\theta_1-K_2)/K_1})$$

or
$$\dot{Y} = -\frac{1}{K_1} \cdot Y \quad \ldots\ldots\ldots \quad 5.6.3$$

The Flow diagrams corresponding to equations 5.6.1(i), 5.6.2 and 5.6.3 in analogue notation are given in Fig.5.6.1.

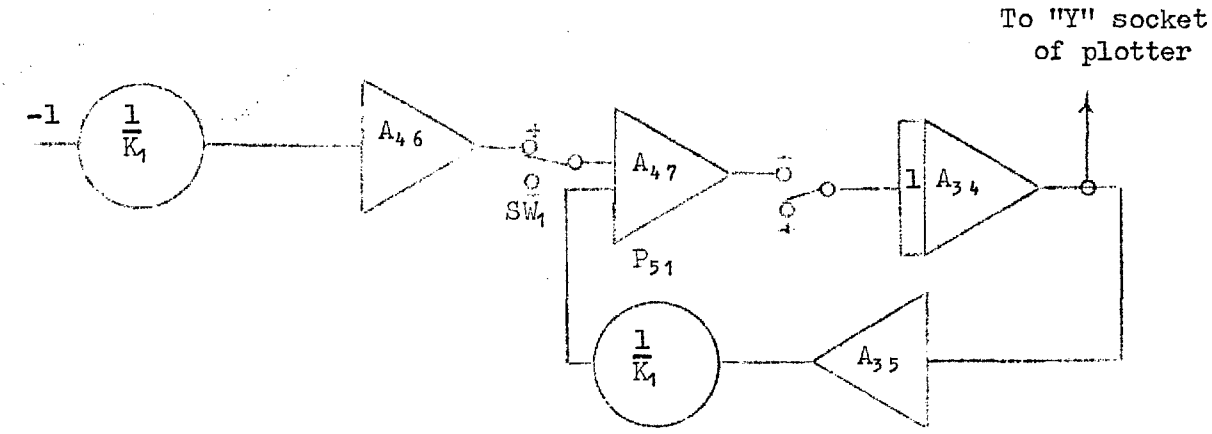

MAIN CIRCUIT

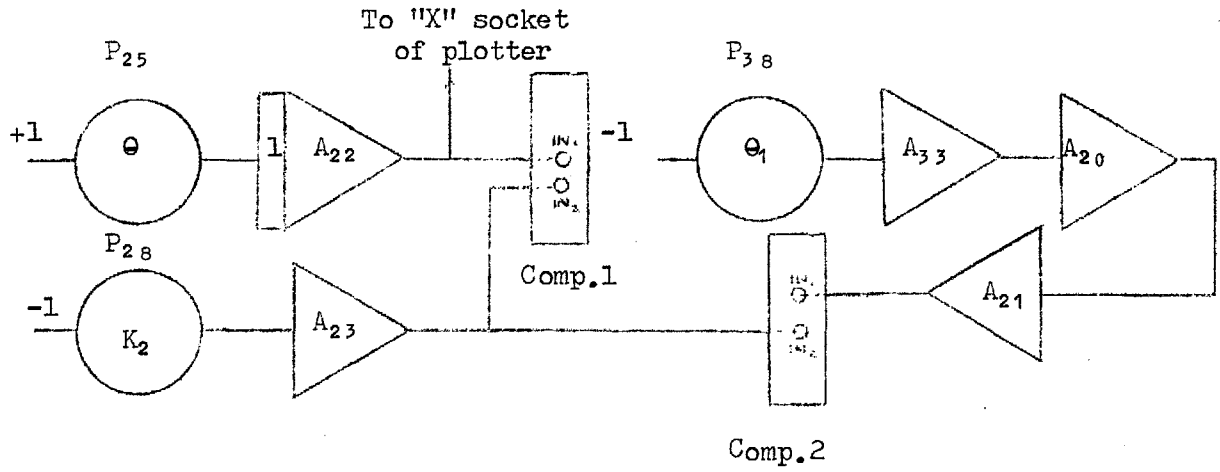

TIME CIRCUIT

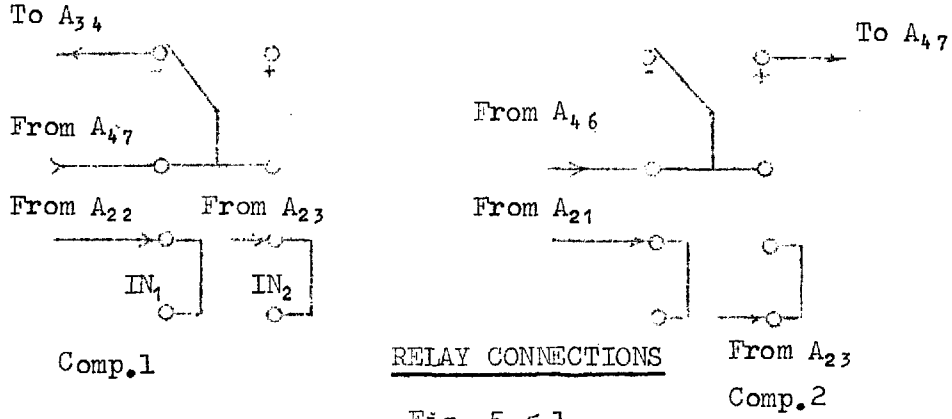

RELAY CONNECTIONS

Fig. 5.6.1.

5.8 Verification of the two parameter model with the analogue computer

The two parameter model was verified using data obtained in the direct simulation experiments, (Set Nos. 22, 33, 47, 55 and 69) and the analogue program given in section 5.7. The mathematical model was simulated on an Electronic Differential Analyser (P.A.C.E. TR 48 computer) and the resulting fit was plotted in the X-Y plane by a P.A.C.E. Variplotter (Type 1100E).

The experimental data were plotted as $C(\theta)/C_i(\theta)$ against θ where $C_i(\theta)$ was the average input concentration. This method of reducing the output concentrations gave the advantage of having the output ordinates in terms of a unit step input.

Since the maximum value of Y in equations 5.6.2 and 5.6.3 never exceeded 1, no amplitude scaling was necessary. A factor of 100 was used to reduce the speed of integration. The potentiometers representing K_1 and K_2 were adjusted by trial and error until the Plotter pen traced out a curve as close to the experimental curve as was possible, thus obtaining a visual best fit. The fits to data sets 22, 33 and 47 are plotted in Fig.5.6.2 and those obtained for data sets 55 and 69 are shown in Fig.5.6.3. The potentiometer settings and the Pen and Arm scaling are given in these figures and the results are tabulated together with the uncorrected "m" and "p" values in Table 5.6.1.

Set No.	Fraction of P.M. (tank vol.) (m)	Fraction of Plug Flow (pipe vol.) (p)	Analogue value (m)	Analogue value (p)
22	0.462	0.538	0.371	0.629
33	0.300	0.700	0.256	0.744
47	0.410	0.590	0.310	0.690
55	0.590	0.410	0.520	0.480
69	0.810	0.190	0.711	0.289

Table 5.6.1.

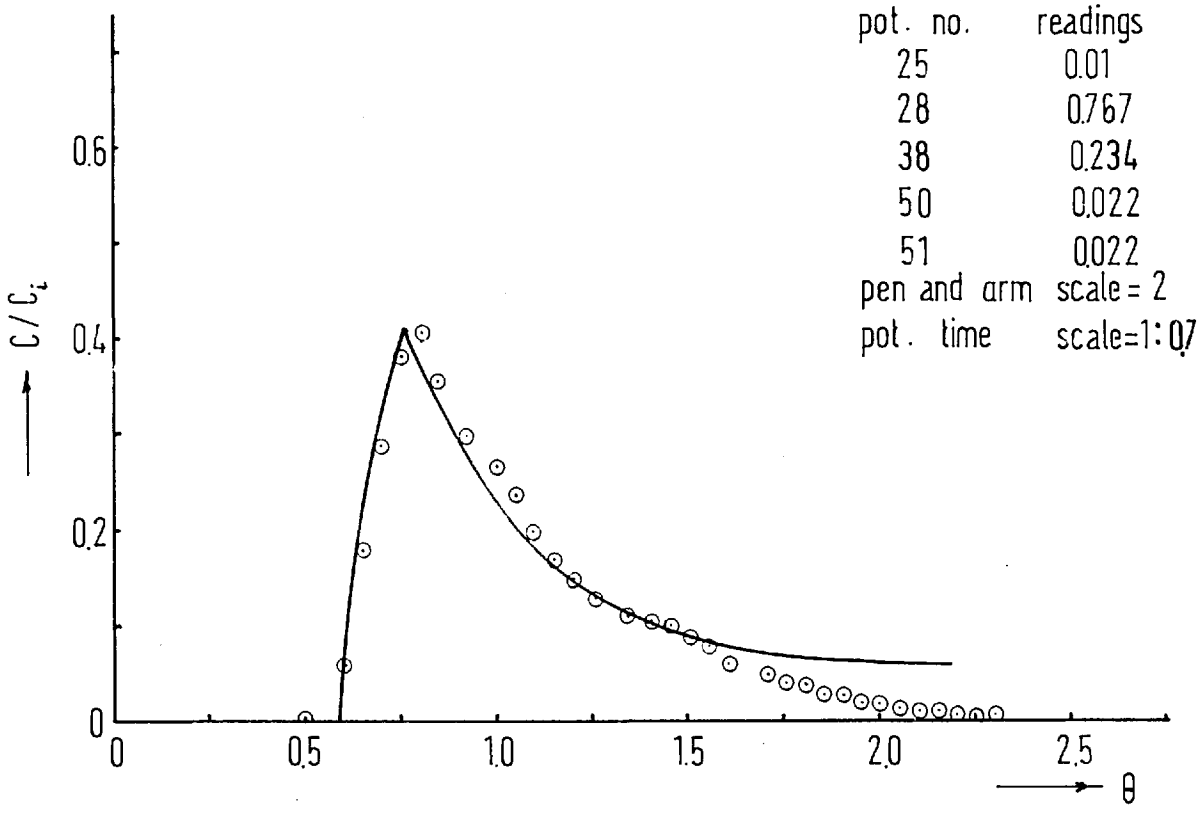
SET NO. 22.
pot. no. readings
25 0.01
28 0.767
38 0.234
50 0.022
51 0.022
pen and arm scale = 2
pot. time scale=1: 0.75
C / Ci
0.6
0.4
0.2
0
0
0.5
1.0
1.5
2.0
2.5
θ

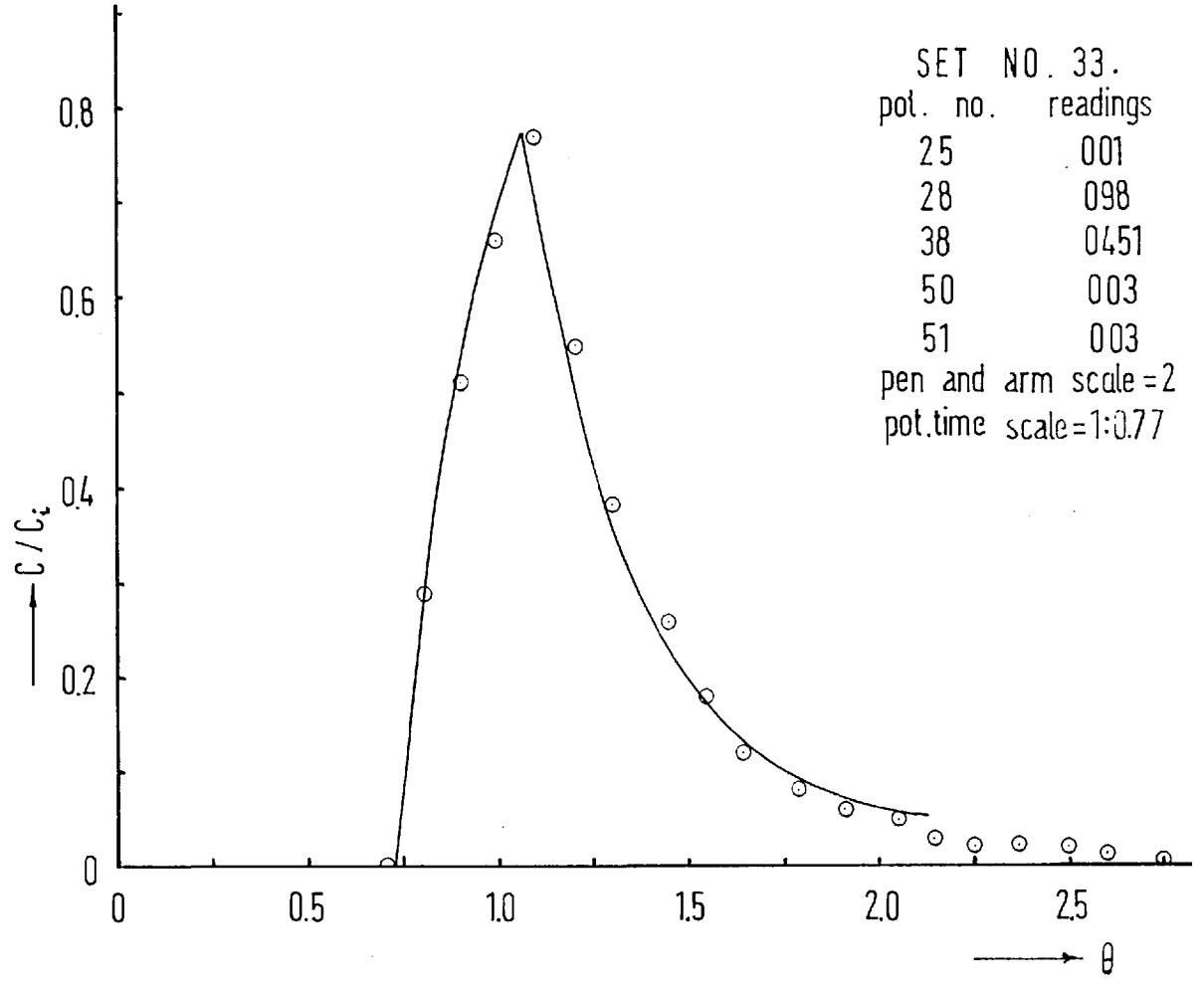
SET NO. 33.
pot. no. readings
25 001
28 098
38 0451
50 003
51 003
pen and arm scale = 2
pot.time scale = 1:0.77
C / Ci
0.8
0.6
0.4
0.2
0
0
0.5
1.0
1.5
2.0
2.5
θ

FIGURES 5.6.2.

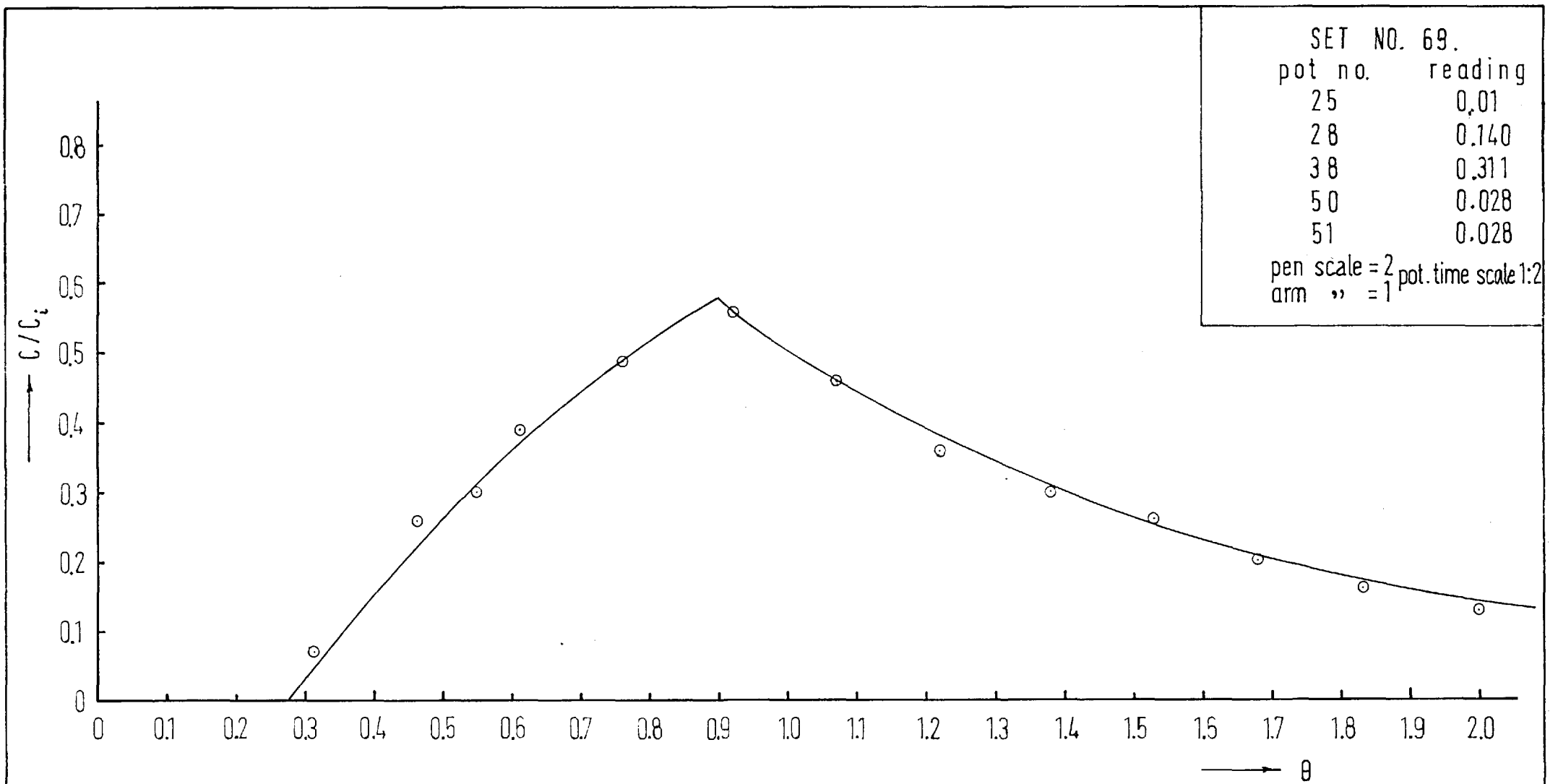
SET NO. 69.
pot no. reading
25 0.01
28 0.140
38 0.311
50 0.028
51 0.028
pen scale = 2 pot. time scale 1:2
arm " = 1
C / Ci
θ
0 0.1 0.2 0.3 0.4 0.5 0.6 0.7 0.8 0.9 1.0 1.1 1.2 1.3 1.4 1.5 1.6 1.7 1.8 1.9 2.0
0 0.1 0.2 0.3 0.4 0.5 0.6 0.7 0.8

FIG. 5.6.3.

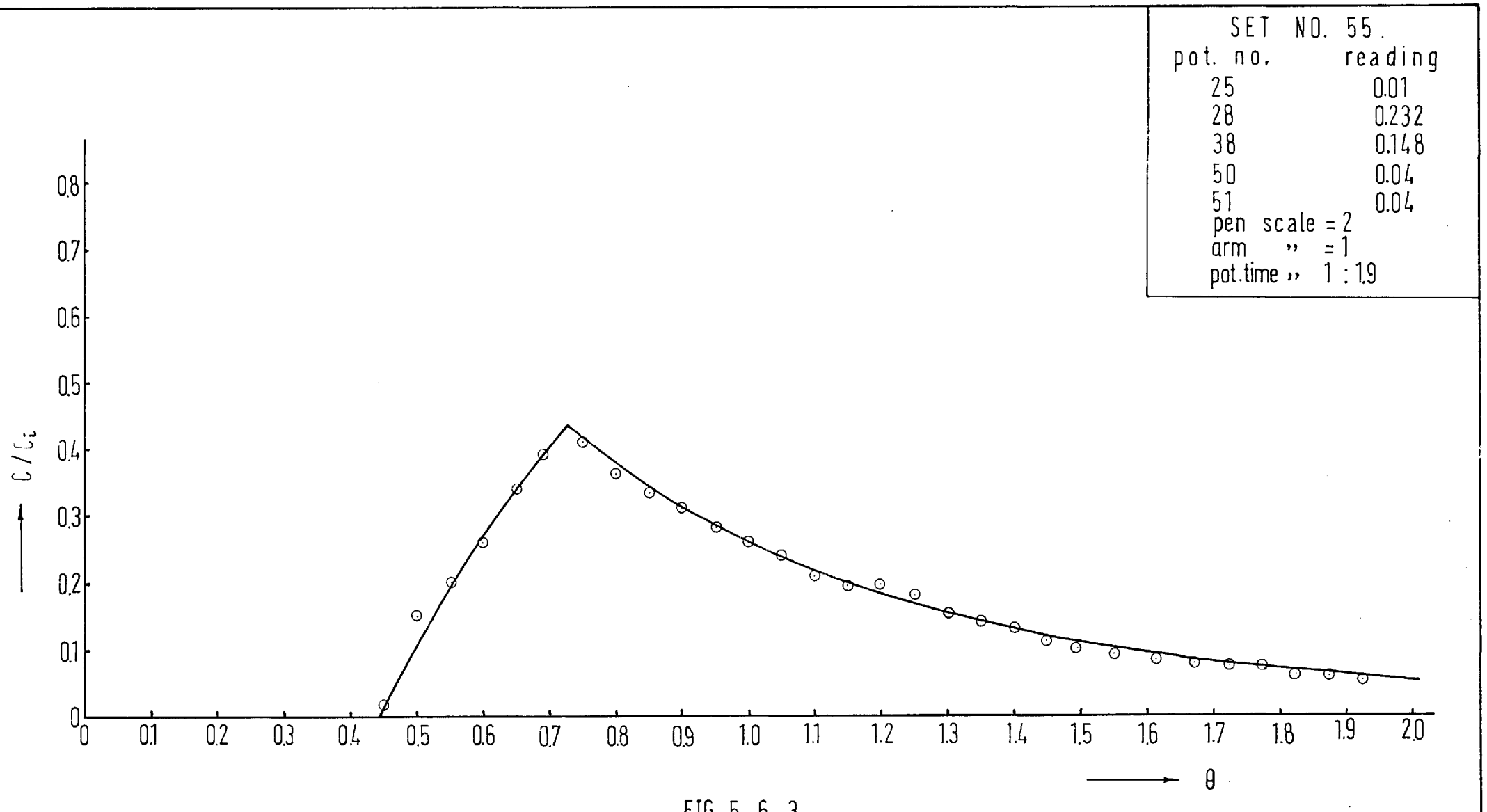
SET NO. 55.
pot. no. reading
25 0.01
28 0.232
38 0.148
50 0.04
51 0.04
pen scale = 2
arm " = 1
pot.time " 1 : 1.9
C / C∞
0
0.1
0.2
0.3
0.4
0.5
0.6
0.7
0.8
0.9
1.0
1.1
1.2
1.3
1.4
1.5
1.6
1.7
1.8
1.9
2.0
θ

FIG. 5.6.3.

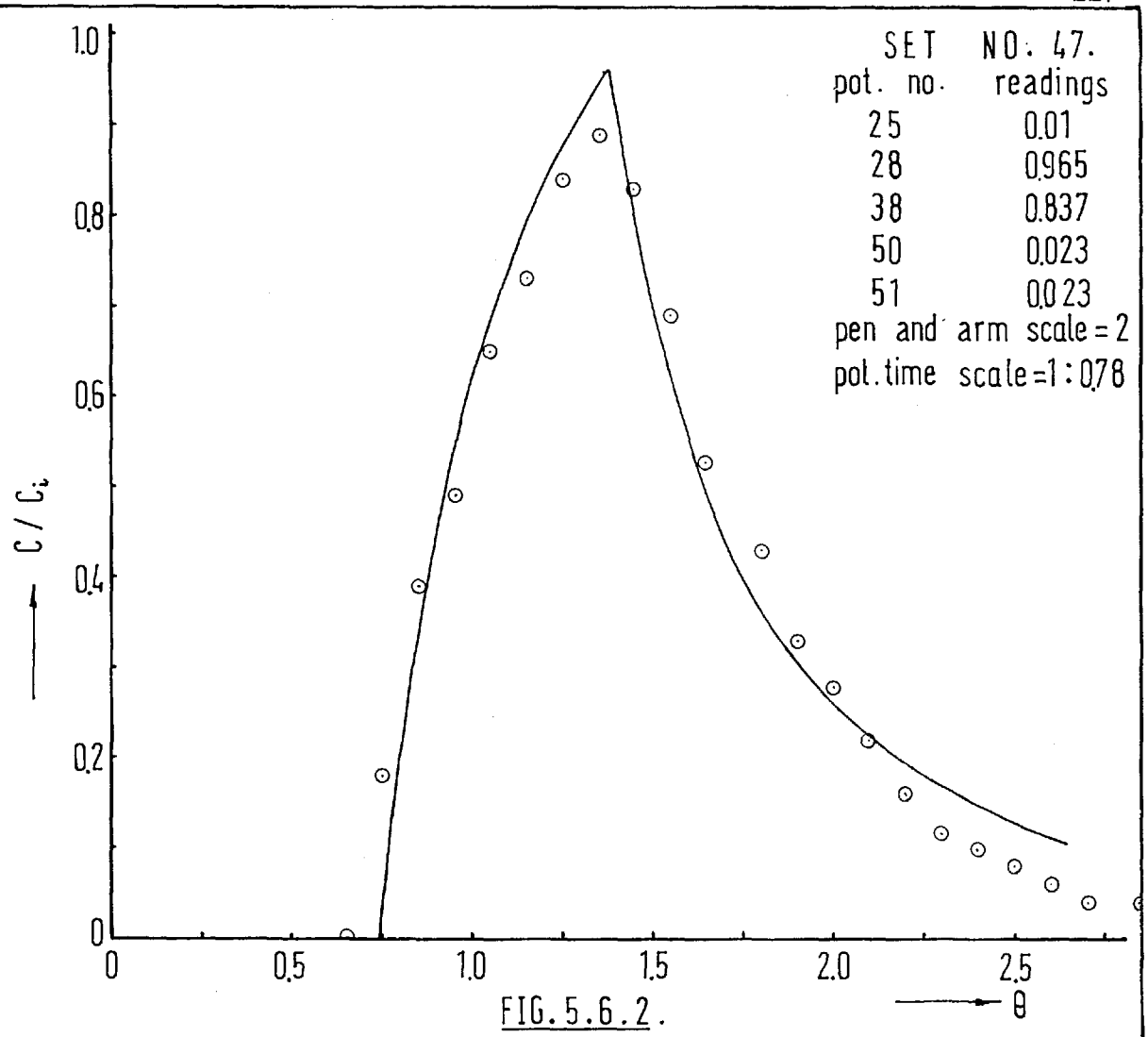

FIG. 5.6.2.

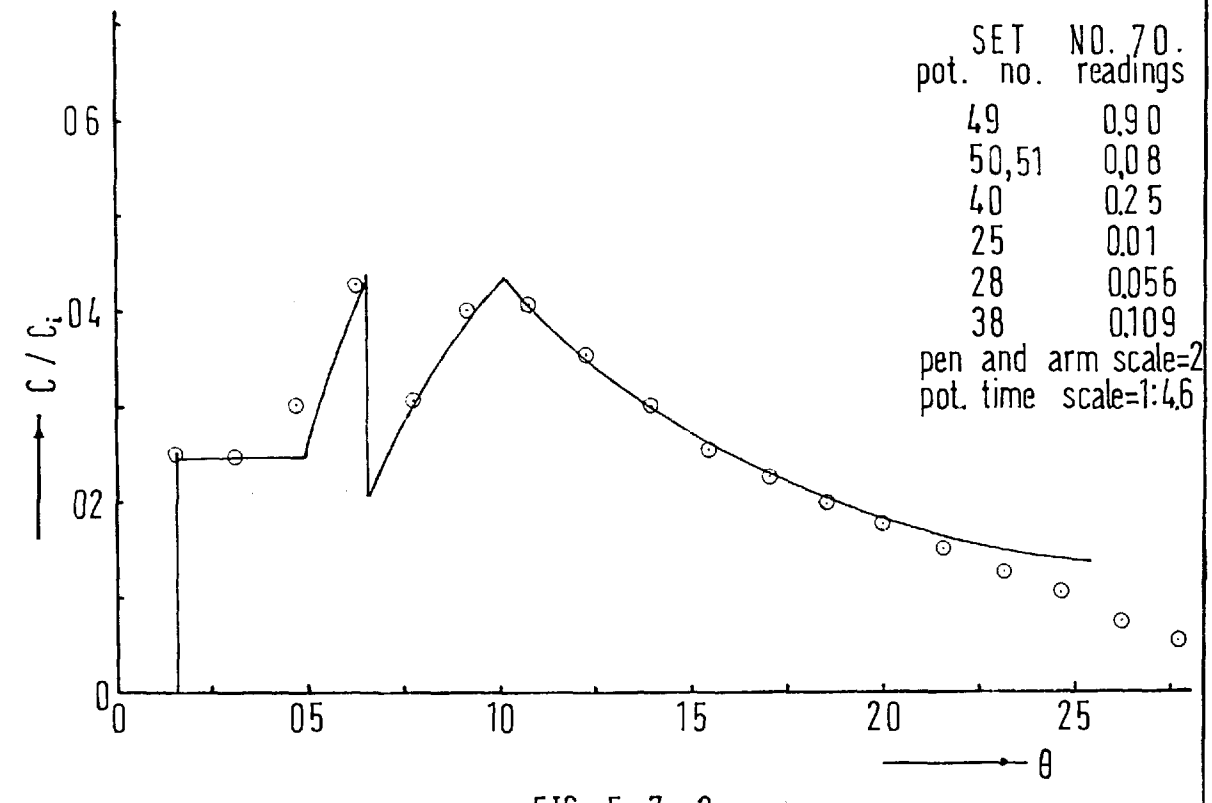

FIG. 5.7.2.

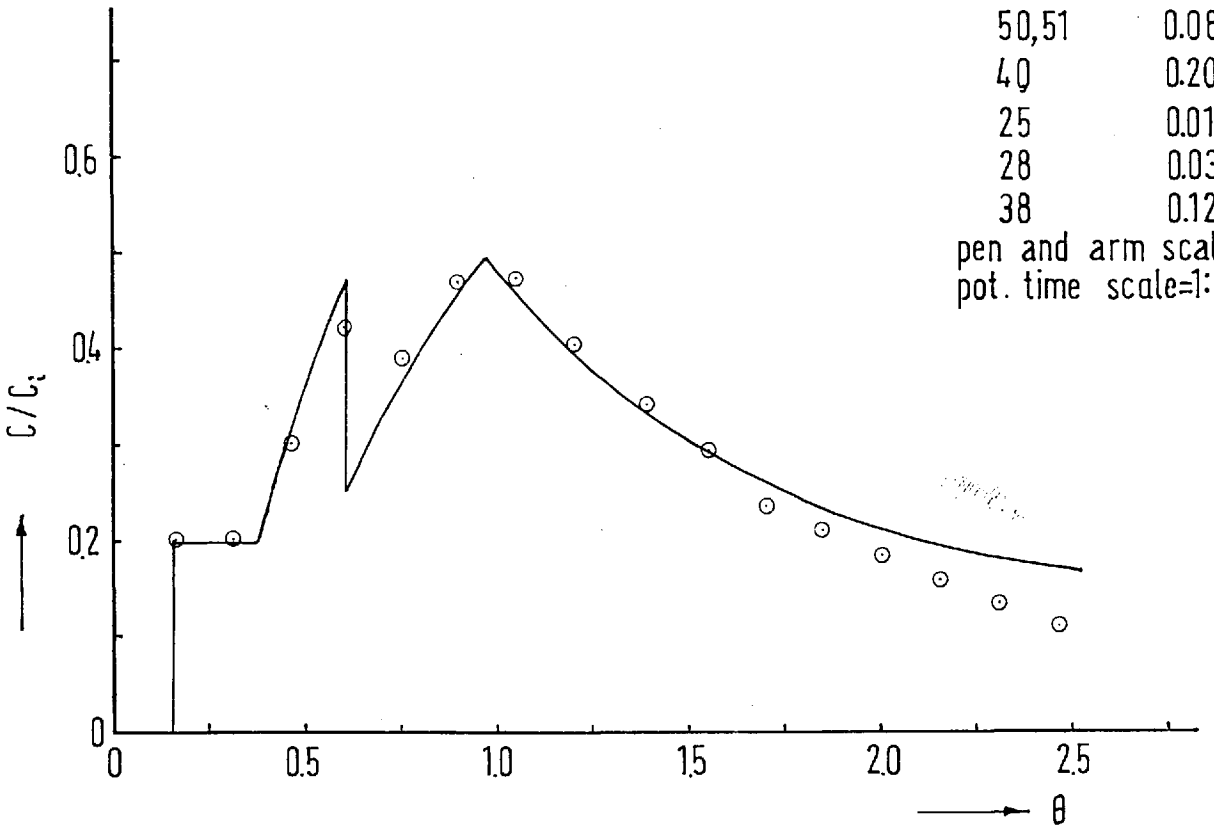
SET NO. 71.
pot. no. readings
49 0.98
50,51 0.08
40 0.20
25 0.01
28 0.038
38 0.126
pen and arm scale= 2
pot. time scale=1:4.76
C / Ci
0.6
0.4
0.2
0
0
0.5
1.0
1.5
2.0
2.5
θ

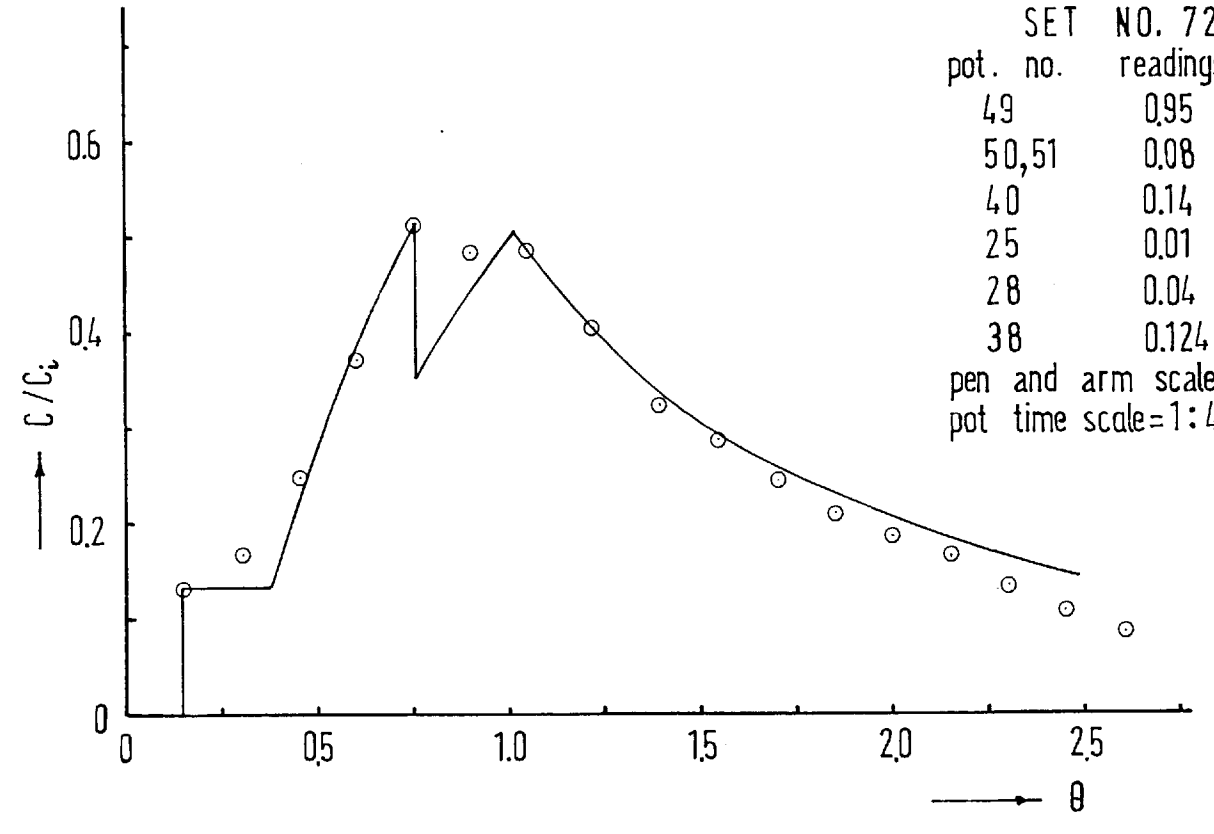
SET NO. 72
pot. no. readings
49 0.95
50,51 0.08
40 0.14
25 0.01
28 0.04
38 0.124
pen and arm scale= 2
pot time scale=1:4.83
C / Ci
0.6
0.4
0.2
0
0
0.5
1.0
1.5
2.0
2.5
θ

FIGURES 5.7.2.

This method of analysis presents one difficulty in that it is difficult to satisfy the constraint m+p = 1. Also losses in potentiometers, ammeters, integrators and other contacts such as relays, require the time scaling of the plot to be adjusted. The values of K_1 and K_2 are normalised by dividing each one by their sum. The results obtained ultimately on comparison with the actual values are found to be reasonably satisfactory.

5.8 Analogue modelling of the four parameter short circuiting model

In this particular case the positive type of shortcircuiting, i.e. the type of short circuit which precedes the main flow was considered. The basic equations are given below:-

(i) $C_o(\theta) = 0$ ..... $0 < \theta < K_3$

(ii) $C_o(\theta) = f$ ..... $K_3 < \theta < K_2$

(iii) $C_o(\theta) = f + (1-f)(1-e^{-(\theta-K_2)/K_1})$ .. $K_2 < \theta < (\theta_1+K_3)$

(iv) $C_o(\theta) = (1-f)(1-e^{-(\theta-K_2)/K_1})$ ..... $(\theta_1+K_3) < \theta < (\theta_1+K_2)$

(v) $C_o(\theta) = (1-f)(e^{-(\theta-\theta_1-K_2)/K_1} - e^{-(\theta-K_2)/K_1})$ .. $\theta > (\theta_1+K_2)$

As the analogue machine available for this study had only two comparators, the following modifications were made. Part (i) was omitted altogether. The origin was shifted to the time K_3 so that part (ii) of the equation remains valid for a time (K_2-K_3), part (iii) remains valid for a time θ_1 and part (iv) for a time $(\theta_1+K_2-K_3)$. Even with this arrangement a minimum of three comparators are necessary. During the analysis the work of the third comparator was done manually. The flow diagram of the model in analogue notation is given in Fig.5.7.1.

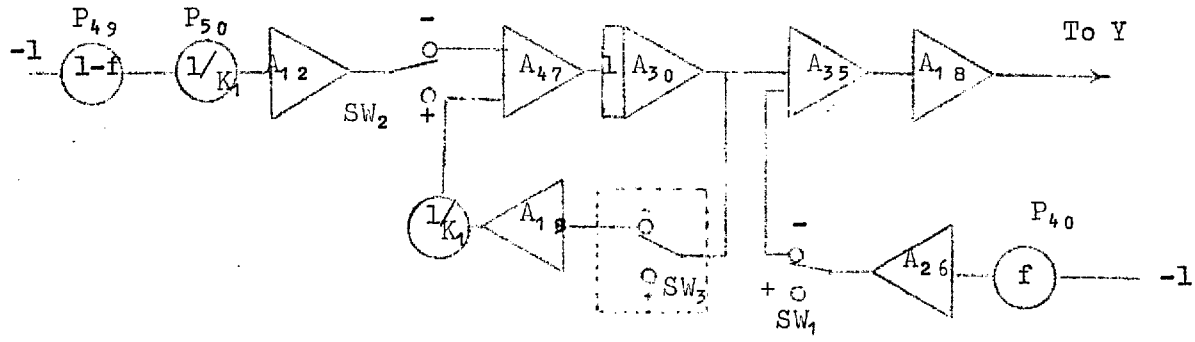

MAIN CIRCUIT

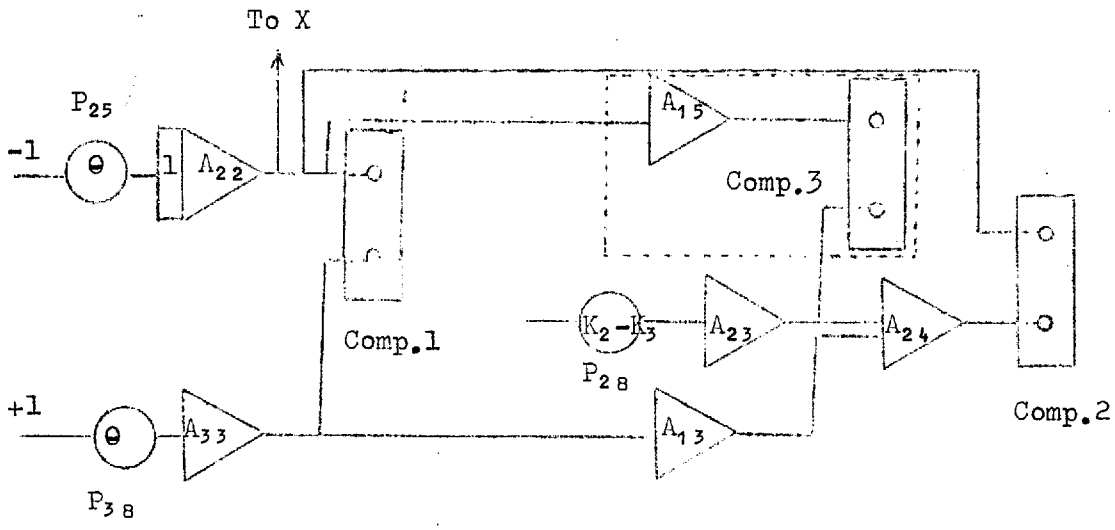

TIME CIRCUIT

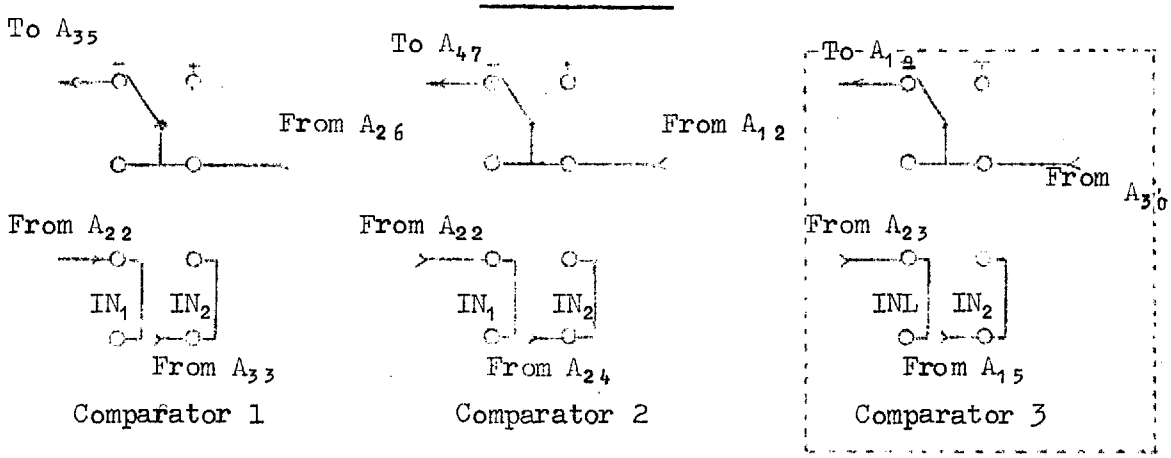

RELAY CONNECTIONS

Fig.5.7.1

5.9. Verification of the four parameter model using the analogue computer

As a third comparator was not available on the computer the parts of the diagram surrounded by dotted lines in Fig.5.7.1 were omitted. The procedure for plotting the output curve and fitting it to the experimental data by setting the potentiometers was the same as in the previous case. The connection between the amplifiers A_{30} and A_{19} was kept open until a time equal to (K_2-K_3) had elapsed, when they were manually connected using the "holding" facility, thus doing the work of the third comparator. The time (K_2-K_3) was measured by the movement of the plotter pen on the graph rather than by stopwatch. The results of the fit are shown in Fig.5.8.2 together with the pot settings, calculated scaling and arm and pen scales. For comparison the results of sets Nos. 70, 71 and 72 are tabulated in Table 5.8.1 along with the actual values. Considering the approximations inherent in an analogue circuit, the results obtained are satisfactory. It should be noted from the transformation of the equation for the analogue program that it is necessary to know the correct value of K_3 in this case before commencing the analysis. If a third comparator had been available the results would have been better, and again various electrical losses contributed to errors in the results.

Set No.	Actual				Analogue			
	m	p	s	f	m	p	s	f
70	0.66	0.326	0.014	0.25	0.555	0.315	0.05	0.25
71	0.66	0.326	0.014	0.20	0.618	0.343	0.04	0.20
72	0.66	0.326	0.014	0.15	0.618	0.350	0.032	0.14

Table 5.8.1.

5.10 Analogue program for the recirculation model

An analogue program for the recirculation model is given below. The relevant equations are restated here for convenience.

(i) $C_o(\theta) = 0$ ..... $0 < \theta < K_2$

(ii) $C_o(\theta) = \frac{1}{(1+f)} (1-e^{-(\theta-K_2)/K_1})$ $K_2 < \theta < (\theta_1+K_2$

(iiia) $C_o(\theta) = \frac{1}{(1+f)} (e^{-(\theta-\theta_1-K_2)/K_1} - e^{-(\theta-K_2)/K_1})$ ...

$(\theta_1+K_2) < \theta < (2K_2+K_3)$

(iiib) $C_o(\theta) = \frac{1}{(1+f)} [1 - e^{-(\theta-K_2)/K_1} + \frac{f}{(1+f)} \{1 - (1+ \frac{\theta-2K_2-K_3}{K_1})$

$e^{-(\theta-2K_2-K_3)/K_1} \}]$ .... $(2K_2+K_3) < \theta < (\theta_1+K_2)$

(iv) $C_o(\theta) = \frac{1}{(1+f)} [e^{-(\theta-\theta_1-K_2)/K_1} - e^{-(\theta-K_2)/K_1} + \frac{f}{1+f}$

$\{1 - (1 + \frac{\theta-2K_2-K_3}{K_1}) e^{-(\theta-2K_2-K_3)/K_1} \}]$

..... $(\theta_1+K_2) < \theta < (\theta_1 +2K_2+K_3)$

or $(2K_2+K_3) < \theta < (\theta_1 + 2K_2 + K_3)$

(v) $C_o(\theta) = \frac{1}{1+f} [e^{-(\theta-\theta_1-K_2)/K_1} - e^{-(\theta-K_2)/K_1} + \frac{f}{1+f} \{(1+ \frac{\theta-\theta_1-2K_2-K_3}{K_1})$

$e^{-(\theta-\theta_1-2K_2-K_3)/K_1} - (1 + \frac{\theta-2K_2-K_3}{K_1}) e^{-(\theta-2K_2-K_3)/K_1}\}]$

..... $\theta > \theta_1 + 2K_2 + K_3$

Again for convenience the origin is shifted by an amount K_2.

In differential form parts (ii) and (iii) can be written as follows:-

(ii) $\dot{Y} = -\frac{1}{K_1} Y + \frac{1}{(1+f)K_1}$ ..... $0 < \theta < \theta_1$

(iiia) $\dot{Y} = -\frac{1}{K_1} Y$ ..... $\theta_1 < \theta < (K_2 + K_3)$

Equation (iiib) can be transformed as follows.

Let $Y = C_o(\Theta)$ in (iiib) above.

Then $$\dot{Y} = \frac{1}{1+f}\left[\frac{1}{K_1}e^{-(\Theta-K_2)/K_1} - \frac{f}{1+f}\left\{-\frac{1}{K_1}\left(1+\frac{\Theta-2K_2-K_3}{K_1}\right)e^{-(\Theta-2K_2-K_3)/K_1}\right\}\right]$$

$$+\frac{1}{K_1}.e^{-(\Theta-2K_2-K_3)/K_1}\Bigg]$$

or $$\dot{Y} = -\frac{1}{K_1(1+f)}\left[1 - e^{-(\Theta-K_2)/K_1} + \frac{1}{(1+f)}\left\{1-\left(1+\frac{\Theta-2K_2-K_3}{K_1}\right)e^{-(\Theta-2K_2-K_3)/K_1}\right\}\right]$$

$$+\frac{1}{K_1(1+f)}\left\{1-\frac{f}{1+f}\left(1+e^{-(\Theta-2K_2-K_3)/K_1}\right)\right\}$$

or $$\dot{Y} = -\frac{Y}{K_1} + \frac{1}{K_1(1+f)}\left\{1-\frac{f}{1+f}\left(1+e^{-(\Theta-2K_2-K_3)/K_1}\right)\right\}$$

Differentiating again

$$\ddot{Y} = -\dot{Y}/K_1 + \frac{1}{K_1(1+f)}\left[\frac{f}{K_1(1+f)}\,e^{-(\Theta-2K_2-K_3)/K_1}\right]$$

or $$\ddot{Y} = -\dot{Y}/K_1 - \frac{1}{K_1^2(1+f)}\left[1-\frac{f}{(1+f)}\left(1+e^{-(\Theta-2K_2-K_3)/K_1}\right)\right] + \frac{1}{K_1^2(1+f)}\cdot\left(1-\frac{f}{1+f}\right)$$

or $$\ddot{Y} = -\frac{\dot{Y}}{K_1} - \frac{\dot{Y}}{K_1} - \frac{Y}{K_1^2} + \frac{1}{K_1^2(1+f)^2} \quad \ldots\ldots (K_2+K_3) < \Theta < \Theta_1$$

Part (iv) can be transformed in a similar way to

$$Y = -\frac{2\dot{Y}}{K_1} - \frac{Y}{K_1^2} + \frac{f}{K_1^2(1+f)^2} \quad \ldots\ldots \Theta_1 < \Theta < (\Theta_1 + K_2 + K_3)$$

$$\text{or } (K_2+K_3) < \Theta < (\Theta_1 + K_2 + K_3)$$

Similarly part (v) yields

$$Y = -\frac{2\dot{Y}}{K_1} - \frac{Y}{K_1^2} \quad \ldots\ldots \Theta > (\Theta_1 + K_2 + K_3)$$

The flow diagram for the model transformed as above is given in Fig.5.9.1 for $K_2 < (\Theta_1+K_2) < (2K_2+K_3) < (\Theta_1+2K_2+K_3)$.

It can be seen from the flow diagram that for operation of this program, at least four comparators are necessary. Moreover the analogue

FIGURE 5.9.1.

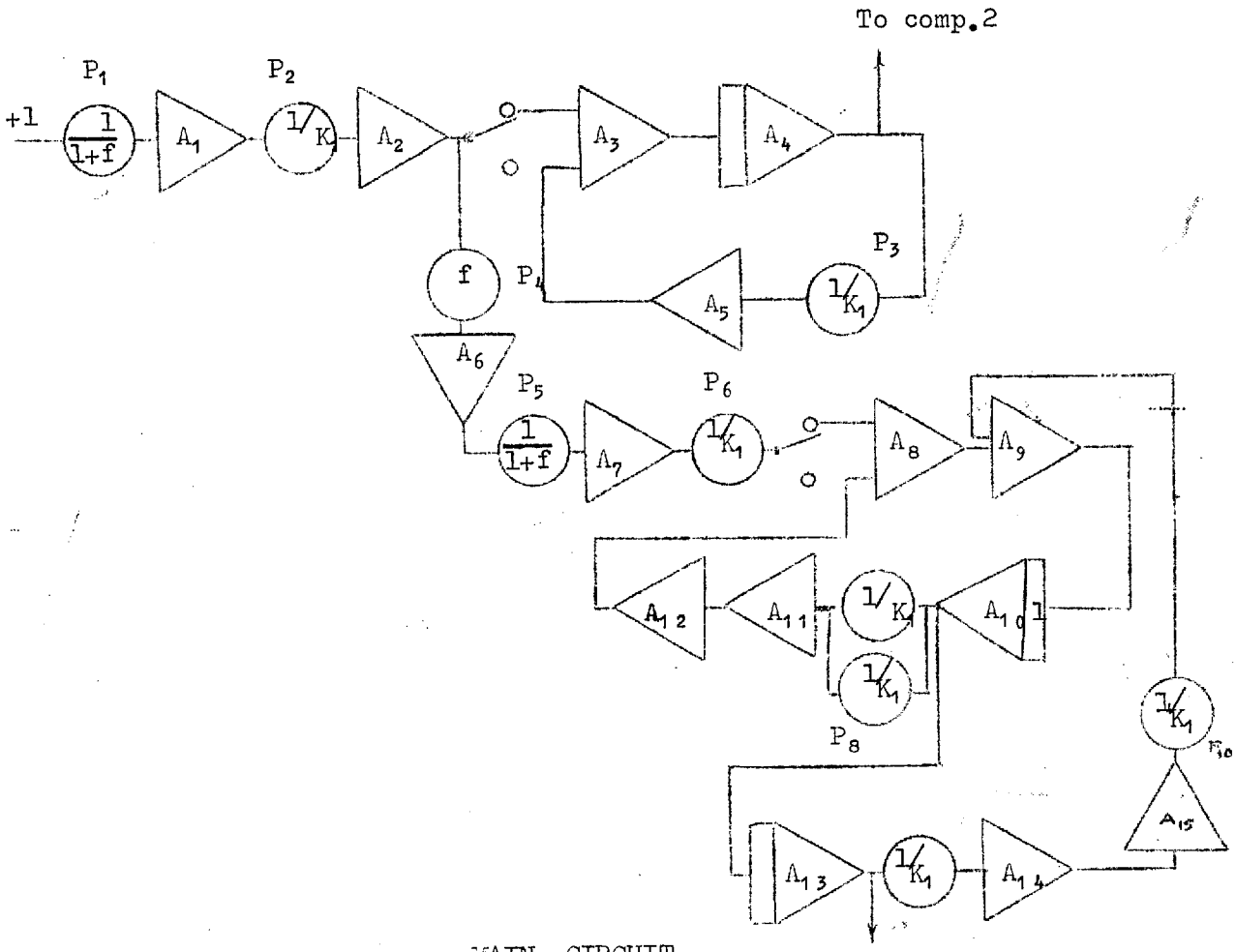

MAIN CIRCUIT

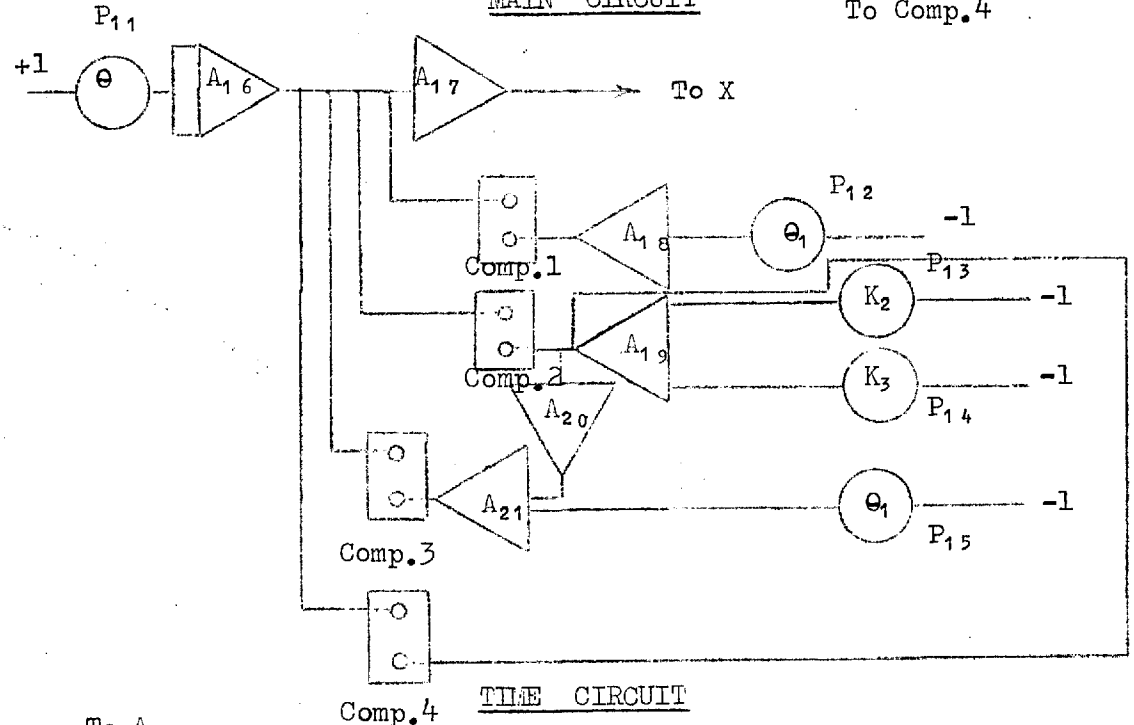

TIME CIRCUIT

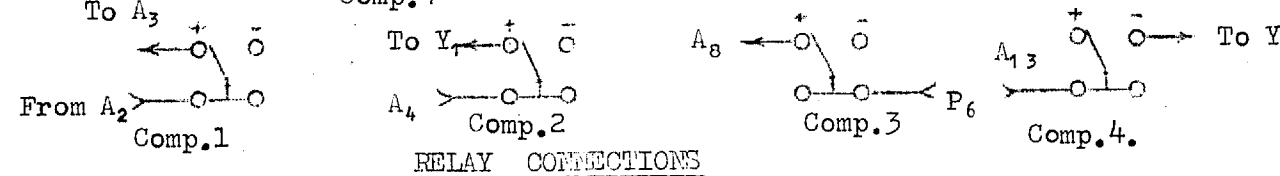

RELAY CONNECTIONS

Fig. 5.9.1.

machine should have two Y plotters with a change over at time (K_2+K_3) from one to the other. The use of two Y plotters can be eliminated by holding at time (K_2+K_3) and manually connecting the amplifier A_{13} to the Y socket directly. The available equipment was found to be unsatisfactory in that the four comparators could not be made to work simultaneously at any one time. Consequently this model could not be simulated satisfactorily in the time available, but it is felt that reasonable results could be obtained on properly functioning equipment.

5.11 Conclusions

Two methods of computer analysis have been illustrated in this chapter, digital and analogue. Although the results obtained from the analogue are approximate, it is a much quicker procedure. For complex cases it is difficult to apply and considerable errors may result. With the digital method using Rosenbrock's optimisation program, generally more accurate results can be obtained without much effort on the part of the analyst. However no account is taken here of the economics involved. It must also be remembered that in either case good optimisation depends on the accuracy with which the initial values of the parameters can be estimated.

CHAPTER VI

DISCUSSION, CONCLUSIONS AND RECOMMENDATIONS FOR FURTHER RESEARCH

6.1. Summary and discussion of work done

In any study of the behaviour of a flow through system, some insight into its hydraulic characteristics is most helpful. Such knowledge is useful in comparing flow-through systems, and also in designing systems to meet particular needs. In many cases the mechanisms that goven the hydraulic behaviour of a flow system are difficult to measure in a physical way. For example it is difficult to measure velocity distributions, or pressure distributions, or density gradients in a sedimentation tank or an oxidation pond containing sewage.

Such systems have been studied by obtaining Flow Curves or Residence Time Distribution curves from tracer tests, and analysing these distributions statistically. However, as was evidenced in Chapter 4, it is difficult to infer anything about the physical behaviour of a system from the statistical parameters of such a distribution curve. In this thesis mathematical models are proposed which have a closer connection with the physical behaviour of the flow in a system and consequently give a more useful interpretation of the flow curves obtained from tracer studies.

In this study the system is considered to be composed of elements such as the perfect mixing element (or zone), the plug flow element, the short circuiting element etc. In the actual system it is clear that such zones cannot be distinguished and do not exist independently. However this compartmentalisation approach is considered to be the best available, and there are precedents for it, for instance in the elementary theory of sedimentation, in which a tank is regarded as consisting of an inlet zone, an outlet zone, a settling zone etc.

In the present study therefore the system is regarded as a number of idealised flow zones combined in series and parallel. Attempts at such modelling which have been made in the past are described and discussed in Chapter 1. Systems were analysed in terms of "C" and "F" diagrams which are the response curves corresponding to an instantaneous input (a Dirac Delta function) or an ideal unit step input.

In most of these analyses the importance of the frontal interface of the tracer, which produces the rising limb of the flow curve has been minimised or neglected. Other omissions in general have been the quantity of tracer injected and the duration of injection. In this analysis care is taken to measure the tracer input as it is considered of prime importance.

Since it is not practicable to produce a pure impulse, a rectangular input pulse of suitable width and height was used. Mathematical treatment of a rectangular input is not too difficult as has been shown in Chapter 2. In that chapter six different mathematical models were proposed. Control theory was applied in the derivation of these, involving a number of approximations and simplifying assumptions. Such approximations are inherent in all mathematical modelling and in the author's opinion do not render the models invalid in this study.

The first of these models, in which plug flow and perfect mixing are combined in series, is useful in analysing simple flow curves with a smooth rise and a smooth fall. In these cases, the time from the first arrival of tracer at the outlet to the peak of the curve, is equal to the duration of the tracer input pulse. The time of first arrival of tracer at the outlet depends on the extent of plug flow and perfect mixing only and is not related to "dead space" volume.

The length of the tail of the curve depends entirely on perfect mixing.

Since short circuiting or differential flow occurs in most systems a four parameter short circuit model was developed which differs from earlier work in that the short circuit is not regarded as instantaneous. A more realistic short circuiting volume is introduced, which is assumed to be a plug flow volume, thus introducing a time constant for the bypassing flow. Thus short circuiting is redefined as a bypassing flow in parallel with the main flow. Depending on whether the short circuiting fraction of the flow reaches the outlet earlier or later than the main flow, it is referred to as "actual" (positive) shortcircuiting or negative shortcircuiting. In this connection "dead space" is redefined after the manner of Levenspiel[9] as the volume occupied by the relatively slow moving fraction of the flow. Thus the volume corresponding to a negative short circuit or "long circuit" can be considered as effective "dead" space. In any case the introduction of a short circuiting volume has made the analysis more flexible. The relative positions and heights of the two peaks of the flow curve, give a guide to making an initial estimate of short circuiting volume and flow.

Since the introduction of a plug flow short circuit results in a sharp rise and sharp fall in the flow curve, a series combination of plug flow and perfect mixing was introduced in the short circuit path, as being more realistic. This model is referred to in the text as the five parameter short circuiting model. The introduction of this type of short circuit smoothes the rises and falls in the flow curve and again makes the model more flexible. It is clear that with this model, either of the parallel flow paths of the model can be considered as the main path. The effect of shortcircuiting time on

the relative positions of the peaks has been discussed in detail in Chapter 2 with the aid of computer generated curves.

The next model considered consists of plug flow and perfect mixing in series as the main flow path, with a plug flow recirculation path in parallel. The resulting transfer function contains exponentials in the denominator and therefore gives a multipole solution. However for simplicity, the denominator is expanded by MacLaurin's series and all terms except the first two are regarded as negligibly small and are omitted. This assumption is true in the case of a small recirculating fraction. For example considering the data of curve 1, Fig.2.7.4, in which $K_1 = 0.546$, $K_2 = 0.254$, $K_3 = 1.2$, $f = 0.1$, when $w = 2$ the value of the magnitude of the term

$$\frac{f}{(1+f)} \cdot e^{-s(K_2+K_3)/(1+K_1 s)}$$

is 0.05 and hence the powers of this term greater than 1 can be neglected. With this truncation, the inversion of the Laplace Transform is not difficult. As a result of retaining only two terms, only one recirculation peak is obtained from the model. This model could be improved by retaining further terms in the series, but this would result in complex mathematics. In any case when the main flow consists of plug flow and perfect mixing in series, it is considered that unless the recirculation flow is large, secondary peaks due to recirculation will not be distinguishable in the tail of the flow curves. Therefore the model is useful for practical applications. However in systems with predominant plug flow the subsequent peaks caused by recirculation will be prominent and distinguishable. For such cases it is necessary to retain further terms in the MacLaurin's series, without much difficulty in inversion.

Two models with three branches in parallel were next examined. The main flow path consists of perfect mixing and plug flow in series.

This main path is combined with a shortcircuiting path and a recirculation path, each of which is plug flow. In the first model none of the recirculated flow passes through the shortcircuiting path, whereas in the second case shortcircuiting of the recirculated flow is possible. With these two models, especially the latter, most flow systems can be simulated. However estimation of the initial values of the parameters is difficult and requires much experience. In all recirculation models it is assumed that macro recirculation takes place from outlet to inlet. Since macro and micro recirculation contribute to perfect mixing, it may be difficult to isolate the recirculation element from the perfect mixing element of the main flow especially when the recirculation time is short compared with the main flow time. It has been found that recirculation lowers the peak produced by the main flow and produces a hump or bulge on the falling part of the flow curve if shortcircuiting is also present. In these models plug flow recirculationonly was considered, whereas a combination of plug flow and perfect mixing recirculation would have given better results. However this would greatly increase the complexity of the mathematics, apart from increasing the number of parameters.

In Chapter 3 a description of the Pulse Technique is given and its application to the models of Chapter 2 is illustrated. The use of a single pulse input instead of a sinusoidal forcing function is necessary for practical reasons. This part of the work is capable of further extension in view of the fact that the Pulse Technique has several advantages over the direct method of Chapter 2. The advantages of the pulse technique are enumerated below:-

(i) Inversion of the Transfer Function is not necessary. Therefore in cases such as the recirculation model, curtailment of the series is not required.

(ii) It is specially useful in the case of complex and high order systems.

(iii) Any arbitrary input pulse shape can be used without extra mathematical complexity.

(iv) If the frequency response of individual elements of a system is known, these can be synthesized on a Bode Diagram to determine the response of the whole system.

(v) Stability and sensitivity analysis can be considered if the frequency response of the system is known.

A single pulse is especially advantageous, apart from its practical advantages, in that it can contain a large number of harmonics so that the response of the system over a wide range of frequencies can be determined. This is especially useful for stability and sensitivity analysis.

In the latter part of Chapter 3, sensitivity analysis was applied for a number of models, and the deductions made were found by experimental verification to be valid. For example, it was found by sensitivity analysis that the introduction of a 5th parameter into the 4 parameter model did not change the sensitivity of the model transfer function very much. This was supported in the analysis of experiments in Chapter 4. In fact sensitivity and stability analysis are more useful in the case of complex high order systems. This part of the work is capable of further extension.

In Chapter 4 verification of the proposed models was undertaken in two stages. Various combinations of idealised flow regimes, or as ideal as it was possible to obtain in the laboratory, were connected together to provide a direct physical analogue to the mathematical model under consideration. Perfect mixing was simulated by intense agitation of water in a vessel using diffused air. Plug

flow was simulated by turbulent flow in a tube. Shortcircuiting and recirculation were simulated again by turbulent flow in tubes, controlled by means of a pump. It was found that the mathematical models could be used to analyse the flow curves produced by various combinations of these elements, and identify the different components, in spite of the fact that the components were by no means ideal.

The fractions of perfect mixing and plug flow in the perfect mixing vessel and plug flow tubing were computed using the two parameter model, which pre-supposes the validity of this model. However in the absence of any alternative approach this was unavoidable.

In the second part of the experimental work, a series of tests were carried out on a model rectangular tank. The outflow curves obtained were analysed by means of the models proposed. The flow rate through the model tank and the height and width of the input pulse were varied in these experiments. The results obtained showed the expected trends. For example an increase in flow velocity through the tank results in an increase in the plug flow fractions and a decrease in the perfect mixing fraction. Short circuiting flows also show a similar trend, decreasing with increasing flow rate and vice versa. This tends to support the new definition of short circuit and effective "dead" space.

In these experiments the input pulses were measured. The time of injection, the quantity of tracer injected and its concentration were measured so that the percentage of tracer recovery could be computed. It was observed that an input pulse of suitably long duration smoothes the outflow curve and the effects of different flow conditions such as short circuiting and recirculation. The use of a long pulse means that tracer can be injected at low concentrations and the rate of flow of injection can be kept at a low level. These measures

ensure that the normal steady flow conditions of the system are not upset during injection.

In spite of the precision with which electrical conductivity was measured during the experiments, errors have given rise to inaccurate tracer recovery values. The most important variable which gave rise to such errors is considered to be temperature. It has been found that at the higher concentrations of salt, the change in conductivity per degree centigrade change in temperature may be as high as 20 $\mu\mho$ and furthermore the relationship between concentration change per degree temperature change and concentration is non linear. Small temperature variations did occur during the course of experiments which were not recorded. However in general it was found that when the experiments were conducted one after the other under identical temperature conditions insofar as was possible, reproducible results were obtained. The importance of temperature control in obtaining reproducible results has also been reported by Tekkipe et al.[20], because of its effect on the flow patterns within the system, particularly when the flow is slow. Other errors which may occur in the measurement of residence time distribution using the conductivity tracer technique, such as stratification within the conductivity cell, incomplete mixing of the flow, method of sampling etc. as reported by White[54] were not found to influence the results of these experiments.

In Chapter 5 the computer techniques used in analysing the flow curves and fitting the proposed models have been presented. It was found that Rosenbrock's[52] optimisation technique was the most useful one for optimising the values of the parameters, but that a great deal depended upon the accuracy with which the initial values were estimated at the beginning of the optimisation process. It was found that the best approach was to study the shape of the output

curve, and assume some initial values for the parameters which govern the shape and position of the peak. Using these initial values some intermediate ordinates on the rising and falling limbs of the curve are computed by hand and the initial estimates are changed accordingly by trial and error. This is a cumbersome procedure but there appears to be no alternative. In the latter part of Chapter 5 the use of an analogue computer for curve fitting was illustrated. For a simple flow curve a simple analogue can be conveniently used as shown, but with more complex models a hybrid computer would have been more useful. There is scope for further work in this direction.

6.2. Comparison with earlier work

In this section a comparison is made between the models proposed in this thesis and a number of models or techniques which have been proposed in the literature on the subject.

Statistical methods illustrated in the latter part of Chapter 4 suffer from the disadvantage that the parameters used, generally calculated by moments, are greatly affected by truncation errors. In this connection the importance of the tail has been studied by the author by generating curves with the two parameter model and determining the mean time by taking first moments about the origin. It has been found that for predominantly plug flow conditions, the mean value so determined is reasonably accurate, but with a high perfect mixing fraction the error in calculation of the mean is great if the tail is prematurely truncated. It has been found that with 90% perfect mixing the error in mean time is 14% even if the area omitted by truncating the tail of the curve is only 4%. Even with 0.002% of the tail area omitted by truncation the error in the calculation of mean time was found to be 1.2%. In this exercise the moments were

computed using the trapezoidal rule with a step size of 0.001. It can be seen that such an error could easily be attributed mistakenly to the existence of "dead" space or a stagnant zone in the system. Apart from possible inaccuracies in the computation of these statistical parameters, they give no great insight into the physical behaviour of the system.

Rebhun and Argaman[4] proposed a method for determining "m", "p" and stagnant volume which is described in Chapter 1. In order to compare the results obtained by their method with the methods proposed here, a number of experiments were performed on the model tank at flows of 5, 10, 12 and 14 litres per minute. The input pulse was reduced in duration of injection to a value of 15 seconds in order to simulate an impulse input, and the concentration consequently was high in order to obtain an accurate result. The flow curves were analysed and $\log[1-F(\theta)]$ versus θ was plotted for each curve, in order to obtain values of m, p, and the "dead" space. The results show that the plug flow fraction remained constant around 40% throughout the flow range from 5 litres per minute to 14 litres per minute. These plots also gave unrealistic "negative" dead space volumes. A typical plot of $\log[1-F(\theta)]$ against θ for a flow of 14 litres per minute is given in Fig.6.2.1. For comparison the results obtained from the two parameter model fit are plotted in Fig.6.2.2 along with the "p" values obtained by Rebhun et al.'s method. The discrepancies between the two methods of analysis are very great. From a realistic standpoint the values obtained from the two parameter model fit are more satisfactory. The more complex models give still better results. Rebhun and Argaman's analysis also gives negative dead spaces in the case of their experiments which they attribute to inaccuracies in experimental technique. This explanation seems unlikely and it is

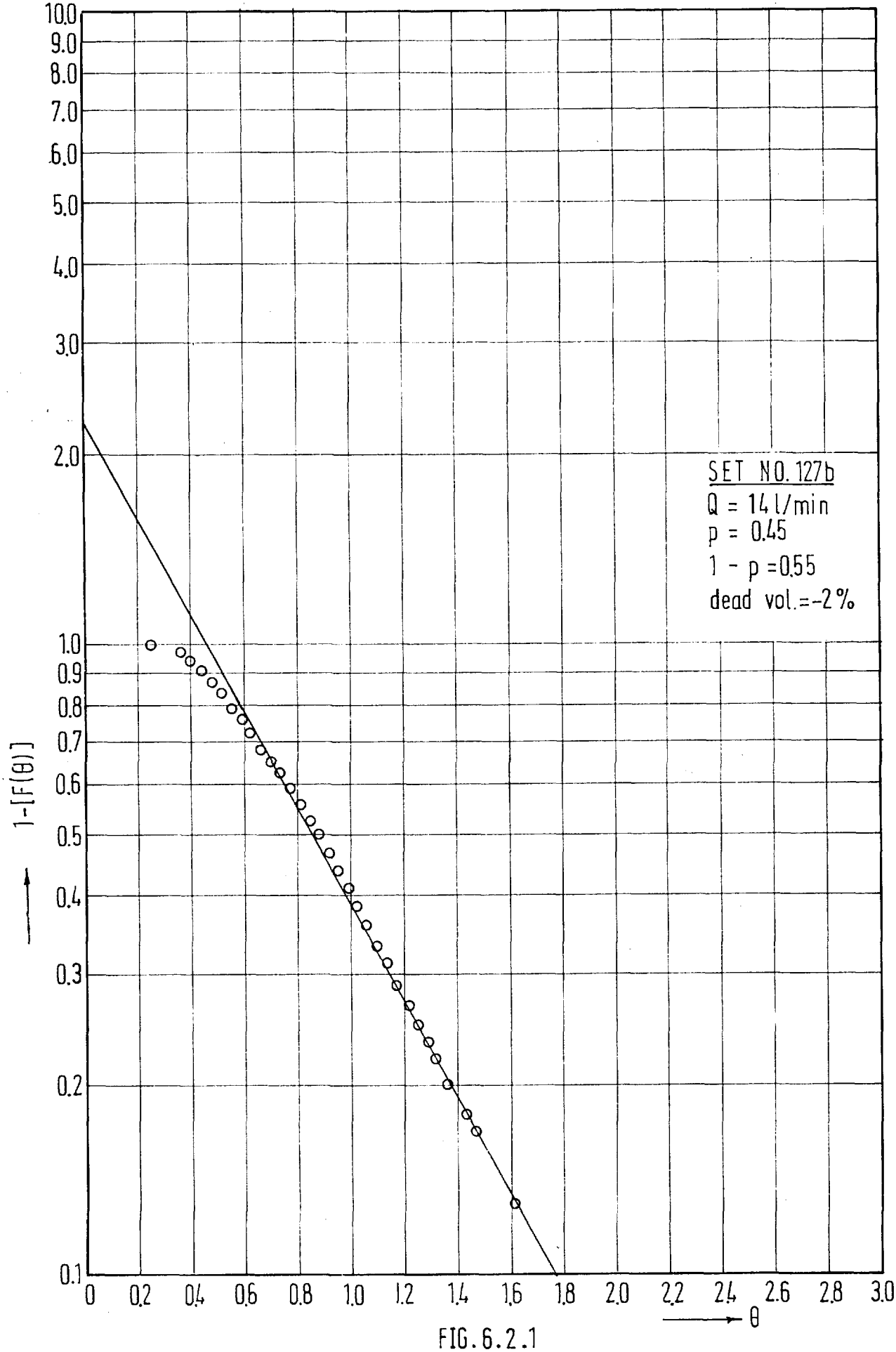
SET NO. 127b
Q = 14 l/min
p = 0.45
1 - p = 0.55
dead vol. = -2 %
1-[F(θ)]
θ
10.0
9.0
8.0
7.0
6.0
5.0
4.0
3.0
2.0
1.0
0.9
0.8
0.7
0.6
0.5
0.4
0.3
0.2
0.1
0
0.2
0.4
0.6
0.8
1.0
1.2
1.4
1.6
1.8
2.0
2.2
2.4
2.6
2.8
3.0

FIG. 6.2.1

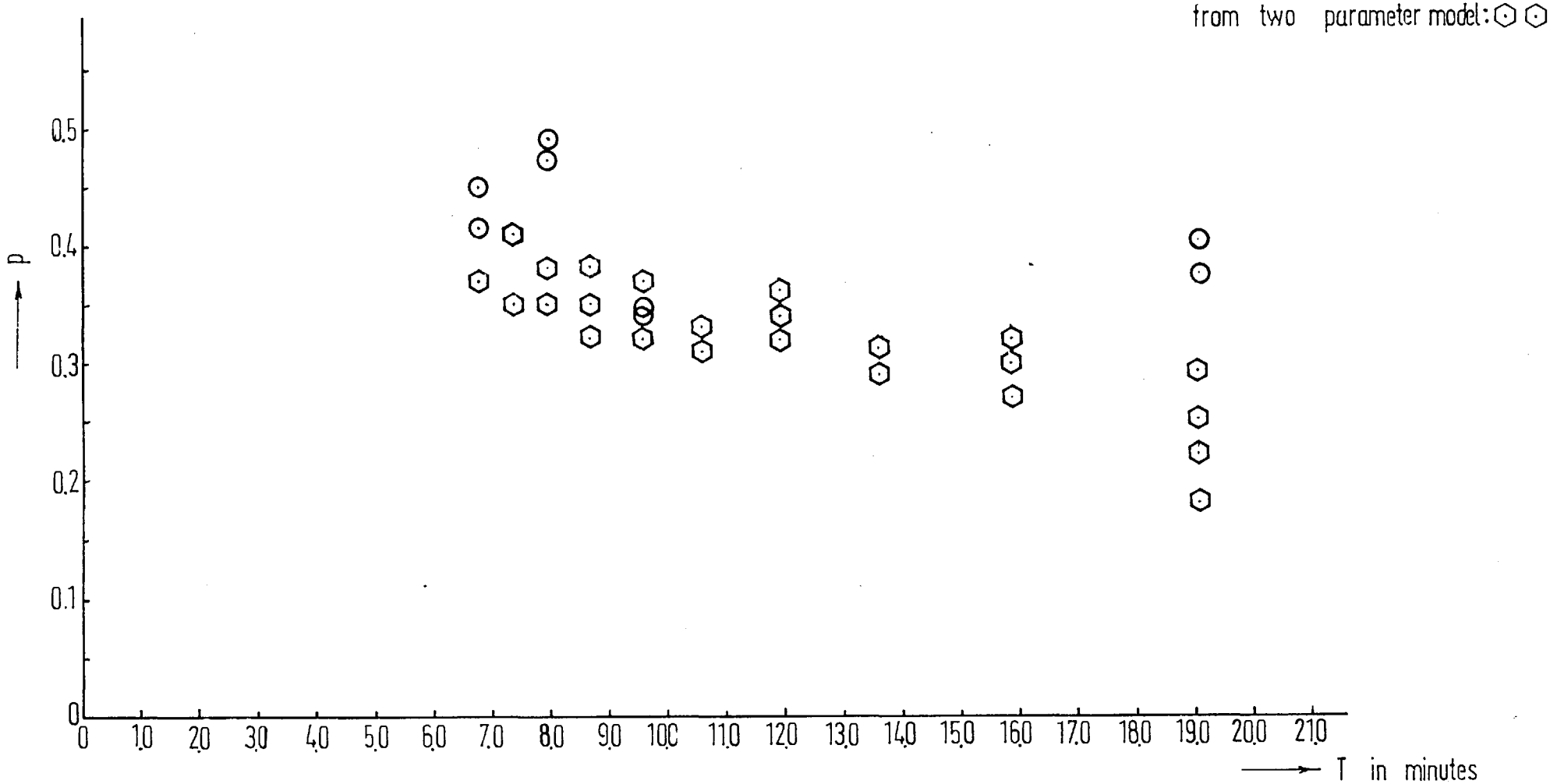
points obtained from
Rebhun and Argaman : ⊙ ⊙
from two parameter model: ⬡ ⊙
p
0.5
0.4
0.3
0.2
0.1
0
0 1.0 2.0 3.0 4.0 5.0 6.0 7.0 8.0 9.0 10.0 11.0 12.0 13.0 14.0 15.0 16.0 17.0 18.0 19.0 20.0 21.0
T in minutes

FIG. 6.2.2a

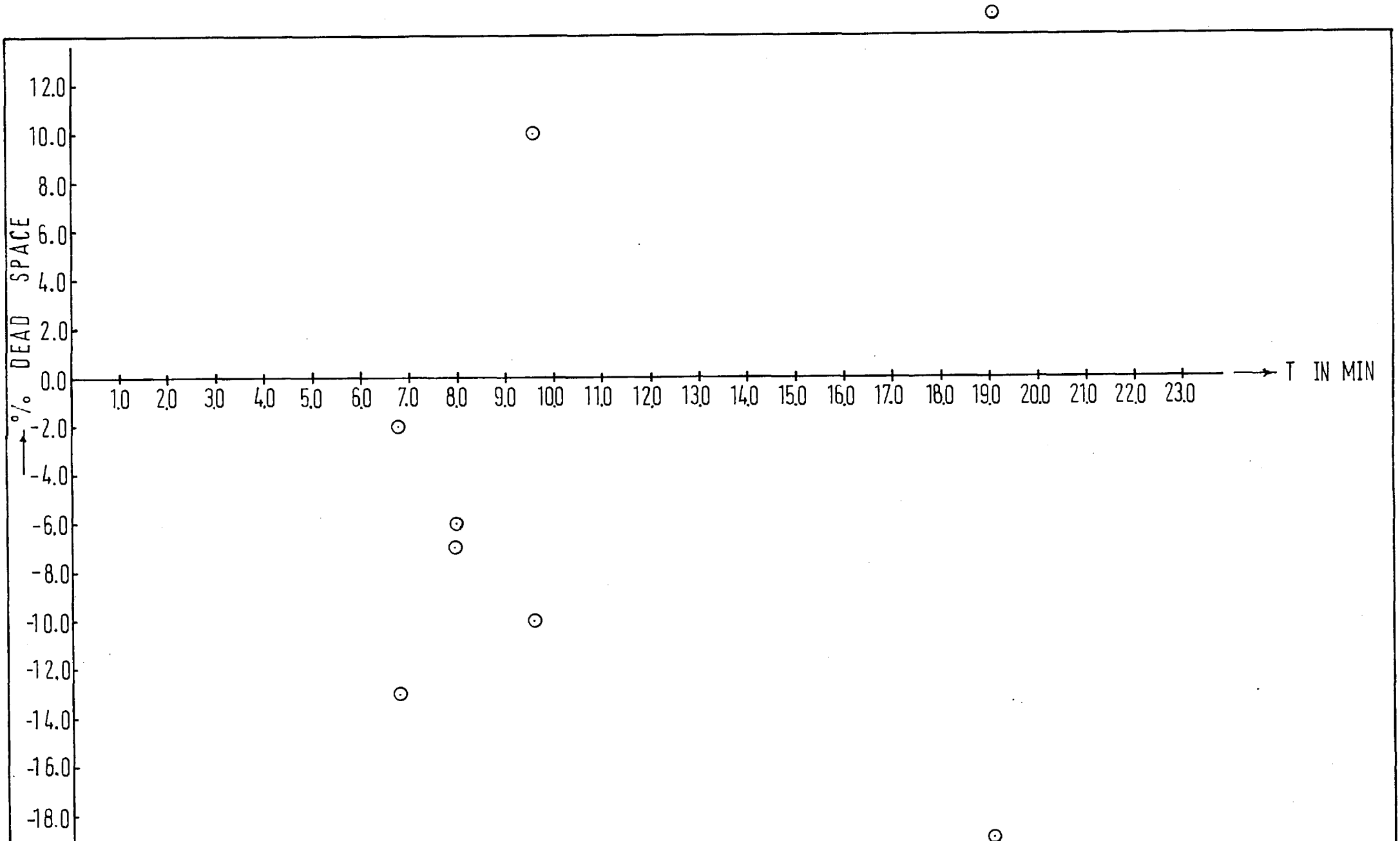

DEAD SPACE OBTAINED FROM REBHUN ETAL'S METHOD.

FIG. 6.2.2b.

suggested here that the analysis in invalid.

Various diffusion models have been put forward in the literature for determining the degree of mixing in flow systems. The basic equation from which the diffusion models are derived is given in Chapter 4 and is reproduced here

$$\frac{\partial C}{\partial t} = D \cdot \frac{\partial^2 C}{\partial x^2} - u \frac{\partial C}{\partial x}$$

Murphy et al.[55](56) used the solution of the above equation given by Thomas et al.[56](57) as follows:-

$$\frac{C}{C_o} = 2 \sum_{n=1}^{\infty} \frac{\mu_n (U \sin \mu_n + \mu_n \cos \mu_n)}{(U^2 + 2U + \mu_n^2)} \text{ Exp. } [U - \frac{(U^2 + \mu_n^2)\theta}{2U}]$$

where $\theta = \frac{t}{T}$, $U = \frac{1}{2} \frac{1}{D/uL}$ and μ_n are constants

$\mu_1, \mu_2, \mu_3 \ldots\ldots \mu_n$. and are given by the roots of the equation

$$\mu_n = \cot^{-1} [(\frac{\mu_n}{U} - \frac{U}{\mu_n})/2]$$

$\frac{"D"}{uL}$ is referred to by Murphy et al. as the Diffusion number and was determined from the peak of the flow curve by making $\frac{d(C/C_o)}{d\theta} = 0$ in the concentration equation given above.

As the level of mixing is an important factor in the design of an aeration tank in an Activated Sludge unit, Murphy et al. have suggested $\frac{D}{uL}$ as an important parameter for design purposes.

For comparison purposes a flow curve obtained experimentally by Murphy et al.[55](55) is reproduced in Fig.6.2.3. Because of lack of information regarding duration of the tracer injection, θ_1 was determined by the author by trial and error. It can be seen that in spite of this the four parameter and five parameter models show a reasonably good fit to the experimental points. It can be seen that the diffusion model of Murphy et al. gives the best fit of the three, but it is

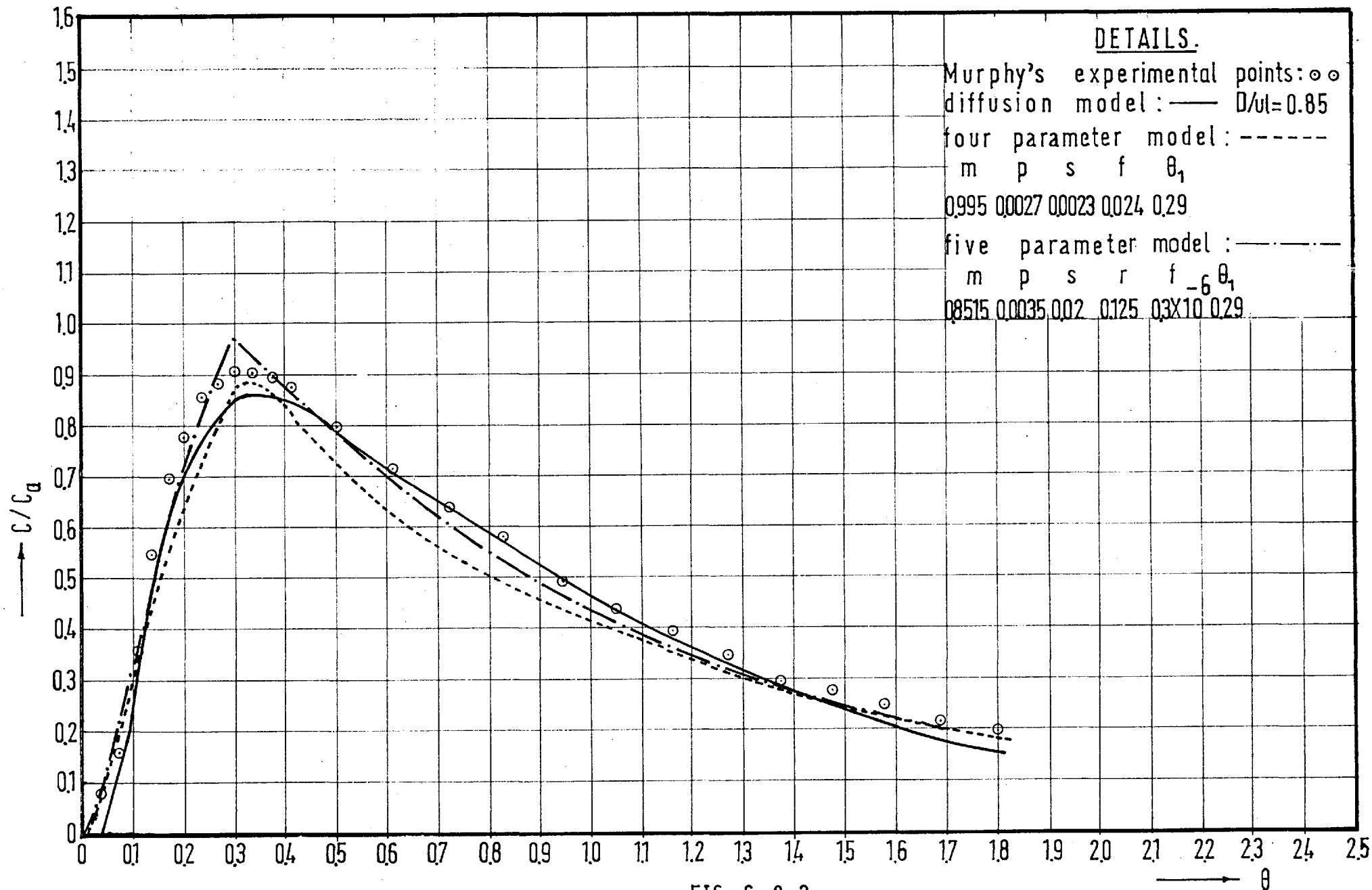
DETAILS.
Murphy's experimental points: ⊙⊙
diffusion model : —— D/ul= 0.85
four parameter model : ------
m p s f θ1
0.995 0.0027 0.0023 0.024 0.29
five parameter model : —·—·—
m p s r f −6 θ1
0.8515 0.0035 0.02 0.125 0.3X10 0.29
C / Cq
θ

FIG. 6.2.3

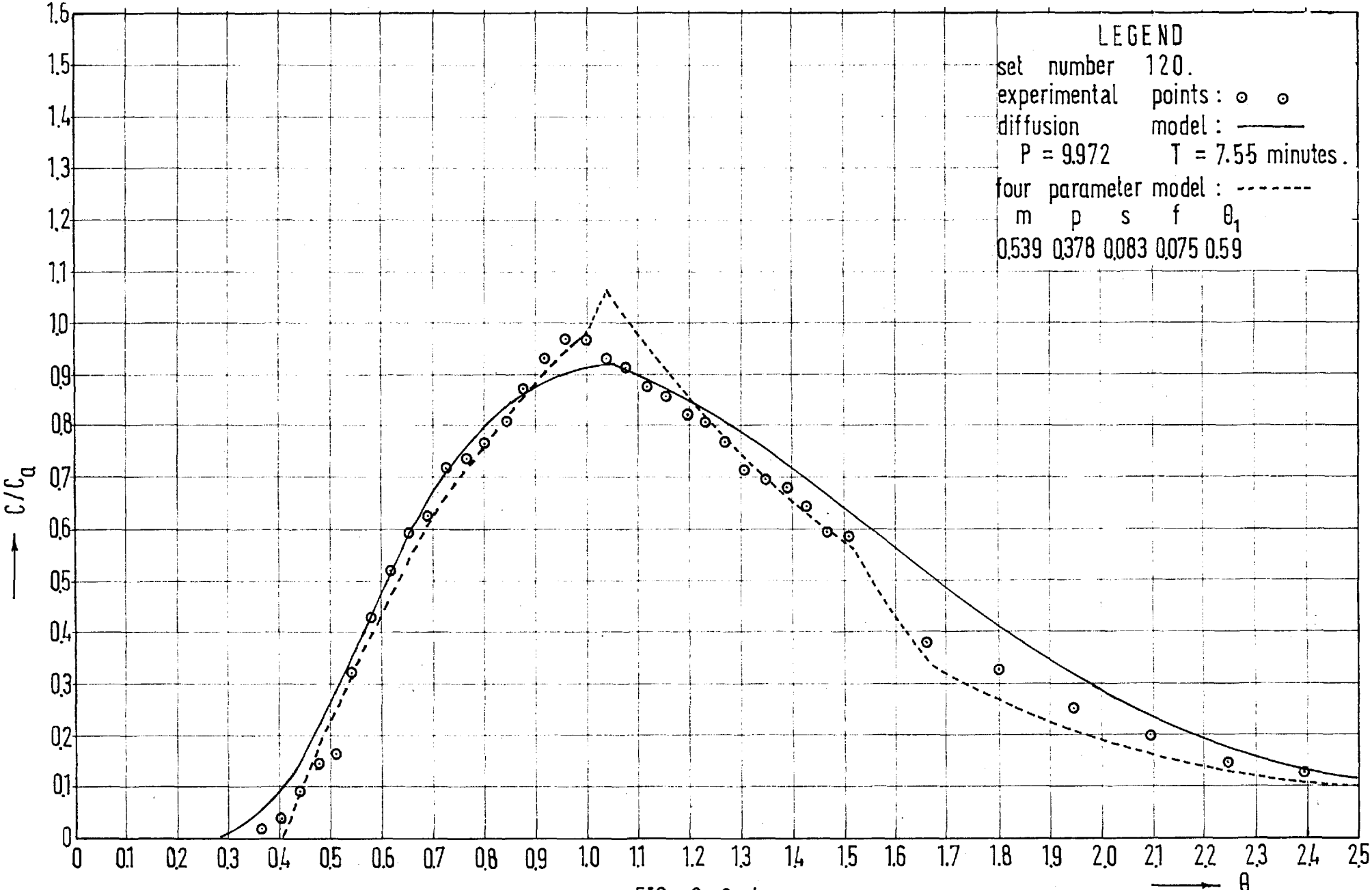
LEGEND
set number 120.
experimental points : ⊙ ⊙
diffusion model : ——
P = 9.972 T = 7.55 minutes.
four parameter model : - - - - - -
m p s f θ1
0.539 0.378 0.083 0.075 0.59
C/Ca
θ
0 0.1 0.2 0.3 0.4 0.5 0.6 0.7 0.8 0.9 1.0 1.1 1.2 1.3 1.4 1.5 1.6 1.7 1.8 1.9 2.0 2.1 2.2 2.3 2.4 2.5
0 0.1 0.2 0.3 0.4 0.5 0.6 0.7 0.8 0.9 1.0 1.1 1.2 1.3 1.4 1.5 1.6

FIG. 6.2.4

suggested by the author that it gives the least information about the flow system. The five parameter model on the other hand indicates that about 15% of the total volume of the tank was relatively stagnant although 98% of the total volume was perfectly mixed. Out of this, about 13% perfect mixing takes place in the stagnant zone. It is suggested that this type of analysis gives a better insight into the hydraulic behaviour of the tank than the one parameter diffusion model above.

A second diffusion model is that used by Krenkel et al.[48] explained in Chapter 4. This model is currently used for the determination of longitudinal mixing. This is a two parameter model in which T is the mean time of flow and P is the Peclet number = $\frac{uL}{D}$. For comparison purposes experimental set No.120 is plotted in Fig.6.2.4 and fitted with Krenkel et al.'s diffusion model, and the author's four parameter model. The latter gives a better overall fit of the data and can take account of the drop in the output curve at $\theta = 1.5$ caused by short circuiting in the system. The diffusion gives a good fit up to the peak, but thereafter deviates from the curve considerably. The four parameter model also gives more information about the flow conditions. A marked disadvantage of the diffusion model is that it cannot be used in the analysis of flow curves with more than one peak.

6.3 Possible uses for the proposed models

Apart from their probable use in the field of Chemical Engineering, the proposed models could be used in the analysis of the flow curves obtained from some of the flow systems and treatment units used in Public Health Engineering, particularly in water and sewage treatment. In cases in which retention of the liquid within the unit for a particular

length of time is the primary function, as in the case of a chlorine contact tank, the merits of different designs can be assessed by carrying out flow tests on existing systems and analysing the results. The type of design which produces the maximum plug flow fraction in this case is the most desirable.

Tests of this type have been performed in the past on sedimentationtanks with somewhat inconclusive results. In many cases the actual experiments performed have not been completely satisfactory. It is essential that in the case of either an impulse input or a thick pulse input that the tracer be fully mixed with the flow before reaching the inlet of the unit. In many cases the tracer slug has been dumped into the flow indiscriminately just upstream of the tank inlet, tending to lead to meaningless results. In a sedimentation tank the extent of plug flow is said to determine the settling efficiency of the tank, greater plug flow being associated with better efficiency. However in the author's opinion more research is necessary to correlate settling efficiency with plug flow or perfect mixing. The immediate value of such analysis is possibly the determination of shortcircuiting or recirculation caused by the existence of density layers.

In studies on the kinetics of bioxidation and nitrification in waste treatment units analysis of this type may be found helpful. Most practical units have flow regimes intermediate between that of an ideal tubular reactor and a perfectly mixed reactor. Information on the degree of longitudinal mixing can be obtained by the use of these models. Similar information could be obtained from studies on oxidation ponds, lakes and river reaches, particularly with regard to short circuiting and recirculation.

These techniques have possible uses in the study of Physiological flow, to which control theory is frequently applied. As early as 1954 Meier et al.[57] introduced the dilution technique to the study of flow and the measurement of volume of blood in arteries and veins. By injecting an indicator dye into the venous system at a suitable point and taking samples at some suitable point downstream, the flow of blood or the volume of the system may be determined. In such measurements it is assumed that the dye is completely mixed on injection. Again the heart may be regarded as a reactor in which mixing is obtained by turbulence. It is considered by many investigators that the ventricles are perfectly mixed compartments and the auricles are plug flow compartments. There is some controversy over these points but Macdonald[58] suggests that in greatly distended hearts approaching failure, the ventricles cease to function as perfectly mixed vessels and large volumes of blood accumulate at the end of the systoles creating stagnant zones in the heart. In such cases the extent of mixing, plug flow, shortcircuit or stagnancy could be conveniently determined by the models proposed in this work. Again according to Macdonald[58] in such studies a prolonged injection of tracer gives better results than jet injection (or an impulse input).

The stimulus response technique has also been used in studies on the kidney[59]. It is considered that a long tail or a secondary peak on the response curve is a symptom of malfunction of the kidney and indicates blockage. The use of the models developed in this study would certainly give more insight into the behaviour of the kidney. In general the response of any part of the body to cardiac output could be analysed by these methods.

6.4 Suggestions for future research

In this thesis a method of analysing the flow into a number of assumed flow zones has been presented. No attempt has been made to take account of any changes which might be taking place in the constituents of the flow or to apply reaction equations to the models in order to determine the overall kinetics of a reactor or unit process such as a sedimentation or chlorination tank. Since in practice most flow systems exhibit changes in fluid composition with time and these are of major interest, it is suggested that future work should concentrate on this aspect. It is felt by the author that the application of reaction equations to these mathematical models of flow may lead to useful results in the prediction of outlet concentrations of the flow constituents.

In addition the following suggestions are made for the use of future investigators:

1. For reproducibility and reliability of experimental data it is essential that the temperature of the fluid flowing through the system should remain approximately constant. This can be attained by thermostatic control of feed water temperature. A system as used by Tekkipe et al.[20] can meet this requirement.

2. It has been observed that as the duration of the input pulse increases, better and better fit of the experimental data with the proposed models is attained. It is felt that there is an optimum height and width of the input pulse for getting the best fit. More research is necessary to determine this optimum.

3. The analysis of the flow curves obtained from field units such as the aeration tank is not yet well defined . It is hoped that analysis of flow curves obtained from models of different scales by the models described in this work will enable future investigators to look more thoroughly into the behaviour of such units as mentioned above .

4. It is felt that the Pulse Technique should be more thoroughly investigated . For accurate measurement of the input and output pulses , a radio active or photo sensitive tracer and an automatic continuous recording device can be used .

APPENDIX

1. Special Functions :

A number of special functions used in Chapters 1 and 2 are described here.

(a) The Unit Step Function $U(t-a)$ is defined as follows :

$$U(t-a) = 0 \quad \text{for } t < a$$

$$= 1 \quad \text{for } t > a$$

If used as a multiplier of a function, it has the effect of wiping out all values of the other function before $t = a$. It is useful in representing pulses and in the step by step reproduction of complicated functions. These properties of the Unit Step Function have been extensively used in Chapter 2.

The Laplace Transform of $U(t-a) = \frac{e^{-as}}{s}$ and $L\,U(t) = 1/s$.

(b) The Dirac Delta Function $\delta(t-a)$ is defined as follows :

$$\delta(t-a) = 0 \text{ for } t \neq a$$

$$= \infty \text{ for } t = a$$

Also $$\int_{a-\epsilon}^{a+\epsilon} \delta(t-a)dt = 1$$

It denotes an Instantaneous Unit Impulse and represents a pulse of infinitesimal duration, infinite intensity and unit magnitude occurring at time $t = a$. If used as a multiplier of a function $f(t)$ as shown below, it "picks out" the value of $f(t)$ at any instant $t = a$.

(i) $\int_b^c f(t).\delta(t-a)\,dt = f(a)$ when $b < a < c$

(ii) Laplace Transform of $\delta(t-a) = e^{-as}$ and $\delta(t) = 1$

(iii) $\frac{d}{dt}(U(t-a)) = \delta(t-a)$.

(c) Convolution : It is an operation which gives the inverse transform of the product of two transforms directly in terms of the original functions.

Let F(t) and G(t) denote any two functions that are sectionally continuous in each finite interval $0 \leq t \leq T$, and let F(s) = L[F(t)], G(s) = L[G(s)]. Then

$$F(s) \cdot G(s) = \int_0^\infty e^{-st} \int_0^t F(\tau) \cdot G(t - \tau)\, d\tau\, dt \text{ and}$$

$$L^{-1}[F(s) \cdot G(s)] = \int_0^t F(\tau) \cdot G(t - \tau)\, d\tau$$

The integration operation as given above to get the inverse of the Laplace transform is known as convolution and is usually denoted as $F(t) * G(t)$.

The various properties of convolution are

(i) It is commutative i.e. $F(t) * G(t) = G(t) * F(t)$.

(ii) It is distributive with respect to addition :

$F(t) * [G(t) + H(t)] = F(t) * G(t) + F(t) * H(t)$.

Also $F * (KG) = K(F * G)$ where K is a constant.

(iii) It is also associative :

$F(t) * [G(t) * H(t)] = [F(t) * G(t)] * H(t)$

As mentioned in Chapter 1, these properties of convolution can be conveniently used for determining the response of a system to any input pulse function F(t), if the response of the system to a Dirac Delta input function is known.

Let G(t) be the response function of the system for a Dirac Delta input. Then the output function C(t) for the input F(t) is obtained by convolution

$$C(t) = \int_0^t F(t-\tau) \cdot G(\tau)\, d\tau.$$

2. Inversion of a number of Laplace Transforms :-

Details of the inversion of a number of the Laplace Transform described in Chapter 2 are given below.

(a) $L^{-1}\dfrac{1}{1+K_1 s}$. It has a single pole at $s = -\dfrac{1}{K_1}$

$$\therefore L^{-1}\frac{1}{1+K_1 s} = \lim_{s \to -\frac{1}{K_1}} \left[\frac{e^{st}}{1+K_1 s}\right]$$

$$= e^{-t/K_1}$$

(b) $L^{-1}\dfrac{1}{s(1+K_1 s)}$. It has two poles, one at $s = 0$ and the other at $s = -\dfrac{1}{K_1}$

$$\therefore L^{-1}\frac{1}{s(1+K_1 s)} = \sum \text{Residues of } \frac{e^{st}}{s(1+K_1 s)} \text{ at the poles.}$$

$$= \lim_{s \to 0} \frac{s e^{st}}{s(1+K_1 s)} + \lim_{s \to -\frac{1}{K_1}} \frac{e^{st}(1+K_1 s)}{s(1+K_1 s)}$$

$$= 1 - e^{-t/K_1}$$

(c) $L^{-1}\dfrac{e^{-K_2 s}}{s(1+K_1 s)} = \left[1 - e^{-(t-K_2)/K_1}\right] . U(t-K_2)$. This is obtained from the Translation Theorem of Laplace Transforms and the deduction obtained from section (b) above.

(d) $L^{-1}[1 / s(1+K_1 s)^2]$. This can be solved from the fundamentals of Laplace Transforms as follows.

$$L^{-1}[1 / s(1 + K_1 s)^2]$$

$$= L^{-1}[(1/K_1^{\,2}) / s(s + \tfrac{1}{K_1})^2]$$

$$= \frac{1}{2\pi i} \int_{\gamma-i\infty}^{\gamma+i\infty} \frac{\frac{1}{K_1^{\,2}}\, e^{st}\, ds}{s\,(s+ 1/K_1)^2}$$

$$= \sum \text{Residues of } [e^{st}/K_1^{\,2}\, s\, (s + 1/K_1)^2] \text{ at poles } s = 0 \text{ and } s = -\frac{1}{K_1}$$

The residue R_1 at $s = 0$ is

$$R_1 = \lim_{s \to 0} \frac{s\, e^{st}}{s\, K_1^2\, (s+\frac{1}{K_1})^2}$$

$$= 1$$

And the residue at $s = -\frac{1}{K_1}$

$$R_2 = \lim_{s \to -\frac{1}{K_1}} \frac{1}{1!} \frac{d}{ds} \left[(s + \frac{1}{K_1})^2 \frac{e^{st}/K_1^2}{s\,(s + \frac{1}{K_1})^2}\right]$$

$$= \lim_{s \to -\frac{1}{K_1}} \frac{1}{K_1^2} \cdot \frac{d}{ds} \left[\frac{e^{st}}{s}\right]$$

$$= \frac{1}{K_1^2} \cdot \lim_{s \to -\frac{1}{K_1}} \left[\frac{s.t.e^{st} - e^{st}}{s^2}\right]$$

$$= \frac{1}{K_1^2} \left[\frac{-\frac{t}{K_1} e^{-t/K_1} - e^{-t/K_1}}{1/K_1^2}\right] = -(1 + \frac{t}{K_1})\, e^{-t/K_1}$$

$$\therefore \sum \text{Residues} = R_1 + R_2 = 1 - (1 + \frac{t}{K_1})\, e^{-t/K_1}$$

(e) $$L^{-1} \frac{e^{-(2K_2 + K_3)s}}{s\,(1 + K_1 s)^2}$$

$$= \left[1 - (1 + \frac{t - 2K_2 - K_3}{K_1})\, e^{-(t - 2K_2 - K_3)/K_1}\right] \cdot U(t-2K_2 - K_3)$$

This is obtained from the Translation Theorem and the deductions of section (d).

3. Dreifke's Trapezoidal Approximation :

(a) In Chapter 5 the Fourier Transform of the function

$$f(t) = f_i\, (1 - \frac{t}{\Delta t} + \frac{t_i}{\Delta t}) + f_{i+1}\, (\frac{t}{\Delta t} - \frac{t_i}{\Delta t})$$

has been presented. Here the details of the solution are given.

$$FT[f(t)] = \int_{t_i}^{t_{i+1}} f_i (1 + \frac{t_i}{\Delta t} - \frac{t}{\Delta t})\, e^{-jwt}\, dt + f_{i+1} \int_{t_i}^{t_{i+1}} (\frac{t}{\Delta t} - \frac{t_i}{\Delta t}) e^{-jwt} dt$$

Now $$\int_{t_i}^{t_{i+1}} f_i\left(1 + \frac{t_i}{\Delta t} - \frac{t}{\Delta t}\right) e^{-jwt}\,dt$$

$$= \int_{t_i}^{t_{i+1}} f_i\left(1 + \frac{t_i}{\Delta t}\right) e^{-jwt}\,dt - \frac{f_i}{\Delta t} \int_{t_i}^{t_{i+1}} t\, e^{-jwt}\,dt$$

$$= f_i\left(1+ \frac{t_i}{\Delta t}\right)\left(-\frac{1}{jw}\right)\left[e^{-jwt}\right]_{t_i}^{t_{i+1}} - \frac{f_i}{\Delta t}\left[t\left(-\frac{1}{jw}\right)e^{-jwt} - \int\left(-\frac{1}{jw}\right)e^{-jwt}\,dt\right]_{t_i}^{t_{i+1}}$$

$$= f_i\left(1+ \frac{t_i}{\Delta t}\right)\left(-\frac{1}{jw}\right)\left(e^{-jwt_{i+1}} - e^{-jwt_i}\right) - \frac{f_i}{\Delta t}\left[t\left(-\frac{1}{jw}\right)e^{-jwt} - \frac{j^2}{w^2}\, e^{-jwt}\right]_{t_i}^{t_{i+1}}$$

$$= \frac{f_i \cdot j}{w}\left[\left(1+\frac{t_i}{\Delta t}\right)\left(e^{-jwt_{i+1}} - e^{-jwt_i}\right) - \frac{1}{\Delta t}\left[t_{i+1}e^{-jwt_{i+1}} - \frac{j}{w}\, e^{-jwt_{i+1}}\right.\right.$$

$$\left.\left. - t_i e^{-jwt_i} + \frac{j}{w}\, e^{-jwt_i}\right]\right]$$

$$= \frac{f_i \cdot j}{w}\left[e^{-jwt_{i+1}}\left(1 + \frac{t_i}{\Delta t} - \frac{t_{i+1}}{\Delta t} + \frac{j}{w\Delta t}\right) - e^{-jwt_i}\left(1+\frac{t_i}{\Delta t} - \frac{t_i}{\Delta t} + \frac{j}{w\Delta t}\right)\right]$$

$$= \frac{f_i \cdot j}{w}\left[e^{-jwt_{i+1}} \cdot \frac{j}{w\Delta t} - \left(1 + \frac{j}{w\Delta t}\right)e^{-jwt_i}\right] \quad \left[\because 1 + \frac{t_i}{\Delta t} = \frac{t_{i+1}}{\Delta t}\right]$$

Again, $$f_{i+1}\int_{t_i}^{t_{i+1}} \left(\frac{t}{\Delta t} - \frac{t_i}{\Delta t}\right) e^{-jwt}\,dt$$

$$= f_{i+1}\left(-\frac{t_i}{\Delta t}\right)\left(-\frac{1}{jw}\right)\left(e^{-jwt_{i+1}} - e^{-jwt_i}\right) + \frac{f_{i+1}}{\Delta t}\left(\frac{j}{w}\, t_{i+1}\, e^{-jwt_{i+1}}\right.$$

$$\left. - \frac{j^2}{w^2}\, e^{-jwt_{i+1}} - \frac{j}{w}\, t_i e^{-jwt_i} + \frac{j^2}{w^2}\, e^{-jwt_i}\right)$$

$$= f_{i+1}\cdot\frac{j}{w}\left[-\frac{t_i}{\Delta t}\, e^{-jwt_{i+1}} + \frac{t_i}{\Delta t}\, e^{-jwt_i} + \frac{1}{\Delta t}\left(t_{i+1}\, e^{-jwt_{i+1}} - \frac{j}{w}\, e^{-jwt_{i+1}}\right.\right.$$

$$\left.\left. - t_i\, e^{-jwt_i} + \frac{j}{w}\, e^{-jwt_i}\right)\right]$$

$$= f_{i+1}\cdot\frac{j}{w}\left[e^{-jwt_{i+1}}\left(-\frac{t_i}{\Delta t} + \frac{t_{i+1}}{\Delta t} - \frac{j}{w\Delta t}\right) + e^{-jwt_i}\left(\frac{t_i}{\Delta t} - \frac{t_i}{\Delta t} + \frac{j}{w\Delta t}\right)\right]$$

$$= f_{i+1} \cdot \frac{j}{w} \left[e^{-jwt_{i+1}} \left(1 - \frac{j}{w\Delta t}\right) + \frac{j}{w\Delta t} e^{-jwt_i} \right]$$

$$\therefore FT_i[f(t)] = \frac{f_i \cdot j}{w} \left[\frac{j}{w\Delta t} e^{-jwt_{i+1}} - \left(1 + \frac{j}{w\Delta t}\right) e^{-jwt_i} \right]$$

$$+ \frac{f_{i+1} \cdot j}{w} \left[\left(1 - \frac{j}{w\Delta t}\right) e^{-jwt_{i+1}} + \frac{j}{w\Delta t} e^{-jwt_i} \right]$$

(b) The regrouping of the terms in equation (3.2.12) by separating the real and imaginary parts is done as follows:

As an example only the first term in the above equation is considered here. The term is

$$f_1 \frac{j}{w} \left[\frac{j}{w\Delta t} e^{-jwt_2} - \left(1 + \frac{j}{w\Delta t}\right) e^{-jwt_1} \right]$$

$$= f_1 \frac{j}{w} \left[\frac{j}{w\Delta t} e^{-jwt_1} \cdot e^{-jw\Delta t} - \left(1 + \frac{j}{w\Delta t}\right) e^{-jwt_1} \right]$$

$$= f_1 \cdot \frac{j}{w} \left[e^{-jwt_1} \left(\frac{j}{w\Delta t} e^{-jw\Delta t} - \frac{j}{w\Delta t} - 1 \right) \right]. \quad \text{From Euler's Relationship,}$$

$$= f_1 \cdot \frac{j}{w} \left[(\cos wt_1 - j \sin wt_1) \left\{ \frac{j}{w\Delta t} (\cos w\Delta t - j \sin w\Delta t) - \frac{j}{w\Delta t} - 1 \right\} \right]$$

$$= f_1 \cdot \frac{j}{w} \left[(\cos wt_1 - j \sin wt_1) \left\{ \frac{j}{w\Delta t} \cos w\Delta t + \frac{\sin w\Delta t}{w\Delta t} - \frac{j}{w\Delta t} - 1 \right\} \right]$$

$$= f_1 \cdot \frac{j}{w} \left[\frac{j}{w\Delta t} \cos wt_1 \cdot \cos w\Delta t + \cos wt_1 \cdot \frac{\sin w\Delta t}{w\Delta t} - \frac{j}{w\Delta t} \cdot \cos wt_1 \right.$$

$$- \cos wt_1 + \frac{1}{w\Delta t} \sin wt_1 \cdot \cos w\Delta t - j \sin wt_1 \cdot \frac{\sin w\Delta t}{w\Delta t} - \frac{1}{w\Delta t} \sin wt_1$$

$$\left. + j \sin wt_1 \right]$$

$$= \frac{f_1}{w} \left[- \frac{1}{w\Delta t} \cdot \cos wt_1 \cdot \cos w\Delta t + j \cos wt_1 \cdot \frac{\sin w\Delta t}{w\Delta t} + \frac{1}{w\Delta t} \right.$$

$$\cos wt_1 - j \cos wt_1 + \frac{j}{w\Delta t} \sin wt_1 \cdot \cos w\Delta t + \sin wt_1 \cdot$$

$$\left. \frac{\sin w\Delta t}{w\Delta t} - \frac{j}{w\Delta t} \sin wt_1 - \sin wt_1 \right]$$

$$= \frac{f_1}{w} \left[\cos wt_1 \left(\frac{1}{w\Delta t} - \frac{\cos w\Delta t}{w\Delta t} \right) - \sin wt_1 \left(1 - \frac{\sin w\Delta t}{w\Delta t}\right) \right.$$

$$\left. + j \left\{ - \sin wt_1 \left(\frac{1}{w\Delta t} - \frac{\cos w\Delta t}{w\Delta t} \right) - \cos wt_1 \left(1 - \frac{\sin w\Delta t}{w\Delta t}\right) \right\} \right]$$

$$= \frac{f_1}{w} \left[\cos wt_1 \cdot \frac{w\Delta t}{2} \cdot \frac{\frac{1}{2}\left(1 - \cos 2\frac{w\Delta t}{2}\right)}{\left(\frac{w\Delta t}{2}\right)^2} - \frac{w\Delta t}{w\Delta t} \cdot \sin wt_1 \left(1 - \frac{\sin w\Delta t}{w\Delta t}\right) \right.$$

$$\left. + j \left\{ - \sin wt_1 \cdot \frac{w\Delta t}{2} \cdot \frac{\frac{1}{2}\left(1 - \cos 2\frac{w\Delta t}{2}\right)}{\left(\frac{w\Delta t}{2}\right)^2} - \frac{w\Delta t}{w\Delta t} \cos wt_1 \left(1 - \frac{\sin w\Delta t}{w\Delta t}\right) \right\} \right]$$

$$= \frac{f_1}{w}\left[\cos wt_1 \cdot \frac{w\Delta t}{2}\left(\frac{\sin\frac{w\Delta t}{2}}{\frac{w\Delta t}{2}}\right)^2 - \frac{w\Delta t}{w\Delta t}\cdot \sin wt_1\ \left(1 - \frac{\sin w\Delta t}{w\Delta t}\right)\right.$$

$$\left. + j\left\{-\sin wt_1 \cdot \frac{w\Delta t}{2}\left(\frac{\sin\frac{w\Delta t}{2}}{\frac{w\Delta t}{2}}\right)^2 - \frac{w\Delta t}{w\Delta t}\cdot \cos wt_1\ \left(1 - \frac{\sin w\Delta t}{w\Delta t}\right)\right\}\right]$$

$$= f_1 \cdot \Delta t\left[\tfrac{1}{2}\left(\frac{\sin w\Delta t/2}{w\Delta t/2}\right)\cos wt_1 - \frac{1}{w\Delta t}\sin wt_1\ \left(1 - \frac{\sin w\Delta t}{w\Delta t}\right)\right.$$

$$\left. + j\left\{-\tfrac{1}{2}\sin wt_1\ \left(\frac{\sin w\Delta t/2}{w\Delta t/2}\right)^2 - \frac{1}{w\Delta t}\cos wt_1\ \left(1 - \frac{\sin w\Delta t}{w\Delta t}\right)\right\}\right]$$

In this way the other terms also of Equation (3.2.13) can be obtained.

4. Deduction of Analogue model for recirculation:

The deductions of the analogue form of the Recirculation Model up to part (iii-b) are given in Chapter 5. The deductions for parts (iv) and (v) are given below:

Part (iv) is written in the form

$$Y = \frac{1}{(1+f)}\left[e^{-(\theta-\theta_1-K_2)/K_1} - e^{-(\theta-K_2)/K_1} + \frac{f}{(1+f)}\left\{1-\left(1+\frac{\theta-2K_2-K_3}{K_1}\right)\right.\right.$$

$$\left.\left. e^{-\frac{(\theta-2K_2-K_3}{K_1}}\right\}\right]$$

Then $$\dot{Y} = \frac{1}{(1+f)}\left[-\frac{1}{K_1}\ e^{-(\theta-\theta_1-K_2)/K_1} + \frac{1}{K_1}\ e^{-(\theta-K_2)/K_1} - \frac{f}{(1+f)}\left\{-\frac{1}{K_1}\left(1+\frac{\theta-2K_2-K_3}{K_1}\right)\right.\right.$$

$$\left.\left. \cdot\ e^{-(\theta-2K_2-K_3)/K_1} + \frac{1}{K_1}\ e^{-(\theta-2K_2-K_3)/K_1}\right\}\right]$$

or,

$$\dot{Y} = -\frac{1}{K_1(1+f)}\left[e^{-(\theta-\theta_1-K_2)/K_1} - e^{-(\theta-K_2)/K_1} + \frac{f}{(1+f)}\left\{1-\left(1+\frac{\theta-2K_2-K_3}{K_1}\right)\right.\right.$$

$$\left.\left. \cdot\ e^{-(\theta-2K_2-K_3)/K_1}\right\} + \frac{1}{K_1(1+f)}\left[\frac{f}{(1+f)}\left(1 - e^{-(\theta-2K_2-K_3)/K_1}\right)\right]\right.$$

or,

$$\dot{Y} = -\frac{Y}{K_1} + \frac{f}{K_1(1+f)^2}\left(1 - e^{-(\theta-2K_2-K_3)/K_1}\right)$$

Differentiating again,

$$\ddot{Y} = -\frac{\dot{Y}}{K_1} + \frac{f}{(1+f)^2 K_1^2}\, e^{-(\theta-2K_2-K_3)/K_1}$$

or, $$\ddot{Y} = -\frac{\dot{Y}}{K_1} - \frac{1}{(1+f)K_1^2}\left\{\frac{f}{(1+f)}\,(1 - e^{-(\theta-2K_2-K_3)/K_1})\right\} + \frac{f}{(1+f)^2 K_1^2}$$

or, $$\ddot{Y} = -2\dot{Y}/K_1 - \frac{Y}{K_1^2} + f/(1+f)^2 . K_1^2$$

.... $\theta_1 + K_2 < \theta < \theta_1 + 2K_2 + K_3$ or

$2K_2 + K_3 < \theta < \theta_1 + 2K_2 + K_3$

Part (v) can be written as

$$Y = \frac{1}{(1+f)}\,[e^{-(\theta-\theta_1-K_2)/K_1} - e^{-(\theta-K_2)/K_1} + \frac{f}{(1+f)}\left\{(1 + \frac{\theta-\theta_1-2K_2-K_3}{K_1})\right.$$

$$\left. . e^{-(\theta-\theta_1-2K_2-K_3)/K_1} - (1 + \frac{\theta-2K_2-K_3}{K_1})\, e^{-(\theta-2K_2-K_3)/K_1}\right]$$

Then on differentiation

$$\dot{Y} = -\frac{1}{K_1(1+f)}\,[e^{-(\theta-\theta_1-K_2)/K_1} - e^{-(\theta-K_2)/K_1} - \frac{f}{(1+f)}\left\{-\frac{(\theta-\theta_1-2K_2-K_3)}{K_1}\right.$$

$$e^{-\frac{(\theta-\theta_1-2K_2-K_3)}{K_1}} + e^{-(\theta-\theta_1-2K_2-K_3)/K_1} + \frac{(\theta-2K_2-K_3)}{K_1}$$

$$\left. . e^{-(\theta-2K_2-K_3)/K_1} - e^{-(\theta-2K_2-K_3)/K_1}\right\}]$$

or,

$$\dot{Y} = -\frac{Y}{K_1} + \frac{1}{K_1(1+f)}\,[e^{-(\theta-\theta_1-2K_2-K_3)/K_1} - e^{-(\theta-2K_2-K_3)/K_1}]$$

Differentiating again,

$$\ddot{Y} = -\frac{\dot{Y}}{K_1} - \frac{f}{K_1^2\,(1+f)^2}\,(e^{-(\theta-\theta_1-2K_2-K_3)/K_1} - e^{-(\theta-2K_2-K_3)/K_1})$$

or

$$\ddot{Y} = -2\dot{Y}/K_1 - Y/K_1^2 \;\ldots\ldots\; \theta > \theta_1 + 2K_2 + K_3$$

REFERENCES

1. MacMullin, R.B. and Weber, M.,
Am. Inst. Chem. Engrs., 31, 409 (1934-35).

2. Danckwerts, P.V.,
Chem. Engg. Sc., 2, 1 (1953).

3. Denbigh, K.
'Chemical Reactor Theory'. Cambridge (1950).

4. Rebhun, M. and Argaman, Y.,
J. San. Eng. Div., Proc. A.S.C.E., 91, S.A. 5, 37 (1965).

5. Villemonte, J.R., Rohlich, G.A. and Wallace, A.T.
Advances in Water Pollution Research, 2, 381 (1966).

6. Coulson, G. and Richardson, E.,
'Chemical Engineering', Vol. II, p.917, McGraw Hill (1955).

7. Naor, P. and Shinnar, R.,
Ind. Eng. Chem., Fundamentals, 2, 278 (1963).

8. Himmelblau, D.M. and Bischoff, K.B.,
'Process Analysis and Simulation', Wiley (1968).

9. Levenspiel, O.
'An Introduction to the design of Chemical Reactors', Wiley (1962).

10. Denbigh, K.,
'Chemical Reactor Theory', Cambridge, pp.86 (1950).

11. Chollette, A. and Cloutier, L.
Can. J. Chem. Eng., June, 105 (1959).

12. Wolf, D. and Resnick, W.,
I. and EC Fundamentals, 2, No.4, p.287, Nov. (1963).

13. Denbigh, K.G.,
Trans. Faraday Soc., 40, 352 (1944).

14. Weber, A.P.
Chem. Eng. Progress, 49, 26 (1953).

15. Colburn, A.P.,
Trans. Am. Inst. Chem. Engrs., 31, 457 (1935).

16. MacMullin, R.B.,
Chem. Eng. Progress, 49, 33 (1953).

17. Sinclair, C.G. and McNaughton, K.J.
Chem. Eng. Sci., 20, 261 (1965).

18. Vermeulen, T.,
'Advances in Chemical Engineering', Vol. II, 147 (1958).

19. Deemter, J.J. van
Chem. Eng. Sci., 13, 190 (1961).

20. Tekkipe, R.J. and Cleasby, J.L.,
J. San. Eng. Div., 94, SA1, 85, Feb. (1968).

21. Villemonte, J.R., Rohlich, J.R. and Wallace, A.T.,
'Evaluation of Oil Water Separator inlet Devices' presented at 31st Mid year Meeting of the American Petroleum Institute, Division of Refining, Houston, Texas, May (1966).

22. Levenspiel, O.
The Can. J. Chem. Eng., p.135, Aug. (1962).

23. Chollette, A., Blanchet, J. and Cloutier, L.,
The Can. J. Chem. Eng., p.1, Feb. (1960).

24. Wallace, T.,
J. San. Eng. Div., 92, SA2, p.179, April (1966).

25. El-Baroudi, M.H.,
J. San. Eng. Div., 92, SA3, p.27, June (1966).

26. Kendall, M.G. and Stuart, A.,
'The Advanced Theory of Statistics', Vol.I, Griffin (London) (1958).

27. Izawa, K.,
'Introduction to Automatic Control', Elsevier Publishing Co. (1963).

28. Ceaglske, N.H.,
'Automatic Process Control for Chemical Engineers', Wiley (1956).

29. Cheng, D.K.,
'Analysis of Linear Systems', Addison-Wesley (1959).

30. Takamatsu, T. and Naito, M.,
Water Research, No.6, 1, 433 (1967).

31. Dooge J.C.I.,
A lecture given on Process Analysis of Hydrological Data in the Civil Engineering Department, Imperial College in 1967.

32. Clements, W.C. Jr. and Schnelle, K.B. Jr.
I. and EC. Process Design and Development, 2, No.2, 94 (1963).

33. Churchill, R.V.,
'Fourier Series and Boundary Value Problems', McGraw Hill (1941)

34. Moskowitz, S. and Racker, J.,
'Pulse Techniques', 3rd Print., Prentice Hall (1954).

35. Kuo, B.C.,
'Automatic Control Systems', 3rd Print., Prentice Hall (1964).

36. Caldwell, W.I., Coon, G.A. and Zoss, L.M.,
'Frequency Response for Process Control', McGraw Hill (1959).

37. Krenkel, A.P., Hays, J.R. and Schnelle, K.B., J.W.P.C.F., 38, 1669 (1966).

38. Law, V.J. and Bailey, R.V., Chem. Eng. Sci., 18, 189 (1963).

39. Draper, C.S., McKay, W. and Lees, S. 'Instrument Engineering', Vol.II, McGraw Hill (1953).

40. Dreifke, G.E., Hougen, J.O. and Mesmer, G., I.S.A. Transactions, 4, 353 (1962).

41. Horowitz, I.M., 'Synthesis of Feedback Systems', Academic Press (1963).

42. Hougen, J.O. and Walsh, R.A., Chem. Eng. Progr., 57, 69 (1961).

43. Manson, M.A., J. Boston Soc. Civ. Engrs., 27, 207 (1940).

44. Hooper, L.J., Trans. Am. Soc. Mech. Engrs., 62, 651 (1940).

45. Ambrose, H. Jr, Baumann, E.R. and Fowler, E.B., Sew. Ind. Wastes, 29, 24 (1957).

46. Fan, L.N. 'Turbulent Buoyant Jets into Stratified or Flowing Ambient Fluids', Report No. KH-R-15, Calif. Inst. of Tech., June, 1967.

47. Thackston, E.L., Hays, J.R. and Krenkel, P.A., J. San. Eng. Div., 93, SA3, p.47, June (1967).

48. Krenkel, P.A., J.W.P.C. Federation, 34, No.12, p.1203, Dec. (1962).

49. Spalding, D.B., Chem. Eng. Sci., 9, 74 (1958).

50. Kelly, L.G., 'Handbook of Numerical Methods and Applications', p.61, Addison-Wesley (1967).

51. Marquardt, D.W., Industrial and Applied Mathematics, 11, 431 (1963).

52. Rosenbrock, H.H., The Computer Journal, 3, 175 (1960-61).

53. Powell, M.J.D., The Computer Journal, 7, 155 (1964-65).

54. White, E.T., The Jl. Imp. Col. Chem. Eng. Soc., 14, 72 (1962).

55. Murphy, K.L. and Timpany, P.L.,
J. San. Eng. Div., 93, SA5, p.1, Oct. (1967).

56. Thomas, H.A. and McKee, J.E.,
Sewage Works Journal, 16, 42 (1944).

57. Meier, P. and Zierler, K.L.,
J. Appl. Physiology, 6, 731 (1954).

58. McDonald, D.A.,
'Blood Flow in Arteries', Edward Arnold (1960).

59. Bland, W.H.,
'Nuclear Medicine', McGraw Hill (1960).